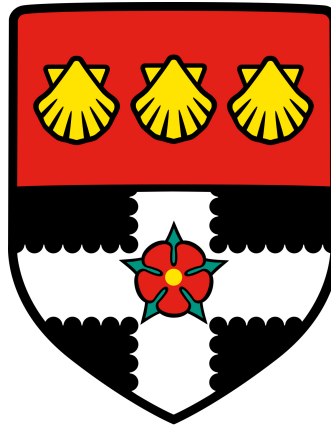# The University of Reading

Investigating the regenerative effects of adipose-derived mesenchymal stem cell conditioned media on sarcopenic and progeric skeletal muscle

Thesis submitted for the degree of Doctor of Philosophy

School of Biological Sciences

Taryn May Morash

October 2017

Declaration

I confirm that this is my own work and the use of all material from other sources has been properly and fully acknowledged.

Taryn May Morash

Taryn Morash

Acknowledgements

Taryn Morash

Abstract

Ageing, defined as the progressive deterioration of molecular, cellular, tissue and whole organism function, is a primary risk factor for numerous diseases, such as cardiovasculature disease, neurodegeneration and cancer. In recent years, advances in our knowledge of key determinant mechanisms that underpin ageing decline, drives the notion that these features can be attenuated and targeted therapeutically, enabling elderly individuals to experience an enhanced quality of life into advanced old age. Sarcopenia comprises the age-related loss of muscle mass, quality and function and contributes to overall frailty, immobility and a greater risk of falls. The use of stem cell-derived conditioned media (CM) holds great clinical potential and recent studies have reported many beneficial effects in a number of tissue models of injury and disease. We want to develop a novel anti-ageing therapy for the treatment of age-associated declines in sarcopenia. First, we characterise the skeletal muscle profile in a novel use of the $Ercc1^{d/-}$ murine model of progeria and compare it to the naturally-aged phenotype. We examine the effects of CM, generated from adipose-derived mesenchymal stem cells (ADMSCs), on skeletal muscle composition, function and satellite cell (SC) activity in sarcopenia and progeria. We show that CM has beneficial regulatory effects on mechanisms underpinning the declines associated with the Hallmarks of Ageing, for example, enhancing mitochondrial function and reducing oxidative stress. Importantly, we also demonstrate that CM harbours pro-angiogenic effects, which we hypothesise is unlikely to impact on skeletal muscle alone. Remarkably, we report the $Ercc1^{d/-}$ mice appear to launch a survival programme and delay the progression of age-related deterioration. A further feature associated with ageing skeletal muscle is the impaired regenerative function and myofibre turnover following injury and daily use. Key factors attributed to this decline in repair involve compromised SC activity as well as the depletion of the stem cell pool, known to occur with age. We want to first, examine the influence of the myofibre microenvironment on SC behaviour. Second, we investigate the use of non-muscle cell types as a source to generate muscle cells. We show that three stem cell types, ADMSC, dental pulp stem cells (DP) and amniotic fluid stem cells (AFS) and one non-stem cell line, MDA-MB-231 (MDA) breast cancer cells, adopted amoeboid-based migration (blebbing) once seeded onto myofibres. We also show that the regulation of the migratory mechanisms, known to be controlled by the Rac and Rho signalling pathways, is conserved in each of these cell types. Remarkably, we also demonstrate that a rapidly growing non-muscle stem cell (AFS), as well as a non-stem cell (MDA) initiate expression of MyoD and furthermore, the AFS cells were directed, through exposure to the myofibre microenvironment, to fuse and form myotube structures that express myosin heavy chain (MHC$^+$).

Taryn Morash

Abbreviations

3D - Three Dimensions

4E-BP - 4E binding proteins

ACh – Acetylcholine

ActRIIB – Activin type IIB receptor

ADMSC – Adipose derived mesenchymal stem cells

ADP – Adenosine diphosphate

AFS – Amniotic fluid-derived stem cells

AGE - Advanced glycation end-products

AKT – Protein kinase B

ALK (1/2) - Activin receptor-like kinase (1/2)

AMP - Adenosine monophosphate

AMPK – AMP-activated protein kinase

ANOVA - Analysis of Variance

ATP – Adenosine triphosphate

bFGF – Basic fibroblast growth factor

bHLH – Basic helix-loop-helix

BMC – Bone mineral content

BMD – Bone mineral density

BMSC – Bone marrow mesenchymal stem cells

°C - Celsius

Ca^{2+} - Calcium ion(s)

CaMK – Ca^{2+}/Calmodulin-dependent protein kinase

CD31 - Cluster of differentiation 31

CD34 - Cluster of differentiation 34

Taryn Morash

CD45 – Cluster of differentiation 45

Cdc42 - Cell division control protein 42 homolog

Cdkn2a/ p16^{INK4a} - cyclin-dependent kinase Inhibitor 2A

CM – Conditioned media

cm - Centimetres

CO_2 – Carbon dioxide

CSA – Cross-sectional area

CTX - Cardiotoxin

DAPI – 4',6-diamidino-2-phenylindole

dH_2O – Deionised water (ultrapure)

DHE - Dihydroethidium

DMD – Duchenne muscular dystrophy

DMEM – Dulbecco's modified eagle medium

DMSO – Dimethyl sulfoxide

DNA - Deoxyribonucleic acid

DP – Dental pulp stem cells

ECM – Extracellular matrix

EDL – Extensor digitorum longus

EDTA - Ethylenediaminetetraacetic acid

EGF – Epidermal growth factor

eIF2 - Eukaryotic initiation factor 2

ER – Endoplasmic reticulum

ERCC1 – Excision repair cross-complementary group 1

Ercc1$^{-/-}$ - Excision repair cross-complementary group 1 null/knockout mouse

Ercc1$^{d/-}$ - Excision repair cross-complementary group 1 mutant mouse (hybrid delta 7 (Δ7)/null)

Taryn Morash

ETC – Electron transport chain

EV - Extracellular vesicle

FAK - Focal Adhesion Kinase

FBS – Fetal bovine serum

FG – Fast-twitch glycolytic

FGF – Fibroblast growth factor

FOG – Fast-twitch oxidative glycolytic

FOXO - Fork-head box O

g – Force of gravity (gravitational)

GAPs - GTPase activating proteins

GDF-8 – Growth and differentiation factor 8

GDF-11 – Growth and differentiation factor 11

GDP - Guanosine diphosphate

GEFs - Guanine nucleotide exchange factors

GF – Growth factor

GFP – Green fluorescent protein

GH – Growth hormone

GM – Growth media

GPX - Glutathione peroxidase

GTP - Guanosine triphosphate

H_2O - Water

H_2O_2 – Hydrogen peroxide

HDAC - Histone deacetylase

H&E - Haemotoxylin and eosin

HGF – Hepatocyte growth factor

Taryn Morash

HIF1a – Hypoxia induced factor 1a

HPR – Hexazotized pararosaniline

HPRT - Hypoxanthine-guanine phosphoribosyltransferase

IGF – Insulin-like growth factor

IL-6 – Interleukin 6

IM – Intramuscular

IMF - intermyofibrillar

IMR-90 – Lung fibroblast IMR-90 cell line

IP – Intraperitoneal

IV – Intravenous

kPa – Kilopascal

MAPK - Mitogen-activated protein kinase

μL – Microliters

μM - Micromolar

μm – Micrometre

MDA - MDA-MB-231 human breast adenocarcinoma cell line

mdx – Mouse model (muscular dystrophy - x-linked)

MEF2 - Myocyte enhancer factor 2

MHC – Myosin Heavy Chain

MHC I - Myosin Heavy Chain type I

MHC IIA - Myosin Heavy Chain type IIA

MHC IIX - Myosin Heavy Chain type IIX

MHC IIB - Myosin Heavy Chain type IIB

mg – Milligrams

MI – Myocardial infarction

Taryn Morash

miRNA – MicroRNA

mL – Millilitres

mM – Millimolar

mm – Millimetres

MMP – Matrix metalloproteinase

MnSOD - Manganese superoxide dismutase

MRF – Myogenic regulatory factor

mRNA – Messenger RNA

MSC – Mesenchymal stem cells

mTOR – Mammalian target of rapamycin

MuRF1 – Muscle Ring-Finger protein 1

MVs - Microvesicles

Myf5 – Myogenic factor 5

MyoD – Myogenic differentiation 1

NAD^+ - Nicotinamide adenine dinucleotide (oxidised)

NADH - Nicotinamide adenine dinucleotide (reduced)

NBT – 4-nitro blue tetrazolium chloride

NCAM - Neural cell adhesion molecule

NER – Nucleotide excision repair

NFAT – Nuclear factor of activated T-cells

NF-κB - nuclear factor kappa-light-chain-enhancer of activated B cells

NICD – Notch intracellular domain

NO – Nitric oxide

O_2^- - Superoxide

O_2 – Oxygen

Taryn Morash

p53 – Tumor suppressor protein 53

P70S6K1 - 70kDa S6 protein kinase

PARP1 - Poly(ADP-ribose) polymerase 1

Pax3 - Paired box protein 3

Pax7 – Paired box protein 7

PBS – Phosphate buffered saline

PCR – Polymerase chain reaction

Penstrep – Penicillin-Streptomycin

PFA – Paraformaldehyde

PGC-1α - Peroxisome proliferator-activated receptor-γ co-activator 1 alpha

PI3K - Phosphoinositide 3-kinase

qPCR – Quantitative (Real-Time) polymerase chain reaction

RBP- Jκ - Recombining binding protein Jκ

RNA - Ribonucleic acid

ROCK – Rho-associated protein kinase

ROS – Reactive oxygen species

RyR – Ryanodine receptor

SA-beta-gal - Senescence-associated beta-galactosidase

SC – Satellite cell

SDH - Succinate dehydrogenase

SEM – Standard error of the mean

SEM – Scanning electron microscopy

SERCA – Sacro/endoplasmic reticulum Ca^{2+}-ATPase

SFCM – Single fibre culture medium

SIRT1 – Sirtiun 1

Taryn Morash

SMA – Alpha smooth muscle actin

SO – Slow-twitch oxidative

SOD - Superoxide dismutase

SR - Sarcoplasmic reticulum

SS - Subsarcolemmal

STAT3 – Signal Transducer and Activator of Transcription

T0 – Time plus zero hours

T2 – Time plus 2 hours

T14 – Time plus 14 hours

T24 – Time plus 24 hours

T48 – Time plus 48 hours

T72 – Time plus 72 hours

TA – Tibialis anterior

TF – Transcription factor

TFAM – Mitochondrial transcription factor A

TGF-β - Transforming growth factor beta

TH - Thyroid hormone

TNF-α - Tumour necrosis factor alpha

TSC (1/2) - Tuberous sclerosis complex (1/2)

UPS - Ubiquitin-proteosome system

VEGF – Vascular endothelial growth factor

v/v – Volume per volume

WT – Wild-type

XPA - Xeroderma pigmentosum

XPF - Xeroderma pigmentosum group F

Taryn Morash

Table of contents

Taryn Morash

Taryn Morash

Taryn Morash

Taryn Morash

Taryn Morash

Taryn Morash

Taryn Morash

Taryn Morash

Table of figures

Taryn Morash

Taryn Morash

22

Taryn Morash

Chapter 1
Introduction

Taryn Morash

Introduction

The overall aim of this project is to investigate the therapeutic effects of stem cell secretory factors on age-related declines in skeletal muscle. Diseases associated with ageing are becoming more prevalent and as a result of improved longevity, this raises questions, as to whether human 'healthspan', can keep up pace with increasing lifespans. There has been a rise in the proportion of elderly individuals in the human population and caring for these individuals into their advanced old age, causes a greater strain on the healthcare and economic systems (Suzman & Beard 2011; Martin & Sheaff 2007).

In recent years, López-Otín and colleagues have enumerated nine 'Hallmarks of Ageing' and these can be described as common biological 'themes' that have been shown to deteriorate over time, leading to age-related declines in function (López-otín et al. 2013). The hallmarks include; 'genomic instability', 'loss of proteostasis', 'stem cell exhaustion', 'cellular senescence', 'telomere attrition', 'altered intercellular communication', 'mitochondrial dysfunction', 'deregulated nutrient-sensing' and 'epigenetic alterations'. It has also been suggested that the overall 'ageing' effect develops through a combination of these hallmarks (López-otín et al. 2013). The perception of ageing in the literature has altered in recent years, to consider ageing as more of a pathology in itself (Beckman & Ames 1998; Aiello et al. 2017; Gladyshev & Gladyshev 2016). Thus, further investigation and an improved understanding of the underlying mechanisms that appear to become 'faulty' over time, could indicate possible therapeutic targets (Martin & Sheaff 2007; Melis et al. 2013).

Overall frailty, defined by declines in energy, physical ability, cognition, fitness and health in the elderly population, has been highly associated with deterioration of the neuromuscular system (Rockwood et al. 2005; Cesari et al. 2006). Skeletal muscle makes up approximately 45-50% of total body mass (Seifter et al. 2005). Sarcopenia is defined as the age-related loss in muscle mass, quality and function and population studies have reported estimations of approximately 20% of people aged 60-70 years old are affected by sarcopenia and this rises once over the age of 80 (up to ~50%) (von Haehling et al. 2010; Baumgartner et al. 1998; Paddon-Jones & Rasmussen 2009; Burton & Sumukadas 2010). Muscle mass has also been estimated to decrease by ~1-3% after the age of 50, annually and contributes to overall frailty, linked directly to a greater risk of falls, fractures and hospitalisation (Doherty 2003; von Haehling et al. 2010; Grounds 2014; Cesari et al. 2006). An extensive study conducted by Janssen and colleagues, calculated the approximate healthcare cost of sarcopenia in the United States of America (U.S.A) as $7.7bn for women and $10.8bn for men, per year, accountable for ~1.5% of total healthcare expenditure (Janssen et al. 2004). It should be noted however, that this estimation was calculated in 2004 and is expected to be higher today.

24

Taryn Morash

The changes that occur in skeletal muscle structure and stem cell function with age have been the focus research area of studies, in a number of different model systems, in animals as well as humans (Alnaqeeb & Goldspink 1987; Ansved & Larsson 1989; Degens, Turek, et al. 1993; Baumgartner et al. 1998; Shake et al. 2002; Frontera et al. 2008; Faulkner & Brooks 1995; Terman & Brunk 2004; Shefer et al. 2006; Collins et al. 2007; Orford & Scadden 2008; Collins-Hooper et al. 2012; Lavasani et al. 2012; Cheung & Rando 2013; Sousa-Victor et al. 2014). However, it is apparent from the literature that there remains the need for a detailed, comprehensive 'ageing skeletal muscle profile', as well as an appropriate experimental set-up to identify, outline and potentially treat, delay or even prevent associated age-related symptoms (Demontis et al. 2013).

Skeletal muscle provides a model tissue to investigate the changes in stem cell maintenance and function with age and sarcopenia delivers a consistent, well-defined experimental model of 'pathology', in order to explore stem cell secretory factors as an anti-ageing therapy (in mice). Collaborators have previously established regulatory approved, clinically compliant, standard operating procedures for the generation of autologous stem cell conditioned media-based therapeutic treatments. The use of stem cell-derived conditioned media holds great clinical potential and recent studies have reported many beneficial effects, observed in a number of tissue models of injury and disease (Kinnaird et al. 2004; Cho et al. 2012; Cantinieaux et al. 2013; Lavasani et al. 2012; Inoue et al. 2013; Pawitan 2014). It is believed that the clinical use of conditioned media will provide a less invasive, more successful, safer alternative to stem cell transplantation (by reducing the likelihood of host rejection in an inflammatory response and the occurrence of neoplasia) and could play essential roles in the amelioration of disease (Cho et al. 2012; Kim et al. 2010).

The aims of the current research project are firstly, to explore how the muscle tissue health and architecture alters with the onset and progression of sarcopenia in naturally-aged mice. This is achieved using a range of experimental parameters conducted at molecular, cellular, tissue and whole organism levels to develop a broad skeletal muscle profile, providing a basis for subsequent experimentation. Secondly, features of skeletal muscle composition, function and regeneration are characterised, in the novel use of a murine model of DNA damage accumulation, in a resultant phenotype of accelerated ageing (progeria). The progeric skeletal muscle profile is assessed in the capacity to mimic the aspects of decline observed in sarcopenia in natural ageing. Thirdly, the potential therapeutic paracrine effects of conditioned media (CM) treatment, generated from adipose-derived mesenchymal stem cells (ADMSC), is examined in both naturally-aged and progeric skeletal muscle. Lastly, the importance of the skeletal muscle myofibre matrix in determining satellite cell (SC) regenerative function, as well as the influence of the myogenic microenvironment on the behaviour and fate of non-muscle cells, is explored.

Taryn Morash

Muscle

Myocytes are the cells that make up muscle and differences in the characteristics, structure and arrangement of these cells determine the muscle type. There are three main types of muscle found in the human body; smooth muscle, cardiac muscle and skeletal muscle (Clark 2005). The latter two forms are distinguishable from smooth muscle by the striations or regular stripes observed across individual myofibres. Thus, cardiac and skeletal muscle are also referred to as 'striated muscle' due to their macroscopic appearance (Pocock & Richards 2006). Cardiac muscle is that of the heart and smooth muscle is located primarily in the walls of blood vessels and hollow organs of the body, including the digestive tract (Campbell 2008). Skeletal muscle is a component of large, multi-cellular animals that, as the name suggests, is attached to the bones via tendons and is responsible for voluntary movement. However, it will be seen that this is not the only function of skeletal muscle. The investigations conducted in the current research project will be focused on skeletal muscle, specifically.

Skeletal muscle

Skeletal muscle in humans comprises approximately 40% of total body weight and is a highly dynamic and plastic tissue (Janssen et al. 2000; Frontera & Ochala 2015). There are over 650 muscles in the human body and they vary greatly in size, shape, attachments and composition. For example, the *Stapedius* of the inner ear is the smallest striated muscle in the human body and averages about 6-7mm in adults (Clement et al. 2002). In contrast, the *Sartorius* muscle extends the length of the thigh bone and although it has a relatively thin diameter, it is also the longest muscle. Therefore, characteristics are extremely variable between muscles, this can be directly linked to the tasks each muscle has to perform and these include a wide range of different functions throughout the body. The main functions of skeletal muscle include: 1. Maintains posture and body position. 2. Permits movement through force generation. 3. Provides support to the soft tissues for example, the muscles of the abdominal wall and pelvic floor. 4. Guards entrances and exits of the mammalian body orifices. 5. Functions as a vital amino acid store and maintains core body temperature through heat production, via the important role played in metabolism (MacIntosh et al. 2006).

Skeletal muscle is known to maintain body posture and balance (involuntary) through interactions via the two sub-pathways of the vestibulospinal tract, the medial and lateral vestibulospinal tracts (Siegel & Sapru 2010). These tracts are responsible for regulating motor-neuronal innervation, in response to sensing external stimuli, to initiate stabilization of the head (and neck) muscles and upright posture through the extensor muscles in the leg, respectively (Brodal 2010). Moreover, a further function of skeletal muscle is that, the *Gastrocnemius* and *Soleus* muscles of the lower leg

Taryn Morash

that constitute the calf, are involved in the 'calf muscle pump' mechanism, which functions in the return of venous blood flow to the upper body from the lower extremities, essential in the prevention of lower leg ulceration and deep vein thrombosis (DVT) (Bryant & Nix 2012; Christopoulos et al. 1989; Meissner et al. 2012).

Macroscopic anatomy of skeletal muscle

Skeletal muscle is comprised of a variety of tissues including blood vessels, nerves and connective tissue. Each muscle is served by one nerve, one artery and at least one vein. All of which tend to enter at one central point and branch extensively throughout the connective tissue layers (MacIntosh et al. 2006). The entire skeletal muscle body is surrounded by a dense connective tissue layer, of which collagenous fibres are a major constituent, termed the epimysium (Rowe 1981). The role of the epimysium is to keep the muscle separate, protecting against friction from other surrounding tissues and bones (MacIntosh et al. 2006). A further collagenous layer, the perimysium, encases fascicles which are bundles of myofibres. Myofibres are a multi-nucleated syncytium of myonuclei, surrounded by a plasma membrane (sarcolemma) and a layer of connective tissue known as the endomysium, of which collagen fibres, laminin and fibronectin are the main components (MacIntosh et al. 2006; Bertolotto et al. 1983; Gulati et al. 1982; Engvall et al. 1990). Myofibres consist of bundles of protein filaments (myofibrils), longitudinally arranged down the length of the fibre, and in turn, actin (thin) and myosin (thick) myofilaments, making up the striated, contractile element (sarcomere) of skeletal muscle (Campbell 2008; Pocock & Richards 2006) (Figure 1.1). The epimysium, perimysium and endomysium are continuous with tendons, which at each end link the muscle body to the bone, which it serves to transmit the mechanical force generated by muscle contraction, to the skeleton (Light & Champion 1984; Pocock & Richards 2006). Additionally, just below the perimysium sheets, arterioles and venules as well as intramuscular nerves, enter and form branching patterns within these regions, as well as serving the endomysium layers. Furthermore, arterioles supply blood to the dense capillary networks that serve individual myofibres (MacIntosh et al. 2006).

Microscopic anatomy of skeletal muscle

Skeletal muscle myofibres, depending on muscle length, can vary from a few millimetres to several centimetres and range from 50 to 100μm in diameter (Pocock & Richards 2006). Myonuclei are organised peripherally within the myofibre, beneath the sarcolemma and there are two distinct subpopulations of mitochondria, the subsarcolemmal (SS) and the intermyofibrillar (IMF) mitochondria (Bruusgaard et al. 2006; Ferreira et al. 2010; Leeuwenburgh et al. 2005). The contractile unit of skeletal muscle, the sarcomere, is repeated as a chain along the length of each

Taryn Morash

myofibril and it is the alignment of these units, that creates the characteristic striations of skeletal muscle (Pocock & Richards 2006). When viewed using polarised light, there are two distinct regions visible, a dark region, known as an A band (anisotrophy), composed of thick (myosin) filaments and a light region, termed the I band (isotrophy), which is made up of thin filaments (actin) (Figure 1.1). Each I band is divided by a characteristic line, termed the Z line, which contains numerous proteins including α-actinin (binds actin filaments) and desmin (links adjacent Z lines for alignment), and the region between two Z lines is the sarcomere unit. In the centre of the dark A band is a region in which thick and thin filaments do not overlap and this results in a zone with a pale appearance, known as the H zone. In the centre of the H zone, adjacent thick filaments form links to create the M line (MacIntosh et al. 2006). The myofibre sarcolemma contains a transverse tubule (T tubule) system which comprises narrow tubules that project transversely from the sarcolemma across each myofibre at the junctions between A and I bands. Each myofibril is surrounded by the sarcoplasmic reticulum (SR), which is the endoplasmic reticulum of skeletal muscle. Where the SR and the T tubules make contact, the SR enlarges to form terminal cisternae. The SR stores and releases calcium and along with regulatory activity of actin filament proteins, troponin and tropomyosin, helps to regulate muscle contraction (Pocock & Richards 2006).

Muscle contraction

The sliding filament model of muscle contraction is dependent on the interactions between the thick (myosin) and thin (actin) filaments. Each myosin molecule contains a rod-like tail and two globular head regions, which contain the ATP binding site and ATPase, where ATP is hydrolysed to ADP and inorganic phosphate. The hydrolysis of ATP converts the myosin head region to a high energy state that subsequently binds actin, forming a cross-bridge, the actin filament is then pulled towards the centre of the sarcomere. It is this movement that causes a shortening of the sarcomere and the filaments slide longitudinally, increasing the overlap between the two types of filament. The cross-bridge is detached when a new ATP molecule binds the myosin head. In a repeated cycle, the free myosin head cleaves the new ATP and attaches to a binding site further along the actin filament (Campbell 2008).

The arrival of an action potential at the pre-synaptic terminal of a neuromuscular junction triggers the release of the neurotransmitter acetylcholine (ACh). Subsequent binding of ACh to the sarcolemmal nicotinic receptors on the myofibre leads to depolarisation, thereby generating an action potential. The action potential spreads along the length of the myofibre via the T tubules and triggers the release of calcium ions (Ca^{2+}) from the terminal cisternae (Campbell 2008). The Ca^{2+} ions bind the troponin complex, displacing tropomyosin, changing its position on the actin molecule. This

Taryn Morash

in turn, exposes the myosin binding sites on the actin filament, allowing myosin/actin coupling to take place, initiating muscle contraction through the sliding filament process. When motor neuron stimulation ceases, the myofibre relaxes and the filaments slide back to their original positions and the Ca^{2+} ions are pumped out of the cytosol back into the SR. Low Ca^{2+} ion levels cause troponin and tropomyosin to return to their starting positions and therefore, inhibits myosin/actin binding once more (Pocock & Richards 2006).
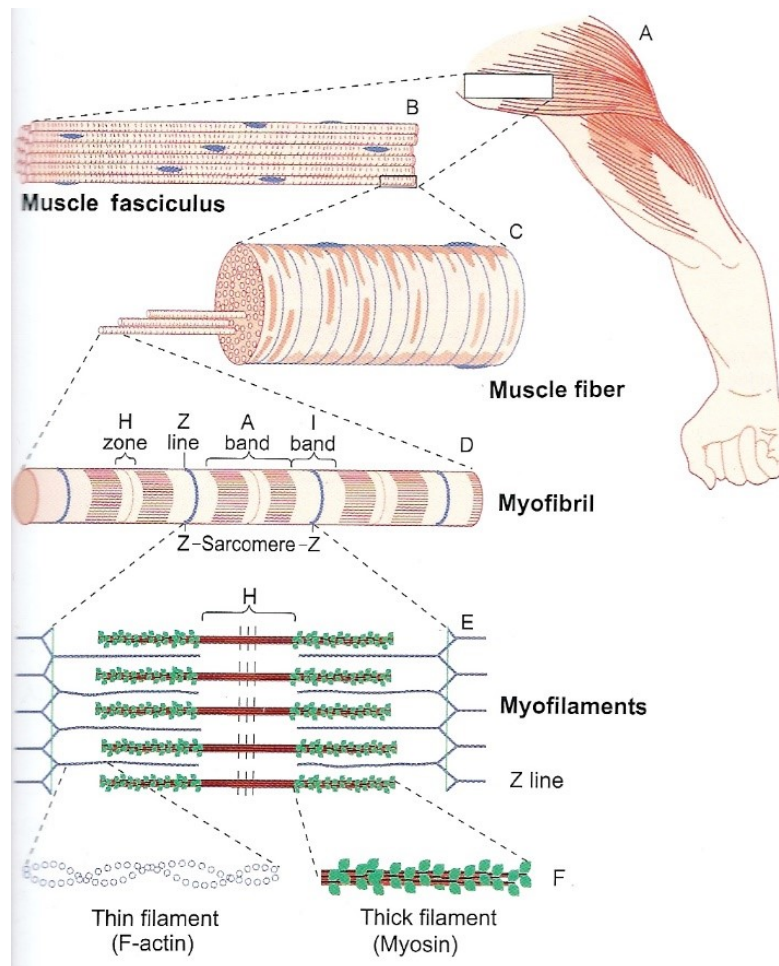
Figure 1.1 Microscopic structure of skeletal muscle. (A) Whole muscle. (B) A muscle fascicule (C) An individual muscle fibre (D) Myofibril structure. (E, F) Myofilament structure and the arrangement of thick and thin filaments (Pocock & Richards 2006).

Taryn Morash

Skeletal muscle myofibre classification, functional diversity and plasticity

A single motor neuron supplies one or more myofibres and together this forms a single motor unit (Burke et al. 1971; Pette & Vrbova 1985). When the neuron is activated, the action potential is transmitted to each myofibre it serves, as per the mechanism previously described. Therefore, the motor unit is the final functional element that generates movement (Pette & Vrbova 1985). Myofibres are highly organised and display a wide range of diversity, which is attributed to a variety of functional capacities and plasticity in their adaptation to functional demand (Goldspink 1999; Degens et al. 1992; Pette & Staron 2000). There are a number of ways that myofibres can be classified and these can be based on among others, physiological, histochemical, biochemical and morphometrical properties, such as contractile capacity, myosin heavy chain (MHC) composition, oxidative capacity and fatigability (Larsson et al. 1991; Alnaqeeb & Goldspink 1987; Pette & Staron 1990) (Figure 1.2). The diversity presented by skeletal muscle myofibres was recognised in early studies describing muscles as 'white' or 'red' which, through later research utilising a combination of physiological and the advance in enzyme histochemical methods, further elucidated these broad differences in appearance, to refer to more specific physical properties, such as myoglobin content and oxidative capacity (Pette & Staron 1990). Burke and colleagues were among the first to classify three distinct myofibre types in the *Gastrocnemius* muscle of cats, based on their physiological and histochemical characteristics, identifying that myofibres within the same motor unit were uniform in type (Burke et al. 1971; Burke et al. 1973). Additionally, Peter and colleagues utilised NADH tetrazolium reductase and succinate dehydrogenase enzymes to study the glycolytic and oxidative capacity of guinea pig and rabbit myofibres with low or high ATPase activity (Peter et al. 1972). These early classifications included (fatigue-resistant) slow-twitch oxidative (SO), (fatigue-resistant) fast-twitch oxidative glycolytic (FOG) and (fast-fatigable) fast-twitch glycolytic (FG) myofibres (Burke et al. 1971; Peter et al. 1972). This thereby, added a further dimension to classifications, where relationships were made between metabolic properties (oxidation) and fatigability and established that 'red' muscle myofibres may be fast or slow (Burke et al. 1971; Burke et al. 1973; Pette & Staron 1990). The vast number of different ways that myofibres can be physiologically, histologically, and biochemically identified and categorised therefore, can make general myofibre classification a challenge (Larsson et al. 1991). However, despite the numerous methods of classifying myofibre types histologically, few have prevailed as universally-used, 'industry-standard' protocols (Pette & Staron 1990; Pette & Staron 2000). One method commonly used to identify different myofibre types is by MHC isoform profile, where distributions within a muscle, between muscle types, as well as across strains and species are extremely varied, further establishing skeletal muscle as a diverse, heterogeneous tissue (Pette & Staron 2000). MHC isoforms are accountable for the myosin ATPase

Taryn Morash

activity and contractile rate of myofibres and have since, been categorised into type I (slow twitch) and type II (fast twitch) groups (DeNardi 1993). Schiaffino and colleagues used anti-MHC isoform rat monoclonal antibodies and immunoblotting analysis to identify the myofibre types and importantly, described three distinct type II sub-populations, including IIA, IIB and intermediate IIX/IID fibres (Schiaffino et al. 1989; DeNardi 1993). Due to the many possible combinations in myosin heavy and light chain isoforms, multiple hybrid myofibre types can be formed (Lowey et al. 1993). This feature, as well as the different classes of motor neurons that serve those myofibres, results in numerous variations in the morphological, biochemical and contractile abilities of the myofibres in a muscle. These features are highly dependent on specific muscle function. For example, muscles required to maintain posture (postural), predominantly consist of slow-twitch myofibres with high resistance to fatigue. Whereas, phasic muscles contain a high proportion of fast-twitch motor units for more rapid movements (Pette & Vrbova 1985). Moreover, the succinate dehydrogenase histochemical stain remains a commonly used qualitative assessment of oxidative capacity in muscle (Takemura et al. 2017; Barnouin et al. 2017; Pette & Staron 2000). The metabolic requirement of each MHC isoform varies significantly for example, slow twitch type I myofibres are generally characterised by a small cross-sectional area (CSA), an abundance of mitochondria, myoglobin and a greater capillary density (Figure 1.2). Fast twitch myofibres such as type IIB typically have a large CSA, few mitochondria, little myoglobin and a rich in glycogen (Figure 1.2). Type IIA and IIX myofibres have intermediate properties (Gundersen 2011; Yan et al. 2011; Duan et al. 2017) (Figure 1.2). Furthermore, Type I and IIA myofibres are more oxidative in their metabolism whereas, type IIX and IIB are predominantly glyocolytic (Schiaffino & Reggiani 1996; Pette & Staron 2000) (Figure 1.2). A range of fibre type-specific isoforms of other muscle proteins also determine differences between myofibre types. Notably, the sarcoplasmic-endoplasmic reticulum Ca^{2+}-ATPase (SERCA) isoforms vary between myofibre type, with SERCA1a highly expressed in types IIX and IIB whereas, SERCA2a is expressed in slow type I and IIA myofibres (Salvatore et al. 2013; Schiaffino & Reggiani 2011). Faster myofibres also maintain a greater abundance of both ryanodine receptor (RyR) calcium release channels and SERCA pumps which, together, regulate the release and ATP-dependent re-uptake of calcium from the cytosol. Therefore, differing abundances of these proteins and SERCA isoform expressions, can regulate the rate of this process, during muscle contraction and relaxation (Schiaffino & Reggiani 2011).

Taryn Morash
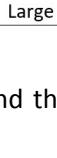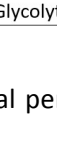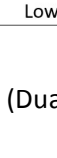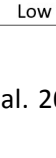
MHC isoform	Twitch duration	Shortening velocity	Myofibre size (CSA)	Fatigue resistance	Metabolism	Force	Mitochondrial density	Capillary density	Energy efficiency
I	Slow	Slow	Small	High	Oxidative	Low	High	High	High
IIA									
IIX									
IIB	Fast	Fast	Large	Low	Glycolytic	High	Low	Low	Low

Figure 1.2 Myofibre isoforms and their physiological performance, adapted from (Duan et al. 2017; Gundersen 2011).

Distribution of myofibres

Distribution of myofibre types varies within muscles and across muscle types and species. For example, examination of the myofibre composition profiles of a large variety of different rat muscles demonstrated that type IIB myofibres comprised the largest proportion of rat musculature, however there were some muscles, such as the *Soleus*, that contained very few, if any type IIB myofibres (Delp & Duan 1996). Furthermore, Armstrong and colleagues have previously shown that the deep extensor and flexor muscles of the limbs in a number of mammals, including rats, pigs, dogs and cats, contain the highest proportion of type I myofibres, whereas the superficial muscles are comprised of a large percentage of type IIB (Ariano et al. 1973; Armstrong & Phelps 1984; Armstrong et al. 1987; Armstrong et al. 1982). Similarly, this is also the case when analysing the distribution of myofibres within a single limb muscle. For example, the deep region contains the majority of the type I myofibres, in contrast very few are located superficially, instead in this peripheral region there is an abundance of type IIB myofibres (Armstrong & Phelps 1984; Fuentes et al. 1998). The distribution and composition of myofibre types are vastly different in the rabbit *Extensor digitorum longus* (EDL), *Psoas* and *Tibialis anterior* (TA) muscles, compared to the mouse and rat, as it has been shown that the predominant myofibre is the type IIX and these muscles do not contain pure type IIB myofibres (Hämäläinen & Pette 1993). The type I distribution however, showed proximo-distal differences in the regionalisation across the hindlimb muscles of these three species. Furthermore, the muscles of the rat hindlimb were all described as 'fast' muscles, with the exception of the *Soleus*, and the patterning of type I distribution was reported to be highly reproducible, with similar trends of declining proximo-distal type I myofibre densities (Wang & Kernell 2001). The composition and distribution of myofibres is known to be directly linked with the functional demand and specific role of a given muscle. For example, anti-gravity or postural muscles, such as the *Soleus*, contain a larger proportion of slow oxidative (type I) myofibres whereas, locomotory muscles are comprised of an

Taryn Morash

abundance of fast glycolytic (type II) myofibres (Suzuki 1995). Significantly greater proportions of type IIB myofibres comprised the muscles analysed in the rat and mouse, relative to the rabbit. Additionally, studies in larger mammals and man have revealed a greater abundance of type I myofibres, when compared to small animals (Delp & Duan 1996; Prince et al. 1976; Johnson et al. 1973). It was proposed that smaller animals have a greater requirement for the use of type IIB myofibres due to their reliance of significantly faster contraction velocities for movement (Hämäläinen & Pette 1993; Suzuki 1995; Delp & Duan 1996). Studies examining myofibre composition in human muscles however, are considerably less abundant than those carried out in animals, particularly those conducted in small rodents (Smerdu et al. 1994). Humans are suggested to have only three (pure) myofibre types (I, IIA and IIX), as very few myofibres, located in the masseter muscles and external oblique were demonstrated to contain type IIB RNA, but not IIB protein (Yan et al. 2011; Smerdu et al. 1994; Horton et al. 2001). In-situ hybridisation analysis, showed that MHC IIX-specific mRNA probes hybridised with those myofibres that histochemically expressed IIB, however the IIB-specific probe only hybridised with a few myofibres histochemically defined as type I in the external oblique muscle, but not with any IIB myofibres in any other examined muscles (Horton et al. 2001).

Transitions in myofibre type

The heterogeneity of myofibres in their physiological, biochemical and metabolic features, is a key determinant of differences in contraction speed and fatigue resistance, enabling diverse muscle groups to carry out a variety of functions and movements. A fundamental and remarkable characteristic of myofibres is their adaptability to changing environmental, metabolic and functional demands controlled by numerous intrinsic signalling pathways (Bassel-Duby & Olson 2006). The adaptability of skeletal muscle was demonstrated using cross-innervation of slow twitch *Soleus* muscle with nerve fibres that normally supply the fast twitch *Flexor digitorum longus*, resulting in an increased contractile speed. Additionally, a corresponding, slower contraction was observed with cross-innervation in the reverse, in fast twitch muscle (Buller et al. 1960). Studies conducted to examine the genetic regulation of these myofibre transitions, have been achieved using exercise, transgenic animal models, electrical stimulation, disease states as well as microgravity. For example, studies conducted in denervated rat, rabbit and cat muscles show that electrical stimulation that mimics patterns of high (intermittent short bursts) and low (prolonged) frequency activities influence the contractile properties of fast and slow muscles, respectively (Lomo et al. 1974; Salmons & Vrbová 1969). A slow to fast switch in myofibre type can be induced, not only through high frequency electrical stimulation, but also by muscle unloading, for example during hindlimb suspension, as well

Taryn Morash

as hyperthyroidism (Caiozzo et al. 1998). Alternatively, a switch in the opposing direction, from fast to slow types, is induced, along with low frequency electrical stimulation, through muscle overloading, as well as hypothyroidism (Nwoye & Mommaerts 1981; Schiaffino & Reggiani 2011). Interestingly, the slow gene programme is difficult to reverse in adult myofibres and tends to persist for a long duration, even in denervated muscle. Therefore, a myofibre transition from slow to fast, which may can result in the disappearance of the slow myofibres, can only be induced by long-term complete inactivity. For example following spinal cord damage in mice or spinal cord injury in humans (Schiaffino & Reggiani 2011). In general, however, the development and maintenance of the slow myofibre phenotype is dependent on innervation by a slow motor neuron. Whereas, the development of fast characteristics is believed to be regulated by thyroid hormone (TH), as well as a high frequency innervation pattern (Pette & Staron 1997; Pette & Staron 2000; Salvatore et al. 2013).

Furthermore, it is well-established that skeletal muscle myofibres undergo phenotypic transitions in chronic disease, such as obesity, ageing, as well as in response to physical activity (Hickey et al. 1995; Inbar et al. 1981; Yan et al. 2011). Specifically, endurance exercise induces a transformation of myofibres from those more glycolytic to an oxidative phenotype within faster type II myofibres, from IIX to IIA, to I in humans and IIB to IIX, to IIA in rats and mice (Green et al. 1979; Andersen & Henriksson 1977; Allen et al. 2001; Schiaffino & Reggiani 2011). Correspondingly, a higher proportion of type IIA and IIX are observed in more sedentary humans (Klitgaard, Bergman, et al. 1990). Molecular genetics-based research has allowed for a more detailed analysis of the underlying regulation of exercise-induced myofibre transitions. Subsequently, studies have established that the activation of the calcineurin/NFAT (nuclear factor of activated T-cells) signalling pathway, is a key determinant for the expression of slow twitch muscle genes, through numerous loss and gain of function, as well as transgenic animal studies (Chin et al. 1998; Yan et al. 2011). Additionally, Ca^{2+}/calmodulin-dependent protein kinase (CaMK) activation of myocyte enhancer factor 2 (MEF2) and the successive derepression of class II histone deacetylases, such as HDAC proteins (4, 5 and 9) is also involved in the transformation of myofibres to those more oxidative (Potthoff et al. 2007; Yan et al. 2011). Furthermore, the AMP-activated protein kinase (AMPK) and peroxisome proliferator-activated receptor gamma coactivator 1-alpha (PGC-1α) interactions (AMPK/ PGC-1α), as well as the p38γ3 mitogen-activated protein kinase (MAPK)/PGC-1α signalling pathways, have been established as functionally important in the response to metabolic stress and energy deprivation, through increased contractile activity, by segmentally initiating exercise-induced myofibre transitions and mitochondrial biogenesis, respectively (Röckl et al. 2007; Garcia-Roves et al. 2008; Lin et al. 2002; Pogozelski et al. 2009).

Taryn Morash

Muscle hypertrophy

In general, muscle mass is dependent on the balance between protein synthesis and degradation and mechanisms of both processes are sensitive to, among others, physical activity/exercise, hormonal regulation, nutritional status, ageing and injury and disease (Frontera & Ochala 2015; Goldspink 1999; Yang et al. 1997; Cartee et al. 1996; Degens & Alway 2003). Increases in adult skeletal muscle mass is believed to be as a result of increases in size (hypertrophy), in response to the greater demand with growth, rather than increased myofibre number (hyperplasia) (Rowe & Goldspink 1969). Myofibre number is believed to reach maximum value at birth and remains unchanged throughout development into adulthood (Glass 2005; Alnaqeeb & Goldspink 1987; Rowe & Goldspink 1969). Adaptation of muscle mass to changing functional demands is a further fundamental characteristic of skeletal muscle plasticity and as such, is of interest where research into preventing muscle wasting is a priority. For example, further understanding of the mechanisms underpinning muscle hypertrophy and atrophy is critical in cases of myopathology and other diseases, cancer, sepsis, HIV/AIDS and prolonged inactivity, as a result of injury and ageing.

Increased muscle loading, for example through resistance training exercise, results in muscle (compensatory) hypertrophy whereas, unloading or prolonged disuse leads to a decreased mass or atrophy. Importantly, these increases in muscle mass can be attributed to increases in myofibril number and size and are therefore, typically accompanied by a greater contractile, force-generating capacity and overall strength (Alnaqeeb & Goldspink 1987; Degens & Alway 2003). Muscle hypertrophy has been studied extensively and can be achieved through surgical denervation of surrounding muscle synergists (in small animals), as well as through resistance training exercise (small animals and humans), among others (Degens et al. 1992; Degens, Turek, et al. 1993; Lowe & Alway 2002; Roman et al. 1993; Welle et al. 1996). Importantly, there are key differences in the type of exercise and the resultant effects on the response and adaptability of skeletal muscle. For example, resistance training brings about changes relating predominantly to increased muscle mass through greatly increased levels of rapid protein synthesis. Whereas, endurance exercise results in more long-term adaptations, including myofibre type transitions from more glycolytic to those more oxidative and mitochondrial mass increases (Baar 2006). Thus in humans, high resistance training through weight-lifting exercise results in increases in the size of FOG (IIA) and FG (IIX/IIB) myofibres (Prince et al. 1976; Staron et al. 1984). Contrastingly in the rat, intensive forelimb exercise, has been shown to increase the proportion and hypertrophy of SO myofibres (Jaweed et al. 1977). Insulin-like growth factor-1 (IGF-1) mRNA expression has been shown to increase in response to overload and stretch, resulting in hypertrophy (Yang et al. 1997). Furthermore, the underlying regulation of signalling mechanisms, modulated by resistance exercise, implicates the activity of insulin and

Taryn Morash

GH/IGF-1 in stimulating the PI3K/AKT/mTORC2 pathway in resistance training-induced protein synthesis, through downstream components including, 4E binding proteins (4E-BP), eukaryotic initiation factor 2 (eIF2) and 70kDa S6 protein kinase (P70S6K1), believed to be the primary controls of initiation (Glass 2005; Baar 2006) (Figure 1.3). The PI3K/AKT/mTORC2 pathway simultaneously, inhibits protein degradation and autophagy signalling through the fork-head box O (FOXO), whilst promoting synthesis (Velloso 2008). Moreover, the CaMK/MEF2 and AMPK/PGC1α signalling pathways are initiated through endurance exercise and are responsible for characteristic activity-induced myofibre transitions (from IIX to IIA and I) (Klitgaard, Bergman, et al. 1990; Andersen & Henriksson 1977; Baar 2006).
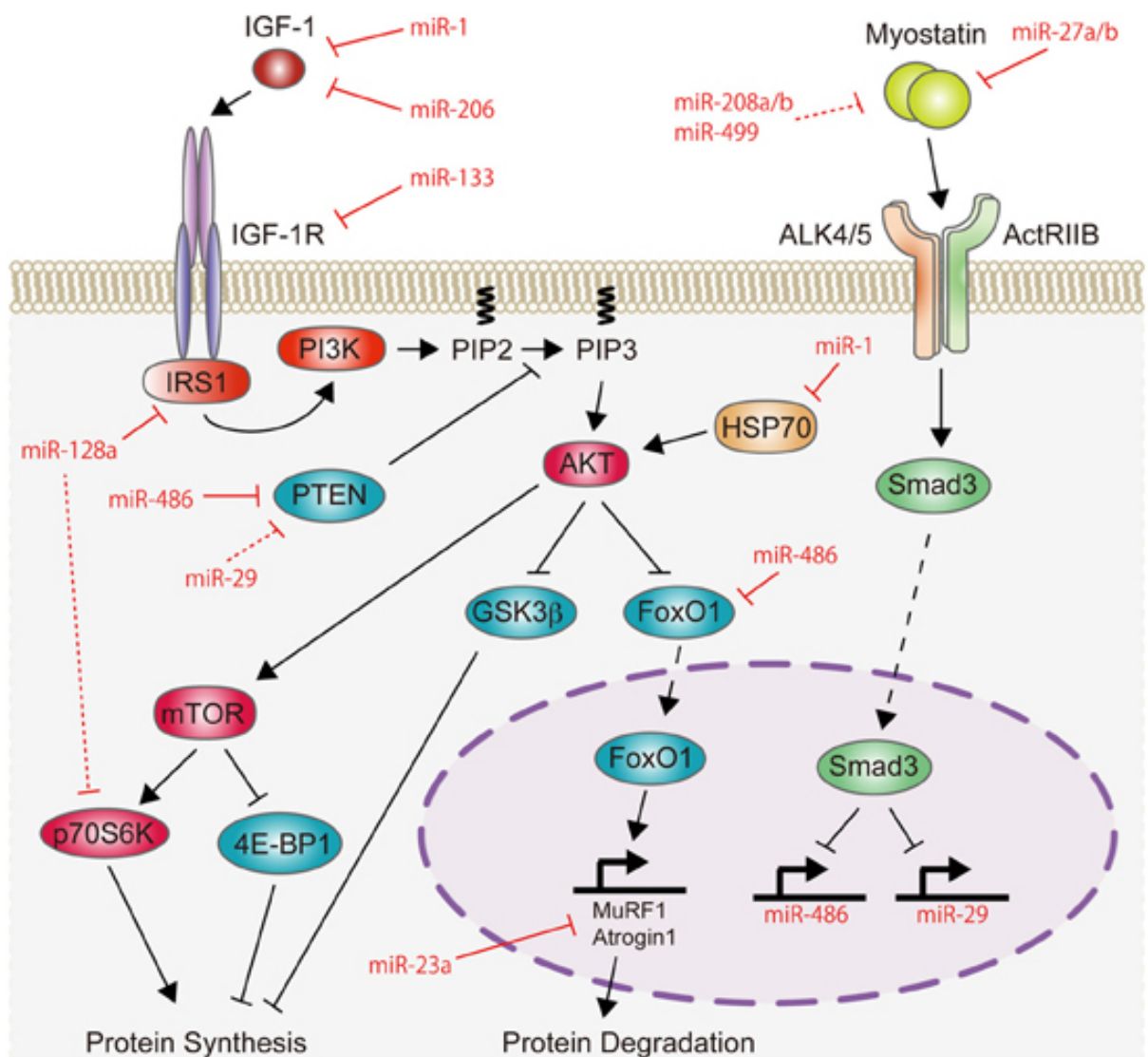
Figure 1.3 Signalling pathways regulating protein synthesis and degradation (Hitachi & Tsuchida 2014).

Taryn Morash

Muscle atrophy

Skeletal muscle is a highly adaptive tissue with very plastic cells regarding their size, where myofibres can undergo hypertrophy in response to increased demand (Schwartz 2008; Rowe & Goldspink 1969). Contrastingly, myofibres also undergo atrophy in response to stimuli such as during sarcopenia, denervation, cachexia (cancer), sepsis, muscular diseases and alternatively, prolonged disuse or inactivity (Lynch et al. 2007). The mechanisms that control the balance between anabolism and catabolism are those that regulate protein synthesis and degradation. A functional shift or dysregulation in either direction can drive the counteracting pathway more strongly, to induce overall outcomes of extensive hypertrophy or atrophy (Lynch et al. 2007). A gross loss of muscle mass is regulated by the following mechanisms, the first is the ubiquitin-proteasome system (UPS), which mediates signalling of ubiquitin ligases MuRF1 and atrogin-1, further regulated by the PI3K/AKT pathway via FOXO, as well as the NF-κB pathway (Glass 2005; Schwartz 2008). The second is the autophagy/lysosome pathway, also coordinated by FOXO signalling (Bechet et al. 2005; Schwartz 2008). Thirdly, the Ca^{2+}-dependent cysteine protease, calpain pathway (Bartoli & Richard 2005; Lynch et al. 2007). Furthermore, TGF-β family member, Myostatin is a key negative regulator of muscle hypertrophy. Myostatin initiates cellular signalling by binding either of the type II activin receptors (IIa or IIb), activating type I receptors ALK4 or ALK5, formation of this receptor complex results in phosphorylation of transcription factors, SMAD2 and SMAD3, which in turn, translocate to the nucleus, bringing about a reduction in protein synthesis and upregulation of degradation (Egerman et al. 2015).

Additionally, apoptosis is believed to play an important role in muscle atrophy and has been shown to occur in the myonuclei, stromal cells as well as the satellite stem cell populations of skeletal muscle (Schwartz 2008; Wang et al. 2014). However, there is evidence of a relatively consistent myonuclear domain, a strictly regulated theoretical amount of cytoplasm supported by a single myonucleus (optimum myonuclei to cytoplasm, DNA to protein ratio), despite fluctuations in myofibre size (Dupont-Versteegden 2006). The mechanism that governs the reduction of myonuclei during atrophy has been shown to resemble that of apoptosis, including characteristics of chromatin condensation and DNA fragmentation. However, it is also believed that alternatively, this process should be described as 'apoptotic nuclear death', as unlike mono-nucleated cells, multi-nucleated myofibres do not appear to completely package up and clear all cellular contents (nuclear and cytoplasmic) (Dupont-Versteegden 2005). This therefore suggests that unlike traditionally-described apoptosis, there appears to be a subset of myonuclei that are more susceptible to apoptotic stimuli to reduce overall total myonuclei numbers per myofibre (Schwartz 2008; Dupont-Versteegden 2005). Apoptosis has been shown to be higher in *Soleus* muscles of aged rats, compared to young, indicated

Taryn Morash

by TUNEL assays as well as increased caspase activity (Leeuwenburgh et al. 2005). Furthermore, a study conducted in mice also showed that there was a distinct rise in apoptosis in aged muscle. A small proportion was identified as the myonuclei however, apoptosis appeared to be concentrated in the stromal cells, endothelial cells of the capillary network, as well as the satellite stem cell population (Wang et al. 2014).

Collagen synthesis and degradation

Like the myofibres themselves, the surrounding ECM is highly complex and can adapt according to mechanical and reparative demands. Mechanical loading begins a signalling cascade from molecular gene expression, transcription, translation, as well as post-translational modifications, to bring about collagen synthesis and degradation (Yasuda et al. 1996). TGF-β and IGF-1 are among the growth factors released during exercise and this is accompanied by an increased procollagen expression and collagen synthesis (Yang et al. 1997; Kjær et al. 2009). Collagen is produced as a triple helical polypeptide chain of procollagen by the fibroblasts (as well as SCs) in the ECM, where the procollagens are cleaved by proteases and assembled into collagen fibrils. Post-translational modifications include enzymatic cross-linking, known to be increased in ageing (Zimmerman et al. 1993; Haus et al. 2007; Wood et al. 2014). ECM component remodelling and degradation in both physiological and pathological conditions is dependent on key matrix metalloproteinase (MMP) activity. In the *mdx* mouse, MMP-2, MMP-9 as well as tumour necrosis factor (TNF-α) activities were increased during degeneration-associated ECM remodelling (Bani et al. 2008). Additionally, increases in Wnt signalling has been implicated in the increased proliferation of muscle resident stromal cells and enhanced collagen deposition (Trensz et al. 2010).

Taryn Morash

Satellite cells

Essential to life is the ability for tissues to undergo repair following damage, caused through injury, disease or normal cellular turn-over, with age. Regeneration typically involves the activation and proliferation of quiescent stem cells located within their tissue-specific stem cell niche, through various extrinsic factors and intrinsic signalling pathways. A stem cell can be described as an unspecialized cell, that retains the ability to divide indefinitely producing two daughter cells; with the capability of remaining quiescent and thereby, contributing back to the stem cell pool in a process of self-renewal, or initiating differentiation towards a specific cellular lineage, regulated by certain external signalling molecules (Weissman 2000).

Mammalian skeletal muscle during adulthood, is a stable post-mitotic tissue which, under normal conditions, requires only periodic fusion of the resident stem cells, satellite cells (SCs), in response to daily wear and tear, to compensate for overall muscle turnover. However, upon injury skeletal muscle maintains a remarkable ability to regenerate damaged myofibres. The degeneration and subsequent regeneration process is highly regulated at molecular, cellular and tissue levels and results in renewal of contractile units, that are fully innervated and vascularised. This process is highly reliant on SCs and the intrinsic factors that govern the underlying mechanisms of their regenerative function, as well as the interactions with the muscle stem cell microenvironment (niche) through extrinsic factors. The resident stem cell population of skeletal muscle, first termed 'satellite cells' by Alexander Mauro in 1961, remain quiescent beneath the basal lamina until activated by external cues, through muscle damage or stress conditions (Mauro 1961; Beauchamp et al. 2000; Bischoff 2004). Once activated, satellite cells then enter the cell cycle, proliferate, migrate and form progenitor (myoblast) cells, that differentiate into myotubes then fuse, replace and incorporate or support damaged muscle (Collins-Hooper et al. 2012; Yin et al. 2013). SC proliferation and differentiation during regeneration is also believed to be influenced by innervation, therefore activity and exercise, the vasculature, hormones including testosterone and thyroid hormone, nutrition as well as the tissue lesion following damage (Yin et al. 2013).

Identification of the satellite cell as the regenerative component of skeletal muscle

Importantly, it was Snow and colleagues that demonstrated that SCs contributed nuclei to regenerating skeletal muscle and this was not carried out by the myofibres themselves (Snow 1977; Snow 1977a). Development of an *in vitro* suspension culture system of individually dissected single myofibres from rat hindlimb muscles, enabled the study of the origin and behaviour of SCs. It was shown that SCs were induced to divide following myofibre dispersal and subsequently, SCs were

Taryn Morash

identified as a viable highly proliferative cell population with the potential to be utilised in regeneration in myopathologies, such as muscular dystrophies (Bischoff 1975). It was later shown that freshly isolated SCs expressed CD34 and Myf5 and it was suggested that these markers could be responsible for maintaining SC quiescence (Beauchamp et al. 2000). Although, more recently, Notch signalling, through the SC-specific deletion of recombining binding protein Jκ (RBP- Jκ), has been demonstrated as having an essential role in maintenance of quiescence in SCs and therefore, the stem cell pool (Bjornson et al. 2012). A further study showed that microRNA-489 suppressed the oncogene, DEK, post-transcriptionally, which similarly implicated microRNA-489 in the preservation of SC quiescence (Cheung et al. 2012). Moreover, manipulation of culture conditions, including serum and growth factor deprivation, loss of cell adhesion and contact inhibition have been shown to drive cells into quiescence, by arresting cell cycle progression in G1 phase. These findings therefore, indicate that SC quiescence is not only regulated by intrinsic mechanisms but also by the extracellular microenvironment.

Satellite cell activation

Studies into the activation of SCs revealed that the external stimuli (mitogens), were shown to be released from crushed skeletal muscles and subsequently were identified as growth factors, including transforming growth factor beta (TGF-β), fibroblast growth factor (FGF), insulin-like growth factor-1 (IGF-1) and hepatocyte growth factor (HGF) (Bischoff 1986a; Allen & Boxhorn 1989; Allen et al. 1995). It was established that IGF-1 increases SC proliferation and differentiation through the myogenic lineage, FGF additionally, increased proliferation and similarly to TGF- β, was also shown to have inhibitory effects of SC differentiation. The influence of the myofibre microenvironment and SC niche, on SC activation, was first reported by Bischoff and colleagues, who observed that SCs on the myofibre surface had a reduced mitogenic response compared to isolated cells (Bischoff 1990).

Satellite cell origin and function in myogenesis

It is well-known that the 'Paired Box' (Pax), family of transcription factors play essential roles during myogenesis (Treisman et al. 1991; Mansouri et al. 1996). Importantly, structurally homologous Pax3 and Pax7 have differing functions during embryonic development. In the mouse and chick, both Pax3 and Pax7 are expressed in the neural crest cells and throughout the embryonic dorsal neural tube (Goulding et al. 1991; Mansouri et al. 1996). However, one key role of *Pax3* and *Pax7* genes is the specification of myogenic stem cells, which enter the myogenic programme during embryogenesis and foetal development (Relaix et al. 2005). Pax3 and Pax7-positive skeletal muscle progenitor cells, derived from the central dermomyotome region of somites, activate myogenic regulatory genes and differentiate into skeletal muscle myofibres or form the proliferating cell population, that in late-

Taryn Morash

stage foetal muscle, are believed to adopt a SC position (Ben-Yair 2005; Gros et al. 2005; Kassar-Duchossoy et al. 2005; Relaix et al. 2005). This therefore, suggests that this population of somite-derived cells also provides the SCs of postnatal skeletal muscle (Gros et al. 2005). Pax3 is crucial for the survival of the progenitor cells, located at the edges of the dermomyotome (particularly those positioned hypaxially), where Pax3 is required for delamination and subsequent migration of progenitor cells to sites of skeletal muscle formation, for example the limbs (Franz et al. 1993; Goulding et al. 1994). Furthermore, Pax3, together with Myf5 has been shown to regulate the activation of MyoD (Tajbakhsh et al. 1997). However, Pax7 is the predominant paralogue expressed in adult human primary myoblasts, suggesting that despite structural similarities between Pax3 and Pax7 proteins, the differential spatial-temporal patterns of expression indicates that they regulate myogenesis in distinctly different cell types during development. Moreover, Seale and colleagues did not detect SCs in Pax7-null mice, thereby suggesting that Pax7 plays a crucial role in specification of the SC lineage in vertebrates (Seale et al. 2000). Pax3 is shown to be expressed in a small subset of the adult SC population, which includes the diaphragm and 50% of the forelimb muscles. However, the majority of the hindlimb musculature is negative for Pax3 and a downregulation of Pax3 has been noted in the hindlimb during foetal development (Otto et al. 2006; Relaix et al. 2006).

Throughout the myogenesis process, in adult skeletal muscle regeneration, markers of myogenic lineage are expressed in a step-wise fashion during cell differentiation, beginning with the expression of Pax7, a marker of satellite stem cell quiescence (Seale et al. 2000; Zammit, Relaix, et al. 2006). Co-expressed is Myf5 (myogenic factor 5) and following SC activation and determination towards a myogenic lineage, sequential expression of other muscle-specific basic helix-loop-helix (bHLH) transcription factor (TF) proteins, belonging to the myogenic regulatory factor (MRF) family, is initiated (Beauchamp et al. 2000; Funk et al. 1991). These factors include the 'master regulatory gene', *MyoD* (myogenic differentiation protein 1) and *Myogenin* and expression leads to the formation of mature muscle cells (Funk et al. 1991; Tapscott 2005; Weintraub et al. 1989; Grounds et al. 1992) (Figure 1.4). However, it has also been shown that the SC population is heterogenous, as subsets of SCs are known to divide asymmetrically and adopt divergent fates. SCs that co-express Pax7 and MyoD, downregulate Pax7 move towards terminal differentiation. However, other subsets appear to alternatively, downregulate MyoD expression, maintaining Pax7 and withdraw from cell cycle, retaining a state of quiescence and thereby, replenishing the stem cell pool (Zammit et al. 2004; Nagata et al. 2006).

The Wnt/β-catenin signalling pathway has been established as a key regulator of cell proliferation and lineage specification. Exogenous Wnt ligands, particularly Wnt1, Wnt3a and Wnt5a, have been shown to be expressed in both the regenerating myofibre and SC population and therefore, it has

been proposed that this signalling is important for SC proliferation during muscle regeneration processes (Otto et al. 2008). Additionally, Notch signalling is known to be important in the control of cell proliferation, differentiation and cell fate determination (Artavanis-Tsakonas et al. 1999). Notch signalling is initiated by the binding of Delta and Jagged ligands to the Notch transmembrane receptors, which through a subsequent enzymatic receptor cleavage, forms the Notch intracellular domain (NICD) and activation leads to NICD translocation to the nucleus, for targeted gene expression (Artavanis-Tsakonas et al. 1999). Notch regulation in skeletal muscle regeneration functions as a response to muscle injury, where the Delta ligand is rapidly upregulated in both the myofibres and activated SCs, resulting in the initiation of SC proliferation. Subsequent Notch inactivation, through the upregulation of the antagonist, Numb, enables differentiated myoblast fusion, as the final step in myofibre repair. Interestingly, as SCs are known to divide asymmetrically, producing two daughter cells with divergent fates, Numb was also localised asymmetrically, resulting in daughter cells with different levels of Numb. Therefore, it is postulated that this feature supports regulation of divergent SC fates (Conboy & Rando 2002). Moreover, activation of Wnt signalling in differentiating myoblasts antagonises Notch signalling and supports terminal differentiation, indicating a large degree of cross-talk interactions between these two well-defined regulatory mechanisms (Yin et al. 2013).
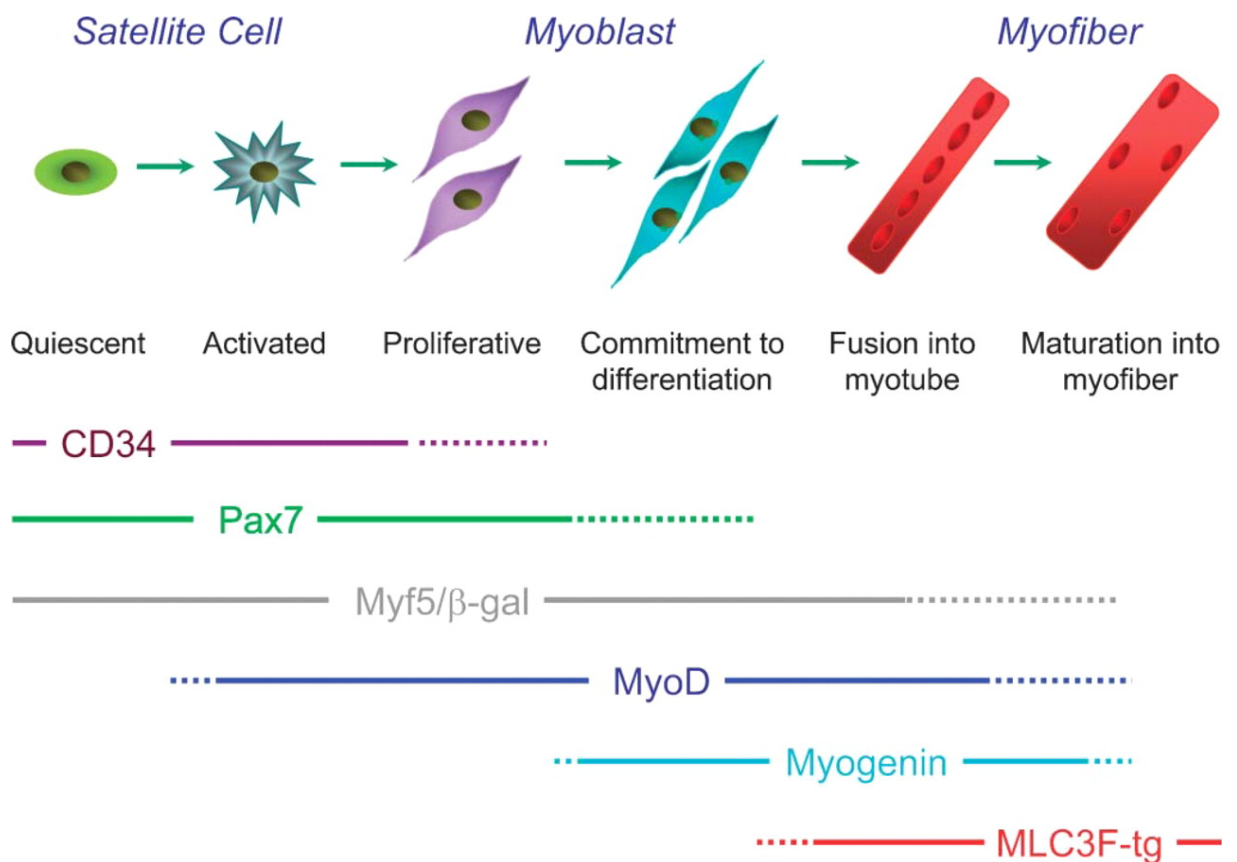
Figure 1.4 Satellite cell markers expressed during myogenesis (Zammit, Partridge, et al. 2006).

Taryn Morash

Studies investigating the differentiation capacity of SCs by induction towards other lineages, alternative to myogenic specification (including adipogenic and osteogenic pathways), have suggested that SCs share multipotential mesenchymal stem cell activity (Asakura et al. 2001; De Coppi et al. 2006). Furthermore, it was shown that the potential therapeutic effects of the *in vitro* culture and transplantation of isolated skeletal muscle-derived (CD34^{+}/45^{-}) stem cells (Sk-34), in the rejuvenation of damaged vascular, muscular and peripheral nervous systems, was due to their vast differentiation capacity (Tamaki et al. 2005; Tamaki et al. 2007). Furthermore, the use of SCs/primary myoblasts in transplantation experiments to supplement, support or alleviate degeneration in skeletal muscle in disease (such as Duchenne Muscular Dystrophy, DMD or ischaemic heart disease), following a myocardial infarction, or muscular injury, remains a potential candidate in cell-based therapy (Partridge 2000; Hagege et al. 2001; LaFramboise et al. 2003). This is despite relatively limited success thus far, due to a large proportion of transplanted cells dying in the first 3 days of introduction into the host tissue, surviving myoblasts are rejected through an immune response or do not migrate further than 200µm away from the site of injection (Siegel et al. 2009; Péault et al. 2007). However, it is in general agreement that for more successful cell-based therapy, there is a requirement for more effective dispersal and engraftment of injected cells (Siegel et al. 2009).

The underlying mechanisms of satellite cell migration

The traditionally-defined mechanism of cell migration is the lamellipodia-based method, usually described as the 'crawling' of cells through the extracellular matrix (ECM). This process occurs through the actin-polymerization-driven extension and branching of plasma membrane protrusions (lamellipodia) from the leading edge of a migrating cell and the myosin II-mediated contraction behind the cell body, at the 'lagging' end (Small et al. 2002; Tyson et al. 2014; Yoshida & Soldati 2006). In order to aid the 'traction' movement generated by the cell, focal adhesion contacts are made with the substratum/ECM as lamellipodia extend from the leading edge and these are broken down at the back as the cell progresses forward (Alberts et al. 2008). Recently however, an alternative, 'novel' mechanism for migration has been described in satellite cells and this is mediated via plasma membrane, vesicle-like 'blebs' contributing visually to 'amoeboid-like' behaviour (Otto et al. 2011). The bleb-based mechanism is initiated through local hydrodynamic modifications in cytosolic pressure, simultaneous weakening of the cortex and subsequent detachment from the plasma membrane. Localized ruptures of the cortex are created and expansion of the membrane results in the protrusion of spherical 'bleb' structures and migration has been shown to be affected by the age of the satellite cell (Charras et al. 2005; Charras & Paluch 2008; Collins-Hooper et al. 2012; Bergert et al. 2012). The blebbing process or 'lifespan' can be subdivided into three main 'phases'

Taryn Morash

including bleb initiation, stabilization and retraction (Tinevez et al. 2009). Both mechanisms have been shown to be implemented by the satellite cell and there is variation in migration speeds dependent on which method is adopted, with the lamellipodia-based motility occurring at a reduced rate compared to blebbing (Otto et al. 2011). As well as this, activated satellite cells have been observed traveling beneath the surface laminin layer of myofibres via the traditional lamellipodia-driven form but tend to assume the faster blebbing method, once having emerged through this layer, to migrate along the surface of myofibres (Otto et al. 2011).

It is now widely believed that the Rac and Rho small GTPase signalling pathways function antagonistically and are responsible for the regulation of cellular migration mechanisms (Sanz-Moreno et al. 2011). Herein, Rac initiates extension of lamellipodia protrusions from the leading edge of a migrating cell and therefore inhibition of Rac activity prevents this form of movement, whereas Rho and associated Cdc42 pathway interactions regulate amoeboid/bleb-based motility (Calvo et al. 2011; Charras & Paluch 2008; Nelson 2008; Sanz-Moreno et al. 2011). Rac and Rho proteins are constituents of subfamilies within the larger Ras superfamily of GTP hydrolases (Nelson 2008; Ridley & Hall 1992; Ridley & Hall 1994). GTPases have been described as 'molecular switches' and function through the binding of guanosine diphosphate (GDP) or guanosine triphosphate (GTP) resulting in conformational changes in shape to alternate between an inactive and active state (Bustelo et al. 2007; Jaffe & Hall 2005; Pollard et al. 2007). Regulation of GTPase activity is controlled by GEFs (guanine nucleotide exchange factors) and GAPs (GTPase activating proteins); the former activates GTPases by exchange of GDP for GTP and the latter (GAPs), initiate breakdown of the bound GTP molecule through hydrolysis and thereby reverts the protein back to its inactive state (Alberts et al. 2008; Bustelo et al. 2007). On activation, interactions with other downstream signalling molecules through particular signalling cascades and effector proteins are initiated in response. These bring about regulation of specific cellular events including cell polarity, cytoskeleton organization, cell migration, progression and regulation of the cell cycle and transcription (Bustelo et al. 2007).

Three human isoforms of Rho (RhoA, B and C), two Rac isoforms (Rac1 and 2) and Cdc42 were identified as distinct branches of the Ras superfamily and studies began into the apparent differences in function between the members, despite sharing a large amount of homology in their GTP binding sites (Chardin 1988; Madaule & Axel 1985). In the early 1990s, recombinant RhoA studies resulted in alterations in fibroblast cell morphology and speculation as to the function of Rho in actin filament organization and formation of stress fibres and focal adhesions was investigated (Paterson et al. 1990; Ridley & Hall 1992). Similar experiments involving Rac1 were then conducted and these suggested that Rac plays a role in plasma membrane 'ruffling', as well as lengthening of lamellipodia protrusions from the cell surface (Ridley et al. 1992). Further investigation revealed that interactions

Taryn Morash

between the Rac and Rho GTPase signalling pathways were common and 'cross-talk' at many levels, between multiple downstream proteins, also occurred frequently (Ridley 2001). A number of chemical inhibitors have been developed to target particular members of the Rho family GTPases and associated downstream effector proteins. Inhibition is a useful tool in cell signalling investigation, as roles of specific target proteins and their interactions within a pathway, can be determined through experimentation where the function is hindered or prohibited. This is achieved by observing the effect on particular cellular processes, through the blocking or 'knocking-down' of constituents in a pathway, in order to effectively observe what function is 'missing' or impaired. For example, studies currently being carried out by Marshall *et al*. involve *in vivo* experimentation and tissue culture assays, to observe the two mechanisms of migration in tumour cells, in order to better understand cancer cell invasion and metastasis (Ahn et al. 2012; Sanz-Moreno et al. 2011). Similarly, in understanding how these signalling pathways function, it is possible to manipulate the cell migration mechanisms utilised by a particular cell type *in vitro*. Importantly, this in turn, enables the observation of the effects that this has on cell speed, overall movement, directionality, morphology and importantly, as with SCs, how these impact on muscle regeneration in general. In recent years however, it is evident from the literature, that there has been a switch in focus towards studies involving the investigation into properties of the stem cell microenvironment or 'niche' and extracellular matrix (ECM), in order to better understand their impacts on cell behaviour (migration, morphology, differentiation and proliferation). Thus, it is postulated that different cell types are governed by the same molecular regulation, regarding their adaptability and response to the microenvironment, to facilitate different methods of motility.

The satellite cell extracellular matrix

In direct contact with the SCs, is a network of ECM components, such as type IV collagen, laminin, fibronectin and glycoproteins, that constitute the myofibre basal lamina, separating the SC population from the muscle interstitium (Sanes 2003). These molecules are predominantly synthesised and secreted by interstitial fibroblasts, but SCs and myoblasts are also known to produce and remodel these components during regeneration (Kovanen 2002). SCs are located between the basal lamina, which comprises a network of collagen IV and the sarcolemma (apical), covered in laminin (Woodley et al. 1983; Collins et al. 2007). The ECM network provides the myofibre with mechanical support, physical strength and elasticity, as well as importantly, enabling binding of SCs and other interstitial cells, for cell to cell and cell to ECM communication, for mechano-sensing and internal signal transduction. For example, α7/β1-integrin binding sites are presented by the basal lamina, for the physical tethering of the internal actin cytoskeleton of SCs, to the ECM for the

Taryn Morash

molecular communication (Song et al. 1992; Burkin & Kaufman 1999; Mayer 2003). Additionally, muscle-specific laminins (laminin-2 and -4), interact with the myofibre surface through integrins and dystroglycan (Gullberg et al. 1999; Sanes 2003). Moreover, essential for the initiation of a rapid response to muscle injury, proteoglycans situated on the surface of SCs, act as receptors in the binding of inactive growth factor precursors in resting, undamaged muscle. These precursors include hepatocyte growth factor (HGF), basic fibroblast growth factor (bFGF), epidermal growth factor (EGF), insulin-like growth factor isoforms (IGF-I and IGF-II), as well as Wnt glycoproteins and are believed to be sequestered from SCs, myofibres, interstitial cells or serum (Yin et al. 2013; Tatsumi et al. 1998; Golding et al. 2007; Machida & Booth 2004; Brack et al. 2008). Upon injury, proteolytic enzymes, such as thrombin, serine proteases and matrix metalloproteinases (MMPs), present in serum or the interstitium, rapidly activate the growth factor precursors. HGF functions during SC activation, migration and proliferation (Allen et al. 1995; Tatsumi et al. 1998; Miller et al. 2000). For example, HGF has been shown to increase aged SC migration speeds along myofibres in culture (Collins-Hooper et al. 2012). FGFs found in skeletal muscle have been associated with the stimulation of myoblast proliferation and myogenic lineage progression and are also known to contribute to the regeneration process through their well-defined roles in angiogenesis (Allen & Boxhorn 1989; Kästner et al. 2000; Floss et al. 1997; Lefaucheur et al. 1996). IGF signalling is highly linked with protein synthesis and myofibre hypertrophy and therefore, as hypertrophy involves the supplementation of myonuclei as the muscle grows, SCs are also activated by IGF signalling (Bark et al. 1998; Barton-Davis et al. 1999; Musarò et al. 1999; Philippou et al. 2007). MMPs, comprise a family of zinc-dependent enzymes responsible for the degradation of ECM components that function in both the degenerative and subsequent regenerative phases in damaged muscle (in particular MMP-2 and MMP-9) (Carmeli et al. 2004; Kherif et al. 1999). Additionally, activated MMP-2 and MMP-9 are known to degrade collagen IV in the muscle ECM, enabling SCs to emerge and migrate across the basement membrane to the lesion site (Nishimura et al. 2008).

Taryn Morash

Hallmarks of ageing

The Oxford English Dictionary definition of ageing describes this as *'the process of growing old'* however from a biological standpoint, the following definition was proposed in 1991: *'a persistent decline in the age-specific fitness components of an organism due to internal physiological deterioration'* (Rose 1991). The phrase *'internal physiological deterioration'* has been used extremely broadly here and importantly, it is what drives this process that is yet unknown and has the attention of a large proportion of the regenerative medicine research field. It is well documented that there is an age-related degeneration in satellite stem cell number and function with the mechanisms underpinning these declines remaining an area still poorly understood. It is apparent from the literature that ageing is almost considered a pathology in itself and therefore something that is potentially treatable. In 2013, Lopéz-Otín and colleagues published a review enumerating the nine hallmarks of ageing, taking a similar format to the 2000 review entitled 'The Hallmarks of Cancer' by Hanahan and Weinberg (López-otín et al. 2013; Hanahan & Weinberg 2000) (Figure 1.5). Hallmarks discussed in the 2013 review included 'stem cell exhaustion', 'genomic instability', 'cellular senescence' and 'telomere attrition' and therefore describes how ageing is appreciated as a multi-stage pathology that can be potentially measured and assayed *in vitro*, as well as within animal models at various levels, for example, this study provides a wide spectrum of characteristics for detailed analysis at the molecular and cellular levels, where the effects of ageing begin (López-otín et al. 2013).
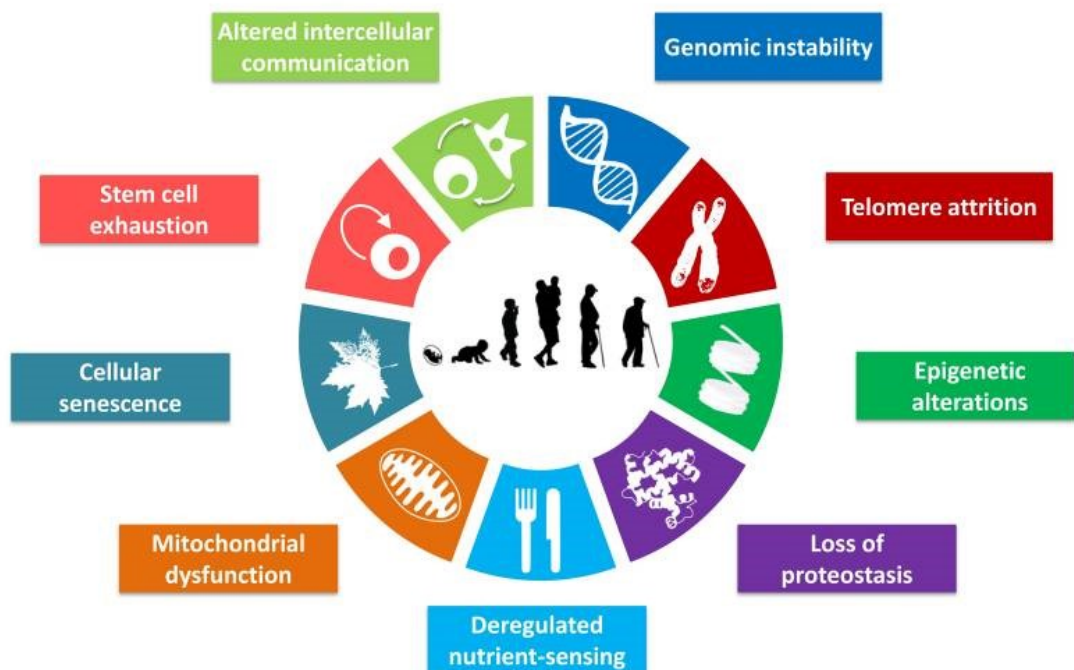
Figure 1.5 The nine Hallmarks of Ageing (López-otín et al. 2013).

Taryn Morash

Modern biological theories of ageing

Modern biological theories of ageing broadly fall into two main categories: 1. Programmed (death) theory and 2. Damage or error (error accumulation) theories and these discuss where ageing begins at the core, on a molecular level.

The programmed theory contains three sub-categories that includes 'programmed longevity' whereby ageing is the result of sequential switching on and off of certain genes, defining senescence (organism) as the point where age-related degeneration arises. This theory encompasses genetic instability as a hallmark of ageing discussed in the review by Lopéz-Otín and colleagues in 2013. Secondly, the 'endocrine theory' describes how hormones control ageing progression through the idea of a 'biological clock'. For example the IGF-1/insulin signalling (IIS) pathway has been implicated in the hormonal monitoring of the ageing process. Thirdly, the 'immunological theory' indicates that the gradual weakening of the immune system with age increases susceptibility to infection and disease, ageing and death.

The damage/error theory can be sub-divided into five categories beginning with the 'wear and tear theory' first described by Weismann in 1882 (reviewed by Rose 1991) as the process of cellular and tissue components gradually wearing with time through their repeated use. The '(Pearl's) rate of living theory' suggests that the quicker the rate of an organism's oxygen basal metabolism, the shorter the lifespan and therefore provides initial foundations to the oxidative stress theory that is widely accepted as a major contributing factor to the overall ageing process and is considered a further hallmark of ageing. However, some argue this does not fully explain the maximum lifespan and has since been altered to take into account features including the variation of fatty acid content of cell membranes between species and some show how rapamycin (TOR) and forkhead transcription factors (FOXO) could be implicated in promoting longevity through growth and stress resistance pathways (Hulbert et al. 2007; Rollo 2010).

The rate of living theory along with the 'free radical theory' similarly, depend on the oxidative stress theory as a basis. The free radical theory specifically, includes damage to cellular components such as nucleic acids, proteins, sugars and lipids caused by superoxide and other free radicals (Harman 1956). Single- and double-strand breaks can occur through such damage and these can accumulate with age. Some natural antioxidants in the form of enzymes, exist in the body and without these, damage and cell death would be greatly increased. Experiments involving the use of antioxidant agents in rodents to prolong longevity, fuel this theory. More recently reactive oxygen species (ROS) signaling has been highlighted as an important pathway contributing to cellular senescence and overall ageing,

Taryn Morash

as an extension to the free radical theory (Afanas'ev 2010). DNA damage occurs at high frequency (>60,000 times, per mammalian cell, per day), but is rapidly repaired through a number of DNA damage repair mechanisms, dependent on the nature of the break (Bernstein et al. 2013). However, faults in these repair processes can lead to an accumulation of un-repaired regions of DNA in somatic cells, over time and can cause mutation and malfunction (Bernstein et al. 2013). In particular, damage to mitochondrial DNA can lead to mitochondrial dysfunction. It is this build-up of naturally occurring DNA damage that results in reduced genetic stability over time and is considered a major contributing characteristic of the ageing process. Furthermore, the 'cross-linking theory', introduced in 1942 by Johan Bjorksten refers to an accumulation of cross-linked proteins with time, which are believed to damage cells and is therefore an underpinning feature of the 'loss of proteostasis' hallmark of ageing commonly discussed in the anti-ageing research field (Bjorksten & Tenhu 1990).

All of the above are examples of damage occurring randomly at a molecular level and are believed to contribute to and constitute the overall effect of ageing. It is postulated that faults occurring at molecular and cellular (as well as extracellular) levels, with DNA damage accumulation and oxidative stress, among multiple others, leads to cellular senescence and therefore, impaired regeneration and cellular turnover. In turn, these effects then impact on overall tissue health and architecture, strength, mobility and other age-related symptoms that can be observed at whole organism levels. Although these molecular alterations arise randomly on a tissue-wide basis, leading to widespread ageing of the organism, the main focus tissue of the current project, skeletal muscle, provides a useful, model tissue as a basis for ageing research. Skeletal muscle regeneration is a process that occurs throughout adult life, it provides a variable to be measured during the ageing process, at all four of the main analysis 'levels', molecular, cellular (and extracellular), tissue and whole organism levels.

Taryn Morash

Sarcopenia

Sarcopenia is termed as the degenerative loss of muscle mass, quality and function with age. Numerous characteristic age-related changes have been previously observed in myogenic ageing studies, conducted at whole tissue, cellular and molecular levels. These include, among many others, myofibre atrophy, decreased muscle weight, variations in muscle diameter, motor neuron denervation, reduced contractile and force-generating capacity, increased myofibre fibrosis, a reduction in skeletal muscle satellite stem cell number and function and increased oxidative stress (Shefer et al. 2006; Collins et al. 2007; Faulkner & Brooks 1995; Alnaqeeb & Goldspink 1987; Wang et al. 2014; Chai et al. 2011). Many of these observations in ageing muscle can be explained, at least in part, by some of the previously discussed hallmarks of ageing, as the underlying mechanisms that decline and become apparently 'faulty' with age. For example, features of mitochondrial dysfunction are known to cause increased oxidative stress and reactive oxygen species (ROS) production. Additionally, decreased regenerative capacity of satellite cells with age, has been shown to be implicated at a molecular level, by loss of reversible stem cell quiescence and instead, causes inappropriate progression through the cell cycle. This in turn, leads to an imbalance in the number of progenitor cells produced and ultimately, a depletion in the number of stem cells that constitute the stem cell pool (Orford & Scadden 2008).

Sarcopenia progression measured at a tissue level, enables the examination of parameters such as myofibre numbers, cross-sectional area, proportion of regenerating myofibres, myosin heavy chain (MHC) isoform myofibre typing and general tissue architecture, which are frequently analysed to monitor the changes that occur to muscle health with age. Studies conducted in black 6 wild-type mice (C57BL/6), indicated an overall loss of muscle mass in the *Gastrocnemius* muscle (from 0.6g-0.34g) with age (from 20-25 months) (Wang et al. 2014). *Gastrocnemius* growth initially followed a similar trend to that of the recorded body weights, with an increase in weight with growth (between 2 and 11 months) until maturation. However, unlike that of the muscle mass, body weight stabilized and did not show the same decrease with old age (25 months) (Wang et al. 2014). A similar, early investigation carried out in rats, showed that EDL (*Extensor digitorum longus*), TA (*Tibialis anterior*) and *Soleus* muscle weights decreased in aged (≥22 months) animals (Alnaqeeb & Goldspink 1987). Along with myofibre atrophy, observed changes to myofibre morphology through analysis of muscle cross-sections from adult to old ages, indicated that aged myofibres changed shape, were less uniform and therefore, bordered fewer direct 'neighbour' myofibres (Wang et al. 2014).

Taryn Morash

Effect of ageing on myofibre composition and size

Skeletal muscle is known to undergo a well-defined shift of myofibre composition with age, to comprise larger proportions of those with a higher oxidative capacity, for example type I myofibres (Larsson & Edström 1986; Alnaqeeb & Goldspink 1987; Chai et al. 2011; Rowan et al. 2011). It is also reported that ageing is associated with the progressive loss of motor neurons. Fast motor neurons are preferentially lost, leading to the subsequent loss of type II myofibres. The switch to a more oxidative phenotype therefore, has been linked to denervation of faster type II myofibres and a corresponding re-innervation by surviving slow twitch motor neurons (Lexell et al. 1988; Lexell 1997; Degens 2007). This re-innervation is also believed to be the result of motor neuronal axon splitting, however, there is some evidence that this ability is hindered in advanced old age (Faulkner & Brooks 1995; Larsson & Ansved 1995; Demontis et al. 2013). Furthermore, denervation/re-innervation events have also been implicated in reduced contractile capacity and the rearrangement of myofibre types and it is proposed that type IIX myofibres are an intermediate form displayed during a slow to fast or a fast to slow shift (Larsson et al. 1991; Pette & Staron 2000; Larsson & Ansved 1995). Myofibres that do not undergo successful re-innervation following motor neuron atrophy, become atrophic themselves. Myofibre atrophy is a key determinant in the loss of muscle mass with age (Lexell et al. 1988; Rowan et al. 2012; Chai et al. 2011). Chai and colleagues reported that the characteristic increased myofibre atrophy and MHC phenotype switch to those more oxidative was more noticeable in the *Soleus* muscle of geriatric mice (29 month-old), compared to the EDL (Chai et al. 2011). However, it is argued that the myofibre type transition to a slow oxidative phenotype, is more achievable in a muscle that is defined as a slow muscle (*Soleus*), from IIA to I, compared to the faster more glycolytic EDL, step-wise from IIB to IIX to IIA (to I, rare) (Schiaffino & Reggiani 2011). Additionally, atrophic myofibres were observed to have a smaller CSA, were non-uniform in shape and myofibres exhibited centrally-located nuclei, a described hallmark of degeneration/regeneration events, in aged and geriatric muscle (Sousa-Victor et al. 2014; Barns et al. 2014).

It has been established that there is a significant degree of muscle loss experienced with advanced age, as by definition, sarcopenia encompasses a decline in muscle mass and function. Degens and colleagues investigated these features in aged rat *Plantaris* muscles and observed that mass, overall strength as a measurement of maximal tetanic force (P_0), as well as resistance to fatigue (through intermittent isometric contractions), were all significantly reduced in old age. It was concluded that both skeletal muscle mass and function were therefore diminished in old age (Degens et al. 1993; Degens & Alway 2003). Thus, Degens and colleagues, examined the capacity to which muscles elicited a hypertrophic response during old age. Denervation techniques carried out in aged rat *Plantaris* muscles, saw a similar response of compensatory hypertrophy to functional demands, in

Taryn Morash

absence of the activity of its hindlimb synergists, suggesting that this feature is not limited by age (Degens et al. 1993).

Despite an accompanying increased connective tissue content with growth, noted during the first year of life (in rats), the decline in force-generation with age, could not be attributed to changes in connective tissue content (Degens, Turek, et al. 1993). It was reasoned that denervation/re-innervation events, loss of myofibrillar proteins and structural modifications in the myosin molecule could all impact on overall contractile strength in ageing. Moreover, age-dependent mutations in the four-and-a-half LIM domain protein 1 (FHL1), located in the sarcomeric I band and focal adhesions, has been implicated in age-associated myopathy, accompanied by myofibrillar and intermyofibrillar (mitochondrial and SR) disorganisation, as well as impaired muscle oxidative, contractile and exercise capacities, increased autophagy and subsequent decreased survival rates (Domenighetti et al. 2014). Additionally, the slowing of myosin maximum shortening-velocity (V_0), has been observed *in vitro* with myosin extracted from the aged *Soleus* (rat), relative to young which therefore, impairs overall contractile potential in aged muscle (Höök et al. 1999). Furthermore, alterations in myosin structure is believed to further impair myosin head binding strength and therefore force-generation, during maximal isometric contraction (Lowe et al. 2001). Frequent degeneration and following regeneration in muscle has been shown to alter the extracellular matrix (ECM) and connective tissue architecture in both dystrophic and aged muscle (Kragstrup et al. 2011; P. A. Marshall et al. 1989). Changes in features other than collagen thickness or abundance, such as increased cross-linking of collagen, advanced glycation end-products (AGE), leads to increased myofibre stiffness and a reduction in force-generating ability (Haus et al. 2007; Lacraz et al. 2015; Kragstrup et al. 2011; Wood et al. 2014).

It has previously been suggested that increased physical activity and exercise training in aged individuals, can counteract age-related changes in morphology and function (Klitgaard, Mantoni, et al. 1990; Roman et al. 1993; Welle et al. 1996; Alway et al. 1996). Fatigue resistance increased with muscle overload (compensatory hypertrophy) in rats, at both a young and old age and tetanic force was increased in trained and hypertrophic muscles (Degens, Veerkamp, et al. 1993; Degens et al. 1993). Unlike in ageing humans however, force-generating capacity and specific tension (force generated by myofibres per unit of cross-sectional area), were not increased during muscle overload in rats of advanced age, instead these features declined (Degens & Alway 2003). Moreover, a prolonged decrease in muscle contractile activity (for example, sedentary lifestyle, bed rest, spinal cord injury, limb immobilisation), is associated with disuse-induced decreased myofibre CSA, muscle mass and force generation, as well as a shift towards a fast myofibre phenotype (Stevenson et al. 2003). Furthermore, these inactivity-associated muscle atrophy is reportedly, mediated through a decrease in protein synthesis (decreased AKT and P70S6K expression and inhibition of eIF4E) and

Taryn Morash

increased protein degradation (increase UPS, atrogin-1 and MuRF signalling) (Stevenson et al. 2003). Thus, training and physical activity carried out during adult life and extended into advanced age, remains a valid, recommended intervention in the prevention of human sarcopenia-related deterioration (Lynch et al. 2007).

Taken with what is known about the underlying mechanisms of hypertrophy and protein synthesis, it is reasoned that the alterations to the regulation underpinning the ageing process, are mimicking those associated with endurance exercise. Regulation of these mechanisms are therefore, concerned with initiating a survival response, encompassing characteristics of cellular maintenance, as a priority over growth, of which, mTOR signalling has a central role (Glass 2005; Baar 2006). Similarly, an unbalanced nutrient intake, such as during starvation, combined with increased energy requirements, promotes catabolism resulting in myofibre atrophy and loss of muscle mass (Koskelo et al. 1990; Elashry et al. 2017). Characteristics of ageing are believed to arise through features that can be described as stochastic, or alternatively, genetic in nature (Garinis et al. 2008; Niedernhofer et al. 2006). Stochastic or spontaneously-occurring events, refer to those arising as a result of exogenous biological, physical or chemical factors, or endogenous features such as, replication errors, hydrolytic reactions or reactive oxygen species (ROS), leading to an accumulation of DNA damage and overall decline (Garinis et al. 2008; Hoeijmakers 2009). The genetic element however, has been associated with the rate of decline and has been linked with the GH/IGF-1 signalling axis, for example, which is a well-defined regulatory pathway involved in maintaining the balance between cellular growth/protein synthesis and cellular death/protein degradation (Garinis et al. 2008; Niedernhofer et al. 2006; Glass 2005; Velloso 2008). Moreover, studies have utilised declining GH/IGF-1 levels to predict longevity in the human population and consequently, these mechanisms have been manipulated and utilised in numerous ageing intervention approaches, with the interest of promoting overall longevity (Dollé et al. 2006; Spindler 2005; Bartke 2005; Milman et al. 2014).

It is proposed that, endurance exercise, starvation and ageing survival responses, elicit the activation of AMPK, which is sensitive to metabolic stress and energy deprivation (low ATP). This subsequently, regulates inhibition, through tuberous sclerosis complex-1 and -2 proteins (TSC1 and TSC2), of mTOR (mTORC1) and downstream initiators (4E-BP2, eIF2 and P70S6K1) of protein synthesis (Baar 2006) (Figure 1.6). Meanwhile, low levels of GH/IGF-1 have been associated with increased longevity and therefore, corresponding downregulation of IGF-1 activity during the age-associated survival response, further limits protein synthesis (Milman et al. 2014; Bartke 2005; Niedernhofer et al. 2006; Garinis et al. 2008). Instead, this activity also results in the inhibition of downstream mTOR (mTORC2) and AKT, in turn, activating FOXO (FOXO 1 and 3), Atrogin-1 and MuRF1-mediated protein degradation, driving autophagy and the sequestering of amino acids, to be recycled for cellular

Taryn Morash

turnover (Sandri et al. 2004; Lee et al. 2004; Mammucari et al. 2007). FOXO is known to interact with sirtuin 1 (SIRT1), activating both mitochondrial transcription factor A (TFAM) and peroxisome proliferator-activated receptor-γ co-activator 1 alpha (PGC1α), among multiple other coactivators, to bring about changes in mitochondrial abundance and function, as well as driving myofibres to a more oxidative phenotype. PGC1α is a critical metabolic sensor of calcium signalling induced by motor neuron activity both by short term and chronic exercise in rodents and humans (Baar et al. 2002; Russell et al. 2003). Furthermore, transgenic expression of PGC1α initiates mitochondrial biogenesis and a switch to a more oxidative phenotype in more glycolytic muscles (Lin et al. 2002). Therefore, mitochondrial biogenesis is increased in response to exercise-induced muscle contraction (Holloszy 1967; Baar et al. 2002). SIRT1 activity is reported to enhance the transcription of antioxidant genes, including manganese superoxide dismutase (SOD2) and thus, functions in the elimination of ROS superoxide (O_2^-), produced by increased oxidative metabolism, from the electron transport chain (ETC). However, SIRT1 functions as a NAD^+-dependent histone/protein deacetylase and an age-related depletion in NAD^+ contributes to the potential limitation of SIRT1 activity in aged muscle (Fang et al. 2016). Additionally, while the upregulation of SIRT1 expression has been documented in numerous pathological situations, levels are believed to be downregulated under chronic oxidative stress conditions (Li 2014). Thus, the beneficial antioxidant activity of SIRT1 is potentially perturbed in age-related dysregulation.

Taryn Morash
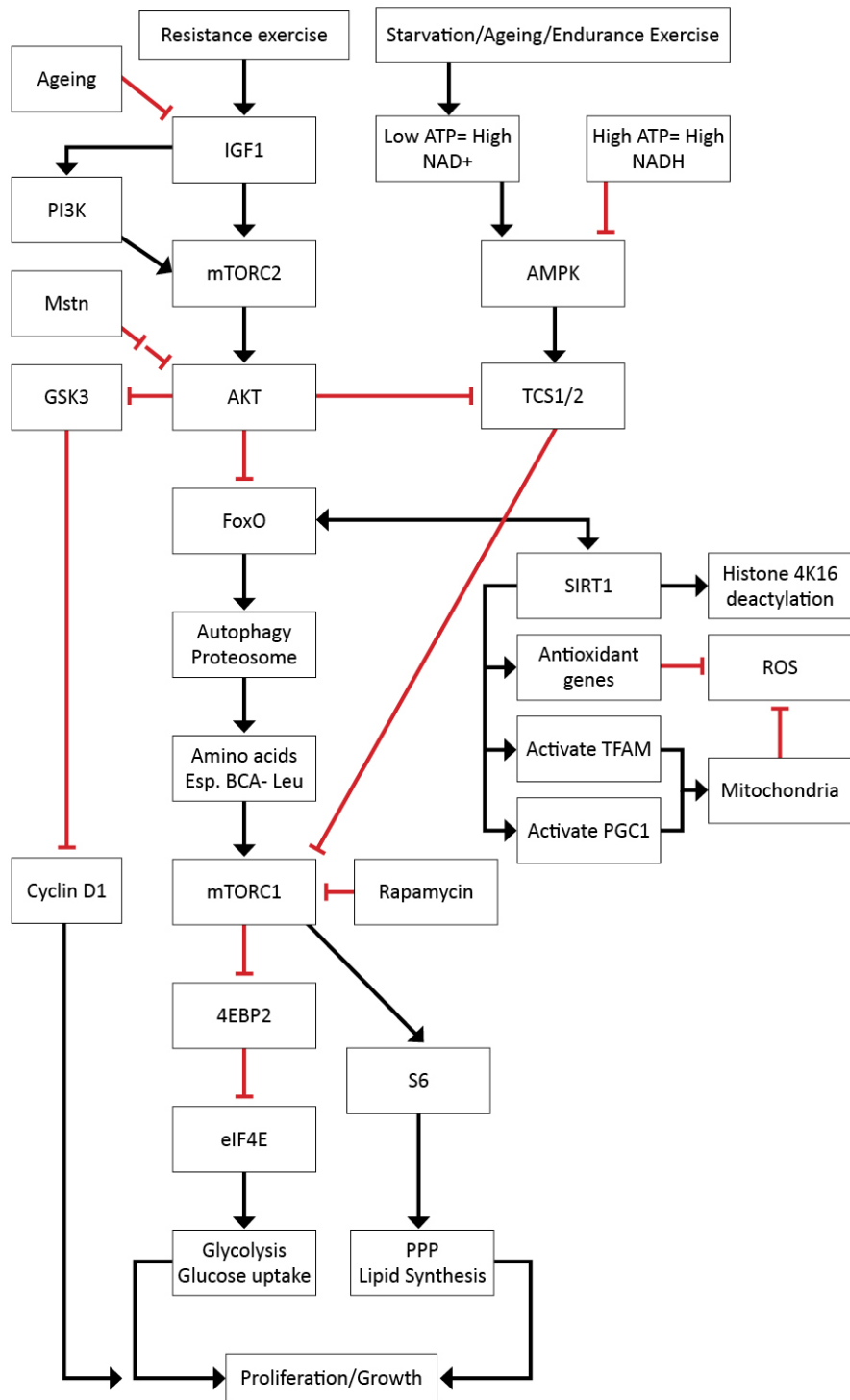
Figure 1.6 Effects of ageing, starvation and exercise on the regulatory pathways involved in protein synthesis, degradation, autophagy and mitochondrial function.

Taryn Morash

Age-related declines in satellite cell number and function

Importantly, effects of the ageing process can be observed at the cellular level during skeletal muscle regeneration, performed by the resident stem cell population, satellite cells (SC). Culture of single myofibres isolated from the murine *Extensor digitorum longus* (EDL) muscle at various ages, enables the analysis of the effects of ageing on the underlying mechanisms of SC function, on the myofibre matrix. It has been previously shown that fewer SCs are present on the myofibres isolated from aged animals compared to young and that activated cells emerged through the basal lamina of the myofibre in a delayed manner and migrated slower (Collins et al. 2007; Shefer et al. 2006; Collins-Hooper et al. 2012). These age-related declines have been attributed to changes in the myofibre niche observed with age (Shefer et al. 2006; Brack et al. 2007; Collins et al. 2007). These observations are in keeping with some of the molecular declines outlined as typical hallmarks of ageing, for example SCs experience cellular senescence and stem cell exhaustion with age, resulting in fewer cells present in the stem cell pool. Delays in activation and emergence could be due to a previously reported reduction in metabolic activity (particularly for protein synthesis and folding), of aged SCs and an increased accumulation of collagen, resulting in a more dense, thicker endomysium that the SC is required to remodel in order to emerge, respectively (Snow 1977b; Marshall et al. 1989).

Reduced SC migration speeds have been previously attributed to altered integrin expression ($\alpha6\beta1$, $\alpha7\beta1$) and as integrins are known to have a high affinity for laminins present as a component of the myofibre basal lamina, changes in integrin abundance or affinity, could lead to altered migration. Notably, however both young and old satellite cells migrate via the bleb-based, 'amoeboid' method of migration, which implies that there are fundamental differences in the bleb dynamics with age, for example, the prolonged extension and retraction times of individual blebs (Siegel et al. 2009; Collins-Hooper et al. 2012).

Alternatively, stem cells enter an irreversible G0 state of cellular senescence where proliferation is permanently ceased and thereby cells no longer retain the ability to be activated for use in a process of repair and regeneration (Cheung & Rando 2013). Cellular senescence is commonly measured in cell culture using a senescence-associated beta-galactosidase (SA-beta-gal) assay that detects a cellular senescent phenotype through histochemical staining using an artificial substrate, X-gal, first used to measure accumulation of senescent cells with age and reported by Dimri and colleagues in 1995 (Dimri et al. 1995; Itahana et al. 2007). A recent study conducted by Sousa-Victor and colleagues in young (2-3 months), adult (5-6 months), old (20-24 months) and geriatric (28-32 months - advanced aged) mice using comparative genetic profiling techniques revealed that maintenance of quiescence into old age and therefore the prolonged regenerative capability of

Taryn Morash

muscle is dependent on the active repression of senescence pathways (Sousa-Victor et al. 2014). In geriatric 'resting' (quiescent) satellite cells, the derepression of p16^{INK4a} (Cdkn2a), a cyclin 4 inhibitor and also a tumour suppressor protein that functions in checkpoint regulation of the cell cycle, causes entry of the stem cell into a senescent state (geroconversion) therefore is rendered incapable of activation for roles in repair responses. The research group carried out ectopic overexpression of p16^{INK4a} as well as silencing studies to observe the effects in young and geriatric cells, respectively. The results were that silencing p16^{INK4a} expression in aged cells caused restoration of quiescence whereas overexpression in young satellite cells prohibited their activation (Sousa-Victor et al. 2014). This study highlights the potential for regeneration that aged stem cells maintain throughout life but apparently 'lose' with altered gene expression and signalling over time. Also this was one of the first studies to use and report on changes that occur in muscle ageing and sarcopenia in an advanced aged or 'geriatric' animals and that perhaps research using 'young', 'adult' and 'old' animals are in fact, using animals where 'old' (<28 months of age), is not old enough and therefore, the vast changes in tissues reported during advanced ageing are not being exhibited and thoroughly explored.

Conboy and colleagues have conducted a series of investigations over recent years and together these studies evaluate the effects of intrinsic signalling and extrinsic factors on stem cell function with age. With relevance to skeletal muscle, Conboy et al. demonstrated the importance of the Notch signalling pathway in satellite cell activation, proliferation and ultimately the initiation of regenerative processes (Conboy & Rando 2002). Although, they showed that artificial activation of the Notch signalling pathway can in turn, restore the activation of aged satellite cells and enhance regenerative capability. These results suggest that the intrinsic regenerative potential is retained in aged satellite cells and that it is the declining extrinsic factors/conditions of the aged microenvironment causing the symptoms of sarcopenia and reduced repair (Conboy et al. 2003; Conboy et al. 2005).

Studies carried out in rats showed that advanced aged muscle, once grafted into young hosts, is regenerated to an equal degree as that in auto-transplanted control animals however when young muscle is grafted into old hosts, regeneration is significantly impaired (Carlson & Faulkner 1989; Carlson et al. 2001). Conboy and colleagues used these findings to form a hypothesis to explore the apparently different array of systemic factors between young and old animals causing these differences in repair capability. They developed a series of heterochronic parabiosis experiments where pairings between young (2-3 months) and old (19-26 months) mice are made, whereby two animals share a circulatory system and therefore, factors present in the young animal are exposed to the old animal and *vice versa*. This provides an alternative experimental procedure, contrasting to tissue transplanting and grafting. Isochronic parabiosis pairings were also generated to use as control

Taryn Morash

systems. Five days post-injury, hindlimb muscles were examined using both haemotoxylin and eosin (H&E) histological staining, as well as immunohistological protocols to study the degree of myofibre regeneration and repair in all parabiosis conditions. This resulted in young conditions (both isochronic and heterochronic parabioses) repairing well however, the isochronic pairing of old animals repaired poorly in comparison, a well-established characteristic of aged muscle tissue.

The repair of the heterochronic parabiosis in old partners conversely, improved regeneration to the level of the young muscle therefore, indicating the defective regenerative potential of aged satellite stem cells can be restored by the systemic factors produced and circulating in serum from a young mouse, either increasing upregulatory factors or reducing inhibitory regulators, or a combination of the two. The authors also comment on these effects being caused by the systemic factors produced and circulating in the young serum, rather than the grafting of young satellite cells into the old animals, having a reparative impact. This was tested in that the young partners were GFP[+] (expressing green fluorescent protein) and on analysis, it was observed that less than 0.1% of repaired myotubes in the aged partner were GFP[+]. Conboy and colleagues suggested that this impaired regeneration in aged muscle could be reversed by appropriate activation of the Notch signaling pathway, previously reported to become defective with age, in particular the upregulation of Notch ligand, Delta. Induction of Delta was reduced in the isochronic aged animals however, the heterochronic parabiosis resulted in activation of Notch through Delta, in aged animals comparable to levels of the young animals. Together these results conclude that the systemic regulatory factors produced in young animals, are able to restore the defective regenerative potential of aged animals, through processes that both increase satellite cell proliferation as well as function (Conboy et al. 2005).

Interestingly, other research groups have also seen rejuvenating effects through the youthful systemic interactions created through the use of heterochronic parabiosis experimental set-ups (Murphy & Thuret 2015). For example, in cardiac ageing studies, a factor that is frequently linked to heart failure is cardiac hypertrophy. Using an old/young parabiosis pairing, regression of the cardiac hypertrophy in old animals was observed and it was concluded that the TGF-β (transforming growth factor beta) superfamily member, GDF11 (growth differentiation factor 11), identified as a circulating factor in the young animals, declined with age (Loffredo et al. 2013). Furthermore, restoring the GDF11 levels in old animals, back to those measured in young animals, echoed the results seen in the parabiosis and reversed the atrophy associated with ageing. Similarly, Sinha and colleagues used parabiosis pairings with young animals and observed improved satellite cell function in aged mice, also implicating the decline in circulating protein GDF11 in old animals, as supplementation with youthful levels of GDF11 had the same beneficial effect (Sinha et al. 2014). However, GDF8

Taryn Morash

(Myostatin), also a TGF-β family member, is highly homologous with GDF11 and a recent study has pointed out a large amount of antibody cross-reaction between GDF11 and Myostatin in previous research (Egerman et al. 2015). Subsequently, this has resulted in controversy and a large amount of disparity in the field regarding the identity of the blood-borne rejuvenation factor (Garber 2016).

Effects of ageing on the skeletal muscle extracellular matrix

The myofibre ECM is known to be comprised of numerous components, such as collagen IV, laminins, fibronectin and glycoproteins, that function critically, in the force transmission and providing structure to the muscle, as well as the anchorage of cells to the basal lamina and cell to ECM communication (Sanes 2003). Structural, biochemical, cellular and functional alterations in the skeletal muscle ECM, contribute to the declines in mechanical characteristics in ageing.

One of the main structural changes known to occur in skeletal muscle with age, is an observed increased collagen content. Studies conducted in both humans and rodents overall, have shown increases in collagen thickness and content with age, at a histological level through examining muscle cross-sections (Kragstrup et al. 2011; Marshall et al. 1989; Alnaqeeb et al. 1984). Furthermore, animal studies indicated that enzymatically facilitated collagen cross-linking increased with age and that physical exercise was observed to reduce cross-link accumulation in aged animals (Zimmerman et al. 1993; Gosselin et al. 1998). In contrast, ageing studies investigating the properties of intramuscular endomysial collagen in human muscle biopsies (from *Vastus lateralis*), indicated that, although there was no significant change in collagen cross-linking levels with age, the advanced glycation end-product (AGE), pentosidine was increased by approximately 200% (Haus et al. 2007; Takahashi et al. 1995). Pentosidine, a derivative of ribose, forms fluorescent cross-links in collagen and could potentially, therefore, disrupt skeletal muscle contractibility, contributed by the 'stiffening' of tissues associated with ageing (Sell & Monnier 1989).

An infiltration of adipocytes into the intermuscular compartments between muscle fascicles is another observation noted in both sarcopenia, as well as some metabolic diseases, such as type 2 diabetes and familial partial lipodystrophy (Dunnigan variety) (Vettor et al. 2009; Garg et al. 1999; Gallagher et al. 2009). Vettor and colleagues through a series of *in vitro* experiments, hypothesised that the adipogenic potential of SCs could account for the presence of adipocytes within skeletal muscle and that an understanding of the molecular signalling pathways underlying the muscle to fat conversion could aid in explaining the increase noted in sarcopenia (Vettor et al. 2009).

Additionally, cellular changes encompass characteristically altered mechanotransduction, reduced SC activation and therefore, perturbed regeneration, among others. Changes to the ECM that impact on

Taryn Morash

cellular function are associated with impaired cell to cell, or cell to ECM communication and perturbed external to internal signal transduction. For example, the focal adhesion kinase (FAK) pathway is known to interact with integrins and transduce intracellular signalling cascades in order to direct alterations in motility via cytoskeletal actin organisation (Mehlen & Puisieux 2006). Additionally, load-induced FAK mechanotransduction activity has been shown to be altered in the aged smooth muscle of the rat aorta, where FAK content and basal phosphorylation were reduced (Rice et al. 2007). Moreover, aged Achilles tendon fibroblasts were shown to have reduced motility and proliferation, as well as poor actin organisation and these altered cell to ECM interactions could be largely attributed to changes in focal adhesion protein localisation (Arnesen & Lawson 2006). These findings, although evident in studies focusing on smooth muscle and connective tissue, could indicate similar dysregulation associated with ageing skeletal muscle. Taken with the reduction in integrin expression in SCs also known to occur with age, could indicate that key pathways involved in mechanosensing, ECM interaction and intracellular regulation of cell migration, among other mechanisms, are compromised with age (Collins-Hooper et al. 2012; Siegel et al. 2009; Mayer 2003).

Naturally-aged skeletal muscle profiling and the requirement for a suitable mammalian model

Although the wild-type C57Bl/6 muscle analysis will allow for a natural-aged 'muscle profile' to be generated, there is an established requirement for an alternative *in vivo* experimental set-up, to fully investigate the progression or accumulation of damage with advancing age and this has become more evident in recent years. Currently, there are limitations to waiting the ~2.5 years to naturally age mice, the heterochronic parabiosis systems (such as mortality risks, technical difficulties regarding the maintenance of parabiont pairings over long periods of time), or young-to-old, old-to-young transplantation techniques (Conboy et al. 2013; Dollé et al. 2011). A review by Demontis and colleagues, discusses both extrinsic and intrinsic factors/defects that occur in muscle during aging, including changes in physical exercise and hormone levels in aged animals as well as alterations in neuromuscular junctions and denervation. Importantly however, the review uses the *Drosophila* 'fruit fly' as a particular focus model and the authors indicate the need for more in-depth studies of sarcopenia, in a more suitable model for ageing (Demontis et al. 2013). Demontis highlighted that fruit fly muscles are small and difficult to compare to sarcopenia in mammals. It was suggested that this is due to differences in the rate of muscle degeneration, attributed to the lack of satellite stem cells in members of the *Drosophilidae* family. The author also states that mice however, are expensive to keep for their greater life-span (2-3 years) and therefore, are not economically viable or practical for more long-term geriatric animal studies (Demontis et al. 2013).

Taryn Morash

The *Ercc1* murine model of progeria

The development of a progeroid animal model which undergoes advanced ageing, living its entire lifespan in a shortened period of time, thus allows for the analysis of the changes that occur with age on a tissue-wide basis, at a more efficient rate. Although with any progeria model developed for this purpose, it would become of high importance to determine if such a model is suitable in mimicking changes associated with natural ageing. Therefore, investigation into the advancement of age-related symptoms, relative to the rate typically noted in natural ageing, would allow for the most accurate comparisons to be drawn during experimentation.

The *Ercc1* knockout murine progeroid model is suggested to effectively mimic alterations occurring in the natural ageing process (Weeda et al. 1997; Dollé et al. 2011). The model is a genetic knockout of the *Ercc1* (*Excision repair cross complementation group 1)* gene encoding the *Ercc1* protein that functions alongside its essential binding partner, *XPF* (*Xeroderma pigmentosum group F*), which together, form an endonuclease complex that participates in excision DNA repair mechanisms.

DNA damage can occur through endogenous cellular processes including DNA replication errors or reactive oxygen species (ROS) or caused by exogenous physical, biological or chemical agents (Hoeijmakers 2009). Naturally occurring DNA damage arises more than 60,000 times per mammalian cell per day (Bernstein et al. 2013). There are a number of different DNA repair mechanisms that have evolved and are implemented, dependent on the nature of the damage, to cope with the majority of these errors including both single-stranded and double-stranded breaks (Lord & Ashworth 2012). A form of single-stranded repair, nucleotide excision repair (NER), is the process implicated in the *Ercc1* mutant, which causes the advanced ageing and shortened lifespan. This is due to the increased, rapid accumulation of DNA damage that has been previously associated with the onset of age-related symptoms and progeroid disorders and is frequently considered a major contributing factor to genomic instability, a characteristic hallmark of ageing (Burtner & Kennedy 2010). The mutated mouse model shares the characteristic NER-deficiency with human progeria syndromes, xeroderma pigmentosum (XP), Cockayne syndrome (CS) and trichothiodystrophy (Dollé et al. 2011). Melton, McWhir and colleagues previously reported liver abnormalities, irregular growth, reduced lifespan and a high mortality rate prior to weaning age (~3 weeks) in a severe *Ercc1* mutant murine model in 1993 (McWhir et al. 1993; Weeda et al. 1997). Hoeijmakers and colleagues describe two *Ercc1* mouse mutants created through specific *Ercc1* gene disruptions by a neomycin marker and restriction site insertions, one is the complete 'knockout', '*Ercc1*$^{-/-}$' (disrupting exon 7), whereas the second is a seven amino-acid carboxy-terminal truncation at the C-terminus of the wild-type *Ercc1* protein, hybrid genotype with the null, which results in a 'knocked down', '*Ercc1 delta* (d/-

Taryn Morash

)' mutation (disrupted exon 10), expressing 10% of the normal level of ERCC1-XPF. The *Ercc1* knockout is therefore the more severe progeroid form with a maximal lifespan reported at ~30 days while the *Ercc1$^{d/-}$* mutation lives to ~30 weeks.

The *ERCC1* model is not the only murine model of advanced age that is currently being explored in the ageing research field. The Hutchinson-Gilford progeria syndrome Zmpste24-deficient mouse (Zmpste24$^{-/-}$) is a model for impaired DNA repair and accelerated cell senescence. Animals typically show symptoms such as slow growth, abnormal gait, kyphosis, alopecia, osteoporosis and bone abnormalities, causing bones to be prone to breakage (Butala et al. 2012; Liu et al. 2013; Young et al. 2005). As this progeroid model is that of early senescence, it could be used experimentally, to answer specific questions regarding the accumulation, clearance and prevention of senescent cells with age. Although the Zmpste24$^{-/-}$ model exhibits overall age-associated symptoms, it is believed that the *Ercc1* mouse can be utilized in the current research project, to aid in answering a broader, more extensive range of hypotheses relating to more tissue types, but particularly, detailing changes that occur in sarcopenia (Young et al. 2005; Dollé et al. 2011). For example, more recently, the *Ercc1$^{d/-}$* mutation was reported to show reduced lifespan and survival as well as whole body and organ weight declines with advanced age (Dollé et al. 2011). The weights recorded for six organs including the heart, liver, brain, spleen, kidney and thymus, showed overall declining trends in weight and it was concluded, that the *Ercc1$^{d/-}$* model exemplifies a 'segmental progeroid phenotype' and this refers to the extent and severity of reported age-related symptoms that were shown to vary between particular organs and tissues (Dollé et al. 2011).

Effect of ageing/progeria on mitochondrial function and oxidative stress

Nuclear DNA repair proteins have been linked to regulation of mitochondrial homeostasis. Coordination of this process is reportedly controlled by nuclear transcription regulators, such as p53, peroxisome proliferator-activated receptor-γ co-activator 1α (PGC1α), hypoxia inducible factor 1α (HIF1α), the fork-head box O (FOXO) and sirtuin members (SIRT1, SIRT6 and SIRT7) and NAD$^+$ availability, as NAD$^+$ is depleted in ageing. SIRT1 activity is NAD$^+$-dependant and among other roles, deacetylates PGC1α, a key positive regulator of mitochondrial biogenesis. Additionally, another NAD$^+$-dependant process implicated in the detection of DNA damage is PARylation, whereby poly(ADP-ribose) polymerase 1 (PARP1), a DNA break sensor, generates PAR in order to initiate signalling involved in the recruitment of PAR-binding DNA repair proteins (Gibson & Kraus 2012; Fang et al. 2016). Imbalances in SIRT1 and PARP1 activity have been linked with ageing and other pathologies and further implicated in Xeroderma pigmentosum (XPA) and Cockayne's syndromes (mutations in genes that encode CSA or CSB proteins) of premature ageing (Mouchiroud et al. 2013;

Taryn Morash

Scheibye-Knudsen et al. 2014; Gibson & Kraus 2012). Studies investigating XPA or CSB patients and cells, showed evidence of altered mitochondrial metabolism and accumulation of damaged mitochondria. The findings of these studies observed reduced SIRT1 activity, attributed to constitutive PARP1 DNA damage detection and this was reversed with inhibition of PARP1 or NAD^{+} precursor supplementation which balanced SIRT1 activity and mitochondrial homeostasis (Fang et al. 2014; Fang et al. 2016; Scheibye-Knudsen et al. 2014).

Early work carried out examining the severity of the full knockout variant of the *ERCC1*-deficiency, revealed the postulated role of p53 as a monitor of DNA damage (McWhir et al. 1993). McWhir and colleagues surmised that tissues under increased levels of oxidative stress, such as the highly metabolically active liver, brain and kidney showed raised levels of p53 (McWhir et al. 1993). Moreover, the brain is believed to be more prone to oxidative injury, due to relatively deficient alternative antioxidant mechanisms (little catalase, glutathione peroxidase, glutathione and vitamin E), compared to other tissues such as the liver (Olanow 1992). Therefore, this is consistent with greater p53 levels occurring in tissues of increased oxidative stress (McWhir et al. 1993). Additionally, Borgesius and colleagues showed increased levels of p53 and caspase-3 in cortical cells of *Ercc1* mutant mice and that the neuronal DNA damage shared characteristics of brain pathology with normal ageing (Borgesius et al. 2011). Tumour suppressor *p53*, also known a master transcriptional regulator, interacts with numerous effector genes involved in a variety of major cellular pathways, including among others, cell cycle progression, apoptosis, autophagy, as well as ROS defence and DNA repair mechanisms (Millau et al. 2009). Thus, p53 activity is implicated in at least two distinct modes of action in roles combating increased levels of oxidative stress, firstly, monitoring the increase and secondly, modulating SOD2 antioxidant activity (Hussain et al. 2004). Furthermore, Feng and colleagues defined the cross-talk between the p53 and mTOR pathways, demonstrating p53 regulation of mTOR activity, including the downstream targets, such as components of autophagy, through activation of AMPK and the TSC1/TSC2 complex (Feng et al. 2005). Upon detection of DNA damage or following genotoxic stress, p53 is activated, initiating starvation/energy depletion-like responses, inhibiting mTOR, protein translation and ribosome biogenesis is halted and autophagy is induced (Feng et al. 2005). Therefore, p53/mTOR activity is shown to be a key regulator in the shift from cell proliferation and growth, to a survival response for cellular maintenance, as well as the response to increased oxidative stress and ROS levels.

Ercc1$^{d/-}$ and skeletal muscle

A handful of studies have so far started investigations into the age-related changes that occur in the *Ercc1*$^{-/-}$ knockout and *Ercc1*$^{d/-}$ mutation, however it is currently believed that there has so far, been

Taryn Morash

only one study published related to the focus tissue of the current research project, skeletal muscle. This landmark study was conducted by Lavasani, Huard and colleagues and aimed to investigate the role of stem cell function in age and therefore decreased regenerative capacity, as a hallmark of ageing, using muscle-derived stem/progenitor cells (MDSPCs) (Lavasani et al. 2012). The MDSPC populations were isolated from the following test groups: young (3 weeks) and old wild-type mice (2 years), progeroid $Ercc1^{-/-}$ (2-3 weeks) and $Ercc1^{d/-}$ (5 months), as well as age-matched wild-type littermates and $Xpa^{-/-}$ (xeroderma pigmentosum complementation group A) mice (3 weeks), that present faulty NER, but do not experience the shortened lifespan that the $Ercc1$-deficient mice do, as controls and these were examined *in vitro*. Results showed among others, a significantly reduced proliferation rate, MDSPC number and prolonged population doubling times in both the old and progeroid MDSPCs. The differentiation capacity was also shown to be compromised in aged and progeroid cells, through the formation of significantly fewer and smaller myotubes. This was confirmed by a reduced expression of myogenic differentiation markers MHC, desmin and myogenin, as well as decreased osteogenic and chondrogenic differentiation potential, compared to that of young wild-type MDSPCs (Lavasani et al. 2012). To investigate whether this transplantation of young MDSPCs would affect the onset of age-related symptoms such as dystonia, ataxia and loss of vision in ageing animals, the delta 'knocked down' variant of the progeroid model ($Ercc1^{d/-}$) was used, in order to be able to allow time for these symptoms to occur, as these are not singularly discernible in the ~30 days lifespan of the full knockout $Ercc1^{-/-}$ mice (Lavasani et al. 2012). The age of onset (weeks) of symptoms including sarcopenia, incontinence, trembling, ataxia, lethargy, kyphosis and dystonia was recorded and an ageing score was determined as the fraction of symptoms delayed between the young MDSPC treatment and PBS injection controls (Lavasani et al. 2012). This indicates the young MDSPCs delayed the onset of age-associated symptoms and therefore, highlights the causal role of impaired stem cell function on the overall global degeneration that occurs with ageing. Furthermore, using a MDSPC co-culture transwell system, Lavasani *et al*. concluded that the beneficial effects the young MDSPCs in $Ercc1^{d/-}$ animals, could be attributed to paracrine 'secreted factors' released from these cells impacting on the implicated host cells, as engraftment and subsequent population expansion of the transplanted cells was limited (Lavasani et al. 2012). This observation holds great significance considering the large volume of work currently being carried out into the release of paracrine factors, microvesicle (MV) particles and the overall effects of a cell's 'secretome' on a neighbouring cell or tissue. Future experimentation utilizing the $Ercc1$ progeroid mouse in the current research project, will explore the potential 'anti-ageing' effects of MV (stem cell-derived conditioned media) treatment in the onset and progression of sarcopenia.

Taryn Morash

The secretome, microvesicles and conditioned media

Microvesicles (MVs) are fragments of plasma membrane that are secreted into the extracellular space from cells either by exocytosis from the endosome compartment, or direct budding and shedding of the surface membrane (Le Bihan et al. 2012). It is now widely believed that MVs are implicated in roles of cell-cell communication, bringing about receptor-mediated alterations to neighbouring cells or the delivery of biochemical molecules as cargo that goes on to be used by receiving cells (Camussi et al. 2010). Vesicles were first reported in 1983 by Pan and Johnstone whilst they examined sheep reticulocyte maturation and since, there has been a large amount of research carried out into the different types of vesicle secreted from cells as part of their paracrine signalling processes (Pan & Johnstone 1983). Many studies refer to these vesicles differently and categorize them based on a variety of biochemical properties and this has led to a large degree of confusion in the literature when referring to the type of vesicle. For example, different nomencultures used to name secreted vesicles have included exosomes, shedding microvesicles, nanoparticles, microparticles, ectosomes, apoptotic blebs, exosome-like vesicles and others (Mathivanan et al. 2010). It has been discussed recently how the classification of types of vesicle requires specification however, Camussi *et al.* use the broader term microvesicles which is then sub-categorized into exosomes and shedding vesicles (Camussi et al. 2010).

Exosomes are membranous vesicles of endosome origin, ranging in size typically from 30-120nm. They are stored as large multivesiclar bodies of the late exosome and fuse with the plasma membrane for release (exocytosis). Shedding microvesicles are larger than exosomes ranging from 100nm to 1μm and form through the budding of the plasma membrane and cytoplasmic protrusions and contents can vary greatly, due to the encompassing of membrane-bound receptors and other proteins, mRNA, miRNA and lipids, as well as the engulfing of cytoplasmic components as buds are formed (Camussi et al. 2010). Mathivanan and colleagues also agree that shedding microvesicles are larger than exosomes and also categorize apoptotic blebs (plasma membrane bodies released from apoptotic or dying cells), as vesicles to be considered separately when using 'microvesicles' or 'exosomes' as a broad term (Mathivanan et al. 2010).

In a vast proteomics analysis study conducted by Le Bihan and colleagues, the exosome and shedding vesicle (microparticle) subtypes were isolated from the conditioned media collected from culturing a primary human skeletal muscle satellite cell line (Le Bihan et al. 2012). The analysis revealed that shedding vesicles contained proteins associated within the endoplasmic reticulum (ER), mitochondria, Golgi, cytoskeleton and cytosol. Proteins identified included, among others, ER resident proteins CALU and HSPA5, actin and tubulins (ACTB and TUBA1B) ribosomal subunits (RPL4

Taryn Morash

and RPL10) and poly(A) binding protein (PABPC1). Contrastingly, exosomes contained proteins from the plasma membrane, such as integrins (ITGA4, ITGA6 and ITGA7), tetraspanins (CD9, CD81 and CD82) as well as those from the sub-plasma membrane (flotillin-1), endosomes (PDCD6IP) and lysosomes (CD63 and LAMP2) (Le Bihan et al. 2012).

Most cell types secrete MVs and their roles in cell-cell interactions and how they function remain poorly understood. Multiple studies have shown that MVs are released from a variety of cell types, with their ability to interact with many different receptor targets (Le Bihan et al. 2012; Pawitan 2014; Kim et al. 2014). As well as this, their apparent 'non-specific' uptake by many other nearby cells, could indicate a beneficial method of biochemical molecule/ component delivery and overall therapy (Camussi et al. 2010). For example, studies examining MVs released from a platelet, leukocyte or endothelial origin may contain different pro-inflammatory and anti-inflammatory factors and circulate in the blood, highlighting a potential therapeutic strategy to treat atherosclerosis (Ardoin et al. 2007). Furthermore, reports have analysed the array of 'secretome' cytokines and growth factors, released from stem cells and the postulated uptake and subsequent horizontal transfer of protein and RNA cargo, results in the translation into functional proteins (Kim et al. 2010; Kinnaird et al. 2004; Le Bihan et al. 2012; Pawitan 2014). Vascular endothelial growth factor (VEGF), fibroblast growth factor-2 (FGF-2) and Interleukin 6 (Il-6) were just three of the identified cytokines to be released from cultured human bone marrow stromal cells (mesenchymal stem cells), in a study focused on a murine hindlimb ischaemia model (Kinnaird et al. 2004). Interestingly, local injection of the conditioned media collected from these human bone marrow mesenchymal cells (BMSC), resulted in improved limb function, reduced tissue damage and atrophy (Kinnaird et al. 2004). Similarly, Cantinieaux and colleagues observed improved motor recovery with BMSC CM following induced spinal cord injuries in rats (Cantinieaux et al. 2013). Mellows and colleagues have recently examined the therapeutic potential of CM, generated under stress conditions and free from all other exogenous molecules, from amniotic fluid-derived stem cells (AFS) (Mellows et al. 2017). It was demonstrated that the AFS secretome promoted stem cell proliferation, migration, as well as protection against cellular senescence, in an acute model of skeletal muscle injury using cardiotoxin (CTX). The biological molecules identified were shown to influence the regulation of a wide-range of cellular processes, such as cell cycle progression, cell to cell communication, cytoskeletal organisation, cell motility, adherence and division, among numerous others. Although isolating the EV fraction from the whole conditioned media content for separate treatment saw major beneficial regenerative effects from both fractions, EVs were shown to harbour a large majority, but not all of the therapeutic regulatory content. Therefore, AFS conditioned media was reported to maintain numerous key regulatory properties, specific to each fraction. As well as this, importantly, it was

Taryn Morash

established that conditioned media treatment facilitates effective tissue regeneration, through the modification of existing, instead of the development of new, signalling mechanisms in the host. This was evident from a large proportion of the EV content comprising miRNA and not mRNA (Mellows et al. 2017). These are just a selection of recent studies that have reported beneficial effects with the use of stem cell-generated conditioned media and the secreted paracrine factor contents, in a variety of tissue models of injury and disease. However, on-going research into the exact properties and mechanisms by which conditioned media, paracrine-driven cell-cell interaction brings about the reparative effects observed, remains an area still poorly understood. Although, the most recent breakthroughs, regarding the numerous cellular processes targeted by conditioned media contents, are beginning to clarify some of the specific regulatory mechanisms involved.

ADMSCs were the chosen cell type in the current study, for CM generation, this is due to a wealth of promising data, reporting amelioration of pathologies, resulting from a wide variety of injury and disease models, either using ADMSCs in whole cell-based or CM approaches. For example, similarly, to BMSC CM regenerative effects, ADMSC CM has been shown to contain pro-angiogenic and anti-apoptotic growth factors, such as VEGF, FGF-2 and HGF which resulted in enhanced blood vessel density, blood perfusion and limb salvage in a mouse hindlimb ischaemia model (Bhang et al. 2014). Furthermore, the role of ADMSC CM in dermal wound healing, found that paracrine factors up-regulated human dermal fibroblast synthesis of ECM proteins, type I and II collagens and fibronectin (Kim et al. 2007). Importantly, it was shown that CM generated from bone marrow-derived mesenchymal stem cells (BMSC) under hypoxic conditions, showed overall increased secretion of HGF and VEGF which improved neurogenesis, motor function and cognition, following a traumatic brain injury in rats (Chang et al. 2013). As opposed to the isolation of MSCs isolated from the bone marrow, dental pulp, umbilical cord or amniotic fluid, ADMSCs are comparatively more easily extracted and minimally invasive, for culture for example, via liposuction. Moreover, previous collaborators have developed a clinically-compliant procedure for the isolation and expansion of CM from autologous ADMSCs. CM is reported to be a safer form of cell-free therapy, without the risks associated with raising an immune response, or the development of neoplasia and other inappropriate differentiation events. These collaborators are currently utilising these methods to treat numerous pathologies and disease, as well as to enhance tissue regeneration following injury or cosmetically, in patients, globally.

Taryn Morash

Importance of tissue microenvironment matrix components and substrate elasticity

Recent studies have aimed to explore the effect of tissue microenvironments and in particular, the rigidity or elasticity of the matrix substrate, on lineage specification of stem cells. In 2006, a study conducted by Engler and colleagues altered the stem cell research field and the way in which the cellular differentiation process is now considered (Engler et al. 2006). It was shown that by mimicking the rigidity of an *in vivo* extracellular matrix (ECM) of a specific tissue in experiments performed *in vitro,* naïve mesenchymal stem cells (MSCs) could be directed towards specific tissue lineages. This was investigated through varying the concentration of bis-acrylamide cross-linking in polyacrylamide gels coated with collagen I to support cellular adhesion and culturing MSC populations on these gels of varying stiffness. For example, the softer matrices, measured using the Young's (elastic) modulus (0.1-1 kPa), best mimic the stiffness of the brain microenvironment and resulted in the MSC specification towards a neurogenic pathway, indicated by cells adopting associated morphologies as well as RNA microarray analysis revealing increased expression of neurogenic markers of mature neurons, such as neurofilament light chain (NFL) and NCAM, signified to play important roles in neural development (Lariviere & Julien 2004; Rutishauser 1984). More rigid substrates (11 kPa) however, that are physiologically relevant to muscle matrix rigidity, indicated increased upregulation of a range of early to late myogenic markers including transcription factors (TF) Pax 3 and 7, MyoD and myogenin and therefore illustrates programming towards the muscle lineage. Matrices engineered to mimic the microenvironment rigidity of collagenous bone (34 kPa), showed greater expression of osteogenic regulators including a TF associated with early osteoblast differentiation, CBFα1 (RUNX2) and osteocalcin a vitamin K-dependent calcium-binding protein vital for bone formation (Gilbert et al. 2002; Hauschka 1986).

Understanding how the ECM impacts on the processes of stem cell differentiation and lineage programming, will provide more appropriate approaches and increase the overall success of stem cell therapy techniques, with particular relevance to tissue regeneration post-injury, in disease as well as with ageing. Use of more physiologically relevant culture matrices (with adjusted rigidity, matrix thickness etc.) for *in vitro* studies, compared to the widely used 'un-natural' tissue culture plastic-based conditions, will provide more appropriate conditions to draw overall more accurate conclusions regarding cell migration, differentiation and behaviour *in vivo*. Another research group for example, investigated the influence of matrix stiffness, mimicking both healthy cardiac muscle compared to damaged tissue post-myocardial infarction (MI), on the specification of transplanted MSCs (Sullivan et al. 2014). In the field of tissue-engineering for example, whereby organic, in-organic or synthetic materials are utilized in *in vivo* or *ex vivo* biological tissue scaffolds or constructs,

Taryn Morash

as a method of aiding tissue transplants and restoring function after injury or disease (Caplan 2007; Jenkins et al. 2003; Totonelli et al. 2012). As such, tissue-engineering is now considered a branch of regenerative medicine (Jenkins et al. 2003). A study conducted in 2012, used a process of detergent-enzymatic decellularisation of rat small intestine, to form a connective tissue scaffold, to act as a matrix to encourage cell re-population after transplantation (Totonelli et al. 2012). Importantly, in addition to providing a great scope for exploration in the wider regenerative medicine research field, the findings of the Engler *et al.* study informs and provides a basis for the experimentation conducted in the current research project.

Taryn Morash

Hypotheses, aims and objectives

Project aim

The main aim of the current research project is to assess the potential therapeutic effects of stem cell-derived conditioned media, on age-related deterioration, associated with the onset and progression of sarcopenia, in skeletal muscle.

Hypothesis 1

Conditioned media generated from adipose-derived mesenchymal stem cells, harbours regulatory properties that attenuate, or even prevent characteristic age-associated changes in skeletal muscle composition and function.

Objectives

1. To develop a broad skeletal muscle profile in naturally-aged C57BL/6 mice, examining characteristics of sarcopenia measured at molecular, cellular, tissue and whole organism levels.

   Although characteristics of age-related decline in skeletal muscle, associated with the onset and progression of sarcopenia, have been studied extensively in numerous muscle types and across species, I aimed to analyse key physiological, histochemical, morphometric and biochemical characteristics of the *Soleus* and *Extensor digitorum longus* (EDL) hindlimb muscles, of young (3 months), adult (6 months), old (24 months) and geriatric (27-30 months) mice, in order to examine how muscle structure and function alter with age. Features examined included, among others, muscle mass, myofibre number, myosin heavy chain myofibre type composition, myofibre cross-sectional area, oxidative capacity, superoxide reactive oxygen species production, as well as capillary density and collagen thickness.

2. To isolate the secretome from adipose-derived mesenchymal stem cells, under stressed culture conditions.

   Although numerous studies have shown the beneficial effects of stem/progenitor cell transplantation in models of skeletal muscle injury and disease, these approaches typically result in poor migration and engraftment of injected cells, suggesting that it is the secreted factors originating from the donor cells that bring about observed regenerative effects (Partridge 2000; LaFramboise et al. 2003; Lavasani et al. 2012). Therefore, I have generated

70

Taryn Morash

conditioned media (CM) from adipose-derived mesenchymal stem cells (ADMSC) under stressed culture conditions, tested in its protective effect against H_2O_2 stress-induced cellular senescence *in vitro*.

3. To utilise the naturally-aged skeletal muscle profile to provide a basis for examining the therapeutic effects of stem cell-derived conditioned media.

   Studies have established that the secretome released in young serum, as well as that from cultured stem/progenitor cells had rejuvenating effects in the skeletal muscle of aged and progeric mice (Conboy et al. 2005; Lavasani et al. 2012). Thus, the *Soleus* and EDL muscles were analysed, using the series of molecular, cellular, tissue and whole organism parameters utilised previously, to examine the paracrine effects in naturally-aged (20 month-old) C57BL/6 mice treated with ADMSC CM.

Hypothesis 2

Conditioned media generated from adipose-derived mesenchymal stem cells, provides therapeutic effects that attenuate features of skeletal muscle composition and function, in the novel use of an $Ercc1^{d/-}$ mutant murine model of progeria.

Objectives

1. To characterise the skeletal muscle phenotype in the *Soleus* muscle of the $Ercc1^{d/-}$ model of progeria.

   Although a large proportion of ageing studies utilise laboratory rodents in order to examine the changes that occur in sarcopenia, there is an increasing requirement for a suitable mammalian model of accelerated ageing to maximise time and economic efficiency of data delivery in ageing intervention research (Demontis et al. 2013). Studies have established that the $Ercc1^{d/-}$ model displays systemic age-associated degeneration, exhibits hallmark features of ageing, including increased oxidative stress and cellular senescence and histopathological characteristics have been extensively studies in the liver, kidney and spinal cord (Dollé et al. 2006; McWhir et al. 1993; De Waard et al. 2010). Therefore, using the series of parameters used to develop the naturally-aged skeletal muscle profile, I characterised the *Soleus* muscle phenotype in the $Ercc1^{d/-}$ mouse.

Taryn Morash

2. To determine the suitability of the *Ercc1*$^{d/-}$ mouse in mimicking well-defined aspects of sarcopenia, as a model of natural ageing.

Studies exploring the wide-spread deterioration in the *Ercc1*$^{d/-}$ model, have established compartment-specific features that mimic 'normal', 'accelerated' and 'extreme' ageing progression (Dollé et al. 2006). It is well known that the decline in overall fitness associated with the ageing process comprises both stochastic and genetic components and this has been linked with a shift in energy consumption, away from synthesis and growth, towards molecular and cellular maintenance (Hoeijmakers 2009; Garinis et al. 2008). This shift has been reported to be a prevalent feature in the *Ercc1*$^{d/-}$ mouse (Dollé et al. 2006). Therefore, it was postulated that evidence for this shift would also be observed in the naturally-aged muscles, where myofibre atrophy and a reduction in myofibre cross-sectional area are reported (Degens, Turek, et al. 1993; Klitgaard et al. 1989; Sousa-Victor et al. 2014). Using the naturally-aged and *Ercc1*$^{d/-}$ *Soleus* muscle profiles, detailed in the previous aims, direct comparisons were drawn between muscle mass, myofibre number, cross-sectional area and composition, among others.

3. To examine the potential beneficial paracrine effects of stem-cell derived conditioned media on phenotypical aspects of the *Ercc1*$^{d/-}$ *Soleus*.

As the *Ercc1*$^{d/-}$ mutant is one of rapidly accumulating DNA damage, it was postulated that features of decline associated with those well-defined in natural ageing, particularly those relating to metabolism and oxidative stress, would be more predominant in the *Ercc1*$^{d/-}$ *Soleus*, compared to naturally-aged muscles. Following similar examination methods as in the naturally-aged aims, the paracrine effect of ADMSC CM was investigated in the *Ercc1*$^{d/-}$ *Soleus*, using the developed array of analyses.

Hypothesis 3

Conditioned media generated from adipose-derived mesenchymal stem cells, increases skeletal muscle satellite cell number and regenerative function in natural ageing and in the *Ercc1*$^{d/-}$ mutant murine model of progeria.

Objectives

Taryn Morash

1. To examine the impact of natural ageing on the underlying mechanisms of satellite cell (SC) function.

It is well known that SCs exhibit delayed activation and emergence, reductions in migration velocity, a lock into premature cellular senescence, proliferation and differentiation potential, with age (Collins-Hooper et al. 2012; Sousa-Victor et al. 2014; Collins et al. 2007). All are essential steps underpinning the process of skeletal muscle regeneration, myofibre turnover and the supply of new myonuclei with muscle hypertrophy (Zammit 2002; Snijders et al. 2009). Thus, in order to provide a basis for subsequent experimentation, these mechanisms of SC activity, were analysed on isolated single myofibre cultures from the EDL muscle of young (3 months) and aged (24 months) C57BL/6 mice. Immunocytochemical protocols for Paired box protein 7 (Pax7) and Myogenic differentiation 1 (MyoD) were used to identify satellite cells, laminin to visualise the myofibre basal lamina and α-smooth muscle actin to examine cell morphology. Time-lapse microscopy allowed SCs to be tracked and migration speeds to be calculated.

2. To characterise the underlying mechanisms of $Ercc1^{d/-}$ satellite cell function.

Although, it has been established that isolated and cultured $Ercc1^{d/-}$ muscle-derived progenitor cells exhibited defective proliferation and differentiation capacities, the other vital aspects of SC activity had yet to be fully characterised, within the single myofibre microenvironment (Lavasani et al. 2012). Thus, the investigation was conducted as in the previous aim, using single myofibres isolated from $Ercc1^{d/-}$ EDL muscles to analyse SC emergence, migration speed, morphology, proliferation and differentiation.

3. To assess the suitability of the $Ercc1^{d/-}$ progeric mouse, as a model of accelerated natural muscle ageing, at a cellular level.

It has been widely accepted that the ageing skeletal muscle myofibre and stem cell 'niche' is also affected by the ageing process and is a key determinant in SC function (Collins 2006; Grounds 2014). This is as opposed to the earlier conclusions suggesting that declines were solely due to a loss of intrinsic potential. The need for an appropriate accelerated ageing model is also evident at a cellular level and would benefit areas of research concerned with enhancing regenerative capacity in aged skeletal muscle, where the interplay between the

Taryn Morash

aged SC and its local microenvironment can be examined, for example during manipulations of the endogenous milieu (Conboy et al. 2003). As with previous aims, results can be directly compared between the naturally-aged and $Ercc1^{d/-}$ satellite cell mechanisms of function.

4. To examine the therapeutic potential of stem-cell derived conditioned media *in vivo* treatment on the underlying aspects of naturally-aged and $Ercc1^{d/-}$ satellite cell function.

It has been shown that the ability of young stem/progenitor cells to restore the proliferative and differentiation dysfunction demonstrated by aged and progeric stem cells which was attributed to the secretome (Lavasani et al. 2012). Thus, as with the previous aim, mechanisms of SC regenerative activity were examined on isolated single myofibres from naturally-aged and progeric EDL muscles.

Hypothesis 4

Skeletal muscle myofibres promote non-muscle stem cells and non-stem cells to adopt myogenic characteristics.

Objectives

1. To determine that the amoeboid-based migratory feature demonstrated by satellite cells, is directed predominantly by the myofibre surface.

It has been established that SCs migrate on myofibres using an amoeboid/bleb-based mechanism (Collins-Hooper et al. 2012; Otto et al. 2011). It is unknown whether the myofibre matrix could induce the bleb-based form of migration in non-muscle cells. Therefore, this was tested by co-culturing myofibres with transplanted adipose-derived mesenchymal stem cells, amniotic fluid stem cells, dental pulp stem cells and a breast cancer cell line, MDA-MB-231 cells and analysing the mode of migration using time-lapse microscopy.

2. To examine the impact of the aged myofibre microenvironment on the migratory and morphological characteristics of resident satellite cells and non-muscle cells.

It was shown that SC migration speed was reduced on aged myofibres (Collins-Hooper et al. 2012). It is unclear whether this feature is determined by a decline in function intrinsic the

aged SC, or directed by the physical properties of the myofibre surface. Thus, the same non-muscle cell types used in the previous aim, were transplanted and co-cultured with myofibres and morphology was analysed using an immunocytochemical protocol for α-smooth muscle actin and migration examined using time-lapse microscopy.

3. To assess the *in vitro* effects of stem-cell derived conditioned media on the morphology and migration speeds of resident satellite cells and non-muscle cells co-cultured with aged myofibres.

   It has been shown that conditioned media treatment enhances the closure of an artificial 'wound', as a migration assay *in vitro* (Mellows et al. 2017). Therefore, the effects of *in vitro* administration of conditioned media on the migration of resident SCs as well as the non-muscle cells on both young and aged myofibres. Furthermore, *in vivo* and *in vitro* administration of conditioned media was compared.

4. To determine whether the molecular mechanisms that underpin the regulation of amoeboid-based migration were the same in each cell type.

   It is well known that Rac and Rho GTPase signalling pathways are central to the regulation of cell morphology and mode of migration, where Rac drives actin filament formation and Rho is responsible for bleb-mediated motility (Sanz-Moreno et al. 2008; Sanz-Moreno & Marshall 2009). Thus, the use of Y-27632 and CK666 (ROCK and Arp2/3) inhibitors were used to block Rho and Rac signalling and examine the impact on the morphological and migratory features of each cell type.

5. To establish the influence of the myofibre surface on non-muscle stem and non-stem cell fate.

   It has been shown that the elasticity or rigidity of a matrix has profound effects of the fate of stem cells (Engler et al. 2006). Thus, the transplanted cell types were examined for myogenic markers after 10 days co-culture on myofibres and subsequently dissociated and examined for myosin heavy chain expression and myotube formation.

Taryn Morash

Chapter 2
Methods

Taryn Morash

Cell culture

Thawing of cells

All cell culture protocols including the preparation of fresh, cell-specific culture media prior to the thawing of cells, were carried out under a laminar flow hood, following a high standard of aseptic tissue culture technique. Aliquots of media (9mL) were pipetted into sterile 15mL centrifuge tubes and pre-warmed to 37°C in a water bath (e.g. one per cell type). Cells were stored in 1.8mL cryovials at approximately -200°C within a liquid nitrogen dewar and to thaw, vials were removed from liquid nitrogen storage and placed directly into a 37°C water bath and agitated gently to speed up the rate of thawing. Under aseptic conditions, the contents (1mL thawed media cell suspension), was pipetted into the 15mL centrifuge tubes of pre-warmed (37°C), fresh, cell-specific culture medium. Cells were then centrifuged at 400g for 5 minutes to form a pellet which was then re-suspended in a further volume of warmed (37°C), fresh media (for example, 1mL) for accurate, manual cell counting using a haemocytometer. After counting, cells were seeded into appropriately-sized tissue culture-treated flasks at an appropriate seeding density for that cell type with fresh media warmed to 37°C. Any non-adherent cells present 24 hours after thawing and seeding were removed through aspiration of the media and fresh media was added. During cell expansion, media was exchanged every 3 days. Cells were grown to appropriate numbers for experimentation ($2.5x10^5$) or to 70% confluency in order to maintain stem cell properties.

Passaging of cells

Once cells had expanded in culture to reach the appropriate number or confluency, cells were dissociated from the culture surface using trypsin (1x TrypLE™ Select 12563-011). Media was removed and replaced with 1x TrypLE™ Select, incubated at 37°C and 5% CO_2 for 5 minutes to allow for complete dissociation. As previously described in the 'Thawing of cells' protocol, cell suspensions were collected into sterile 15mL centrifuge tubes and centrifuged at 1,200 rpm for 5 minutes, re-suspended in 1mL of warmed (37°C), fresh media for accurate, manual cell counting using a haemocytometer. $2.5x10^5$ cells of each type were required for use in cell transplantation experiments and were pipetted into sterile 35mm culture petri dishes (Sarstedt 82.1135.500) containing 1mL of Single Fibre Culture Medium (SFCM) and intact isolated single myofibres (approximately 700 per hindlimb muscle) and left to adhere for 2 hours. Cells required for further expansion in culture were passaged and counted as described and seeded at appropriate densities with media changes every 3 days. Alternatively, cells no longer required for expansion were frozen down for long-term storage.

Taryn Morash

Freezing cells for long-term storage

Dissociated cells, as previously described in the protocol for 'Passaging of cells', were counted and centrifuged for 5 minutes at 400g and instead, were re-suspended in warmed (37°C) freezing media and pipetted into 1.8mL cryovials ($5x10^5$ or $1x10^6$ cells per 1mL freezing media per cryovial). Cryovials were cooled at a slow rate of 1°C per minute in a Mr Frosty™ freezing container (Thermo Fisher Scientific 5100-0001) stored at -80°C overnight. Cryovials were then transferred from -80°C to a liquid nitrogen dewar for long-term storage at approximately -200°C.

Preparation of nitric acid-treated cover slips for cell culture

Round cover slips were washed in 65% (v/v) nitric acid (previously prepared under a fume hood) overnight with gentle agitation. Cover slips were then washed 3 times with distilled H_2O for 30 minutes each with gentle agitation and washed a further time in 70% ethanol in a new glass beaker. Under aseptic conditions, cover slips were carefully laid out to air dry on a layer of clean tissue and once dry, cover slips were autoclaved. Nitric acid cover slips were used to analyse the differentiation of dissociated AFS, MDA and SCs from myofibres and the potential to form of myotubes using the MHC+ immunocytochemical protocol (discussed later in 'Myotube formation culture' section).

Collagenase solution preparation

For two EDL muscles (one mouse dissection), a 1mL aliquot of 2mg/mL type-1 collagenase solution was prepared in DMEM.

Preparation of culture plates

Following sterile tissue culture conditions, 1mL of SFCM was added to each required well of 12-well culture plates (Greiner 665180). Where inhibitor was used, the required inhibitor was added to SFCM at the required concentration and made up to a total volume of 1mL in each well. The plates were placed in an incubator at 37°C and 5% CO_2 for the required period of time.

Cytoskeletal inhibitor preparation

The ROCK inhibitor (Y-27632 dihydrochloride, Abcam ab120129) was used at a concentration of 10μg/mL. The Arp2/3 inhibitor (CK666, Abcam ab141231) was used at a concentration of 150μM. The required concentrations of inhibitors were made up in SFCM to a total volume of 1mL per culture plate well. Cells were added to the culture wells of isolated single myofibres and after allowing 2 hours for cell adherence, myofibres (with transplanted cells) were transferred to wells of a new culture plate and incubated with 1mL SFCM (control) plus inhibitor treatments.

Taryn Morash

Conditioned media generation

Phosphate buffered saline (PBS) preparation for conditioned media (CM) generation

CM was generated in 1x PBS that was prepared in-house and sterilised through autoclaving for 20 minutes at approximately 120°C. Aliquots of PBS were prepared in 8.9mL OptiSeal™ ultracentrifuge tubes (Beckman Coulter 361623) and centrifuged using an Optima XPN-80 ultracentrifuge at 70,000g for 120 minutes. Under aseptic conditions, care was taken to avoid disruption of any pelleted material, whilst the ultracentrifuged supernatant from each tube was removed, combined and stored at room temperature.

Generation of conditioned media (CM) from hADMSCs

Dissociated hADMSCs in suspension were aliquoted into sterile 1.5mL micro-centrifuge tubes ($1x10^6$ cells per tube) and washed in 1mL previously prepared sterile ultracentrifuged PBS. Cells were pelleted through centrifugation at 400g for 5 minutes and re-suspended in a further 1mL ultracentrifuged PBS. The wash step was repeated a further 2 times. A final volume of 400μL ultracentrifuged PBS was added to the cell pellet and centrifuged a further time at 400g for 5 minutes. Pellet cultures were incubated at room temperature for 24 hours, re-pelleted at 400g for 5 minutes prior to the careful aspiration of the (T24 CM) supernatant, avoiding any disturbance to the pellet. The CM aspirations were combined and centrifuged at 4,000g for 20 minutes to pellet any cell debris, then separated into 500μL aliquots and stored at -20°C to ensure one single freeze-thaw cycle in preparation for use in each experiment. Pellet cultures were incubated an additional 24 hours at room temperature in a further 400μL of fresh ultracentrifuged PBS prior to the aspiration of the (T48 CM) supernatant, following the previously outlined protocol for the collection of T24 CM and the process was repeated for the generation of T72 CM.

Post-CM generation hADMSC differentiation to adipogenic lineage

Expanded hADMSCs following CM generation were prepared for adipogenic differentiation in 4-well dishes (surface area of $1.9cm^2$) at a seeding density of 4,000 cells per cm^2 and were cultured in standard conditions (37°C and 5% CO_2) in hADMSC-specific media until 90% confluent. Growth media in the 'test' wells was replaced with StemPro® Adipogenesis basal medium (Life Technologies A10410-01), StemPro® Adipogenesis Supplement (Life Technologies, Thermo Fisher Scientific A10065-01), as per the manufacturer's instructions whereas, the 'control' wells continued to be cultured in growth media. Cells were cultured for 21 days with fresh media changes every 3 days. After 21 days, cells were gently washed in PBS following careful aspiration of the media to avoid

Taryn Morash

disruption to the very confluent cell layer. Cells were then fixed in 4% (w/v) PFA/PBS for 15 minutes, washed 3 times with ultrapure deionised water (dH$_2$O) and washed with 60% (v/v) isopropanol for 5 minutes. Cells were then air-dried and incubated at room temperature in a working solution of Oil Red O stain (see 'Appendix 1 - Materials') for 30 minutes with gentle agitation. Following staining, any excess dye was removed with 4 consecutive dH$_2$O washes for 5 minutes each and cells were allowed to air dry. Cells were visualised and imaged using a brightfield microscope at low magnifications (for example, 10 or 20x). Successful differentiation of mesenchymal stem cells towards an adipogenic lineage was identified by positive Oil Red O staining of oil droplets within the cells.

Post-CM generation hADMSC differentiation to osteogenic lineage

Expanded hADMSCs following CM generation for osteogenic differentiation were prepared using the protocol as followed with adipogenic differentiation. Cells in 'test' wells were cultured with StemPro® Osteocyte/Chondrocyte basal medium (Life Technologies, Thermo Fisher Scientific A10069-01), StemPro® Osteogenesis Supplement (Life Technologies, Thermo Fisher Scientific A10066-01) as per the manufacturer's instructions. Cells were subsequently fixed in 4% PFA/PBS for 15 minutes, washed 3 times with dH$_2$O and incubated at room temperature in a working solution of Alizarin Red S stain for 30 minutes with gentle agitation. Following staining, as per the adipogenic differentiation protocol, cells were washed with dH$_2$O, air dried and imaged using a brightfield microscope (for example, 10 or 20x). Successful differentiation of mesenchymal stem cells towards an osteogenic lineage was identified by positive Alizarin Red S staining of calcium deposits within cells.

Post-CM generation hADMSC differentiation to chondrogenic lineage

For chondrogenic differentiation, hADMSCs, (post-CM generation) were cultured at very high density (1x10^6 cells per 15mL centrifuge tube) as pellet cultures, centrifuged at 400g for 5 minutes, to allow for the formation of cellular spheroids. 'Test' pellet cultures were cultured with StemPro® Osteocyte/Chondrocyte basal medium (Life Technologies, Thermo Fisher Scientific A10069-01), StemPro® Chondrogenesis Supplement (Life Technologies, Thermo Fisher Scientific A10064-01), in standard conditions (37°C and 5% CO$_2$) for 21 days. Media was changed every 3 days with care taken to avoid disturbance to the spheroids. After 21 days, cells were gently washed and fixed as per the adipogenic differentiation protocol and were incubated at room temperature in a working solution of Alcian Blue stain overnight, in the dark. Following staining, any excess dye was removed with 2 consecutive washes with the destaining solution for 20 minutes each. Cells were visualised and imaged using a brightfield microscope at low magnifications (for example, 10 or 20x). Successful

Taryn Morash

differentiation of mesenchymal stem cells towards a chondrogenic lineage was identified by positive Alcian Blue staining of acidic polysaccharides (for example glycosaminoglycans) in cartilage deposits within cells.

Cellular senescence assay

Cells that have entered replicative senescence, a feature associated with ageing and the reduced rate of stem cell-mediated repair, are frequently observed using the X-gal staining protocol. This method was first reported by Dimri and colleagues to quantify the number of cells expressing β-galactosidase following initiation of cellular senescence, histochemically identifiable at pH 6, *in vitro* (Dimri 1995). IMR-90 lung fibroblast cells were expanded in culture to 70% confluency and passaged following the previously detailed cell culture protocols, into the wells of 2 separate 12-well plates (surface area of $3.5cm^2$) at a seeding density of 50,000 cells per well. Cells were cultured until 70% confluent, the media was aspirated from each well and cells were washed in sterile PBS. 900µL of fresh growth media was added to each well and for the 'PBS control' wells 100µL previously prepared sterile ultracentrifuged PBS was added to make a 1mL final volume. For the 'test' wells however, the required concentrations of conditioned media previously generated from hADMSCs was added to each well and made up to a final volume of 1mL ultracentrifuged PBS. For example, 1% CM required 900µL of fresh growth media, 10µL CM and 90µL PBS. Cells were cultured for 24 hours after which the media was aspirated from each well and replaced with 1mL 100µM H_2O_2 in growth media and incubated for 2 hours, in order to initiate cellular senescence. The cells were then washed with sterile PBS twice prior to 48 hours incubation in 1mL fresh growth media in standard conditions (37°C and 5% CO_2). After 48 hours, cells were passaged from the 12-well plates and each well was re-seeded into 3 wells of a 24-well plate (surface area of $1.8cm^2$) at a density of 800 cells per well and cultured for a further 24 hours to adhere. Cells were then fixed with 0.2% glutaraldehyde, 2% PFA for 5 minutes, rinsed twice with sterile PBS and incubated for 18 hours at 37°C in the dark with 250µL per well senescence staining solution. Following staining, the cells were washed twice with PBS and twice with methanol and then air-dried prior to analysis. Cells were visualised and counted manually using an inverted microscope (Zeiss A1 Inverted Epifluorescent Microscope) and the proportion of positively-stained (blue) senescent cells were recorded for each condition. For example 'stressed' and 'unstressed' controls cultured in the presence and absence of H_2O_2, respectively and those conditions pre-treated with CM at various concentrations.

Taryn Morash

Animal maintenance and use

Ethical approval

The experiments were performed under a project license from the United Kingdom Home Office in agreement with the Animals (Scientific Procedures) Act 1986. Healthy animals were maintained and housed in accordance to the Animals (Scientific Procedures) Act 1986 (UK) within the Biological Resource Unit at the University of Reading under standard environmental conditions (20-22°C, 12-hour light-dark cycle) and provided food (standard pelleted diet) and water *ad libitum*.

Maintenance of heterozygous ERCC1 mutant mouse populations

To maintain sufficient young and healthy experimental mouse populations within the Biological Resources Unit, regular breeding pairs were set up and monitored. The ERCC1 mutants were reported to be embryonically lethal on a single inbred laboratory mouse strain by the research groups that developed the ERCC1 mouse model (Weeda, et al. 1997). This feature resulted in the requirement to breed and maintain populations of two separate mouse strains (C57BL/6 and FVB), both heterozygous for the ERCC1 mutation for the knockout (+/-) as well as the knocked-down, 'delta' mutant (d/+), giving rise to a total of four heterozygous breeding populations (+/- C57BL/6, +/-FVB, d/+ C57BL/6 and d/+ FVB). Regular breeding of animals from each of these heterozygous populations with a wild-type mouse of the same inbred strain, continuously maintained healthy cohorts. All of the heterozygous breeding animals live the full, expected lifespan of non-mutant, wild-type mice and do not experience any of the impairments or health issues associated with progeric, full knockout (-/-) or delta mutant (d/-) animals. However, to give rise to the progeric ERCC1 delta mice used in experiments for the present study, heterozygous +/- animals from one strain/background were bred with heterozygous d/+ animals on the other strain/background. For example, as FVB females were found to breed more successfully and produced larger litter sizes (average 8-10 pups each compared to 5-7 pups per C57BL/6 litter), an example breeding pair comprised of a female FVB (+/-) and a male C57BL/6 (d/+).

Isolation of genomic DNA for genotyping of ERCC1 litters

Ear clip samples were collected into 1.5mL micro-centrifuge tubes and placed on ice. Chemical digestion of the ear tissue was initiated by adding 100μL of 50mM sodium hydroxide (NaOH) to each sample followed by brief vortexing. Samples were incubated at 95°C on a heat block for 1 hour with gentle shaking. The chemical digestion was stopped by neutralisation with 10μL of 1.5M Tris buffer (pH 7.4) and samples were centrifuged at 13,000 rpm for 1 minute. The solutions of crudely isolated

Taryn Morash

genomic DNA were then used in a genotyping polymerase chain reaction (PCR) protocol or stored at -20°C.

Polymerase chain reaction (PCR) protocol for the genotyping of ERCC1 litters

ERCC1 primers (listed in 'Appendix 3') were used in a primer 'cocktail' solution and were combined with other essential PCR components including taq polymerase, a deoxynucleotide (dNTP) mix and a buffer solution containing magnesium chloride ($MgCl_2$) to formulate a 'master mix', made in-house. Aliquots of the 'master mix' were then added to 5μL volumes of the isolated DNA solutions in 0.2mL PCR tubes (Eppendorf 0030 123.332) and run on the following cycle programme on a Bio-Rad T100 Thermal Cycler:

1. Incubate at 95°C for 5 minutes

2. Incubate at 92°C for 30 seconds

3. Incubate at 59°C for 30 seconds

4. Incubate at 72°C for 50 seconds

5. Cycle steps 2-4 for 32 times

6. Incubate at 72°C for 5 minutes

7. Cool to 18°C

8. End and store at 4°C

Gel electrophoresis for the genotyping of ERCC1 litters

Agarose was dissolved in 1x Tris-acetate-EDTA (TAE) to make a 2% (mini)gel containing 5% SYBR safe DNA gel stain (Thermo Fisher Scientific S33102), with care taken to avoid creating air bubbles. Once set, the gel was submerged in TAE buffer in the electrophoresis chamber, the combs were removed and samples were loaded into wells along with Orange G loading buffer (Thermo Fisher Scientific R0631) (for example 5μL Orange G added to 15μL PCR reaction product). The first well of each row however, was loaded with 5μL 100bp DNA ladder (Promega G2101) and following a 40-minute electrophoresis run at 70V, the resulting presence and sizes of bands, visualised and imaged using an ultraviolet (UV) transilluminator system, were used to determine the genotypes of ERCC1 mice. Band sizes of 246bp, 390bp and 500bp indicated the presence of a wild-type, ERCC1 mutant and ERCC1 delta allele, respectively.

Taryn Morash

In vivo experimentation

Intraperitoneal (IP) injection of CM for *in vivo* experimentation

Under aseptic conditions, sterile PBS was added to individual conditioned media aliquots (in sterile 1.5mL micro-centrifuge tubes), calculated based on animal body weight, consistent between all treated animals in each cohort, as per the doses described below. Vehicle-treated control doses were prepared using comparable volumes of sterile PBS. The doses of solution to be injected were prepared in 1mL insulin syringes (31G needle). Animals were restrained by the scruff of the neck, following good animal handling technique. Briefly, the scruff was grasped with the thumb and forefinger and the tail tucked away by the little finger. Whilst restraining the mouse in a horizontal position in one hand, the other hand is free to inject the doses intraperitoneally. The needle was inserted into the posterior quadrant of the abdomen, a small distance away from the midline (right-side of the animal, between the midline and the hind-limb) at a 45° angle pointed upwards and away to avoid the bladder. Following injection, animals were returned to their cages and monitored at 30-minute intervals for up to 2 hours to ensure animals remained healthy and in a good condition. Mice were weighed weekly to ensure accurate dose calculation and to further monitor the health of the animals.

CM/PBS I.P injection schedules for *in vivo* experimentation

The CM used in all experiments (both *in vivo* and *in* vitro) was collected in the same batch for consistency and was tested for protection against H_2O_2 stress-induced cellular senescence as well as post-CM cell differentiation *in vitro* assays, using the protocols previously described. Naturally-aged 20-month-old mice (C57BL/6) were injected (I.P) with 15µL/g doses of CM, (or PBS vehicle control) every 2 weeks, over a time period of 4 months (until 24 months of age), resulting in 8 injections in total. Animals were euthanised and tissues harvested 2 weeks after the final I.P injection.

ERCC1 delta mice (and wild-type littermate controls) were injected (I.P) with 30µL/g doses of the same batch of tested CM as used in the naturally-aged *in vivo* experiment, (or PBS vehicle control) every 2 weeks over a time period of 6 weeks (from 9 weeks to 13 weeks of age), resulting in 3 injections in total. Animals were euthanised and tissues harvested 2 weeks after the final I.P injection at 16 weeks of age.

Measurement of mouse forelimb grip strength

Forelimb grip strength measurements were made using a digital force gauge (Chatillon DFM-2). The force gauge was fixed firmly to the bench with the metal grip bar extruding from the bench surface.

Taryn Morash

The force meter was tared to zero and the mouse was gently lifted by the tail and held at a height in which the mouse could firmly grasp the bar. The grip was inspected to confirm that the mouse had a good, symmetrical grasp with both front paws. At a slow, consistent speed, the mouse was pulled back, away from the grip strength meter, until the grasp was broken. At this point, the force gauge measured the peak/maximal force in grams and the value was recorded. The process was repeated 3 times per animal with at least 1-minute intervals between testing to allow the mouse to rest and to avoid habit formation. Peak values as well as average force were used during analysis, normalised to body weight.

Measurement of motor coordination and balance through rotarod performance testing

Motor coordination was measured through performance testing using an accelerating rotarod system (Panlab/Harvard Apparatus LE 8500). Mice were acclimatised to the rotarod system set to a start speed of 4 rpm. The mouse was gently placed on the rotating rod, facing away from the direction of rotation to ensure the mouse walked forward for a 1-minute duration. The mice were monitored to ensure they did not attempt to turn in their lane or grasp onto the rotating rod to avoid walking. Between 1-minute trial runs, animals were returned to their cages for 10-minute rest intervals and the apparatus was cleaned with a mild, animal-safe cleanser. The procedure was repeated for a total of 3 times. Following adequate acclimatization and rest period, the mouse was placed on the rotating rod as previously described and after 10 seconds of steady walking, the acceleration programme was initiated until the mouse fell and triggered the measurement to be recorded on the system. Apparatus was cleaned with a mild, animal-safe cleanser and the process was repeated 3 times separated by 15-minute rest intervals. A note of the latency to fall (seconds) and the rotating speed at fall (rpm) were made and these parameters analysed between treatment/genotype/age groups.

Euthanasia procedure

Mice were humanely euthanised using Schedule 1 killing through carbon dioxide (CO_2) asphyxiation and death was confirmed by cervical dislocation.

Taryn Morash

Skeletal muscle analyses at whole muscle level

Extensor Digitorum Longus (EDL) muscle dissection from mouse

Myofibres were isolated from the *Extensor digitorum longus* (EDL) muscle of the hindlimb. The mice were euthanised using schedule 1 killing by carbon dioxide (CO_2) asphyxiation and EDL muscle dissection occurred immediately following death was confirmed. A 70% ethanol spray was used to sterilise the hind leg fur and surrounding area. A scalpel blade was used to make incisions in the skin around the thigh (proximal to the EDL or TA muscles to avoid damage), pulling distally with the thumb and forefinger, over and away from the footpad the skin is carefully removed. An incision was made and using the same distal pulling action, the remaining skin on the footpad was removed in order to reveal the distal tendons attached to the digits. Grade 4 forceps were used to remove the connective tissue (fascia) layer covering the TA and EDL muscles. The distal tendon of the TA muscle was located and incised using curved microscissors approximately 1cm below the TA muscle body and using grade 4 forceps, pulled proximally towards the knee, revealing the extent of the EDL muscle beneath. The forceps were used to locate the four distal tendons of the EDL raising each superior to the footplate and freeing the tendons from the ankle cartilage by gently pulling posterior to the muscle body. The two proximal tendons of the EDL were incised using microscissors furthest from the muscle body as possible, leaving the majority of the tendons intact and freeing the EDL muscle, whilst the muscle was kept taut using forceps to pull proximally to the knee. The muscle was removed from the limb and incubated at 37°C and 5% CO_2 in the previously prepared 1mL aliquot of 2mg/mL type-1 collagenase solution for single myofibre digestion or frozen for histological analyses.

Dissection of the *Tibialis Anterior* and *Soleus* muscle from mouse

The *Tibialis Anterior* (TA) muscle lies superior to the EDL in the hindlimb and in order to access the EDL, the distal tendon of the TA was incised using microscissors and the muscle lifted anteriorly to reveal the extent of the EDL beneath. It is at this point in the procedure therefore that the TA be dissected from the hindlimb if required. Careful incision of the proximal-most region of the TA where it arises from the lateral condyle of the tibia allowed for muscle removal. The *Soleus* however is located in the posterior compartment of the hindlimb with the *Gastrocnemius* lying superficial to the *Soleus* and arises from the fibula (and some fibres from the medial border of the tibia) running posterior to insert (along with the *Gastrocnemius*) into the calcaneus (heel bone) via the Achilles tendon. The *Gastrocnemius* was required to be gently dissected away and removed from the *Soleus* muscle body, leaving the Achilles tendon intact. As well as this, the *Soleus* required careful removal from the muscles beneath (for example the *Flexor digitorum longus*). The proximal tendon of the

Soleus was lifted with forceps and incised using microscissors followed by the lifting and cutting of the distal (Achilles) tendon to complete dissection.

Snap-freezing of tissue

In preparation for the euthanisation, dissection and subsequent snap-freezing of mouse tissue, a beaker of 200mL iso-pentane was frozen following immersion into a dewar of liquid nitrogen. Freshly dissected tissue (after fresh weight was measured) was then positioned appropriately (muscle laid straight) on a small, $2cm^2$ piece of aluminium foil and lowered onto the frozen iso-pentane. The freezing of the tissue occurred rapidly (snap-frozen) indicated by the muscle appearing whiter in colour. Once completely frozen, the tissue was carefully removed from the foil strip using forceps and quickly placed into labelled microfuge tubes on dry ice (forceps and tubes were pre-cooled in dry ice before use to minimise tissue thawing). Eppendorfs were transferred from dry ice to -80°C freezers for storage.

Preparation of muscle tissue for cryosectioning

Prior to the removal of frozen tissue from -80°C storage, a glass beaker ethanol bath was super-cooled on dry ice. $1cm^2$ aluminium foil cubes were prepared and filled with O.C.T embedding medium (TAAB O023) and the snap-frozen tissue mounted into the O.C.T cube and rapid freezing was enabled by plunging into the super-cooled ethanol bath to avoid thawing. The muscle tissue was cryosectioned transversely at a 10µm section thickness using a Bright OTF cryostat (OTF/AS-001/HS). Serial muscle sections (approximately 12 sections, therefore equivalent to ~120µm per muscle mid-belly region) were mounted onto glass slides (Menzel-Glaser J2800AMNZ), air-dried at room temperature for 30 minutes and stored at -80°C for future processing.

Haematoxylin and eosin (H&E) histological staining protocol

Glass slides with mounted tissue sections were removed from -80°C storage, incubated at room temperature for 30 minutes to dry and washed in 1 x PBS for 2 minutes followed by an 18-minute incubation in Mayer's haematoxylin to stain the nucleic material. The haematoxylin stain was removed using a 2-minute wash in distilled water and 2 dips in acidic alcohol (see 'Appendix 1 – Materials'). The slides were immersed in running water for 5 minutes and then washed in 70% ethanol for 1 minute. Next, the protein material was stained by a 1% eosin solution for 2-3 minutes and to finish, underwent a series of ethanol washes (90%, 100%, 100%, 100%) to dehydrate before clearing the samples with xylene (2 washes, 3 minutes each). Cover slips were mounted using DPX mounting medium (Fisher Scientific 10050080). Slides were allowed to air dry and sections were then visualised and imaged using a brightfield microscope at low magnifications (for example, 5 or 10x).

Taryn Morash

Succinate dehydrogenase (SDH) histological staining protocol to determine muscle oxidative capacity

As per the H&E staining protocol, frozen tissue sections were air-dried at room temperature for 30 minutes. A border surrounding the sections was drawn using an 'ImmEdge' hydrophobic barrier pen (Vector Laboratories H-4000). The NBT and succinate stocks were mixed with phenazine methosulphate to form the incubation medium, just prior to use and was kept out of strong light. The incubation medium was added directly to samples at room temperature and allowed to develop for approximately 2-4 minutes (for *Soleus* and EDL muscles) until a blue/purple colour was visible. Samples were washed in distilled water for 1 minute to stop the staining reaction and fixed in formol calcium for 15 minutes before mounting glass cover slips using 'Hydromount', a water-based mounting medium (National Diagnostics HS-106). Sections were then visualised and imaged using a brightfield microscope at low magnifications (for example, 5 or 10x).

Endothelial marker CD31 histological staining protocol to identify vasculature

Tissue sections were air-dried and prepared with a hydrophobic border, as per the SDH staining protocol. Once dry, the sections were washed with PBS for 5 minutes and incubated sequentially, for 15 minutes each, with the Avidin and Biotin components of an Avidin/Biotin Blocking Kit (Vector Laboratories SP-2001). Sections were then washed in 0.05% Tween 20 (Sigma-Aldrich P9416) in PBS (PBS-T) for 5 minutes and incubated in wash buffer for 30 minutes as an antigen blocking step to avoid any non-specific antibody binding. Following this, the wash buffer was removed and the rat anti-mouse CD31 primary antibody (Bio-Rad MCA2388) (pre-diluted at 1:150 in wash buffer for 30 minutes) was added to the sections and incubated for 1 hour at room temperature. To remove any un-bound antibody, sections were then washed 3 times in PBS-T for 5 minutes each. The rabbit anti-rat HRP secondary antibody (Abcam ab6734) (pre-diluted at 1:200 in wash buffer for 30 minutes) was added to the sections and incubated for 1 hour at room temperature. To remove any un-bound antibody, sections were then washed a further 3 times in PBS-T for 5 minutes each. Following the manufacturer's instructions, sections were then incubated for 10 minutes in Vectastain Elite ABC-HRP solution (Vector Laboratories PK-6100) and washed a further 3 times in PBS-T for 5 minutes each. Following the manufacturer's instructions, sections were then incubated in DAB Peroxidase (HRP) Substrate solution for approximately 4-5 minutes until sections had stained a grey colour. Staining development was stopped with a 1-minute wash in distilled H_2O. Slides were then incubated in a series of 100% ethanol dehydration steps (3 times, 1 minute each) and a further incubation in xylene for 1 minute, before glass cover slips were mounted on each slide using DPX mounting

Taryn Morash

medium (Fisher Scientific 10050080). Slides were allowed to air dry and sections were then visualised and imaged using a brightfield microscope at low magnifications (for example, 5 or 10x).

Immunohistochemistry

Glass slides were removed from -80°C storage and prepared as per the SDH histological staining protocol. Samples were washed twice in PBS and care was taken to avoid disrupting the section adherence. PBS was replaced with permeability buffer and incubated at room temperature for 15 minutes, followed by further washing stages, three times with PBS, then once with wash buffer as a blocking step to avoid any non-specific-binding, for 30 minutes. The wash buffer was removed from the sample and primary antibody (pre-diluted in wash buffer at room temperature for 30 minutes) was added and incubated for 1 hour at room temperature. The sample was washed 5 times in wash buffer to remove any unbound primary antibody and the first secondary antibody (pre-diluted in wash buffer at room temperature for 30 minutes in the dark) was added and incubated for 1 hour at room temperature in the dark. The sample was washed 3 times in wash buffer to remove any unbound secondary antibody. Finally, samples were covered with a cover slip affixed with mounting medium and DAPI, for analysis. With the Myosin Heavy Chain (MHC) isoform protocol, primary and secondary antibodies were added sequentially and pairs of slides (serial sections) were divided accordingly between alternative pairings of the three MHC isoforms (i.e. slide 1: Type IIA and type I, slide 2: type IIA and type IIB) to avoid cross-reactivity (IgG targets).

Imaging of muscle sections and data analysis

Muscle sections were processed for immunohistochemical or histological staining protocols and viewed using the Zeiss AxioImager or Zeiss AxioSkop microscope systems, AxioCam MRm camera and AxioVision software (version 4.9.1) 5x magnification images were captured and stitched/merged together using Adobe Photoshop CS4 image manipulation software to form photographs of the overall muscle section. Myonuclei, SDH positive myofibres and total myofibre/ myofibre typing (ratio of type I, type IIA and type IIb myofibres) counts were carried out on stitched whole muscle section 5x images. CD31 positive capillary counts were carried out on 20x magnification images within $1mm^2$. The 'ImageJ' software 'Cell Counter' plug-in analysis tool was used to count myofibres/cells/capillaries. 10x magnification images were captured (representative, comparable locations in muscle) in order to perform cross-sectional area (CSA) analysis of myofibres using the 'Outline' measurement tool in the AxioVision (version 4.9.1) software.

Taryn Morash

Quantitative real-time polymerase chain reaction (qPCR)

Muscles were wrapped in aluminium foil and submerged into liquid nitrogen, following this, muscles were pulverised into a powder and transferred to 1.5mL microfuge tubes with a flat base. 500µL of TRIzol reagent (Invitrogen 15596-018) was added to each tube and the sample solubilised using a tissue homogeniser. Total RNA was prepared from muscle samples using the RNeasy® Mini Kit (Qiagen 74104) and RNase-Free DNase Set (Qiagen 79254), according to the manufacturer's instructions. According to the RNA concentrations, measured using the Nanodrop 2000 (Thermo Fisher Scientific), 0.5µg of total RNA was reverse transcribed using the RevertAid H Minus First Strand cDNA Synthesis Kit (Thermo Fisher Scientific K1631), following the manufacturer's instructions. From each sample 5µL was used to prepare arbitrary dilutions of 5 standards. The optimal efficiencies of each primer (housekeeping gene and genes of interest) fall between 90 and 110%. Relative mRNA levels were analysed by quantitative real-time PCR (qPCR), using the following cycling protocol: 15 seconds at 95°C, 60 seconds at 60°C, on a StepOnePlus™ Real Time PCR system, using the Applied Biosystems SYBR Green PCR Master Mix (Thermo Fisher Scientific 4309155) and StepOne software v.2.1. Primers were designed using the primer designing tool on the NCBI Blast website and the primers listed in Appendix 3. All data were normalised to the housekeeping gene, hypoxanthine-guanine phosphoribosyltransferase (hprt).

Taryn Morash

Skeletal muscle analyses at cellular level

Mouse EDL single myofibre isolation

The rate of enzymatic digestion and separation of the EDL myofibres in the 1mL aliquot of 2mg/mL type-1 collagenase solution was increased through regular agitation and swirling, every 15 minutes. After monitoring for 1.5-2 hours, the majority of the myofibres were observed as separated, individual myofibres in suspension. Using a sterile, tapered glass pipette the fibres were transferred to a washing dish and viewed under a stereomicroscope. In order to isolate as many myofibres as possible, any bundles of fibres were carefully aspirated and washed twice in DMEM (incubated to 37°C) to remove residual collagenase and then washed twice in SFCM (incubated to 37°C) to replace the DMEM. At this stage, fibres were either cultured or fixed at time-zero (T0).

Single myofibre culture

The desired number of myofibres (for example 10 per well for time-lapse, ~50 for later fixing etc.) were transferred from the wash dish after isolation to previously prepared wells containing 1mL SFCM (incubated to 37°C) in a 12-well plate. For the cell transplantation experiments, 2.5×10^5 AFS, ADMSC, DP or MDA cells were divided between culture dish wells, added and allowed to adhere for 2 hours. After 2 hours, fibres (and therefore attached cells) were transferred to a new dish containing warmed (37°C), fresh SFCM (or adapted LT-SFCM for long-term culture of myofibres, T120 and T240) and incubated at 37°C and 5% CO_2 for the required culture period. Alternatively, 12-well plates were placed within a time-lapse microscopy system surrounded by a temperature- and CO_2-controlled chamber for the generation of time-lapse cell migration data. Myofibres were fixed at various relevant time-points for further analysis (for example immunocytochemistry).

Myotube formation culture

Incubation of isolated myofibres with single fibre culture media (SFCM) enriched with a higher concentration (5%) of chick embryo extract (LT-SFCM), allowed for a prolonged culture period of 10 days (T240). Transplanted AFS and MDA cell/myofibre co-cultures were set-up as per the previously outlined protocol and following 10 days culture, were incubated in 1x TrypLE™ Select for 10 minutes at 37°C to dissociate the cells from the myofibres. The cell/myofibre suspensions were filtered through 70μm cell strainers to remove whole myofibres and hyper-contracted debris, isolating the remaining dissociated cell fraction. The isolated cells were then seeded into wells of a 12-well plate lined with sterile nitric acid-treated cover slips and cultured in fresh cell-specific growth media under standard conditions (37°C and 5% CO_2), until a 95% confluency level was reached. Additionally, AFS

Taryn Morash

and MDA cells expanded in the absence of myofibres, were also seeded and grown to 95% confluency in normal growth media or LT-SFCM as 'control' cultures. Once 95% confluency was reached, growth media was aspirated and replaced with myogenic differentiation media in all conditions with the exception of the 'growth media control' treatments. Cells were incubated in standard conditions (37°C and 5% CO_2), with media changes every 3 days and cell morphology was monitored daily for the formation of myotubes using a brightfield microscope. After 7 days, myotube formation was evident and cell cultures were fixed in 4% PFA/PBS and washed, prior to further processing for analysis, for example immunocytochemical protocols.

Fixing isolated myofibres

Myofibres were fixed by adding 4% paraformaldehyde/phosphate buffered saline (PFA/PBS) solution to the wash dish containing the fibres (after isolation) at a volume ratio of 1:1, resulting in a final concentration of 2% PFA/PBS and left for 15 minutes at room temperature then washed 3 times in PBS to replace the PFA/PBS fixative. Stored in phosphate buffered saline (PBS) at 4°C, for later analysis in transparent 1.5mL microfuge tubes (Axygen MCT-150).

Immunocytochemistry

This protocol was carried out as per previously described with the whole muscle 'Immunohistochemistry' protocol and differs only in that the following details the treatment of cells/myofibres instead of whole muscle sections, as well as differences in the antibodies used. The fixed myofibres, stored at 4°C were washed twice in PBS and care was taken to avoid removing the myofibres from the microfuge tube during washing. PBS was replaced with permeability buffer and incubated at room temperature for 15 minutes, followed by further washing stages, three times with PBS, then once with wash buffer as a blocking step, for 30 minutes. The wash buffer was removed from the sample (myofibres) and the primary antibody (pre-diluted in wash buffer at room temperature for 30 minutes) was added and incubated for 1 hour at room temperature. The sample was washed 5 times in wash buffer to remove any unbound primary antibody and the first secondary antibody (pre-diluted in wash buffer at room temperature for 30 minutes in the dark) was added and incubated for 1 hour at room temperature in the dark. The sample was washed 3 times in wash buffer to remove any unbound secondary antibody. Finally, myofibres were mounted onto a glass microscope slide and covered with a cover slip affixed with mounting medium and DAPI, for analysis.

Taryn Morash

Time-lapse microscopy and imaging of satellite stem cell migration

Myofibres both treated with inhibitor and untreated (control) were viewed in culture plates under a time-lapse microscope (Nikon Eclipse TE200) over a time period of 12 hours. Points along single myofibres were located using the microscope at 20X magnification and were photographed every 15 minutes for a total time period of 12 hours.

Biological sample preparation for critical point drying and scanning electron microscopy (SEM) EMLAB (Electron Microscopy Laboratory) protocol

Myofibres were fixed with the 4% PFA/PBS solution using the previously described method, washed three times in PBS and then washed in distilled water for 15 minutes. Samples were dehydrated through an acetone series (30%, 50%, 70%, 80%, 90% and three times at 100%) at room temperature and were left for 15 minutes at each step in the series. (Solvent/distilled water solutions each made up to 10mL in total). Samples were placed in a sample holder, covered with fresh dry solvent (acetone) and dried in the critical point dryer (Balzers CPD 030 – using liquid CO_2). The dehydration method was repeated ten times to ensure all acetone had been replaced by liquid CO_2. Sample stubs were prepared with carbon disc covers. The gaseous CO_2 was vented off and immediately the dehydrated myofibre samples were mounted onto the prepared stubs and coated with gold in an Edwards S150B sputter coater for 3 minutes. A dessicator was used to store the samples for future imaging and analysis using the SEM (FEI 600F).

Proliferation

Myofibres were cultured for 48 hours in total and fibres were fixed at T14, T24 and T48. Immunocytochemistry was carried out following the previously described protocols using antibodies against Pax7 and MyoD and myofibres were mounted onto glass microscope slides with mounting media and DAPI for analysis. The myofibres were viewed under a Zeiss AxioImager fluorescence microscope using three fluorescent filters and cells were counted based on whether they were observed as positive for Pax7, MyoD or both. Proliferation was calculated as number of cell per fibre, number of cell clusters per fibre and separately, cluster size (cells per cluster).

Myofibre image and movie analysis

All movie analysis was carried out using the freeware analysis programme, 'ImageJ' (version 1.46). Time-lapse movies were first registered to allow for the movement of the myofibre that would otherwise contribute inaccurately to the distance travelled by the satellite cell using the sister freeware programme of ImageJ, 'Fiji' (version 1.0). Individual satellite cells were manually tracked

Taryn Morash

using the plug-in 'MTrackJ'. Bleb dynamics were quantified manually using ImageJ. Different stages of cell emergence and proliferation of individual satellite cells were manually assessed using quantification of live images through the Zeiss AxioImager, AxioCam MRm camera and AxioVision software (version 4.9.1) system.

Statistical analysis

Calculations carried out were to determine that the data was normally distributed as well as to ascertain the mean, standard deviation (SD) and standard error of the mean (SEM), followed by statistical analysis. Student's t-tests or, where applicable, one-way analysis of variance (ANOVA) tests among groups of data were used with post-hoc Tukey multiple comparison tests (also known as Tukey's range test or Tukey-Kramer test) between treatments to determine significance. Where appropriate, two-way ANOVA tests were conducted to assess the interaction between groups and treatments. A level of 95% significance is represented by a P-value (p) *<0.05*, 99% significance *(p <0.01)* and 99.9% significance *(p <0.001)*. Error bars represent standard error of the mean (SEM). Statistical analysis was performed using 'GraphPad Prism' statistical software (version 6). The following animal numbers were as follows for histological analyses: Young (3), Adult (6), Old (5), Old CM (5) and Geriatric (3). qPCR analyses comprised of 3 samples per age group/treatment cohort. Isolated single myofibre analyses were conducted on ≥15 healthy myofibres from 3 animals per age group/condition at all times.

Taryn Morash

Chapter 3

Development of an ageing skeletal muscle profile and the therapeutic effects of conditioned media

Taryn Morash

Introduction

The following series of *in vivo* experiments investigated the hypothesis that conditioned media (CM) generated from adipose-derived mesenchymal stem cells (ADMSC), maintains regulatory properties that attenuate, delay or even prevent characteristic age-associated alterations in skeletal muscle composition and function. Numerous characteristic alterations have been previously observed with the onset and progression of sarcopenia in human and animal studies, conducted at whole tissue, cellular and molecular levels. These features include, among many others, myofibre atrophy, decreased muscle weight, variations in muscle diameter, motor neuron denervation, reduced contractile and force-generating capacity, increased myofibre fibrosis, a reduction in skeletal muscle satellite stem cell number and function and increased oxidative stress (Shefer et al. 2006; Collins et al. 2007; Faulkner & Brooks 1995; Alnaqeeb & Goldspink 1987; Wang et al. 2014; Chai et al. 2011). Development of a broad skeletal muscle profile in naturally-aged C57BL/6 mice provides a basis to test the potential anti-ageing, therapeutic effects of ADMSC CM treatment.

Using a protocol established by a collaborator, CM was generated from ADMSCs under hypoxic-stressed and nutrient deprived conditions, in order to induce the stem cells to produce and secrete survival factors. A study has shown that the total protein secreted by MSCs was greater under hypoxic compared to normoxic conditions (Kinnaird et al. 2004). Additionally, the factors that were demonstrated to be up-regulated included FGF-2, IL-6, TGF-β, TNF-α and VEGFa, key to angiogenesis and regulation of inflammation, for example. Briefly, ADMSCs were expanded under normal growth conditions to the required number of cells, washed to remove any exogenous growth factors originating from the growth media, and pelleted in separate 1×10^{6} PBS cell cultures. Conditioned media was collected at T24, 48 and 72 (hours) time-points with fresh PBS replaced at each, however, the T24 fraction was utilised in the present study. Colleagues have shown that protein concentration and nucleic acid content of the T24 and 48 fractions released by ADMSCs, under these conditions, are similar and in the third time-point (T72), this content is decreased (In press, *Frontiers in Immunology*). The development of an *in vitro* senescence assay to test the efficacy of ADMSC CM has been developed and proven to be robust among colleagues (Mellows et al. 2017). Properties maintained by CM have therefore, been shown to protect against cellular senescence and this assay was used in the same way in the current study, to indicate CM efficacy prior to the novel treatment to study ageing skeletal muscle. Following testing, animals were injected intraperitoneally (I.P) with ADMSC CM from 20 months of age for a duration of 4 months.

Taryn Morash

Results

Conditioned media from adipose-derived mesenchymal stem cells demonstrated protective effects against cellular senescence

Firstly, the efficacy of ADMSC CM as a regulator of cellular senescence was assessed. CM used at concentrations of 1% and 10%, reduced the proportion of positively-stained senescence-associated β-gal cells, following H_2O_2 treatment, to the levels of the unstressed control (p = <0.05 and <0.01, respectively) (Figure 3.1 A). Secondly, the ADMSCs were demonstrated to retain multipotency and differentiated towards, chondrogenic, osteogenic and adipogenic lineages, following the collection of CM (Figure 3.1 B, C, D, E, F).
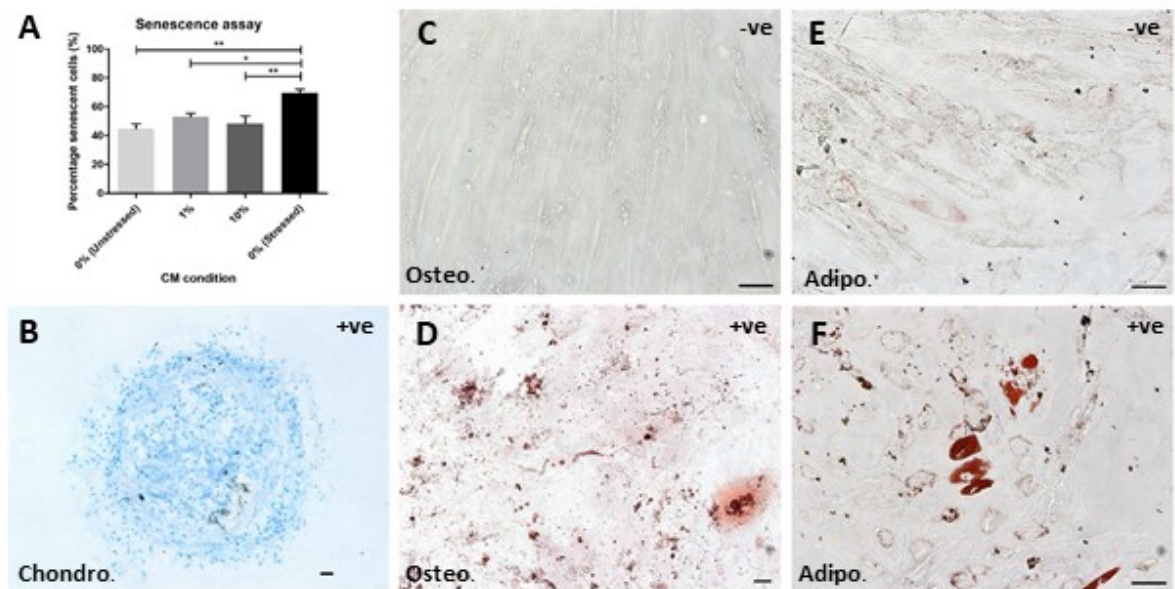
Figure 3.1 ADMSC-derived CM protects against cellular senescence and differentiation assays indicate post-CM generation stemness. **(A)** Senescence assay showing that CM (1%, 10%) protects against cellular senescence (SA-B-gal) in a cultured IMR90 lung fibroblast cell line **(B)** Post-CM ADMSCs in pellet culture (21 days), were induced towards a chondrogenic lineage before being stained with Alcian Blue stain. A positive result would be the cellular spheroid staining blue. Of note, growth media pellet cultures also stained positively and appeared as shown here. **(C)** Undifferentiated ADMSC growth media control for osteogenesis. **(D)** Post-CM ADMSCs cultured for 21 days towards osteogenic lineage prior to Alizarin Red S staining. Positive differentiation results in mineralisation staining red. **(E)** ADMSC growth media control for adipogenesis, starting to differentiate towards adipogeneic lineage. **(F)** Post-CM ADMSCs cultured for 21 days towards adipogeneic lineage prior to Oil Red O staining, with internal fat droplets staining deep red in colour. Scale bar 100µm. *p<0.05, **p<0.01, One-way ANOVA with Tukey post hoc testing.

Taryn Morash

Body weight changes in natural ageing

Body weights for the four age groups, young (3 months), adult (6 months), old (24 months) and geriatric (27-30 months), were recorded to provide information about the growth of wild-type (WT), female C57BL/6 mice during the progression of natural ageing (Figure 3.2 A). The initial growth phase from young to adult ages was observed with an increase in body weight from an average of 18 to 42g. Mass further increased during old and geriatric ages to 43 and 45g, respectively, however when tested, these differences were statistically non-significant.

Additionally, weights were recorded weekly to monitor animals regularly throughout the *in vivo* CM IP experimental time-periods. Firstly, body weights for the Old CM-treated cohort appeared lower than the PBS vehicle control animals however, this difference was not statistically significantly different and indicated a large amount of variation in weight within each cohort (Figure 3.2 B). Secondly, percentage weight change relative to the starting weight was calculated and where the reduction in the body mass of the animals treated with CM was significantly different at week 90 (p = <0.05) (Figure 3.2 C). Percentage weight change during the latter weeks then became increasingly variable, particularly within the Old CM cohort.

Strength and activity assessment shows a decline in grip strength with age

Animal functional studies were conducted to examine the maximum force exerted in the aged animal cohorts (CM or PBS vehicle), as assessed using a grip strength monitor, as well as motor coordination measured using rotarod performance testing. Average grip strength decreased incrementally with age, where forces normalised to body weight, measured in all latter months tested (21 to 24), were all significantly reduced when compared to that at 20 months old (p = <0.05 and <0.01) (Figure 3.2 D). Further declines in maximum force were observed after 21 months (p = <0.05 and <0.01), in a step-wise fashion, which decreased again from 22 to 23 months of age (p = <0.01). Subsequently, grip strength remained consistent and did not alter significantly between 23 and 24 months. Moreover, average force exerted by animals treated with CM, followed a similar declining trend with age as those measured in the PBS vehicle control cohort (Figure 3.2 E). However, the CM-treated animals measured a greater average grip strength in the latter weeks of the experiment, when compared to the PBS controls, to a statistically significant degree at 23 months (100 weeks) old (p = <0.05). Thereafter, force between the two treatment groups remained consistent.

Rotarod performance assessment indicated a large degree of variation in organismal motor coordination from 20 to 24 months of age (Figure 3.2 F). Initially, activity increased from 20 months to a peak performance measured at 21 months (p = <0.05). Following this, rotarod activity returned

Taryn Morash

to similar levels measured at the start of the experiment (20 months). Furthermore, CM treatment had no additional effects on motor coordination measurements during the progression of natural ageing from 20 to 24 months (Figure 3.2 G).
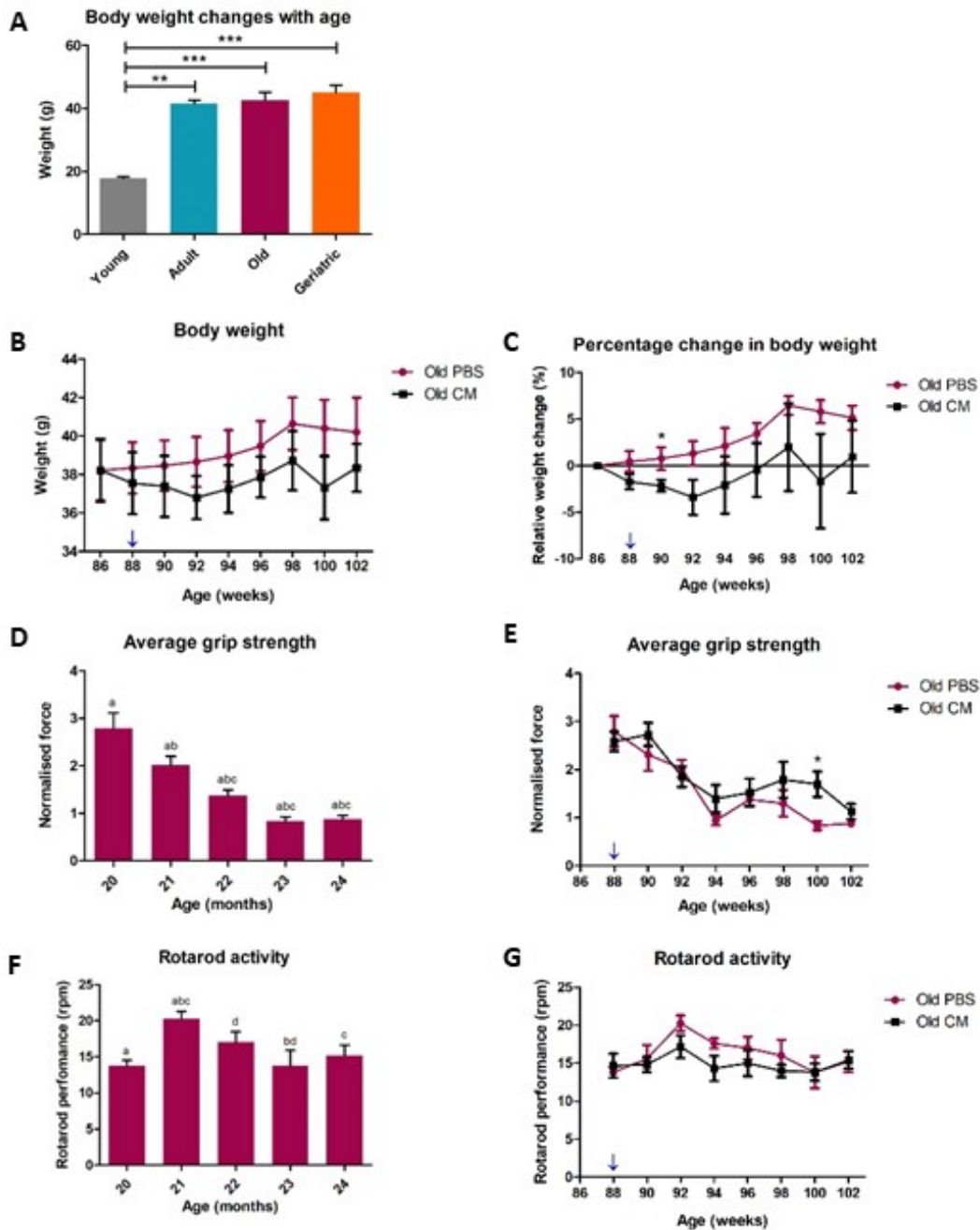
Figure 3.2 Investigating the effect of ADMSC CM (CM) on body mass, grip strength and rotarod performance with age. **(A)** Body weights of young (3 months), adult (6 months), old (24 months) and geriatric (27-30 months) C57BL/6 mice. **(B-C)** CM does not significantly impact on the body weights of old mice. **(D)** Functional assessment of the average grip strength of old mice, force normalised to body weight showed a decline in force exerted with increasing age. Significance indicated by

Taryn Morash

sequential letter pairings, from left to right (p = <0.05). **(E)** Grip strength was largely unaffected by CM in old mice, differing at 100 weeks of age only. **(F)** Rotarod activity in old mice was variable. Significance indicated by letter pairings (p = <0.05). **(G)** Rotarod activity in old mice was not influenced by CM treatment. The initiation of the CM/PBS treatment programme (blue arrows). *p<0.05, **p<0.01, ***p<0.001, **(A, D, F)** One-way ANOVA with Tukey post hoc testing, **(B, C, E, G)** Individual student's t-tests.

Increased fresh skeletal muscle weight with initial growth and declines with age evident in most hindlimb muscles analysed

Fresh hind-limb muscle weights were recorded at the time of dissection, prior to freezing and processing. All muscles analysed increased in weight from young ages and peaked at either adult or old ages, during the initial growth phase of the animals (p = <0.05). *Soleus* and EDL muscles increased from approximately 9mg at young ages to 13 - 14mg at old age (p = <0.05) (Figure 3.3 A, B). The TA increased from 38 to 48mg from young to adult ages (p = <0.001) (Figure 3.3 C). The *Gastrocnemius* peaked at approximately 140mg from 95mg between young and adult ages (p = <0.001) and the *Plantaris* increased from 14 to 22mg (p = <0.001) (Figure 3.3 D, E). Both the EDL and *Gastrocnemius* muscles remained at weights similar to those recorded at peak growth into advanced ageing and any changes shown were not statistically significant. The *Soleus* and TA muscles however, showed statistically significant decreases in weight during advanced ageing, after peaking during initial old ages (p = <0.05). Whereas, the *Plantaris* peaked at an adult age and decreased earlier in the ageing process (p = <0.001). CM treatment did not significantly affect the muscle weights in old age in the EDL, TA, *Gastrocnemius* or *Plantaris*. In the *Soleus* however, CM reduced the muscle weight at old age to those similar to geriatric, adult as well as young ages, approximately 9 - 10mg (p = <0.01).

Taryn Morash
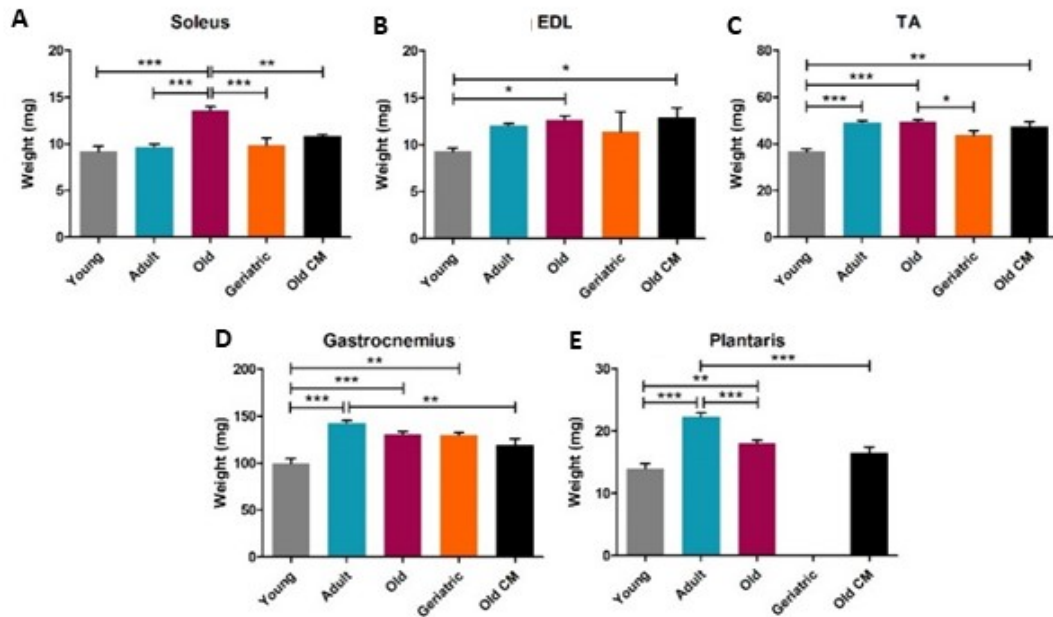
Figure 3.3 Fresh hindlimb muscle weights of young (3 months), adult (6 months), old (24 months), geriatric (27-30 months) and old CM-treated C57BL/6 mice. **(A)** *Soleus* weight. **(B)** EDL weight. **(C)** TA weight. **(D)** *Gastrocnemius* weight. **(E)** *Plantaris* weight (Geriatric data not available). *$p<0.05$, **$p<0.01$, ***$p<0.001$, One-way ANOVA with Tukey post hoc testing.

MHC isoform myofibre composition shift to a slower phenotype in the ageing *Soleus* muscle

The myofibre type (for example slow-twitch type I, fast-twitch type IIA, IIX and IIB) differs between muscle type, depending on function and has been shown to alter with age and the onset of sarcopenia (Alnaqeeb & Goldspink 1987; Chai et al. 2011; Rowan et al. 2011; Larsson & Edström 1986). The *Soleus* muscle consists of a higher proportion of type I, slow-twitch myofibres, has a high capillary density, high resistance to fatigue and high oxidative capacity (Alnaqeeb & Goldspink 1987; Omairi et al. 2016).

To ascertain an indication of how contractile, motor neuron innervation and metabolic functions might be changing during ageing, the myosin heavy chain (MHC) myofibre composition was examined. MHC was visualised and analysed using immunohistochemical staining of transverse cross-sections of the maximal, 'mid-belly' region of frozen *Soleus* muscles. Positive expression of the different MHC isoforms, types I, IIA and IIB (and negative IIX myofibres), as well as the total myofibre number were quantified for all four age groups, young, adult, old and geriatric, as well as old age with CM treatment.

Taryn Morash

Total myofibre numbers in the *Soleus* remained relatively consistent, approximately 850 - 950 myofibres, during young, adult and old ages (Figure 3.4 A). In advanced ageing however, myofibre numbers were significantly decreased to an average of 770 (p = <0.05). CM did not significantly increase the average number of myofibres in old age.

Regarding the MHC myofibre typing, it was shown that during the growth phase between young and adult, the percentage of type I myofibres increased significantly from 35 to 48%, respectively (p = <0.05) and to 56% at old and geriatric ages (p = <0.001, respectively) (Figure 3.4 B, C). Meanwhile, concordantly, the percentage of type IIA myofibres reduced from 54 to 44% during the young to adult growth phase, respectively (p = <0.01) (Figure 3.4 B, D). Percentages of type I and IIA after this age (adult), did not vary significantly and the *Soleus*, a predominately oxidative muscle, continued to remain approximately 60% type I into geriatric ages. IIX and IIB myofibre types represented only a small percentage (less than 5%) of the myofibres comprising the slow twitch *Soleus* muscle and shows a further switching of the fastest type IIB myofibres to slower types (for example type I), where there were no IIB observed at old and geriatric ages, relative to young and adult ages (p = <0.01 and <0.001, respectively) (Figure 3.4 B, E). CM treatment in old age had no significant effects on the MHC myofibre type composition (Figure 3.4 A-F).

Taryn Morash
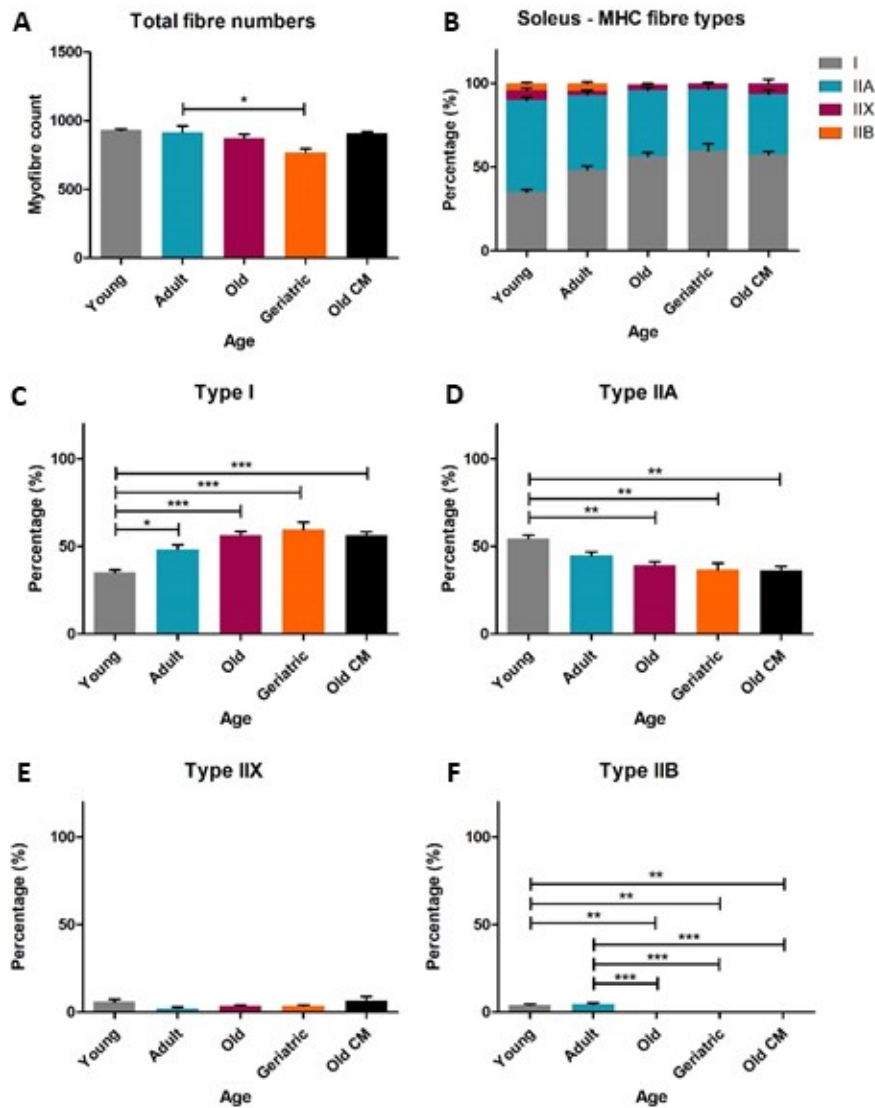
Figure 3.4 The effect of ADMSC CM (CM) and ageing on Myosin heavy chain (MHC) isoform myofibre composition of the *Soleus* muscle. **(A)** Quantification of the total myofibre number in the *Soleus*, saw a reduction at a geriatric age. **(B)** Overall MHC myofibre type composition shows a switch to a slower phenotype with increasing age. **(C)** Proportion of MHC type I myofibres increases with age. **(D)** Proportion of MHC type IIA myofibres decreases with age. **(E)** Proportion of MHC type IIX myofibres remains unchanged. **(F)** Proportion of MHC type IIB myofibres decreases with age. $*p < 0.05$, $**p < 0.01$, $***p < 0.001$, One-way ANOVA with Tukey post hoc testing.

Changes in myofibre cross-sectional area (CSA) in the ageing *Soleus* muscle

In analysing the myofibre cross-sectional area (CSA), it can be determined what morphometric changes occur in ageing myofibres, which has been shown to be a key determinant of muscle force-

Taryn Morash

generating capacity and contributes to the overall effects or symptoms of sarcopenia (Degens & Alway 2003; Larsson & Edström 1986; Ansved & Larsson 1989). CSA analysis was performed and recorded by MHC myofibre type in order to establish any fibre type-specific trends.

Cross-sectional area of type I myofibres did not change dramatically between the four age groups or with CM treatment in the *Soleus* (Figure 3.5 A). Type IIA myofibres showed an increased CSA, peaking at old age ($1800\mu m^2$) when compared to young ($\sim1000\mu m^2$, p = <0.01) and maintaining this level of hypertrophy into advanced ageing (Figure 3.5 B). The CSA of type IIX myofibres however, was extremely variable due to the low number of IIX myofibres that represented only a very small proportion (less than 5%) of the *Soleus*, as previously discussed (Figure 3.5 C). Similarly, the observed increase in the IIB CSA between young and adult ages was not statistically different due to the large range in size of the small proportion of IIB myofibres, leading to variability in the data (Figure 3.5 D). There was no significant difference in CSA in any of the myofibre types in old age treated with CM (Figure 3.5 A, B, C).
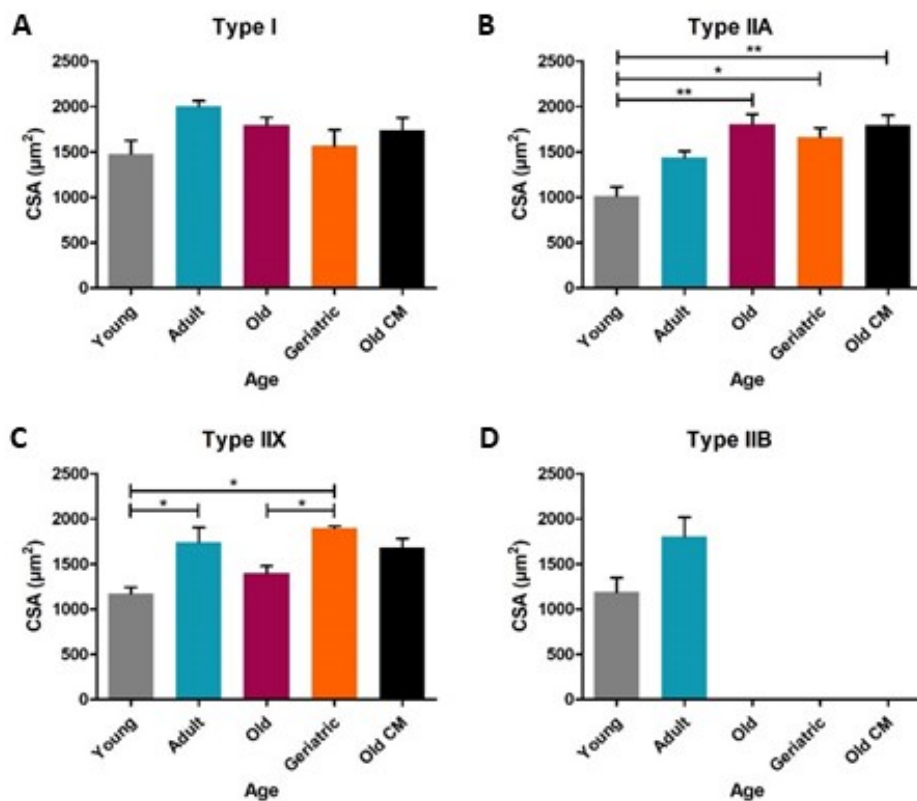
Figure 3.5 Determining the influence of ADMSC CM (CM) and ageing on Myosin heavy chain (MHC) isoform myofibre cross-sectional area (CSA) of the *Soleus* muscle. **(A)** MHC type I myofibre CSA. **(B)** MHC type IIA myofibre CSA. **(C)** MHC type IIX myofibre CSA. **(D)** MHC type IIB myofibre CSA. *p<0.05, **p<0.01, One-way ANOVA with Tukey post hoc testing.

Taryn Morash

Oxidative capacity is reduced in the ageing *Soleus*

It is reported in the literature that there is a switch from faster, glycolytic myofibres to those of a slower, more oxidative nature in the ageing *Soleus* (Alnaqeeb & Goldspink 1987; Rowan et al. 2011; Larsson & Edström 1986). Along with accumulation of DNA damage and loss of proteostasis during ageing, mitochondrial dysfunction and increased oxidative stress are also key factors that can exacerbate overall functional decline (López-otín et al. 2013; Pieczenik & Neustadt 2007). Therefore, importantly, parameters that indicate the degree that metabolic function and some of these aspects of the 'hallmarks of ageing' were altered in the naturally aged *Soleus* muscles, were investigated in the current study.

The histological succinate dehydrogenase (SDH) staining protocol was carried out on *Soleus* muscle transverse cross-sections to analyse the metabolic status of myofibres. SDH-positive oxidative myofibres formed approximately 55 – 60% of the total myofibres during young, adult and old ages (Figure 3.6 A). Although, at geriatric ages, the percentage oxidative myofibres decreased to 45% (p = <0.05).

Despite the proportion of oxidative myofibres at old age being maintained at levels observed at young and adult ages, CM treatment significantly increased the average oxidative myofibres to 69% of the total (p = <0.01). The increase observed with CM treatment in old animals was also statistically significant when compared to both young and adult age groups (p = <0.05).

Vasculature organisation of the *Soleus* remains constant during ageing but CM treatment increases myofibre capillary density

In order to further investigate the mechanisms underpinning the changes observed in metabolic function in advanced ageing as well as CM treatment, vasculature organisation was explored. Firstly, the number of capillaries was measured through the quantification of CD31+ cells per myofibre.

The number of capillaries serving each fibre was shown to increase during the initial young to adult growth phase (2.5 to 3.8, respectively, p = <0.05) (Figure 3.6 B). This capillary density profile was seemingly maintained in the ageing *Soleus* at old and geriatric ages. As with the trend observed previously with the percentage oxidative myofibres and furthermore, despite the capillary density profile being maintained at adult levels into old age, treatment with CM further increased the number of capillaries per fibre to 4.3 (p = <0.05).

Secondly, qPCR analysis of a member of the vascular endothelial growth factor (VEGF) family of genes responsible for roles in regulating angiogenesis and vasculogenesis was analysed in the ageing *Soleus* and indicated that relative levels of mRNA expression between the four age groups (young,

Taryn Morash

adult, old and geriatric) were not significantly different (Figure 3.6 C). The CM group showed increased levels of *VEGFα 165* when compared to the geriatric age group ($p = <0.05$) but was not significantly different to the old control or any other group.

Reactive oxygen species (ROS) production is greater in the ageing *Soleus* and CM harbours apparent antioxidant properties

It is well established in the literature that mitochondrial dysfunction is highly implicated in multiple pathological and toxicological conditions as well as age-related degeneration, including sarcopenia (Pieczenik & Neustadt 2007). As well as this, DNA, but particularly mitochondrial DNA (mtDNA), is extremely susceptible to damage and one of the sources of damage is reactive oxygen species (ROS) produced by the mitochondria themselves (Pieczenik & Neustadt 2007). Therefore, as a measure of oxidative stress in the ageing muscles in current study, the ROS, superoxide (O_2^-) was detected using a small-molecule fluorescent dye known as dihydroethidium (DHE). DHE fluorescence intensity was measured within small and large myofibres of *Soleus* muscles for each age group, as well as with CM treatment in old age. Firstly, it was observed that there was a higher intensity of DHE fluorescence within the centre of smaller myofibres than larger-sized myofibres however this difference was statistically significant in geriatric age group only ($p = <0.01$) (Figure 3.6 D). When analysing the small myofibres only, it appeared that superoxide production increased slightly with age with levels peaking at geriatric age (with a relative intensity of approximately 9 to 13.3a.u.) (Figure 3.6 E). Although due to a large amount of variation, the increase observed was not statistically different to younger age groups. Interestingly, a decreased DHE fluorescence intensity was measured in old age when treated with CM when compared to the 'old' control and geriatric groups ($p = <0.01$ and <0.05, respectively). A statistically significant increase in DHE intensity was noted in the large myofibres between young and old age groups ($p = <0.05$) and the reduction seen with CM treatment in old age was not statistically different from the aged control (Figure 3.6 F).

Mitochondrial superoxide dismutase (SOD2) is a manganese superoxide dismutase (MnSOD) that catalyses the mutating of O_2^- into hydrogen peroxide (H_2O_2) which in turn, is transformed into H_2O by catalase, glutathione peroxidase (GPX) or peroxidredoxin III (PRX III) (Pieczenik & Neustadt 2007; Green et al. 2004). Therefore, SOD2 is an enzyme responsible for mitochondrial antioxidant activity and as previously shown with DHE analysis, an increase in superoxide levels within myofibres could indicate dysfunctional antioxidant regulation. Next, qPCR analysis was carried out to investigate any observed changes with age in SOD2 gene expression. It was shown that SOD2 levels did not alter significantly from young to advanced old ages and remained consistent throughout the murine lifespan (Figure 3.6 G). Moreover, CM treatment had no additional effects on expression.

Taryn Morash
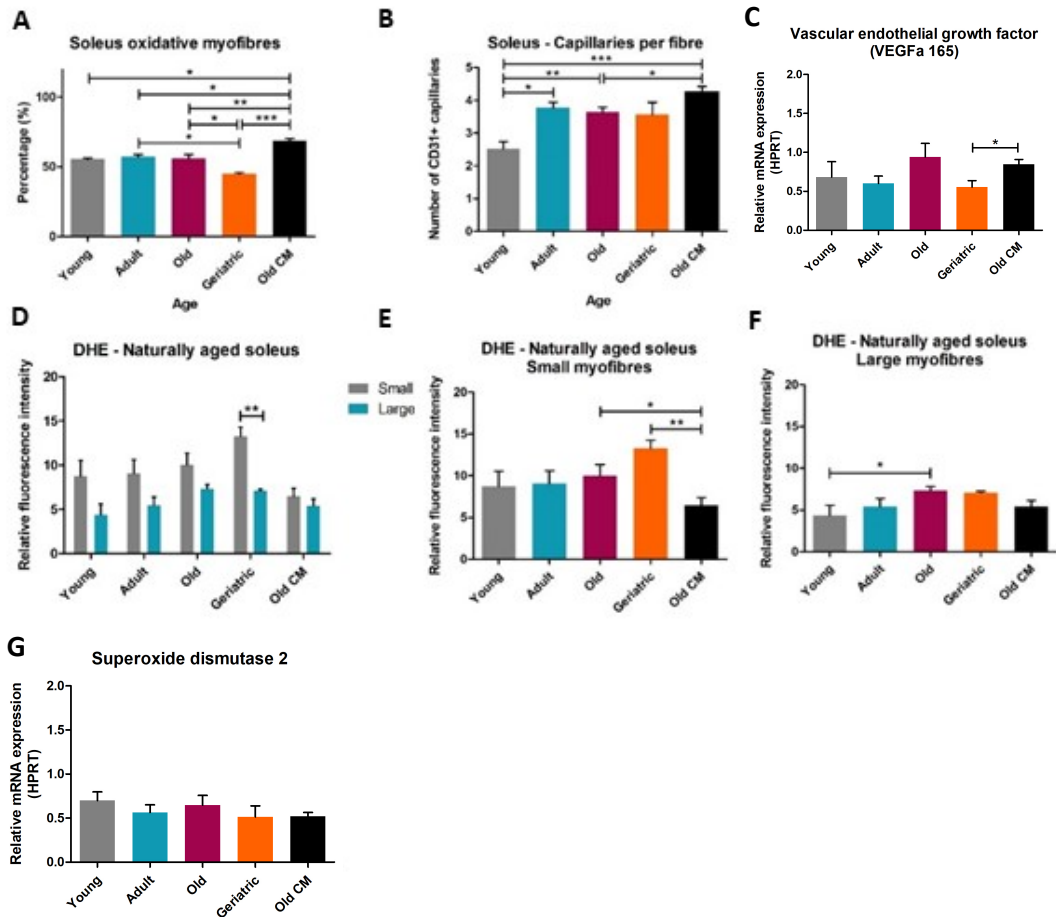
Figure 3.6 The effect of ADMSC CM (CM) and ageing on the metabolic status, vasculature organisation and mitochondrial function of the *Soleus*. **(A)** Proportion of myofibres positive for succinate dehydrogenase (SDH) staining to assess the oxidative capacity. **(B)** Capillary density (CD31+ cells per fibre). **(C)** VEGFa 165 mRNA expression. **(D)** Dihydroethidium (DHE) fluorescence intensity indicating ROS production is greater in small myofibres **(E)** Quantification of ROS production in small myofibres. **(F)** Quantification of ROS production in large myofibres. **(G)** Antioxidant superoxide dismutase 2 (SOD2) mRNA expression. *p<0.05, **p<0.01, ***p<0.001, **(A-C, E-G)** One-way ANOVA with Tukey post hoc testing. **(D)** Individual student's t-tests.

Changes in collagen IV density and dystrophin glycoprotein complex (DGC) components of the ageing *Soleus* extracellular matrix (ECM) and CM modifies connective tissue content

Collagen is a key component, along with other proteins and lipids, of the basal lamina of skeletal muscle and it is has been previously reported in the literature that collagens become more dense and tightly cross-linked, losing elasticity with age. Therefore, these changes in the extracellular matrix

107

Taryn Morash

components impact on the muscle's overall contractility, as well as on the essential mechanisms underpinning satellite cell regeneration following damage or injury, such as emergence through the basal lamina and migration.

Collagen IV, a basement membrane component surrounding each myofibre, was analysed using an immunofluorescence protocol of transverse cross-sections of the ageing *Soleus*. Collagen thickness was measured and categorised based on border type, dependent on MHC myofibre types. For example, borders between type I myofibres and those between non-type I myofibres.

Firstly, there was a notable difference between the two types of border with non-type I borders having a thicker collagen layer than type I in adult and old ages, with and without CM treatment (p = <0.05 and <0.01) (Figure 3.7 A). Secondly, with age, collagen thicknesses increased incrementally with the growth of the animal from young to adult (p = <0.001) and again into old age (p = <0.05) in borders between type I myofibres (Figure 3.7 B). Thickness subsequently decreased from a peak thickness of 2.9µm at old age to 2.4µm at geriatric ages (p = <0.01) but did not reduce to levels previously measured at young ages, 1.7µm (p = <0.001). Interestingly, CM treatment reduced collagen thickness in old age from 2.9µm to 2.3µm (p = <0.001).

Collagen thickness of borders between non-type I myofibres also showed similar trends as those observed with type I. A steady increase in collagen width was measured during the initial growth phase from young to adult and further still from adult to old age to a peak thickness of 3.5µm (p = <0.05, respectively) (Figure 3.7 C). As before, CM attenuated the collagen thickness (2.8µm) in the basement membrane of myofibres in *Soleus* muscles from old-aged mice (p = <0.05).

Moreover, collagen content within ageing *Soleus* muscles was further investigated using qPCR analysis to determine the relative expression levels of genes coding for components of collagen I and collagen IV (*Col1A1* and *Col4A1*, respectively). Collagen I is a highly abundant, key structural protein of skin, bone, dentin, tendons and the endomysium of myofibrils as well as in fibrous scar tissue following repair (Light & Champion 1984; Orgel et al. 2006).

Collagen I analysis indicated an evidently large degree of variation, therefore any observed differences were not statistically significant (Figure 3.7 D). Although, there was a statistically significant decrease in collagen IV expression in geriatric *Soleus* muscles when compared to all other age groups (p = <0.05) (Figure 3.7 E). Additionally, treatment with CM had no effect on the mRNA level of collagen IV at old age.

Two further genes that code for essential components of the dystrophin glycoprotein complex (DGC), responsible for linking the myofibre cytoskeleton to the extracellular matrix, were examined using

Taryn Morash

qPCR analysis. Dystrophin is located on the inside surface of the myofibre sarcolemma (plasma membrane) and has the primary role of connecting actin filaments with other supporting signalling and adaptor proteins to the endomysium for the structural and mechanical stability of myofibres during muscle contraction. Sarcoglycans, although constitute a sub-set of the DGC bound to dystrophin, are the transmembrane protein component of the complex. Components of the DGC are believed to have essential sensing and signalling roles in mechanotransduction, in response to myofibre loading. Along with the lack of dystrophin in Duchenne muscular dystrophy (DMD), the structural integrity of the myofibre basal lamina, extracellular matrix interactions, as well as this mechanosensing response, are all implicated (Goldspink 1999). Dystrophin and beta-sarcoglycan, members of the DGC, were examined in the present study to investigate the possible shared myo-pathological dysfunction demonstrated in DMD, in ageing. Furthermore, changes in DGC components could indicate a source of muscle weakness and declined force-generating capacity in ageing.

The relative mRNA of both dystrophin (coded by the *DMD* gene) and beta-sarcoglycan (*sgcb*) during ageing showed a similar trend of increased expression between adult and old age (p = <0.05 and <0.01, respectively) (Figure 3.7 F, G). There were no significant differences in the expression of these genes coding ECM binding proteins in any other age groups nor in old age with CM treatment.

Taryn Morash
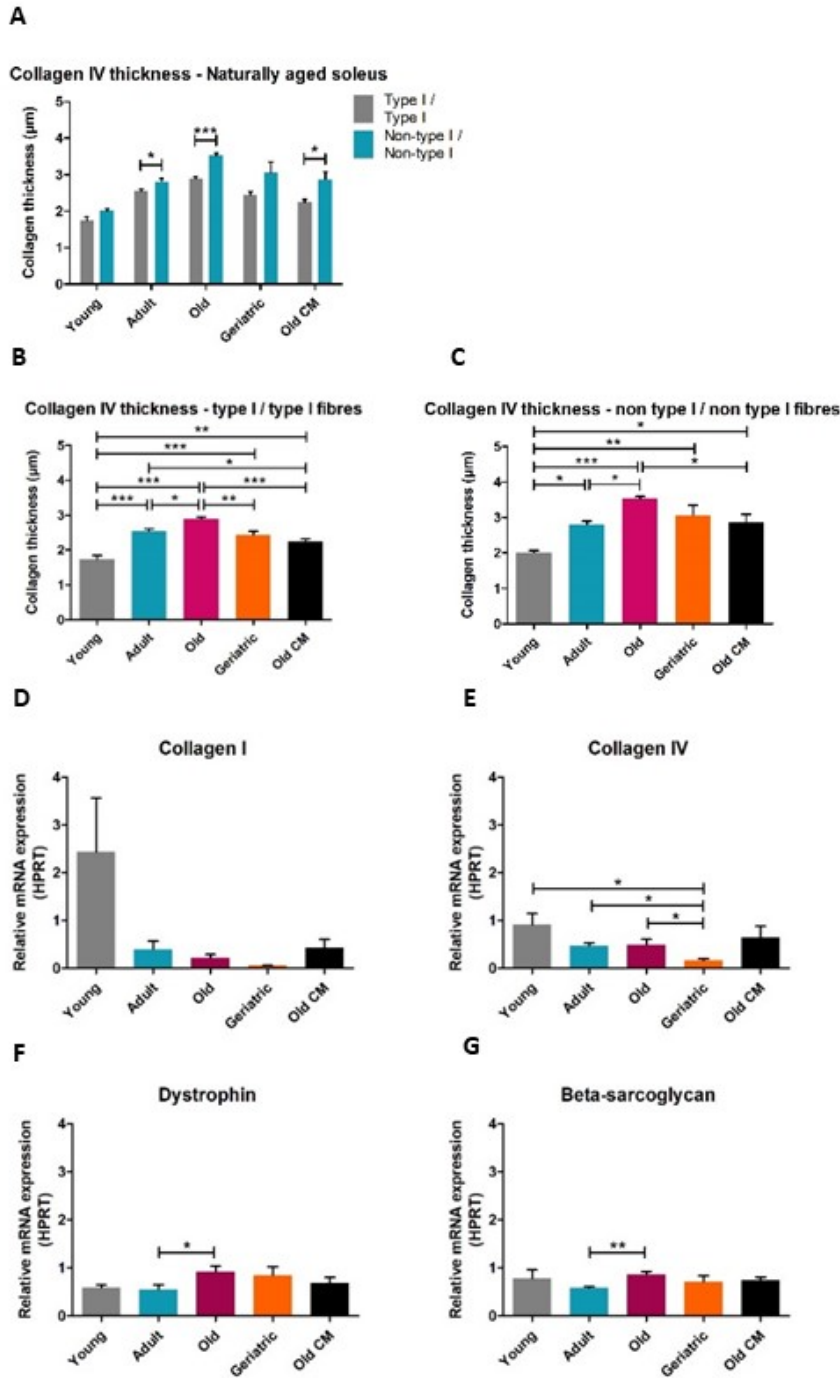
Figure 3.7 Investigating the influence of ADMSC CM (CM) and ageing on collagen content and structural components of the dystrophin glycoprotein complex (DGC) in the *Soleus*. **(A)** Collagen IV thickness between MHC myofibres, type I border with another type I. Non-type I border with a second non-type I myofibre **(B)** Collagen IV thickness in type I myofibre borders **(C)** Collagen IV thickness in non-type I myofibre borders **(D)** Collagen I mRNA expression **(E)** Collagen IV mRNA expression **(F)** Dystrophin mRNA expression. **(G)** Beta-sarcoglycan mRNA expression. *p<0.05,

Taryn Morash

MHC isoform myofibre composition shift to an even faster phenotype in the ageing EDL muscle

The ageing profile of the *Soleus*, a muscle more oxidative in nature, was then compared to that of the EDL, a faster, more glycolytic muscle type. This aimed to establish the extent of the impact of observed changes associated with the onset of sarcopenia in two distinct, metabolically diverse hindlimb muscles. As with the *Soleus*, transverse cross-sections of the EDL muscle were examined using an immunohistochemical protocol for the visualisation and analysis of the MHC isoform content of individual myofibres. MHC fibre types (I, IIA, IIX and IIB) were quantified across the maximal, mid-belly region of each EDL at young, adult, old and geriatric ages including an old age cohort treated with CM.

Firstly, total myofibre number indicated a reduction with age from approximately 1100 myofibres at young and adult ages to 840 at old-age (p = <0.05 and <0.001, respectively) (Figure 3.8 A). Myofibre number at geriatric age however, was not significantly different from that at any other age group. There was also no statistically significant difference in the total number of myofibres in old age with CM when compared to the control old-aged group.

Secondly, MHC myofibre typing analysis showed less than 1% of the total fibres in all age groups were slow-twitch type I (Figure 3.8 B, C). Additionally, between 10 - 17% of total myofibres, consistently across all four age groups as well as CM treatment, were type IIA (Figure 3.8 B, D). However, there was an observed reduction in the percentage of IIX myofibres with age (Figure 3.8 B, E). From adult to old age, the percentage of IIX fibres decreased from 14.5 to 8.4% (p = <0.001). Moreover, geriatric EDLs contained the smallest proportion of IIX fibres (4.9%), significantly fewer than at young (12.7%) and adult (14.5%) ages (p = <0.05 and <0.001, respectively) as well as at old age with CM, 10.5% (p = <0.05). CM treatment did not significantly affect the percentage of IIX fibres at old age. Furthermore, an observed switch to an even faster phenotype with age was noted, with an increased proportion of total myofibres identified as type IIB from adult (68%) to old (78%) ages (p = <0.001) (Figure 3.8 F). Although significantly greater than the proportion measured in adulthood (p = <0.05), treatment during old age with CM was not statistically different from the old age control cohort.
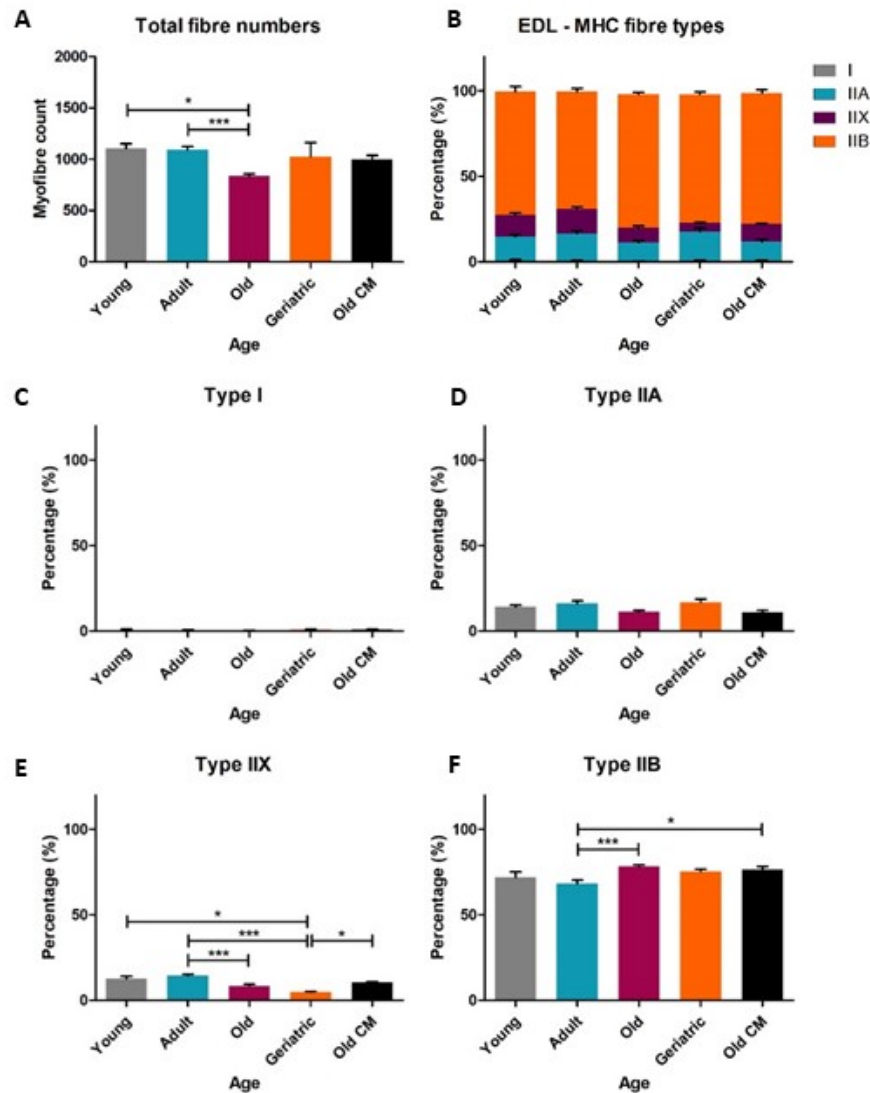
Figure 3.8 Examining the effect of ADMSC CM (CM) and ageing on Myosin heavy chain (MHC) isoform myofibre composition of the EDL muscle. **(A)** Quantification of the total myofibre number. **(B)** Overall MHC myofibre type composition. **(C)** Proportion of MHC type I myofibres. **(D)** Proportion of MHC type IIA myofibres. **(E)** Proportion of MHC type IIX myofibres. **(F)** Proportion of MHC type IIB myofibres. *$p<0.05$, ***$p<0.001$, One-way ANOVA with Tukey post hoc testing.

Changes in myofibre cross-sectional area (CSA) in the ageing EDL muscle

As in the *Soleus*, Myofibre CSA was measured by MHC isoform in order to further examine any myofibre morphometric changes in the ageing EDL. Average type I myofibre CSA did not vary with age, unlike those measured in type IIA fibres that indicated an age-related increase, peaking at geriatric age (~630µm^2), statistically significant when compared to the young (~440µm^2) age group (*p*

Taryn Morash

= <0.05) (Figure 3.9 A, B). Type IIX and IIB myofibres, like type I, appeared to exhibit a reduced degree of variation with age progression, regarding relatively consistent average CSAs between all age groups (650 – 800µm², 1300 – 1400µm² and 400 - 500µm² approximate size ranges, respectively) (Figure 3.9 C, D). CM treatment showed a decreased CSA in type IIB myofibres when compared to the adult age group (p = <0.05) however, CM did not affect myofibre size in old age.
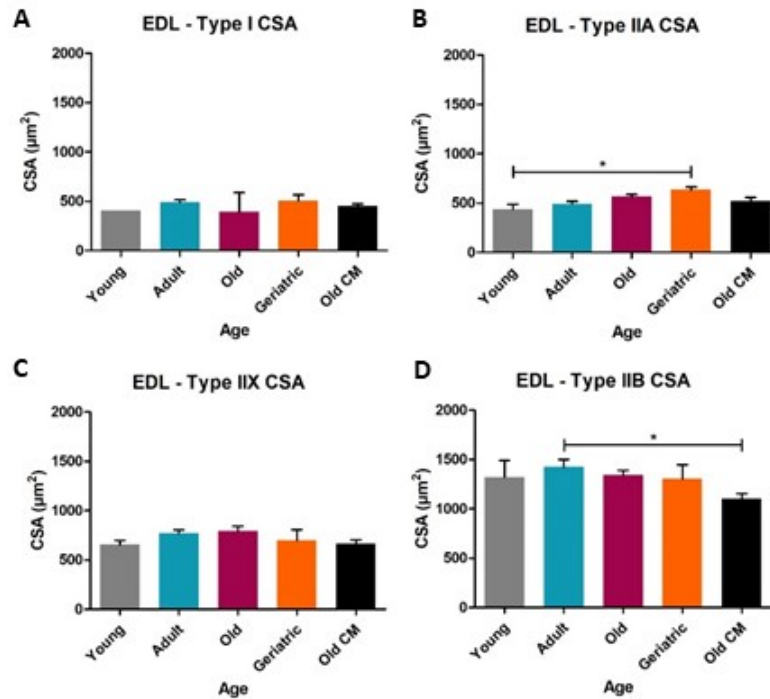
Figure 3.9 The effect of ADMSC CM (CM) and ageing on Myosin heavy chain (MHC) isoform myofibre cross-sectional area (CSA) of the EDL muscle. **(A)** MHC type I myofibre CSA. **(B)** MHC type IIA myofibre CSA. **(C)** MHC type IIX myofibre CSA. **(D)** MHC type IIB myofibre CSA. *p<0.05, One-way ANOVA with Tukey post hoc testing.

Oxidative capacity remains unchanged in the ageing EDL

As previously discussed, unlike the *Soleus*, the EDL is a predominantly glycolytic muscle with distinctly diverse metabolic characteristics. In order to better understand some of the changes observed in the more glycolytic muscle with age as well as those reported in the literature, metabolic function in the ageing EDL was investigated.

To examine the metabolic status of myofibres, the histological succinate dehydrogenase (SDH) staining protocol was carried out on transverse cross-sections of the EDL muscle from 5 cohorts, at young, adult, old and geriatric ages as well as with CM treatment during old age. It was observed that

Taryn Morash

approximately 45 - 49% of total myofibres were SDH-positive during young, adult, old and geriatric ages (Figure 3.10 A). CM treatment during old age did not significantly increase the percentage of SDH-positive myofibres compared to any other age or treatment group.

Vasculature organisation is not altered by CM treatment in the ageing EDL

As discussed, a key component of metabolic function is oxygen delivery and as previously shown with the SDH analysis, there were no observed changes in the proportion of oxidative myofibres in the ageing EDL muscle and CM treatment during old age did not have any significant effects. Vasculature organisation was investigated in order to further understand the features under-lying metabolic regulation and how these are affected during ageing of a primarily glycolytic muscle. As with the *Soleus*, CD31+ cells were quantified per myofibre to examine the effect of CM during old age on the number of capillaries. However, unlike in the *Soleus*, CM had no effect on the number of CD31+ cells at old age in the EDL. (Figure 3.10 B).

Reactive oxygen species (ROS) production increases in the large myofibres of the ageing EDL and CM displays antioxidant potential

ROS production and oxidative stress, as previously discussed, are believed to have key negative impacts on mitochondrial function and the onset and progression of age-related degeneration (Pieczenik & Neustadt 2007; López-otín et al. 2013). Therefore, as before with the *Soleus*, dihydroethidium (DHE) fluorescence intensity within myofibres was measured to detect mitochondrial superoxide (O_2^-) ROS production. DHE fluorescence intensity was compared in both small and large myofibres of muscles from animals treated with CM during old age and compared to that in adult EDLs. As seen in the *Soleus* muscle, there was a statistically greater intensity of DHE fluorescence within the centre of smaller myofibres compared to larger-sized myofibres in both adult and old ages as well as with CM treatment ($p = <0.05$ and <0.001, respectively) (Figure 3.10 C). DHE intensity did not significantly differ in the smaller myofibres with age nor with CM treatment (Figure 3.10 D). However, the increase in fluorescence intensity between adult and old age and the subsequent reduction with CM treatment, were statistically significant ($p = <0.05$ and <0.01, respectively) (Figure 3.10 E).

Myofibre collagen IV density increases with age in the EDL

As collagen thickness is believed to be a key component implicated in reduced contractile ability in disease as well as in sarcopenia as previously discussed, additionally in the current study, the collagen IV thickness was measured in the EDL. As carried out previously with the *Soleus* muscle, collagen IV was visualised using an immunofluorescence protocol of transverse cross-sections and

Taryn Morash

thickness was measured by MHC myofibre border type. For example, borders between type IIB myofibres and those between non-type IIB myofibres.

An observed difference in collagen IV thickness between MHC border type was indicated. A thicker layer of collagen in non-type IIB borders was measured when compared to that between type IIB myofibres, this difference however was statistically significant in old-age only, 2.6 and 2.2µm, respectively (p = <0.05) (Figure 3.10 F). When analysing the thickness of collagen in type IIB borders alone, an incremental increase with age was noted, with a thickness of 1.7 - 1.8µm at young and adult ages, peaking at 2.5µm at a geriatric age (p = <0.05) (Figure 3.10 G). Similar trends were observed when analysing the thickness of collagen IV between non-type IIB myofibres. For example, a peak thickness was also measured at a geriatric age, which showed a significant increase from 2µm at adult ages to 2.8µm at geriatric age (p = <0.05) (Figure 3.10 H). The collagen thickness in both type IIB and non-type IIB borders, between adult and old age, was statistically non-significant. Furthermore, CM treatment did not significantly affect type IIB collagen IV thickness in old age, in either MHC border type.

Taryn Morash
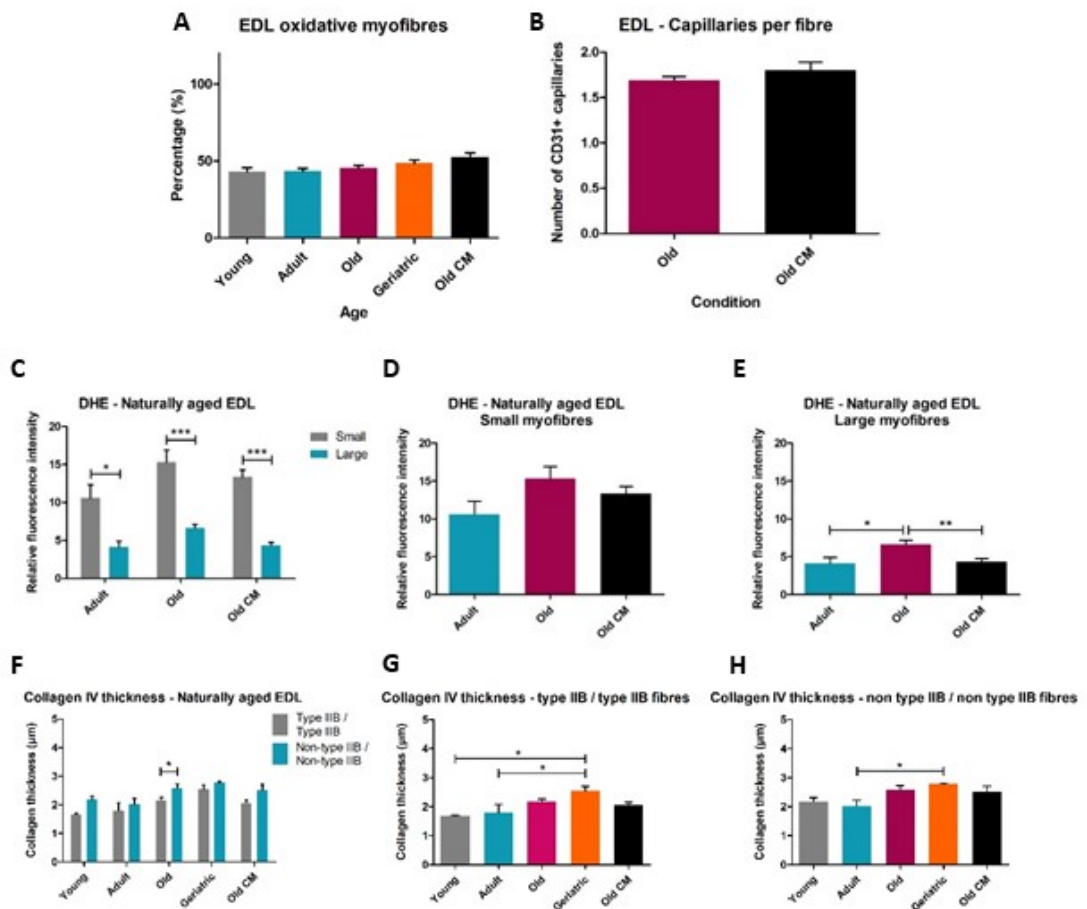
Figure 3.10 The effect of ADMSC CM (CM) on the metabolic status, vasculature organisation, mitochondrial function and collagen content of the ageing EDL. **(A)** Proportion of myofibres positive for succinate dehydrogenase (SDH) staining to assess the oxidative capacity. **(B)** Capillary density (CD31+ per myofibre). **(C)** Dihydroethidium (DHE) fluorescence intensity indicating ROS production is greater in small myofibres **(D)** ROS production in small myofibres. **(E)** ROS production in large myofibres. **(F)** Collagen IV thickness between MHC myofibres, type IIB border with another type IIB. Non-type IIB border with a second non-type IIB myofibre **(G)** Collagen IV thickness type IIB/ type IIB myofibre border **(H)** Collagen IV thickness non-type IIB/ non-type IIB myofibre border *p<0.05, **p<0.01, ***p<0.001, **(A, D, E, G, H)** One-way ANOVA with Tukey post hoc testing. **(B, C, F)** Individual student's t-tests.

Taryn Morash

Discussion

The hADMSCs that were used to generate the CM in the present study, were a commercially available cell line that have been fully characterised in their expression of numerous stem cell markers of multipotency, including CD29, CD44, CD73, CD90, CD105 and CD166 while being negative for CD14, CD31, CD45 and Lin1. It is well-established that ADMSC multipotency can be demonstrated by the ability to differentiate towards not only an adipogenic lineage, but also towards osteogenic and chondrogenic specifications (Baglio et al. 2012; Condé-Green et al. 2016). Importantly, this feature was retained following CM generation in the present study, indicating that the secretome collected was indeed that produced by stem cells. Additionally, it was observed that ADMSC growth media control cells also initiated progression down their typical adipogenic lineage, evident by the formation of lipid droplets in the adipogenesis control cultures. Furthermore, it was noted that under pellet culture conditions, to facilitate the differentiation towards a chondrogenic lineage, the growth media control ADMSCs were also observed as positively-stained for Alcian blue, visibly no different to the positive differentiation media culture. This indicates that the pellet culture system alone was sufficient in directing ADMSCs to a chondrogenic lineage. Therefore, this indicates the importance of growth factor influences and those directed by culture and ECM conditions in directing ADMSC lineage specification. Nevertheless, these findings demonstrate the differentiation potential of the ADMSCs following CM generation. CM was also tested using a robust assay and a protective effect against H_2O_2 stress-induced cellular senescence, was observed. CM treatment tested at concentrations of both 1 and 10% resulted in a reduction in positively-stained SA-β-gal cells to the level of the unstressed control. However, it should be noted that the unstressed control displayed an unexpectedly high proportion of senescent cells, nevertheless, the efficacy of CM treatment in providing protection despite this, was evident. This finding indicates that importantly, properties maintained by the CM in the present study demonstrate regulatory effects involved with the mechanisms of senescence, cell cycle arrest and survival. Of which, these are key mechanisms known to become dysregulated with age, leading to decreased proliferation and differentiation capacities, for example.

The design of the naturally-aged *in vivo* CM series of experiments has enabled the investigation of a variety of research parameters at a range of tissue levels, in order to develop a broad murine ageing profile of multiple aspects, in order to assess the potential therapeutic effect of ADMSC CM. (**A**) It was determined that sarcopenia was indeed evident by the loss of muscle mass, however this was primarily observed at a geriatric age. (**B**) Key phenotypical features were explored and indicated a reduced total myofibre number, an increase in metabolic dysfunction, increased ROS production and

Taryn Morash

evidence of a fast to slow MHC switch of myofibres in the ageing *Soleus*. There was however, a switch in the reverse direction, from fast to an even faster phenotype in the EDL. (**C**) ADMSC CM treatment in aged animals did not appear to influence features such as the overall myofibre number, size or type, although there is some evidence for potential modification of signalling pathways involved in angiogenesis, oxidative metabolism, reduced ROS production/increased antioxidant activity, as well as collagen organisation.

Measurements recorded at a whole organism level indicated that with an initial growth phase in young female C57BL/6 mice, body mass dramatically increased between 3 and 6 months of age. Hereafter, weight appeared to plateau, into old and advanced old age. This finding is consistent with those in other studies, although some also describe that the increase in weight continues until 12 months, at which point thereafter, remains constant or in some cases, declines into advanced old age (Glatt et al. 2007; Halloran et al. 2002; Lessard-Beaudoin et al. 2015; Marino 2012; Fahlstrom et al. 2011). Mice are reported to undergo a rapid increase in body mass with initial growth, during the first 4 weeks and continue to grow and gain weight over a considerable portion of their life-span (Fahlstrom et al. 2011; Turturro et al. 1999; Glatt et al. 2007). Changes in body mass with age have been attributed to, among others, alterations in features of body composition. For example, one study conducted in mice up to 20 months of age, described steady increases in body mass and total body bone mineral density (BMD), as well as a distinct increase in percentage body fat between 6 and 12 months (Glatt et al. 2007). In humans, peak bone mineral density is achieved between the ages of 10 and 19 years and bone mineral content (BMC) however, this continues to increase until approximately 35 years of age (Halloran et al. 2002). Additionally, in human ageing studies, body compositional parameters such as lean mass, BMD and BMC were all significantly reduced in old age (Halloran et al. 2002; Jiang et al. 2015; Riggs et al. 1981). Moreover, it has been suggested that age-related changes in bone architecture and mass in mice were remarkably similar to those observed in human ageing (Halloran et al. 2002). Interestingly however, the old and geriatric animals in the current study did not experience this decline in body mass, which has been reported by some others in advanced old age, despite the geriatric animals having a particularly frail appearance and structure at the experimental end-point. The old animals, contrastingly, had a reasonable amount of white adipose tissue visible upon tissue harvesting at the experimental end-point. This potentially indicates a certain level of inactivity in old age. As it is also well-known in the literature, that actively contracting muscle, during exercise for example, releases myokines which, among other characteristics, modifies the metabolic phenotype of adipose tissue, enhancing browning and fatty acid oxidation (Boa et al. 2017; Pedersen 2009).

Taryn Morash

Functional tests have been used as assessments of motor function and strength and reportedly, young C57BL/6 mice improve rotarod performance remarkably between 1 and 3 months of age. However, this parameter as well as grip strength measurements are both shown to decline with age (Fahlstrom et al. 2011; Serradj & Jamon 2007). Therefore, the decreasing average grip strength in the relatively short experimental duration in the current study, from 20 to 24 months of age, is in keeping with the declining trends described in the literature, however, this was not the case with rotarod testing. Studies utilising extracted slow (β) myosin, in an *in vitro* motility assay, showed that the changes to myosin with age contributed to slowed actomyosin interaction, effecting overall force-generating capacity (Höök et al. 1999).

Characterisation of the skeletal muscle phenotype in natural ageing

With an observed decline in grip strength exerted by aged animals, it can be reasonably postulated that aspects associated with the onset and progression of sarcopenia in the current study, are evident. By definition, sarcopenia has been attributed to a loss of muscle mass with age. Additionally, this is also accompanied by a reduction in contractile force-generating capacity associated with a certain degree of dysregulation and dysfunction of the musculature in ageing human and animal studies (Brooks & Faulkner 1991; Degens & Alway 2003; Klitgaard, Mantoni, et al. 1990; Larsson & Edström 1986; Rittweger et al. 2004). Initially increasing muscle mass with the normal post-natal growth phase of the animal, has been attributed to compensatory hypertrophy in response to a greater demand and load from initial increases in body weight and that fibre number usually remains constant during this phase (hypertrophy over hyperplasia) (Rowe & Goldspink 1969). The findings in the current study appear to be consistent therefore, with what has previously been reported in the literature, regarding the evidence for normal growth-related compensatory hypertrophy. Following this, weight subsequently decreased in most hind-limb muscles into old or geriatric ages. Thus, providing further indication of the onset and development of sarcopenia in the animals studied in the described series of experiments.

Despite the grip strength analysis being used to measure the force exerted by the forelimb muscles, we can postulate that declines in function, although differing between muscle types, are universal in the ageing muscle compartment. The *Soleus* muscle was selected for investigation, at a tissue level, into the changes that occur with age, due to the metabolic status being typically more oxidative in nature, primarily consisting of type I and IIA myofibres. In contrast, the EDL, was used not only to explore the effects of ageing on single myofibre cultures, but was examined and compared histologically at a whole muscle level, to the *Soleus*, as a representative muscle with relatively greater numbers of more glycolytic myofibres. A key feature of sarcopenia is myofibre atrophy, as

Taryn Morash

well as this, there is a well-established switch to those with a higher oxidative capacity with age (Alnaqeeb & Goldspink 1987; Chai et al. 2011; Rowan et al. 2011; Larsson & Edström 1986). Both were characteristics evident in the *Soleus* muscle of the current study, with distinctly fewer myofibres present at a geriatric age. As well as an apparent increase in slower MHC type I myofibres compared to young, with a corresponding decrease in faster type IIA. This switch in myofibre type has been associated with denervation of faster type II (IIX and IIB) and subsequent re-innervation of neighbouring slow-twitch myofibres, also believed to be the result of motor neuronal axon splitting (Faulkner & Brooks 1995; Demontis et al. 2013; Larsson & Ansved 1995). It has also been suggested that denervation/re-innervation processes resulted in rearrangement of myofibre types, namely IIX as an intermediate form assumed by myofibres under-going a slow to fast or a fast to slow shift (Larsson et al. 1991; Pette & Staron 2000). Further evidence of denervation/re-innervation with age, reported in the literature, is the presence of larger motor units, occupying a larger territory evident by MHC IIX grouping (Larsson et al. 1991). Alternatively, endocrine influences have been investigated regarding their effects on myofibre type composition. Thyroid hormones have been shown to be the hormones with the most substantial effect on changes in myofibre types, in particular, hypothyroidism initiates fast to slow transitions, whereas, hyperthyroidism causes transitions in the reverse direction, from slow to fast (Nwoye & Mommaerts 1981; Caiozzo et al. 1998; Li et al. 1996; Pette & Staron 2000). Therefore, changes in thyroid hormones with age may contribute, along with changing demand and load as well as selective motor neuron denervation and re-innervation to the overall changes seen in myofibre phenotype and alteration to force-generating capacity (Pette & Staron 2000). Additionally, denervation has been attributed to the majority of myofibre atrophy observed in aged rats (Rowan et al. 2012). It was also shown that type IIA myofibres appeared to be eliminated at a more advanced rate compared to faster types in the ageing rat *Soleus* and slower types seem to be less susceptible to atrophy (Larsson & Edström 1986; Rowan et al. 2011). Furthermore, a study conducted in human vastus lateralis muscles saw that type IIB myofibres are most susceptible to atrophy in ageing (Lexell et al. 1988). The findings of the current study are therefore, also in agreement with aspects of myofibre atrophy and the reported changes to MHC myofibre phenotype in the ageing *Soleus*.

The opposite trend however, was evident in the EDL, where an apparent switch from fast type IIX myofibres to an even faster phenotype was observed, with an increase in type IIB myofibres from adult to old age. Other than hyperthyroidism, a shift in this direction is typically the result of disuse, suggesting that the animals in the present study may have been experiencing a degree of inactivity, sufficient to elicit a phenotype change in the EDL but not in the *Soleus*. However, this type of slow to fast shift is more frequently linked to more complete disuse, for example from limb immobilisation

Taryn Morash

(Leeuwenburgh et al. 2005; Schwartz 2008; Schiaffino & Reggiani 2011). Reasons for the EDL shift discrepancy could also indicate that the characteristically slower *Soleus* muscle, could be more susceptible to influences towards an even slower phenotype (switch from IIA to I) and has a shorter transition 'journey' to travel in comparison to the faster EDL (IIB to IIX to IIA to I) (Schiaffino & Reggiani 2011). Otherwise, however, the reasons for this discrepancy with those previously reported are not clear. Although, despite the general agreement of a fast to slow shift, some other (human) studies, have alternatively, shown unchanged myofibre type proportions in ageing (Lexell et al. 1986; Lexell et al. 1988; Grimby et al. 1984; Kosek 2006).

Myofibre loss during old age was also apparent in the EDL, indicated by the considerable reduction in myofibre numbers compared to younger ages. Myofibre numbers observed at a geriatric age were slightly greater than those seen in old age. An explanation for this trend could be that frail myofibres, or those undergoing atrophy or degradation, split longitudinally giving the impression of greater numbers present (Alnaqeeb & Goldspink 1987). Suggesting that sarcopenia shows similar attributes to myo-pathological conditions, such as observed myofibre branching instead of supposed hyperplasia in Duchenne muscular dystrophy (DMD) (Faber et al. 2014). Although, it would be expected that in this case, there would be myofibres with greatly variable and reduced CSAs present (Alnaqeeb & Goldspink 1987). This trend was somewhat evident in the variation of type IIX and IIB CSA at geriatric ages. Analysis of serial sections spanning the entire length of the muscle would however, give a greater understanding of this phenomenon (Alnaqeeb & Goldspink 1987). As in the *Soleus*, CSA of the relatively small proportion of type IIA myofibres in the EDL, presented a degree of hypertrophy at a geriatric age. However, the number of IIA myofibres as well as total oxidative capacity remained comparatively unchanged. Aside from potential explanations of hypertrophy in old and advanced old ages relating to those of compensatory growth, in response to other aspects of loss of function or force-generating inefficiencies in aged muscle, or due to an increasing demand or load with increased body mass, underlying causes of this observed feature are largely unknown. As declines in muscle mass with age are usually attributed to a loss in myofibre number, a change in myofibre type or a reduction in myofibre size or a combination of the three (Alnaqeeb & Goldspink 1987). The apparent loss of larger fast-twitch type II myofibres in the current study, despite some evidence of hypertrophy, was sufficient to equal an overall net decline in ageing *Soleus* mass. Contrastingly, in the EDL, a decline in muscle mass was not evident, despite a distinct reduction in myofibre numbers at old age. However, a combination of an increased proportion of IIB (largest CSA) and slight hypertrophy in IIA appears to be sufficient to combat any potential reductions in mass attributed to the myofibre loss. However, increased ECM deposition and thickening may also contribute to this.

Taryn Morash

The switch to an overall slower myofibre phenotype, observed in the *Soleus*, could indicate a number of abnormalities in regulation and function with age. Some of these aspects were thereby investigated further in this series of analyses. Firstly, it can be hypothesised that the fast to slow shift is compensating in regards to impaired oxygen delivery. For example, decreased vascular density and blood flow has been reported in the literature, in the brain as well as in skeletal muscle, in both humans and rodents (Groen et al. 2014; Bell & Ball 1990; Sonntag et al. 1997; Degens, Turek, et al. 1993). Degens and colleagues in particular, report overall capillary loss with age (Degens, Turek, et al. 1993). However, this was not the case in the present study, as the number of capillaries per myofibre in the *Soleus*, did not undergo the loss reported during old age and this was further backed up by the consistent *VEGFa165* expression also observed. Additionally, capillary proliferation was found, along with compensatory myofibre hypertrophy, in the *Plantaris* and that this feature was not lost in aged rats, only delayed in response to demand and CSA increases (Degens et al. 1992; Degens, Turek, et al. 1993). The type IIA myofibres in the aged and geriatric *Soleus* muscles in the present study, indicated significant hypertrophy, which could also be described as 'compensatory'. This term however, is being used in regards to the potential need to combat the loss of force-generating units with the simultaneous decreases in number of type IIA myofibres also seen, rather than compensatory relative to increased demand in response to exercise training.

As features of impaired oxygen delivery were not evident, compensatory hypertrophy and a switch to those myofibres with a higher oxidative capacity could also suggest dysfunctional mitochondrial activity, highlighting that there may be a change in how the oxygen is being used to make ATP. Analysis of SDH activity in the *Soleus* further indicates that this may be the case. Despite an increase in the proportion of type I myofibres, but consistent with the reduction in type IIA (also known to be fast oxidative; FO), SDH activity reveals an overall decline in oxidative capacity in advanced old age. Moreover, mitochondrial dysfunction is shown to be highly implicated in numerous pathological and toxicological conditions, including sarcopenia (Pieczenik & Neustadt 2007; Bua et al. 2002; Wei et al. 1998). In fact, increased oxidative stress, being one of the nine 'Hallmarks of Ageing', is therefore believed to be a main contributing factor to organismal senescence (López-otín et al. 2013). Harmful accumulation of reactive oxygen species (ROS), superoxide (O_2^-), is known to exacerbate the problem, further damaging mtDNA (Pieczenik & Neustadt 2007; Wei et al. 1998). Additionally, as skeletal muscle is a tissue that consumes high amounts of oxygen, consequently this results in higher concentrations of accumulated ROS. Levels of O_2^- ROS production in the current project, were higher in the smaller myofibres, in both the *Soleus* and EDL, compared to large myofibres. This finding correlates to those myofibres with a smaller CSA typically being type I (and a small proportion of type IIA) and traditionally, are more mitochondria-rich and concordantly, more oxidative in nature

Taryn Morash

(Alnaqeeb & Goldspink 1987; Degens et al. 1992; Omairi et al. 2016). O_2^- ROS production was subsequently shown to increase in both small and large myofibres in the ageing EDL and *Soleus*, to a significant degree however, in the large myofibres of both muscles. This is consistent with the previously described fast to slow shift in the *Soleus*, suggesting that larger (typically more glycolytic fast twitch) myofibres such as type II, during the switch to slower type I, were reprogrammed to have a higher capacity for oxidative metabolism, thereby producing more ROS. Whereas, in the EDL, the fast to an even faster shift in myofibre type, suggests that a greater amount of dysfunctional oxidative metabolism, leading to O_2^- production, may be occurring in a proportion of these larger myofibres, despite typically being more glycolytic in nature. Moreover, it is very unlikely that smaller more oxidative myofibres (type I and IIA), that were measured to have average CSAs of <500μm^2, were analysed as part of the 'large' myofibre category in the DHE ROS analysis. Further signifying that it was indeed type IIX and IIB myofibres that showed this increased O_2^- production in old age. Therefore, these findings, taken together, are in agreement with what is known regarding accumulated ROS and increased oxidative stress in ageing muscle.

The factors most likely resulting in increased ROS production during ageing include abnormal oxidative phosphorylation (ox-phos) respiratory function and deficiencies in antioxidant defence mechanisms. The latter was investigated and it was hypothesised that impaired or deficient mitochondrial antioxidant activity is a main factor contributing to the observed increased ROS production in ageing. Alternatively, increased antioxidant activity with age would suggest a functional response to a detection of greater oxidative stress. Mitochondrial superoxide dismutase 2 (SOD2), an antioxidant enzyme known to catalyse the transformation of O_2^- into H_2O_2, is known to be up-regulated following exercise-induced oxidative stress and ROS production (Pieczenik & Neustadt 2007; Davies et al. 1982; Karnati et al. 2013). This is believed to be mediated by redox-sensitive transcription factor nuclear factor κB (*NF-κB*), which once activated and following nuclear translocation, binds to target DNA sequences including *mtSOD* (SOD2), resulting in *SOD2* up-regulation (Ryan et al. 2008; Gomez-Cabrera et al. 2005; Ji et al. 2004). Studies conducted in rat muscles also indicated that while training-induced increases in SOD2 were observed in young animals, training was insufficient in providing any additional protection against oxidative stress in aged animals (Leeuwenburgh et al. 1994). *SOD2* mRNA expression levels however, remained constant with age in the *Soleus* muscles of the current study. Firstly, this could indicate that antioxidant activity is not affected in the aged murine *Soleus* muscle and that the ROS production is occurring at such an increased rate that SOD2 cannot keep pace. Secondly, another explanation could be that, although SOD2 is known to be up-regulated by oxidative stress, it also requires various stages of post-translational modification to be catalytically active (Ryan et al. 2008). Additionally, a

Taryn Morash

number of proteins (such as cyclins, cyclin-dependent kinases as well as p53) interact with and alter SOD2 activity via various post-translational modifications (Candas & Li 2014). Therefore, as it was the mRNA levels that were analysed in this series of experiments, a constant expression at a molecular level may have been all that was required and regulatory fluctuations in the enzyme may have been evident when exploring at the protein level instead. Suggesting that there may have been altered transcription of SOD2 mRNA initially, subsequently resulting in changes in protein levels which in turn, acted as a feedback mechanism, further regulating transcription of SOD2 mRNA. Or more essentially, post-translational modification is responsible for a large proportion of SOD2 activity and response to oxidative stress. Furthermore, investigation for example, into the levels of activated *NF-κB*, as well as western blot analysis of the NF-κB and SOD2 translated proteins, would be of particular interest to the present body of research, in order to give a better understanding of this process in ageing.

Collagen is the main supporting component of skeletal muscle and comprises the majority of connective tissue. There are three main distinct collagens characterised in skeletal muscle, type I collagen of the epimysium, perimysium and tendon. Type III is a component of the perimysium and type IV is located in the basement membrane of myofibres therefore, endomysium (Light & Champion 1984). Collagen has been shown to become denser with age (Alnaqeeb et al. 1984; Marshall et al. 1989). It has also been shown that an increased amount of cross-linking of collagen fibrils with age results in the overall stiffening of connective tissue layers (Zimmerman et al. 1993; Kragstrup et al. 2011). Furthermore, characteristically altered features such as these are believed to impact on skeletal muscle contractility, force-generating capacity and interfere with myofibre signal transduction and mechanosensing ability. Examination of the myofibre extracellular matrix and connective tissue components in this series of experiments indicated that, in keeping with what is reported in the literature, collagen thickness increased in old age in the *Soleus* muscle and at geriatric ages in the EDL. However, in geriatric ages in the *Soleus*, collagen thickness subsequently reduced, suggesting potential connective tissue loss into advanced old ages. However, the diminished collagen mRNA expression levels in the *Soleus*, at a geriatric age, appear to support the finding of reduced collagen content and suggests that this was achieved through gene down-regulation. Key structural dystrophin glycoprotein complex (DGC) components, dystrophin and beta-sarcoglycan, both appeared to be up-regulated between adult and old ages in the *Soleus*. An explanation for this could be compensatory in response to potential reductions in structural integrity of the ageing myofibre, perhaps in the degradation of collagenous fibril content or indeed that of other basal lamina or DGC components. Moreover, the importance of the DGC and surrounding extracellular matrix anchor and signalling proteins to mechanotransduction, in response to myofibre stretch and overload, have been

Taryn Morash

implicated in Duchenne muscular dystrophy (Goldspink 1999). Suggesting that the up-regulation of dystrophin and beta-sarcoglycan in old age, is avoiding similar myo-pathological dysfunction associated with DMD, regarding how a muscle signals and responds appropriately to loading.

The effects of CM generated from ADMSCs on naturally-aged skeletal muscle phenotype

In recent decades, the therapeutic effects of adult stem cells and their self-renewal and multipotent capabilities have dominated the research field of regenerative medicine. Numerous studies involving the introduction of a variety of different stem cell types into sites of tissue damage or injury, have been conducted, in order to examine the regenerative capabilities. Stem cells are proposed to proliferate and differentiate, overall contributing to the host tissue. However, despite varying success of engraftment and even in sites where injected or introduced stem cells are no longer present, therapeutic effects have continued to be observed in the host tissue. Such findings fuel the notion of a paracrine effect whereby, stem cells have been shown to secrete an array of regulatory molecules, as a form of cell to cell communication. Key to the current study, this concept has sparked numerous investigations into the beneficial effects of a young secretome in an aged host or environment.

Work carried out by colleagues, analysed the CM isolated from amniotic fluid stem (AFS) cells (Mellows et al. 2017). Two separate compartments, the extracellular vesicle (EV) and the free secretome fractions were shown to contain an abundance of molecules specific to each fraction, that were shown to promote regeneration in a cardiotoxin-induced injury model in mouse TA muscles. Further analysis of the EV fraction revealed that it was rich in miRNA, rather than mRNA and it is suggested that this is the key regulatory mechanism under-lying therapeutic paracrine activity. Importantly, miRNA known to target specific signalling pathways in areas key to the current project include, metabolic process, response to stress, mitochondrion organisation and ageing. The AFS CM was isolated in the same way, utilising the same protocol, as the ADMSC-derived CM in the current study, free of exogenous molecules.

The measurements carried out at a whole organism level, showed that old animals treated with CM, initially appeared to have a slightly reduced body weight during the 4-month *in vivo* CM study. With a significant decrease noted after the first CM injection in percentage weight change. A large amount of variation in the animal weights was also noted and resulted in albeit minimal differences. However, this could suggest that CM had impacts on the features of lipid metabolism, body composition and body fat previously mentioned. Mellows and colleagues showed that one of the biological processes targeted by the miRNA present in the secreted EV CM fraction from AFS cells, was lipid metabolism (Mellows et al. 2017). Further analysis of the ADMSC-derived CM used in this

Taryn Morash

project is required in order to elucidate key determinant molecules present that could contribute to the changes observed.

Grip strength measurements in the aged animals decline to the same degree with and without CM treatment, indicating that CM did not alter the force-generating ability in aged animals. Moreover, CM treatment in old age resulted in a reduction in *Soleus* weight, despite the key determinants of muscle weight regarding myofibre number and size, were seemingly unchanged with CM. A further component capable of altering muscle weight is connective tissue content. However, discordantly, a decreased collagen IV (basement membrane) thickness and mRNA expression was observed with CM treatment in old age and collagen I (a more structural collagen type and a constituent of tendon) levels were not affected. In the EDL, there were no apparent changes to muscle weight, total myofibre number or size with CM treatment in old age and additionally, collagen IV thicknesses remained constant. These results together indicate that CM treatment does not harbour the ability to significantly alter features underlying overall hyperplasia or hypertrophy in the naturally aged *Soleus* or EDL muscles.

However, *Soleus* muscles from aged CM-treated mice showed an increased number of capillaries per myofibre, which is in keeping with some of the reported findings in the literature, implicating pro-angiogenic paracrine signalling in neovascularisation following tissue damage. One study investigated the therapeutic effects of the exosome fraction CM from CD34^{+} cells isolated and purified from the peripheral blood in an ischaemic hindlimb injury model (Mathiyalagan et al. 2017). The EV CM was shown to be rich in pro-angiogenic miRNA such as endothelial cell miR-126-3p which subsequently regulated genes associated with angiogenesis including, vascular endothelial growth factor (VEGF), angiopoietin 1 and 2 (ANG1 and ANG2), matrix metallopeptidase 9 (MMP9) and thrombospondin 1 (TSP1). Results suggested that treatment with the EV CM mediated tissue repair in the hindlimb, via pro-angiogenic paracrine signalling. Moreover, the colleagues investigating AFS CM alongside this project, revealed in the hindlimb cardiotoxin (CTX) injury model that more efficient tissue regeneration was promoted with AFS CM treatment and this was associated with an increase in vascularisation. Analysis of the miRNA target processes showed that AFS CM contained those involved in angiogenesis and the circulatory system. Despite, alternative cell types used to create the CM in the studies previously described, the results of the present study would support the hypothesis that the ADMSC CM also contains pro-angiogenic regulatory factors or molecules. However, further analysis of the ADMSC CM is required in order to investigate this further.

In the naturally-aged EDL however, unlike the *Soleus*, capillary density was not altered by CM treatment. An explanation for this difference is that the *Soleus* muscle is a highly-vascularised muscle

Taryn Morash

relative to the EDL, therefore it requires an increased rate of oxygen delivery in order to carry out oxidative metabolism. Remarkably, CM treatment in the aged *Soleus*, appears to have also significantly improved the oxidative capacity and this seems to have been accompanied by the increased capillary density. Therefore, it can be postulated that key therapeutic targets of the ADMSC-derived CM content includes mechanisms of not only angiogenesis but also components of oxidative metabolism. As previously mentioned, AFS-derived CM has been shown to possess miRNA that target genes associated with mechanisms of metabolism, stress response and mitochondrial organisation, among many others (Mellows et al. 2017). Furthermore, *in vitro* studies, from the research prospective of radiotherapy treatment in obese melanoma patients, reported protective effects of adipocyte-derived CM, through reduced oxidative stress and improved cell survival, in malignant melanocytes (Coelho et al. 2017). Moreover, CM treatment drastically reduced the amount of O_2^- ROS detected, to those levels observed in small, juvenile and adult myofibres in the *Soleus*. This finding is in agreement with that of both improved oxygen delivery and oxidative capacity, to levels significantly more than those observed in juvenile mice. Decreased amounts of O_2^- ROS were also observed in the large myofibres of the EDL, in the absence of any changes in capillary density or oxidative capacity. Taken together, the findings of this series of experiments suggest that CM generated from ADMSCs not only retains the potential to modify signalling pathways associated with angiogenesis and metabolism, but additionally harbours possible therapeutic, antioxidant properties. More research however, is required in order to define the miRNA content of the ADMSC-derived CM used in the present study.

In conclusion, this series of experiments developed a natural ageing skeletal muscle profile giving insights into a variety of physiological, immunohistological and biochemical parameters in two distinctly different hindlimb muscles of mice, the *Soleus* and EDL. Additionally, this body of work investigates a novel approach of utilising conditioned media (CM) generated from a fully-characterised human adipose-derived mesenchymal stem cell (ADMSC) line, under stressed (hypoxic and nutrient-free) culture conditions, as a potential therapeutic treatment of well-established age-associated declines, in the onset and development of sarcopenia, in naturally-aged mice. After establishing that sarcopenia was indeed evident by the observed loss of muscle mass in the geriatric muscles examined, other key phenotypical features were explored. Features in keeping with what is established in the literature include reduced total myofibre number, an increase in metabolic dysfunction, resulting in greater ROS production and evidence of a fast to slow MHC switch in the ageing *Soleus*. In contrast, a switch in the reverse direction, from fast to even faster type, was seen in the ageing EDL and the reasons underlying this shift remain unclear. CM treatment in aged animals did not appear to influence features such as the overall myofibre number, size or type. However,

Taryn Morash

there is evidence for potential modification of signalling pathways involved in angiogenesis, oxidative metabolism, reduced ROS production/antioxidant activity, as well as collagen organisation. Future work continuing this area of research will benefit from examination of CM effects in geriatric animals, due to the observation of the majority of characterisitics associated with sarcopenia at a geriatric rather than old age, in the current project. Additionally, it would also be essential to administer CM treatment in young control animals in order to determine any effect CM properties have on the maturation and early growth phase of skeletal muscle.

Furthermore, the more oxidative *Soleus* muscle appears to have been affected to a larger degree than the typically more glycolytic EDL, in the characteristics of natural ageing noted in this series of experiments. In addition, this series of results further highlights the importance of murine experiments in the field of ageing research. The mouse is an effective ageing mammalian model, as evident from the relatively consistent changes established in the literature, in numerous species including humans, as well as the ability for effective analysis in a relatively short period of time (for example the lifespan of 2-2.5 years). Moreover, this natural ageing skeletal muscle profile has provided a basis for comparison of the changes that occur in the progeric *ERCC1* delta murine model in the following chapter of results. Importantly, this will investigate the hypothesis that the *ERCC1* delta mutant mouse is a good model of ageing skeletal muscle and mimics those changes reported in natural ageing.

Taryn Morash

Chapter 4

Characterisation of the skeletal muscle phenotype in the *Ercc1*$^{d/-}$ murine model of progeria

Taryn Morash

Introduction

A large proportion of the studies conducted in order to establish the changes that occur in ageing skeletal muscle, as well as multiple other tissues and organ systems, utilise the laboratory mouse. Moreover, numerous parallels can be drawn between the murine and human ageing processes, making the mouse a beneficial and universal model of natural ageing. However, there is a growing need for a suitable mammalian model of accelerated ageing. This is due to the high costs associated with housing mice for their 2 – 3 year lifespan, which in turn, impacts on experimental cohort size. Additionally, intervention approaches designed to study and potentially treat symptoms associated with natural ageing ultimately, often extend over the full lifespan of the animal, thus resulting in a reduced efficiency of data delivery.

The creation of nucleotide excision repair (NER)- and DNA interstrand cross-link repair-compromised *ERCC1*-mutant mouse models, that exhibited remarkably reduced lifespans and premature cellular senescence, allows for a relatively short-term experimental model of accelerated ageing. These progeroid models exhibit components of both stochastic and genetic age-associated decline in fitness. Additionally, they have also been reported to display a shift in energy consumption towards a survival response of molecular and cellular maintenance, over that dedicated to proliferation, synthesis and overall growth (Niedernhofer et al. 2006). The more severe *ERCC1* knockout (-/-) mouse lives a full lifespan within approximately 30 - 40 days whereas, the truncated *ERCC1* delta (d/-) mutant, which functions at only 10% of normal NER activity has been shown to live up to approximately 6 months (Weeda et al. 1997). The *Ercc1*$^{d/-}$ mutant has been reported to display systemic age-associated degeneration with compartment-specific features that mimic 'normal', 'accelerated' and 'extreme' ageing progression (Dollé et al. 2011). The histopathological characteristics of the *Ercc1*$^{d/-}$ mouse have been extensively studied in liver and kidney, as well as the neurodegenerative abnormalities in the spinal cord (Weeda et al. 1997; Dollé et al. 2011; De Waard et al. 2010). The potential of the *Ercc1*$^{d/-}$ mouse therefore, to be used as an effective model of sarcopenia in skeletal muscle, remains to be explored.

The utilisation of the *Ercc1*$^{d/-}$ progeroid mouse in this series of experiments, allows for development of a skeletal muscle profile in a model of accelerated ageing. The *Ercc1*$^{d/-}$ model is associated with hallmark features of ageing, including increased oxidative stress and cellular senescence. Therefore the paracrine effects of ADMSC-derived CM will be tested as a potential therapy for any observed myo-pathological qualities. Characteristics of the progeric skeletal muscle phenotype can be subsequently compared to those associated with onset and progression of sarcopenia in natural ageing. Firstly, as in the naturally-aged series of experiments, analysis was carried out at a whole

Taryn Morash

organism and tissue level. Animal cohorts included the *Ercc1$^{d/-}$* (d/-) mice and their (+/+) littermate controls, treatments comprised of ADMSC-derived CM or PBS-vehicle, +/+ PBS, +/+ CM, *Ercc1$^{d/-}$* (d/-) PBS and *Ercc1$^{d/-}$* CM. Treatments were injected intraperitoneally (I.P) at two week intervals, when animals were 9, 11 and 13 weeks of age and muscle was investigated at 16 weeks.

Taryn Morash

Results

Significantly reduced body weight in the *Ercc1$^{d/-}$* progeroid mice

Body weight and overall animal health were monitored daily throughout the *in vivo* experimental time-period due to the severe nature and rate of degeneration in the *Ercc1$^{d/-}$* mice, particularly during the latter days of the 8-week study. Body weight was measured in grams (g) and most striking was the drastically reduced weight of the *Ercc1$^{d/-}$* progeric mice (d/-) compared to the littermate controls (+/+), evident at each weekly interval throughout the experiment (p = <0.001) (Figure 4.1 A). At week 9, the first week of the experiment, the average starting body weight of the control animals was 32.4g whereas, the progeric animals weighed 15.9g. The control animals subsequently continued to grow and increase in body mass, peaking at week 16, the final week of the study, at an average of 41.6g. Contrastingly, the *Ercc1$^{d/-}$* animals remained at a constant average weight throughout the experiment, dropping to 15g at the lowest at week 11, peaking at 16.3g during week 14 and ending at a final weight of 15.9g, the same as the average weight when the study commenced.

Furthermore, the previously discussed trends in body weight were supported when analysing the percentage change in body weight. These results indicated that by week 11, the degree by which body weight changed from that recorded at the start of the study, between +/+ (12.1% increase) and *Ercc1$^{d/-}$* (5.1% decrease) animals, was significantly different (p = <0.05) (Figure 4.1 B). This difference was maintained throughout the experiment as the control animals continued to increase in body mass, gaining 28.8% of the starting weight at week 16 (p = <0.001). *Ercc1$^{d/-}$* percentage weight change fluctuated between the lowest (5.1% decrease) and peak weight at week 14 (3% increase).

CM treatment did not affect progeric *Ercc1$^{d/-}$* body weight

Moreover, with such a dramatically reduced body weight in the *Ercc1$^{d/-}$* mutant mouse, the following step was to establish if there were any effects of CM treatment on overall body weight. Firstly, body weights fluctuated within a 1g range throughout the experiment (15.9 – 16.8g) (Figure 4.1 C). However, these differences were not statistically significant at any of the weekly intervals. Percentage change in body weight analysis were also not statistically different at any of the weekly intervals (Figure 4.1 D). Interestingly, both cohorts ended the study at week 16 with an average percentage change of 0%. Therefore, CM treatment had no effect on body weight and weight did not change significantly from the start to the end of the study.

Taryn Morash

CM treatment initially appeared to reduce control body weight

The effects of CM treatment on control littermates was investigated by also injecting a control cohort intraperitoneally (I.P) with the same batch of CM as the progeric *Ercc1$^{d/-}$* animals, following the same I.P injection schedule. Similarly to the other experimental cohorts, body weight was monitored and recorded as an indication of overall animal health and growth, with and without CM treatment.

Weight gain patterns in both the control (+/+) PBS-vehicle and control CM appeared to be similar, both gaining weight at a linear rate (Figure 4.1 E). The average weight of the control PBS cohort was greater than that of the control CM group at all of the weekly intervals throughout the 8-week study. However, it was noted that average starting weights between the cohorts varied by approximately 3g, with control PBS weighing more than the CM group, prior to the first I.P injection, although the difference was statistically non-significant. Average body weight recorded at the end of the study were also not statistically different between the two cohorts. Percentage change in body weight removed any misleading effect the slight differences in average starting weight may have had on the overall results. However, any observed differences in percentage increase in body weight were not statistically significant, at any of the weeks measured throughout the experiment (Figure 4.1 F).

Strength and activity assessment indicates a functional deficit in the *Ercc1$^{d/-}$* mice

Functional studies assessed the force exerted, using a grip strength monitor, by the *Ercc1$^{d/-}$* mice in comparison to the littermate controls, with and without CM treatment. Additionally, motor coordination was examined using rotarod performance testing. Normalised grip strength was not statistically different between the control and *Ercc1$^{d/-}$* mice, despite the overall greater average control normalised force compared to *Ercc1$^{d/-}$* (Figure 4.1 G). Furthermore, CM treatment in controls did not significantly alter grip strength relative to the control PBS-vehicle cohort. The control CM cohort was distinctly greater than those measured in the *Ercc1$^{d/-}$* mice (PBS and CM, $p = <0.01$ and 0.05, respectively). CM treatment in the *Ercc1$^{d/-}$* however, did not have any additional effects compared to the *Ercc1$^{d/-}$* PBS. Moreover, control rotarod performance was visibly greater than in the *Ercc1$^{d/-}$* animals, despite this, statistically the difference between +/+ (PBS) and *Ercc1$^{d/-}$* (PBS) controls was non-significant (Figure 4.1 H). Both control PBS and control CM animals exhibited double the rotarod activity compared to *Ercc1$^{d/-}$* treated with CM ($p = <0.05$, respectively). When the genotypes were compared separately however, CM treatment had no discernible effects.

Taryn Morash
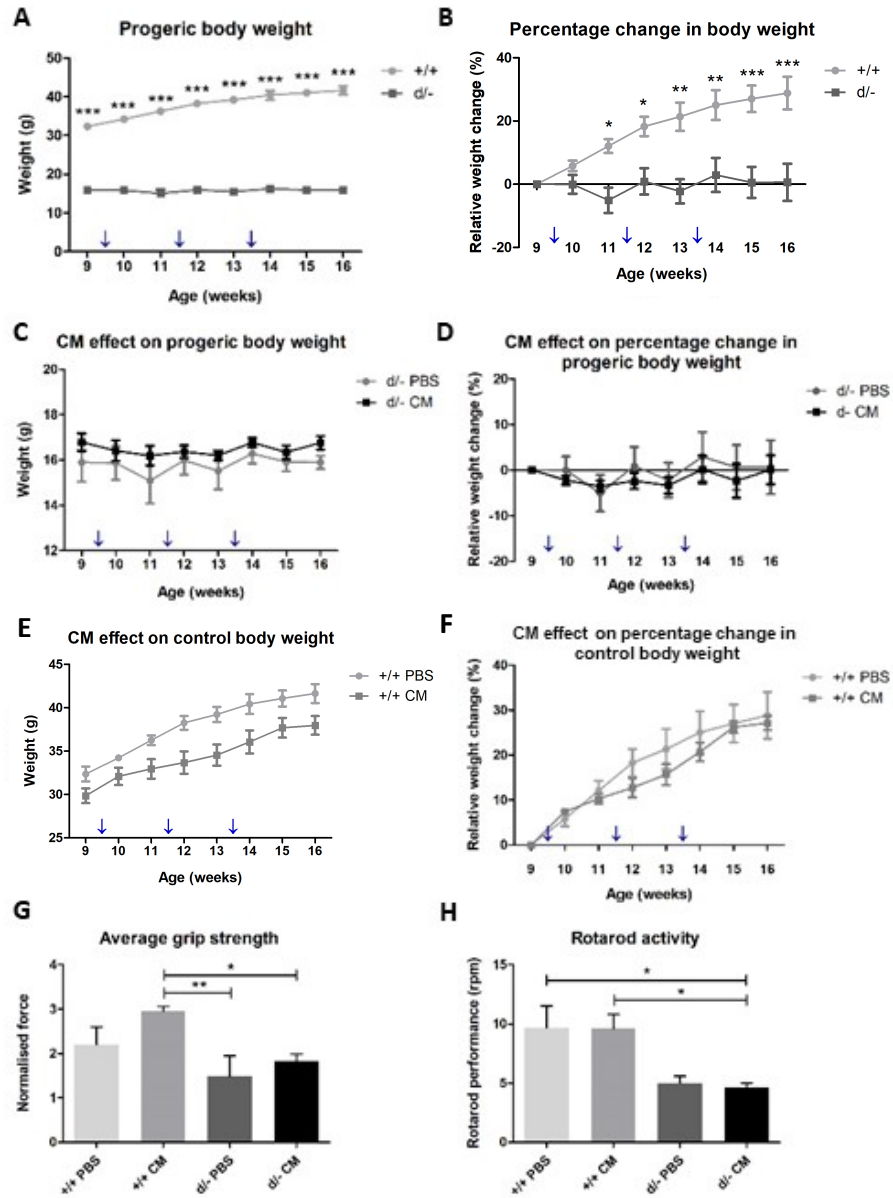
Figure 4.1 Determining the effects of ADMSC CM (CM) on body weight, grip strength and rotarod performance in *Ercc1*$^{d/-}$ progeric mice. **(A)** Drastically reduced body weights of the *Ercc1*$^{d/-}$ (d/-) mice compared to (+/+) littermate controls. **(B)** The percentage change in body weight of *Ercc1*$^{d/-}$ and control mice. **(C)** CM does not impact on the body weights of *Ercc1*$^{d/-}$ mice. **(D)** Percentage change in body weight of *Ercc1*$^{d/-}$ mice. **(E)** The effect of CM on the body weights of control mice. **(F)** CM does not alter the body weight of control mice. **(G)** Functional assessment of average grip strength of *Ercc1*$^{d/-}$ and control mice, force normalised to body weight. **(H)** The effect of CM on rotarod activity in *Ercc1*$^{d/-}$ and control mice. The administration of CM/PBS treatment (blue arrows). *$p<0.05$, **$p<0.01$, ***$p<0.001$, **(A-F)** Two-way ANOVA (repeated measures) with Tukey post hoc testing. **(G-H)** One-way ANOVA with Tukey post hoc testing.

Taryn Morash

Fresh skeletal muscle weight revealed distinctly smaller hindlimb muscles in the *Ercc1$^{d/-}$* mouse

A greatly reduced weight was observed in all hind-limb skeletal muscles (*Soleus*, EDL, TA, *Gastrocnemius* and *Plantaris*) of the *Ercc1$^{d/-}$* mice, compared to those of the littermate controls ($p =$ <0.01 and <0.001) (Figure 4.2 A, B, C, D, E). Additionally, there were no discernible differences in muscle weight in *Ercc1$^{d/-}$* or control animals treated with CM in any of the hind-limb muscles (Figure 4.2 F).
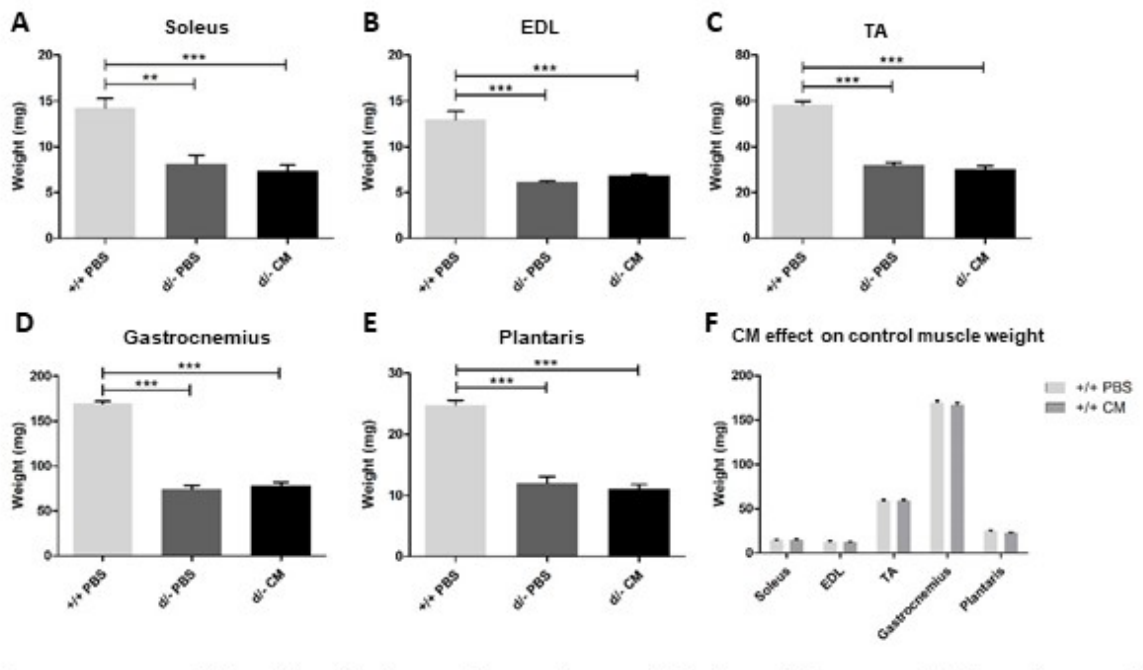
Figure 4.2 *Ercc1$^{d/-}$* fresh hindlimb muscle weights are half that of the control. (d/- PBS), *Ercc1$^{d/-}$* ADMSC CM-treated (d/- CM), (+/+ PBS) and (+/+ CM) littermate controls. **(A)** *Soleus* weight **(B)** EDL weight **(C)** TA weight **(D)** *Gastrocnemius* weight **(E)** *Plantaris* weight. **(F)** The effect of CM treatment on control muscle weights. **p<0.01, ***p<0.001, **(A-E)** One-way ANOVA with Tukey post hoc testing. **(F)** Individual student's t-tests.

MHC isoform myofibre composition is unchanged in the *Ercc1$^{d/-}$ Soleus* muscle compared to control

MHC myofibre composition was investigated using immunohistochemical staining of transverse cross-sections of the 'mid-belly' region of frozen *Soleus* muscles. A well-established shift to a slower MHC phenotype is reported in natural ageing therefore importantly, analysis of MHC content in the *Ercc1$^{d/-}$ Soleus* was carried out to give an indication of any potential changes to physiology and

Taryn Morash

function in the model of progeria. Positive expression of the different MHC isoforms, types I, IIA and IIB (very few in *Soleus*) (and negative IIX myofibres), as well as the total myofibre number, were quantified for all four cohorts, control and *Ercc1$^{d/-}$* animals, with and without CM treatment.

The average total number of myofibres in the control *Soleus* was approximately 840, indicating that CM had no effect on this parameter in the controls (Figure 4.3 A). The total myofibres was reduced to an average of 704 in the *Ercc1$^{d/-}$* animals, significantly lower than the control CM group (p = <0.05) but this reduction was not statistically significant when compared to that of the control PBS (Figure 4.3 A). CM treatment did not have any discernible effect on total myofibre number (Figure 4.3 A).

When analysing the MHC myofibre types, it was noted that, despite the *Soleus* muscle traditionally being comprised of a higher percentage of type I, slow-twitch myofibres as a majority, this was not the case with the littermate control animals (Figure 4.3 B). The myofibre type representing the largest proportion of the *Soleus* muscle in the controls was type IIA (approximately 51%), with 37% of the muscle formed of type I myofibres. In the *Ercc1$^{d/-}$* *Soleus* however, 42% of the muscle was represented by type I myofibres as a majority although this was not statistically significantly more than the percentage of type I myofibres in the control (Figure 4.3 C). The percentage of type IIA myofibres observed was slightly decreased in the *Ercc1$^{d/-}$* muscles when compared to the controls, from 51% to 39%, however this difference was not statistically significant (Figure 4.3 D). Although, the type IIA percentage was significantly increased with CM treatment in the *Ercc1$^{d/-}$* muscles (p = <0.05). Percentages of all other MHC myofibre types (IIX, IIB as well as hybrid I / IIA) remained consistent between control and *Ercc1$^{d/}$* cohorts, as well as with CM treatment, with no other changes observed (Figure 4.3 E, F, G). Additionally, MHC myofibre typing analysis was carried out in the *Soleus* muscles from the control CM and compared to that of the control PBS. It was noted that the percentage of type I myofibres increased from 37% to 40% in the control cohort treated with CM (p = <0.05) while all other fibre type proportions remained consistent (Figure 4.3 H).

Taryn Morash
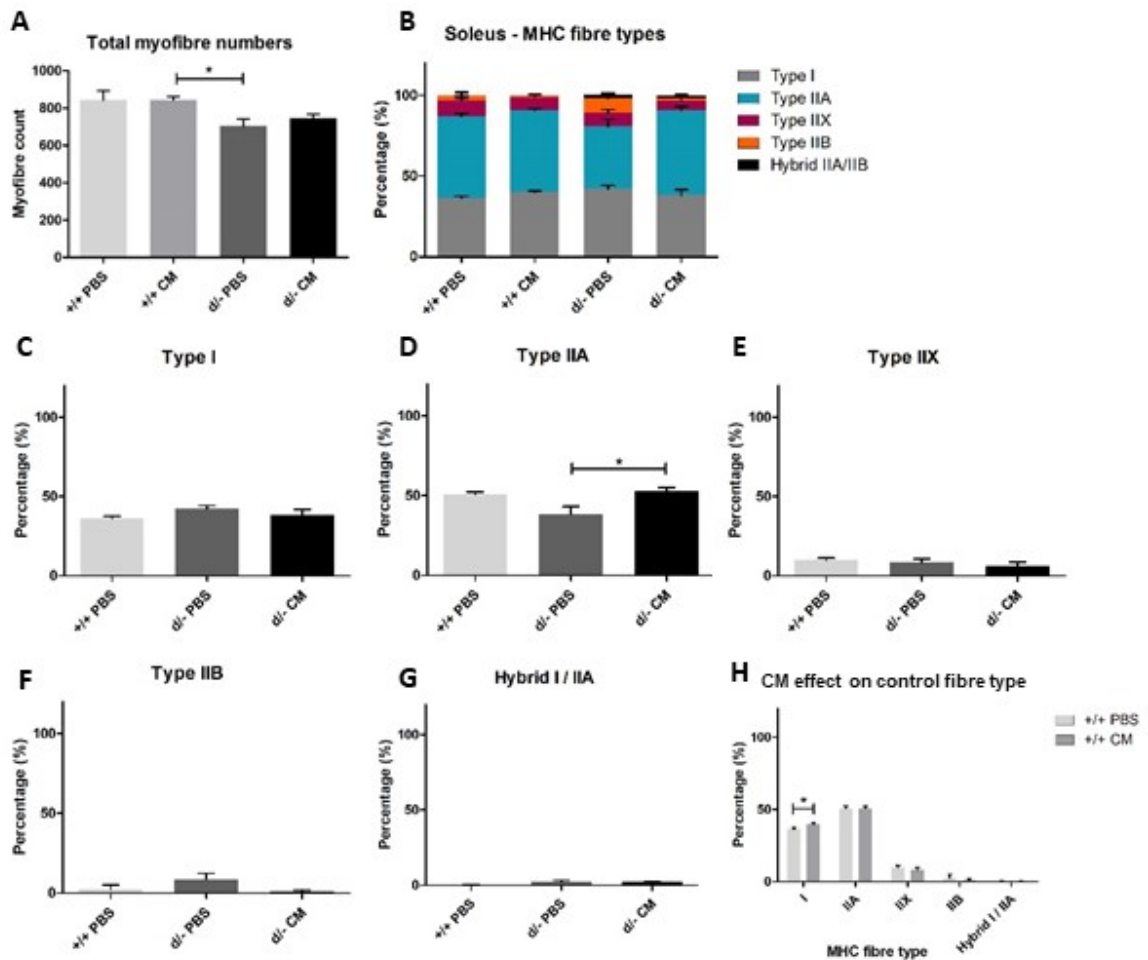
Figure 4.3 Investigating the effect of ADMSC CM (CM) on Myosin heavy chain (MHC) isoform myofibre composition of the *Ercc1$^{d/-}$ Soleus*. *Ercc1$^{d/-}$* (d/- PBS), *Ercc1$^{d/-}$* CM-treated (d/- CM), (+/+ PBS) and (+/+ CM). **(A)** Quantification of total myofibre number. **(B)** Overall MHC myofibre type composition. **(C)** Proportion of MHC type I myofibres. **(D)** Proportion of MHC type IIA myofibres. **(E)** Proportion of MHC type IIX myofibres. **(F)** Proportion of MHC type IIB myofibres. **(G)** Proportion of MHC hybrid type I /IIA myofibres. **(H)** The effect of CM treatment on control *Soleus* composition. *$p < 0.05$, **(A, C-G)** One-way ANOVA with Tukey post hoc testing. **(H)** Individual student's t-tests.

Ercc1$^{d/-}$ myofibre cross-sectional areas (CSAs) were similar to control

One of the key components that can determine force-generating capacity is myofibre size. Muscle growth usually comprises an increase in myofibre number (hyperplasia), and/or increases in myofibre size (hypertrophy). As the *Ercc1$^{d/-}$* model has been reported to shift resources away from growth to focus on genomic preservation and lifespan extension, it is of interest to investigate possible effects of this in skeletal muscle and to relate this feature to function. As with the naturally-aged muscles,

Taryn Morash

myofibre CSA was analysed by MHC myofibre type in the progeric *Soleus*. Overall, CSA between the myofibres of the control, *Ercc1$^{d/-}$* and *Ercc1$^{d/-}$* CM cohorts was highly consistent in each MHC myofibre type. Type I myofibres observed, had a reduced area when treated with CM in the progeric muscles (1330µm^2) when compared with the *Ercc1$^{d/-}$* PBS (1510µm^2) and control PBS (1540µm^2) (Figure 4.4 A). There was a similar trend shown in the type IIA myofibres, where CM appeared to decrease CSA in the *Ercc1$^{d/-}$* muscles (1170µm^2), compared to that of the progeric control (1220µm^2) and control CSA (1300µm^2) (Figure 4.4 B). However, these differences were statistically non-significant. Additionally, despite the control cohort appearing to have larger CSA in type IIX and IIB myofibres and CM seeming to have decreased the CSA of IIB myofibres, these differences were not statistically significant (Figure 4.4 C, D). Therefore, control and *Ercc1$^{d/-}$* myofibres were similar in size and CM treatment had no additional effects on this parameter. Furthermore, CM treatment had no significant effect on myofibre CSA in the littermate controls (Figure 4.4 E).
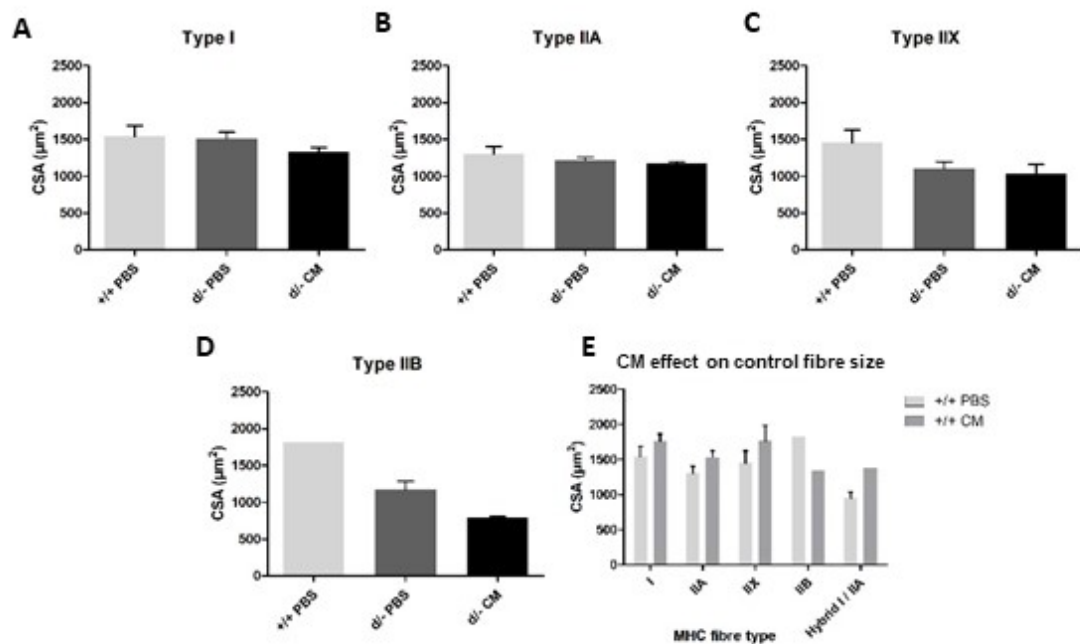
Figure 4.4 Examining the effect of ADMSC CM (CM) on Myosin heavy chain (MHC) isoform myofibre cross-sectional area (CSA) in the *Ercc1$^{d/-}$ Soleus*. *Ercc1$^{d/-}$* (d/- PBS), *Ercc1$^{d/-}$* CM-treated (d/- CM), (+/+ PBS) and (+/+ CM). **(A)** MHC type I myofibre CSA. **(B)** MHC type IIA myofibre CSA. **(C)** MHC type IIX myofibre CSA. **(D)** MHC type IIB myofibre CSA. **(E)** CM treatment does not impact on control fibre size. **(A-D)** One-way ANOVA with Tukey post hoc testing. **(E)** Individual student's t-tests.

Taryn Morash

Oxidative capacity is consistent in the *Ercc1*$^{d/-}$ *Soleus* relative to control

Further to investigating the changes to metabolic function and oxidative capacity that occur during the onset and progression of natural ageing, these characteristics were subsequently examined in the progeric *Ercc1*$^{d/-}$ model. As before, to analyse the myofibres more oxidative in nature as a percentage of the total, the histological succinate dehydrogenase (SDH) staining protocol was carried out on *Soleus* muscle transverse cross-sections. These results indicated that the percentage of oxidative myofibres in the *Ercc1*$^{d/-}$ *Soleus* muscles (52%) was not statistically different from the average observed in the control (57%) (Figure 4.5 A). Moreover, CM treatment had no additional effect on the oxidative capacity in the progeric *Soleus* nor on that seen in the littermate control (Figure 4.5 B).

Capillary density is reduced in the *Ercc1*$^{d/-}$ *Soleus* and CM may harbour pro-angiogenic properties

As previously discussed, oxygen delivery and therefore vasculature organisation can give key insights into any changes to the metabolic regulation of muscle during ageing. To further assess this key aspect as part of the development of a skeletal muscle profile for the *Ercc1*$^{d/-}$ mutant mouse model of progeria, CD31+ cells were analysed and quantified using an immunohistochemical protocol to examine capillary density.

It was observed that the average number of CD31+ cells was 2 cells per myofibre in the *Ercc1*$^{d/-}$ progeric *Soleus*, which was notably fewer when compared to the control where 2.5 cells served each myofibre (p = <0.05) (Figure 4.5 C). Furthermore, CM treatment increased the capillary density to that observed in the control (2.5 cells per myofibre), however this increase was not statistically significant when compared to the *Ercc1*$^{d/-}$ PBS nor the control cohorts. Despite, a further increase seen in the capillary density in the control with CM treatment, to 2.8 cells per myofibre, this difference was also proved to be statistically non-significant (Figure 4.5 D).

A similar trend was noted when examining the relative mRNA expression of VEGFa 165 through qPCR analysis. The expression level of VEGFa 165 was lowest in the *Ercc1*$^{d/-}$ PBS cohort however any differences observed were statistically not significant (Figure 4.5 E).

Reactive oxygen species (ROS) production is increased with CM treatment in the *Ercc1*$^{d/-}$ *Soleus*

As previously discussed, one of the sources of DNA damage is through excessive production of ROS such as superoxide (O_2^-) and is also a hallmark characteristic of mitochondrial dysfunction during ageing. As the *Ercc1*$^{d/-}$ mutant mouse is that which mimics progeria and is itself a consequential

model resulting from insufficient nucleotide excision repair (NER) mechanisms and therefore accumulated DNA damage, the degree that ROS production contributed to the development of sarcopenia in this model were examined. As before, O_2^- was identified using the DHE immunohistochemical fluorescence protocol and the intensity was analysed within myofibres of both small and large CSAs of $Ercc1^{d/-}$ and control littermate *Soleus* muscles, with and without *in vivo* CM treatment.

Firstly, relative DHE intensity was higher in the small myofibres of the $Ercc1^{d/-}$ *Soleus* (11.6) in comparison to the control (8.5), although this increase was not statistically significant (Figure 4.5 F). ROS production in small myofibres in the *Soleus* from $Ercc1^{d/-}$ CM-treated animals however was the highest (13.2) and was statistically increased from that of the control (p = <0.05) but not significantly different from that of the $Ercc1^{d/-}$ PBS cohort. In contrast, CM treatment in the control animals had no effect on DHE intensity measured in the small myofibres (Figure 4.5 G). As previously observed in the naturally aged *Soleus* data, DHE fluorescence intensity was greater in the centre of myofibres with a smaller CSA in both $Ercc1^{d/-}$ PBS and CM (p = <0.05 and <0.001, respectively) as well as control PBS and CM conditions (p = <0.05 and <0.01, respectively) (Figure 4.5 H). Furthermore, the increase in ROS production was also observed in the large myofibres of progeric *Soleus* muscles but notably so in the CM-treated cohort when compared to the control (p = <0.01) (Figure 4.5 I). As observed with the smaller myofibres, CM treatment in the control animals did not affect DHE intensity in the larger myofibres (Figure 4.5 J). Finally, as in the natural ageing experiment, SOD2 gene expression was analysed in the progeric study to provide insights into mitochondrial antioxidant activity. Quantitative PCR analysis indicated a slightly increased level of SOD2 (0.9 relative gene expression) in the control PBS *Soleus* muscles, compared to all other cohorts (approximately 0.5) however the observed difference was statistically not significant (Figure 4.5 K).

Taryn Morash
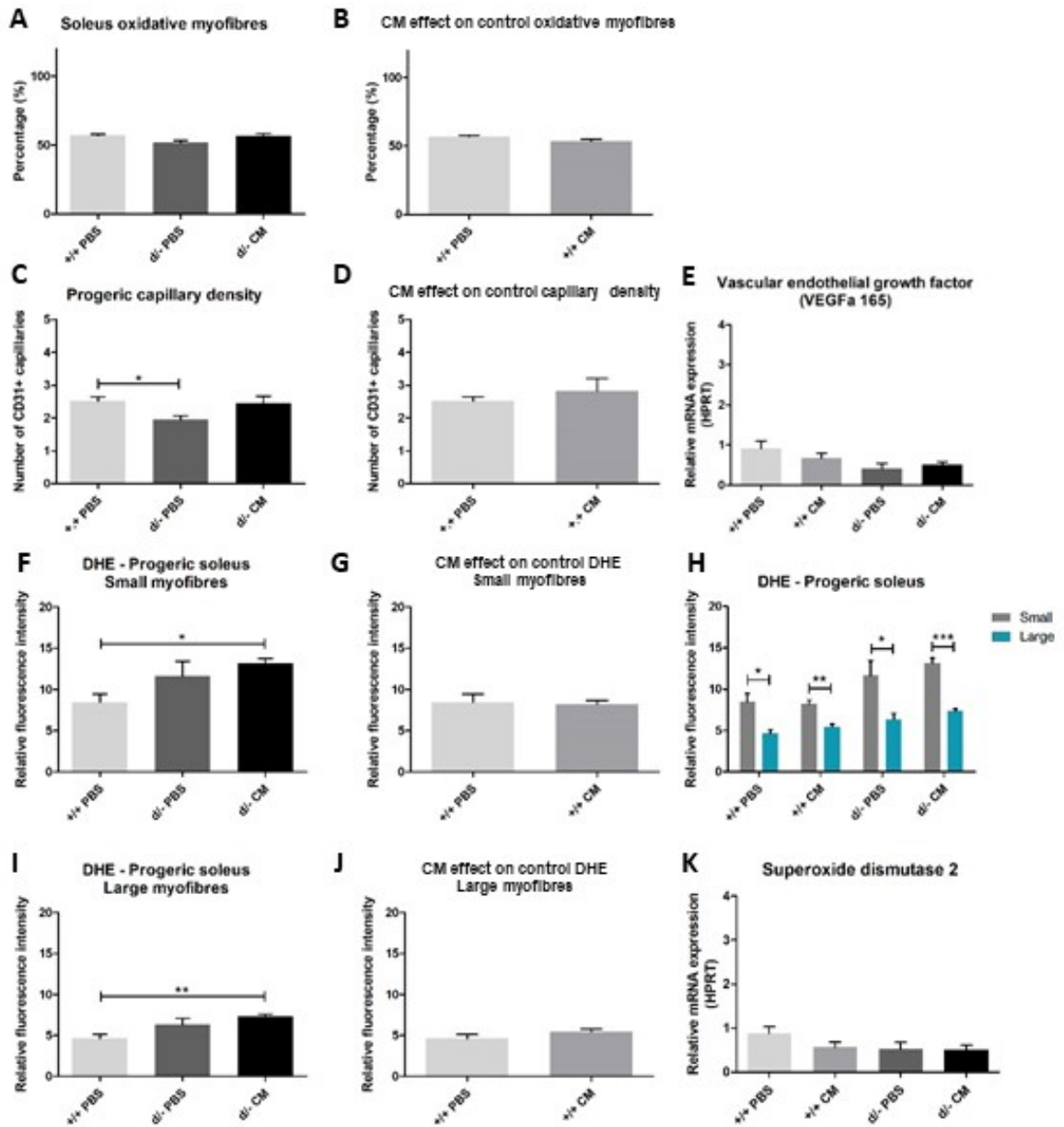
Figure 4.5 Investigating the influence of ADMSC CM (CM) on the metabolic status, vasculature organisation and mitochondrial function of the *Ercc1$^{d/-}$ Soleus*. *Ercc1$^{d/-}$* (d/- PBS), *Ercc1$^{d/-}$* CM-treated (d/- CM), (+/+ PBS) and (+/+ CM). **(A)** Proportion of myofibres positive for succinate dehydrogenase (SDH) staining to assess the oxidative capacity. **(B)** CM treatment does not affect control oxidative capacity. **(C)** Capillary density (CD31+ cells per myofibre). **(D)** CM treatment does not impact on control capillary density. **(E)** VEGFa 165 mRNA expression. **(F)** ROS production in small myofibres. **(G)** CM treatment does not influence ROS production in littermate controls (small myofibres). **(H)** ROS production is greater in small myofibres. **(I)** ROS production in large myofibres. **(J)** CM treatment does not influence ROS production in littermate controls (large myofibres). **(K)** Antioxidant

Taryn Morash

superoxide dismutase 2 (SOD2) mRNA expression. *p<0.05, **p<0.01, ***p<0.001, **(A, C, E, F, I, K)** One-way ANOVA with Tukey post hoc testing. **(B, D, G, H, J)** Individual student's t-tests.

Changes in the extracellular matrix (ECM) of the progeric *Soleus* muscle

Increases in collagen layer thickness are well established in the process of natural ageing and is a feature that is implicated in overall muscle signalling and contractile function in old and geriatric ages. In the present study, collagen thickness analysis was also carried out in *Soleus* muscles of the *Ercc1$^{d/-}$* mouse. Collagen IV thickness analysis was conducted as before, by MHC myofibre border type of transverse *Soleus* cross-sections visualised using immunofluorescence.

Initially, collagen appeared to be thicker in non-type I borders when compared to those of type I myofibres in all control and *Ercc1$^{d/-}$* conditions however these increases were statistically non-significant (Figure 4.6 A). Furthermore, when analysing the two border types individually, despite an observed slight increase in thickness in progeric borders (both type I and non-type I) compared to control, there were no significant changes in collagen IV content in the *Ercc1$^{d/-}$ Soleus* and CM had no additional effect (Figure 4.6 B, C). In the littermate controls, CM treatment also had no discernible effect on collagen thickness (Figure 4.6 D). Furthermore, qPCR analysis carried out indicated no notable variation in ECM content regarding collagen I and IV, dystrophin and beta-sarcoglycan relative mRNA expression, in the *Ercc1$^{d/-}$ Soleus* muscle compared to that of the control, nor with CM treatment (Figure 4.6 E, F, G, H).

Taryn Morash
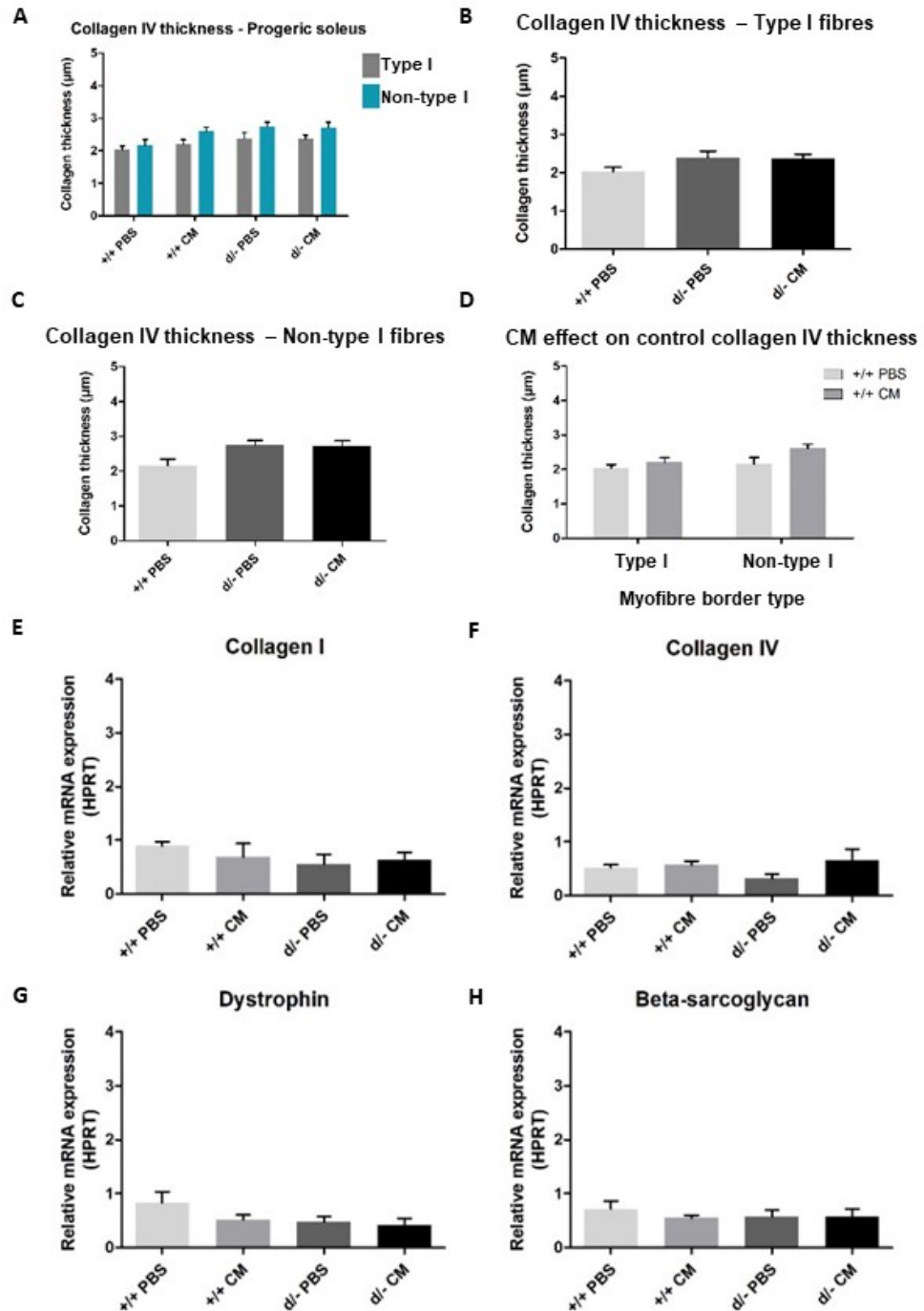
Figure 4.6 Examining the influence of ADMSC CM (CM) on collagen thickness and structural components of the dystrophin glycoprotein complex (DGC) in the *Ercc1*[d/-] *Soleus*. **(A)** Collagen IV thickness between MHC myofibres, type I border with another type I. Non-type I border with a second non-type I myofibre **(B)** Collagen IV thickness between type I myofibres **(C)** Collagen IV thickness between non-type I myofibres **(D)** CM treatment does not affect collagen IV thickness in either border type in littermate controls **(E)** Collagen I mRNA expression **(F)** Collagen IV mRNA expression **(G)** Dystrophin mRNA expression. **(H)** Beta-sarcoglycan mRNA expression. **(B, C, E-H)** One-way ANOVA with Tukey post hoc testing. **(A, D)** Individual student's t-tests.

Numerous characteristics of *Ercc1*$^{d/-}$ skeletal muscle reflect sarcopenia in natural ageing while others appear amplified

A further hypothesis to be investigated was that the *Ercc1*$^{d/-}$ mutant mouse provided a good mammalian model of progeria and mimicked characteristics of degeneration associated with the onset and progression of sarcopenia in natural ageing. To that end, parameters investigated as part of developing a muscle profile for the *Ercc1*$^{d/-}$ animals were compared to that formed for naturally ageing muscle, in the previously reported experiments of the current project. For example, *Ercc1*$^{d/-}$ hind-limb muscles were shown to have substantially reduced muscle weight in all muscle types, when compared to those of old, naturally-aged animals (p = <0.001) (Figure 4.7 A, B, C , D, E). Furthermore, the observed significant reduction in progeric muscle mass was also evident when compared to weights recorded at a geriatric age in the EDL (p = <0.05), TA (p = <0.001) and *Gastrocnemius* (p = <0.001) muscles (Figure 4.7 B, D).
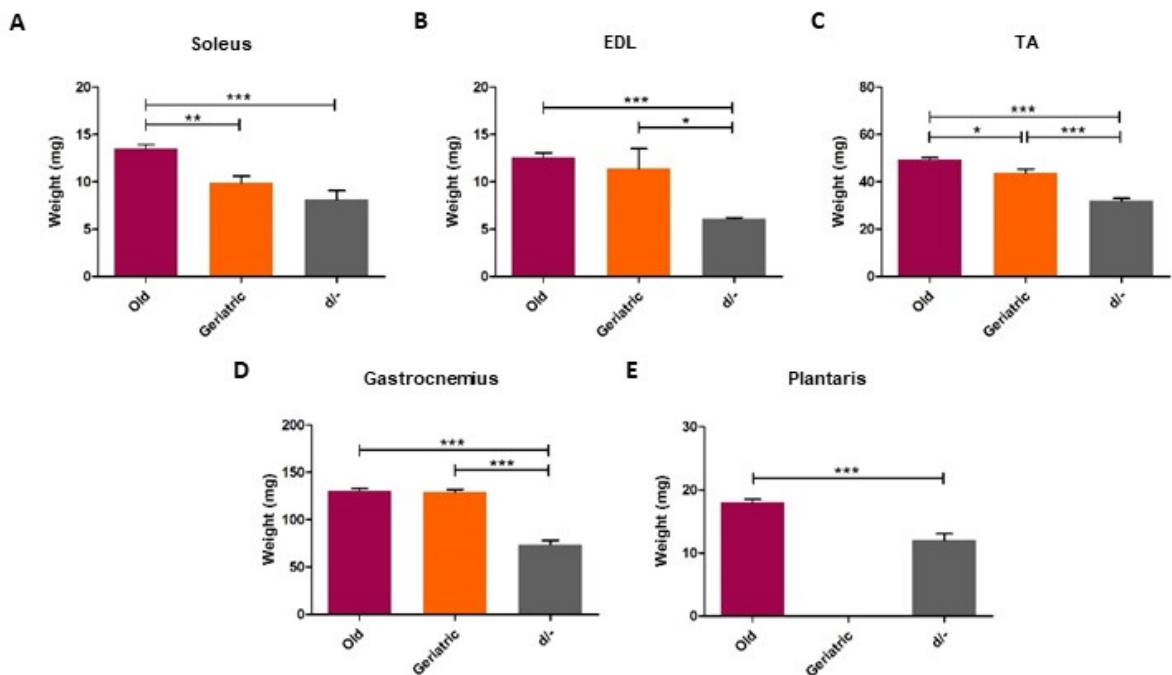
Figure 4.7 Substantially reduced *Ercc1*$^{d/-}$ fresh hindlimb muscle weights compared to natural ageing. **(A)** *Soleus* weight **(B)** EDL weight **(C)** TA weight **(D)** *Gastrocnemius* weight **(E)** *Plantaris* weight. *p<0.05, **p<0.01, ***p<0.001, **(A-D)** One-way ANOVA with Tukey post hoc testing. **(E)** Individual student's t-tests.

Taryn Morash

Furthermore, myofibre type analysis indicated that $Ercc1^{d/-}$ Soleus muscles had remarkably different MHC composition to that of naturally-aged animals. Firstly, the $Ercc1^{d/-}$ cohort showed a greatly reduced proportion of type I myofibres, 42% compared to 56% at old age and 60% at geriatric age (p = <0.05 and <0.01, respectively) (Figure 4.8 A). However, type IIA proportions were no different between the $Ercc1^{d/-}$ and naturally-aged Soleus (Figure 4.8 B). Moreover, as the amount of type I myofibres decreased, the proportional deficit shifted to the fastest phenotypes as percentages of type IIX (p = <0.01), IIB (p = <0.05) and hybrid type I / IIA (p = <0.01) increased when compared to those analysed at old age (Figure 4.8 C, D). The same trend was seen when compared to geriatric ages (p = <0.05, <0.05 and 0.01, respectively).

CSAs of myofibres analysed between naturally aged and $Ercc1^{d/-}$ Soleus muscles was not statistically different in type I myofibres, however type IIA myofibre size was significantly reduced in $Ercc1^{d/-}$ muscles, compared to old age (p = <0.05) (Figure 4.8 E, F). Type IIX CSA was also smaller, ~1100μm^2, in $Ercc1^{d/-}$ myofibres compared to geriatric ages, ~1900μm^2 (p = <0.001), therefore this indicated that $Ercc1^{d/-}$ IIX myofibres were more similar in size to those measured at old age 1400μm^2 (Figure 4.8 G). There were no observed type IIX myofibres present in the old and geriatric Soleus (Figure 4.8 H).

Taryn Morash
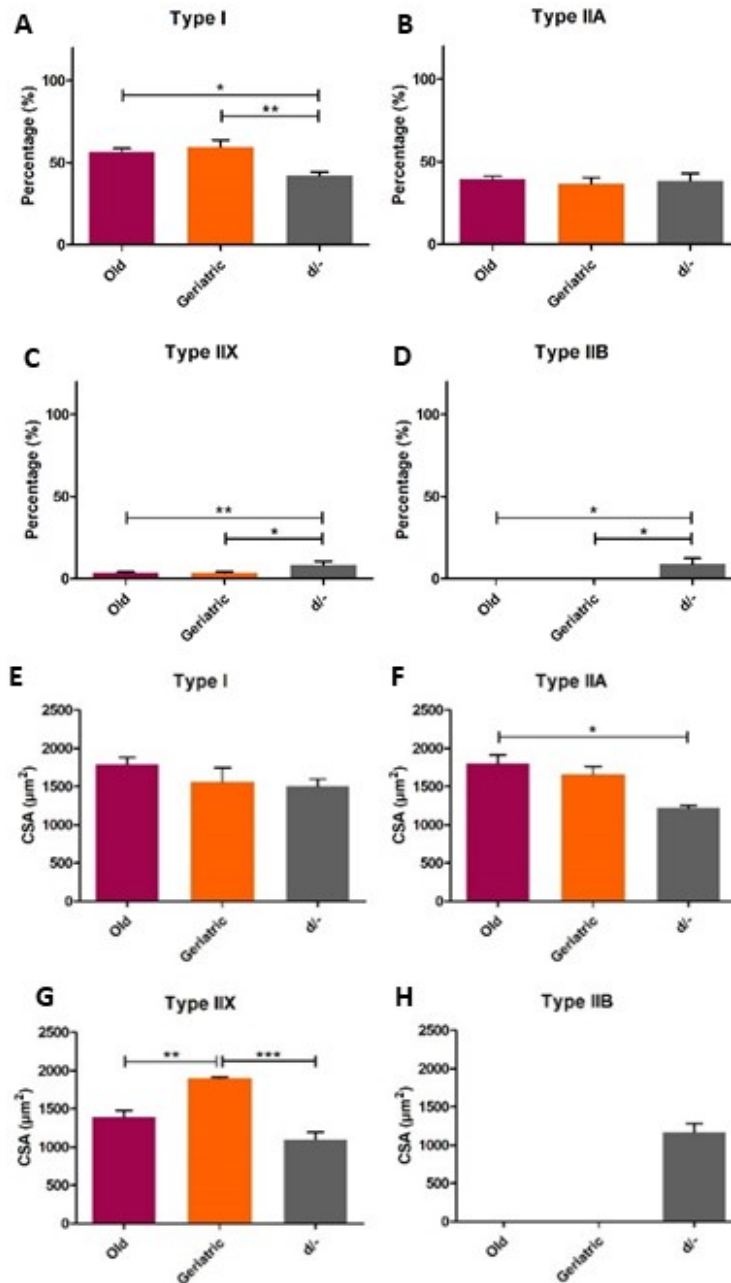
Figure 4.8 Myosin heavy chain (MHC) isoform myofibre composition and size indicates an alternative myofibre phenotype in the *Ercc1$^{d/-}$ Soleus* compared to natural ageing. **(A)** Proportion of MHC type I myofibres **(B)** Proportion of MHC type IIA myofibres. **(C)** Proportion of MHC type IIX myofibres. **(D)** Proportion of MHC type IIB myofibres. **(E)** MHC type I myofibre CSA. **(F)** MHC type IIA myofibre CSA. **(G)** MHC type IIX myofibre CSA. **(H)** MHC type IIB myofibre CSA. *p<0.05, **p<0.01, ***p<0.001, One-way ANOVA with Tukey post hoc testing.

Taryn Morash

Regarding the parameters analysed to determine potential changes in metabolic status and function, such as the percentage oxidative myofibres (SDH), ROS production (DHE) and SOD2 gene expression, the differences noted in old and geriatric ageing and in the *Ercc1*$^{d/-}$ *Soleus* were not statistically significant, indicating a degree of consistency (Figure 4.9 A, D, E, F).

Contrastingly, the capillary density in the *Ercc1*$^{d/-}$ muscle demonstrated an extremely reduced number of CD31+ cells (2 cells per myofibre) compared to the old and geriatric *Soleus* with an average of 3.6 cells each (p = <0.01) (Figure 4.9 B). At a molecular level however, qPCR analysis indicated that there was statistically no variation in mRNA expression of VEGFa 165 between the *Ercc1*$^{d/-}$ progeric model and that in old and geriatric ages (Figure 4.9 C).

Similarly, the collagen IV borders between both MHC type I and non-type I myofibres were found to be thinner in the *Ercc1*$^{d/-}$ *Soleus*, significantly so (type I), when compared to the collagen thickness in old age (p = <0.05) but interestingly, statistically no different to those measured at geriatric ages (Figure 4.9 G, H). Quantative PCR analysis of collagen mRNA expression it was seen that both collagen I and IV levels were consistent between naturally aged old and geriatric groups when compared to that of the *Ercc1*$^{d/-}$ *Soleus* (Figure 4.9 I, J). Expression of DGC component, dystrophin, in *Ercc1*$^{d/-}$ muscles however, was significantly lower than old age (Figure 4.9 K). Beta-sarcoglycan mRNA levels were also consistent between naturally aged and *Ercc1*$^{d/-}$ progeric muscle (Figure 4.9 L).

Taryn Morash
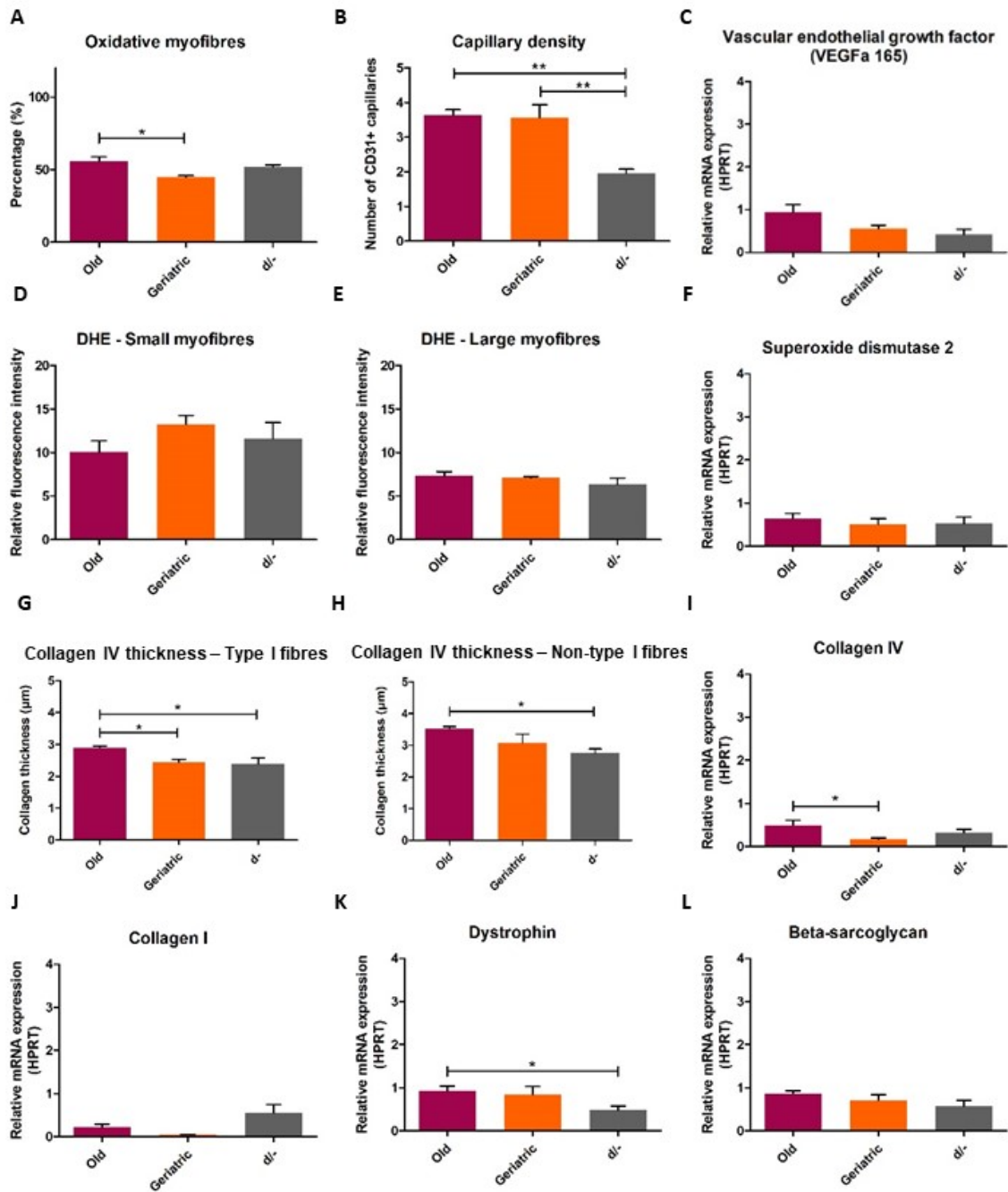
Figure 4.9 Assessing the suitability of the *Ercc1*$^{d/-}$ model of progeria in mimicking natural ageing. The following characteristics of metabolic status, vasculature organisation, mitochondrial function and structural and ECM components are compared in the *Soleus*. **(A)** Oxidative capacity. **(B)** Capillary density (CD31+ cells per myofibre). **(C)** VEGFa 165 mRNA expression. **(D)** ROS production in small myofibres. **(E)** ROS production in large myofibres. **(F)** Antioxidant superoxide dismutase 2 (SOD2) mRNA expression. **(G)** Collagen IV thickness in type I myofibre borders **(H)** Collagen IV thickness non-type I myofibre borders **(I)** Collagen IV mRNA expression **(J)** Collagen I mRNA expression **(K)** Dystrophin mRNA expression. **(L)** Beta-sarcoglycan mRNA expression. *p<0.05, **p<0.01, One-way ANOVA with Tukey post hoc testing.

148

Taryn Morash

Discussion

Characterisation of the skeletal muscle phenotype in the *Ercc1*$^{d/-}$ murine model of progeria

The first objective of this current series of experiments was to characterise features of the *Ercc1*$^{d/-}$ skeletal muscle phenotype. Secondly, as with the naturally-aged study, the experiments were designed in order to additionally determine the effects of ADMSC-derived CM as a potential therapy. The CM treatment was assessed in its capability to impact on hallmark components such as increased oxidative stress, associated with the *Ercc1*$^{d/-}$ model, or any age-related, myo-pathological traits, utilising the parameters employed previously for analysis at a whole organism and muscle level. Thirdly, comparisons were made in order to establish how reliably or accurately the *Ercc1*$^{d/-}$ model displays and mimics characteristics associated with sarcopenia in natural ageing.

This series of experiments has enabled the development of a progeric skeletal muscle profile, detailing the observed differences in physiological, immunohistological and biochemical characteristics of the naturally-aged and *Ercc1*$^{d/-}$ *Soleus* muscle. As with the naturally-aged animal experimentation, parameters were measured at whole organism, tissue, cellular and molecular levels and the effect of CM treatment on these features were recorded. Firstly, observations and measurements recorded at a whole organism level included regular body weight and health checks. Dramatic reduction in body weight (>15% within 2 weeks), along with the development of features such as prominent spine or ribs, sunken hips, hunched body position, matted fur, slow respiration, not responsive to touch stimuli, rectal or uterine prolapse, skin lesions or visible tumours would have been of sufficient health concern for that animal to be sacrificed via a Schedule 1 method. Fortunately, body condition did not decline to this severe extent in any of the progeric animals and although body weight fluctuated slightly, it did not deteriorate anywhere near to this degree. Body weights of the *Ercc1*$^{d/-}$ animals were remarkably reduced compared to their control littermates throughout the experimental duration. This is in keeping with findings reported in the literature, where it is reasoned that the additional conclusion that *Ercc1*$^{d/-}$ cells enter premature replicative senescence, could be an underlying cause of the stunted growth, very small phenotype and drastically reduced lifespan of the *Ercc1*$^{d/-}$ mice (Weeda et al. 1997; De Waard et al. 2010; Dollé et al. 2011). Additionally, it was noted that at the experimental end-point, when the animals were 16 weeks old, the *Ercc1*$^{d/-}$ mice displayed a number of the previously reported age-related signs and symptoms, such as tremors, incontinence, kyphosis, ataxia, dystonia, forelimb and hindlimb clasping as well as having an overall frail appearance (Lavasani et al. 2012). Although a certain amount of weight gained during the early growth phase can be attributed to fat, percentage body fat has been

149

Taryn Morash

shown instead to increase rapidly after 6 months of age (Glatt et al. 2007). Skeletal muscle however, develops rapidly during post-natal growth, between the initial 3 – 4 weeks and continues into adulthood. In studies conducted in rodents, whole-body muscle mass is reported to increase 50-fold during the initial growth phase and of the total gained mass of the growing animal, muscle contributes 50% of the overall increase (Gokhin et al. 2008). Muscle growth is the result of increases in myofibre number (hyperplasia) or increases in myofibre size (hypertrophy). As mouse EDLs are believed to have the entire complement of myofibres at birth, remaining unchanged in studies of myofibre number between 1 – 8 weeks of age, muscle mass increases are therefore attributed primarily to myofibre hypertrophy (White et al. 2010; Gokhin et al. 2008; Stickland 1981). Furthermore, the animals in the current study were 9 weeks old at the start of the experiment and muscle hypertrophy is likely to be the main contributing factor in control body weight increases. The $Ercc1^{d/-}$ animals however, are reported to experience stunted growth and visibly this was evident at the start of the study by animal size alone (Weeda et al. 1997; Dollé et al. 2011; De Waard et al. 2010).

Strength and activity testing revealed that there was a large degree of variation in the data, however despite this, very strong trends indicated overall decreased grip strength and rotarod performance displayed by the $Ercc1^{d/-}$ animals. Functional tests such as these are used universally in the research field to give an indication of functionality. A decreased functionality therefore could be expected in the $Ercc1^{d/-}$ mice given their overall reduced body size however, this may also provide an initial indication of muscular deficits and decreased force-generating capacity. This reduction is consistent with a reduced force measurement previously observed in natural ageing.

In the $Ercc1^{d/-}$ animals however, along with reduced body mass, muscle weights were also significantly reduced when compared to those in control littermates. This is in keeping with muscle mass declines reported in natural ageing, in the literature, as well as in the majority of the naturally-aged hindlimb muscles of the previous series of experiments discussed (Rogers & Evans 1993). Taken with what is known regarding the key determinants behind muscle growth, this finding therefore indicates potential impairments in cell proliferation or the underlying mechanisms of hypertrophy or both. This was further investigated and total myofibre number did appear to be fewer than in the control (significantly so when compared to control CM cohort). It should be noted that initial development of $Ercc1^{d/-}$ is reportedly normal and it is after this time that rapid mutation accumulation occurs, along with the appearance of characteristics associated with premature ageing (Dollé et al. 2006). This therefore suggests that cell proliferation during early muscle development was not affected and instead, directs thinking towards myofibre loss as the explanation behind reduced myofibre number. This is in keeping with the previously reported entry of $Ercc1^{d/-}$ cells into

Taryn Morash

premature cellular senescence (Weeda et al. 1997). Work carried out by De Waard and colleagues revealed increased motor neuron loss and denervation of skeletal myofibres in the $Ercc1^{d/-}$ mice (De Waard et al. 2010). Additionally, as apoptosis has been linked to myofibre atrophy in sarcopenia, it is postulated that among others, caspase levels for example, will indicate a higher instance of apoptosis occurring in the $Ercc1^{d/-}$ muscles (Dupont-Versteegden 2005; Wang et al. 2014). However, further exploration into apoptotic signalling pathways is required in order to provide a better understanding of this activity in the surmised myofibre atrophy in the $Ercc1^{d/-}$ mouse. Moreover, while investigating qualitative features of hypertrophy, the $Ercc1^{d/-}$ myofibres appeared to maintain a trend towards a reduced cross-sectional area compared to controls, particularly in the faster myofibres types (type IIX and IIB). These results are overall in-keeping with what is already well-established, regarding a metabolic shift towards maintenance and away from proliferation and growth, in the interest of extending longevity (Garinis et al. 2008; Niedernhofer et al. 2006). Furthermore, it would indicate that the mechanisms regulating muscle growth are also somewhat dampened in the $Ercc1^{d/-}$ Soleus, as a survival response. It should be noted that these faster myofibre types are less abundant in the Soleus, which subsequently resulted in small degrees of variation becoming amplified in the data, equalling overall statistical non-significance. Therefore, it would be of interest to further investigate the underlying mechanisms of both protein synthesis and protein degradation, hypertrophy and atrophy, in $Ercc1^{d/-}$ muscle. For example, western blot analysis of IGF-1 and PI3K/AKT signalling pathway, responsible for the balance between protein catabolism and anabolism, would aid in elucidating the details of this shift in muscle. Examination of the molecular activity of downstream components of AKT such as mTORC1, 4E-BP2 and e1F4E, associated with protein synthesis or FOXO1/3, Atrogin-1 and MuRF1, connected to the regulation of degradation, could be used to provide further understanding of the trend observed.

Further qualitative analysis revealed no discernible differences in MHC myofibre phenotype in the $Ercc1^{d/-}$ Soleus compared to control. This finding is therefore unlike the shift to a slower, more oxidative phenotype observed in natural ageing. This seems to be a surprising result, when the loss of motor neurons and increased denervation through associated degeneration, are a previously reported phenomenon in the $Ercc1^{d/-}$ animals (De Waard et al. 2010). The process of denervation/re-innervation is believed to be a main cause of myofibre typing transitions (Larsson & Ansved 1995; Larsson et al. 1991; Faulkner & Brooks 1995). However, this could suggest that myofibre atrophy, resultant of extensive motor neuron degeneration, may have been too detrimental to any potential for re-innervation. Additionally, this suggests that also unlike natural ageing, the faster myofibre types do not seem the most susceptible to atrophy (Larsson & Edström 1986; Rowan et al. 2011). Indicating that more wide-spread atrophy occurred in $Ercc1^{d/-}$, which lead to an overall reduced

Taryn Morash

myofibre number, however this was not type-specific. Furthermore, contrastingly to natural ageing, but in keeping with the consistent MHC phenotypes, there was no evidence of a change in the percentage oxidative myofibres in the $Ercc1^{d/-}$ Soleus muscle. However, there was evidence of reduced capillary density, suggesting that oxygen delivery may not be as efficient in $Ercc1^{d/-}$ muscle. This therefore, is in-keeping with findings of capillary loss associated with natural ageing (Degens et al. 1993).

Moreover, ROS production, although showing slightly increased levels above the control in the $Ercc1^{d/-}$ mice, was not statistically significant. An explanation for this trend could suggest that at the rate O_2^- ROS was being generated as a by-product of dysfunctional oxidation, it could also have been sequestered at a reasonably equivalent efficiency by antioxidants. However, further analysis revealed that SOD2 expression levels in the $Ercc1^{d/-}$ Soleus, were unchanged compared to that of the control. As it is known that SOD2 expression increases in response to oxidative stress, it could be reasoned that the albeit slight increases in O_2^- ROS, were not sufficiently detected in the $Ercc1^{d/-}$, in order to induce an increase in SOD2 expression. Moreover, SOD2 requires a number of post-translational modifications to become catalytically active and function is also regulated further at a protein level, for example by cyclins and p53 (Ryan et al. 2008; Candas & Li 2014). Therefore, it would be of interest to measure SOD2 protein levels to further understand SOD2 function in the $Ercc1^{d/-}$ as, with an absence of regulation at a gene expression level, the protein level may provide a better understanding of its activity. Additionally, as superoxide is just one of the ROS that can play a role in overall damage of DNA, mtDNA, lipids, proteins, oxidative phosphorylation enzymes for example, there are also many other free radicals that can do just as much damage if levels are not maintained by the range of antioxidant mechanisms. For example, glutathione peroxidase (GPX), is downstream from SOD2, that functions in the detoxification of H_2O_2 to water (Pieczenik & Neustadt 2007). Therefore, as $Ercc1^{d/-}$ has been previously linked with high levels of oxidative stress, other sources would merit further investigations.

The effects of CM generated from ADMSCs on $Ercc1^{d/-}$ Soleus muscle phenotype

Research carried out by Lavasani and colleagues in 2012 provided the basis for the hypothesis that *in vivo* CM treatment will have beneficial therapeutic effects in the skeletal muscle of $Ercc1^{d/-}$ mice. This landmark study reported that *in vivo* administration of young muscle progenitor/stem cells into the $Ercc1^{d/-}$ progeroid mice resulted in extended lifespan and 'healthspan'. Furthermore, improved characteristics of regeneration, including proliferation, differentiation as well as tissue vascularisation, were evident even in the absence of transplanted donor cells (Lavasani et al. 2012).

Taryn Morash

This essential finding therefore infers rejuvenation potential released by young/healthy cells acting through a paracrine effect via 'secreted factors'. Using the previously established series of parameters, investigating at whole organism and tissue levels, the potential therapeutic properties of ADMSC CM is assessed in the *Soleus* muscle of *Ercc1*$^{d/-}$ mice.

Ercc1$^{d/-}$ body weight appeared to be unaffected by CM treatment. However, in the control, weight was reduced compared to the PBS-vehicle controls, after the second and third IP injections. An explanation for this could be that previously mentioned in the naturally-aged experimentation, where it was suggested that CM could modulate features of body composition and body fat through signalling targets associated with lipid metabolism, as seen in the miRNA analysis of the CM generated from AFS cells (Mellows et al. 2017). Although, the control littermates had relatively less visible fat than the old animals at the experimental end-point and as previously discussed, skeletal muscle mass increases are known to contribute to a large proportion of body weight gain, occurring at a rapid pace during the early growth phase of mice (Gokhin et al. 2008). It could be suggested that CM treatment instead impacted on the rate of hypertrophy when compared to control PBS. However, when this data was analysed as the percentage change in body weight, this previously observed difference did not reach statistical significance.

As in the naturally-aged series of experiments, CM appeared to have no additional effects in aspects of grip strength and rotarod performance, muscle weight, myofibre number or myofibre size in the *Ercc1*$^{d/-}$ *Soleus*. CM treatment however did appear to increase the proportion of type IIA myofibres from a slightly reduced percentage in the *Ercc1*$^{d/-}$ muscles to a control level. This could suggest that CM potentially prevented loss of the faster type IIA myofibres, which is the type that is reportedly more susceptible to myofibre denervation and damage than slower types, as previously discussed (Larsson & Edström 1986; Rowan et al. 2011). Alternatively, CM may have caused a myofibre switch to a faster oxidative type IIA, indicating that where there was a large amount of myofibre loss observed in the *Ercc1*$^{d/-}$ *Soleus*, which is attributed to motor neuron degeneration, CM may be assisting successful re-innervation by surviving motor neurons. CM treatment in the control also appeared to have no further impact on these aspects of muscle physiology and phenotype. Unlike the previous findings in the naturally-aged *Soleus*, the oxidative capacity and capillary density parameters in both control and *Ercc1*$^{d/-}$, appeared relatively unaffected by CM treatment. There was a slight, albeit non-significant increase in the *Ercc1*$^{d/-}$ capillary density to a level more akin to that observed in the control, therefore suggesting as before, that CM may hold pro-angiogenic potential. This again would be in-keeping with a pool of miRNA targets identified in the AFS-derived CM analysis (Mellows et al. 2017). ROS production however in both large and small myofibres, was remarkably greater in *Ercc1*$^{d/-}$ muscles with CM treatment. This is seemingly counterintuitive for a

Taryn Morash

potential therapy in a model of progeria, where oxidative stress and damage through ROS production would only exacerbate the situation. A possible explanation for this could be that as O_2^- ROS generation is known to be a by-product of 'normal', functional oxidative metabolism within mitochondria, if in the instance that CM increased the rate of metabolism, utilising the 'faulty' machinery, O_2^- ROS may have been produced at an advanced rate. Secondly, accumulated O_2^- ROS may also be due to inadequate antioxidant activity or regulation. Similar to the findings in natural ageing, SOD2 mRNA levels remained unchanged between control and $Ercc1^{d/-}$ conditions, with and without CM treatment. Therefore, it could be postulated that post-translational modulation of antioxidant activity was instead more regulated in a more negative direction with CM. Thirdly, the damage caused through dysfunctional mitochondrial activity in the $Ercc1^{d/-}$, may have reached an irreversible state, thus any potential beneficial impacts on metabolism and stress response, maintained by the CM, now has little therapeutic effect. This additionally, could also be the reason behind the relatively unchanged oxidative capacity and capillary density. Collagen IV thickness, expression of collagen types I and IV as well as DGC complex components, dystrophin and beta-sarcoglycan also appeared to be unaltered with CM treatment.

In a model of such severe and rapid systemic DNA damage accumulation and subsequent, systematic organ failure and despite stunted growth, the *Soleus* phenotype, in regards to some of the physiological parameters analysed, was not as drastically altered as initially expected. With some evidence of myofibre loss, surmised to be the outcome of the previously described shift to a survival response. Where energy reserves are focused away from proliferation and synthesis and instead, are directed towards pathways of genomic and cellular maintenance, autophagy and biological material recycling. Taken together, this could potentially signify distinct differences in CM treatment efficacy, in altering components of regulation to bring about seemingly beneficial, therapeutic (pro-angiogenic, antioxidant, ECM component) changes in naturally-aged muscle, compared to seeing relatively little impact in the severe model of premature ageing. As concluded in the natural ageing series of experiments, the therapeutic value of CM seems to be the ability to regulate (potentially through miRNA), the signalling and behaviour of resident stem and existing somatic cell populations, to carry out regeneration or to combat age-related decline. This therefore, may be possible in a system where the survival response and shift towards maintenance may not be quite so strong. Whereas it appears that CM treatment in the $Ercc1^{d/-}$ model is not as capable of regulating mechanisms of regeneration, to counter the rapid onset of wide-spread decline. This suggests that, in a model displaying such an extreme survival response and postulated systematic default to cellular conservation, autophagy and death, the control of these mechanisms is not so easily overridden by the therapeutic paracrine effect of CM. Overall, it could be hypothesised that CM has more beneficial

Taryn Morash

therapeutic value in systems undergoing slower, more chronic features of decline and dysregulation. Suggesting that there is perhaps a threshold at which point the paracrine effect of properties harboured by CM, may no longer be able to aid in balancing features of such advanced and somewhat over-whelming signals of decline and dysregulation.

Numerous characteristics of *Ercc1*$^{d/-}$ skeletal muscle reflect sarcopenia in natural ageing while others appear amplified

A key objective of the project was to determine the extent that the *Ercc1*$^{d/-}$ mouse model mimics features of sarcopenia in natural ageing. The first main finding when comparing some of the aspects of *Soleus* physiology and myofibre phenotype was that *Ercc1*$^{d/-}$ muscle weights were all remarkably lower than those measured in old and geriatric animals. This is not surprising when the well-documented runted phenotype of the *Ercc1*$^{d/-}$ is considered (Weeda et al. 1997; De Waard et al. 2010; Dollé et al. 2011). This finding is even more remarkable as, despite the evidence of sarcopenia in the old and geriatric animals, as well as the particularly frail appearance of the geriatric cohort at the experimental end-point, the *Ercc1*$^{d/-}$ muscles were so strikingly smaller. Regarding MHC composition, as previously mentioned, the naturally-aged muscles exhibit an established switch to a slower myofibre phenotype. Whereas, this shift was not observed in the *Ercc1*$^{d/-}$ *Soleus*. This therefore, is represented when the proportions are directly compared. Further indicating that *Ercc1*$^{d/-}$ *Soleus* muscles contain greater numbers of faster type IIX and IIB myofibres, whereas there are very few present in old and geriatric muscle. It is surmised that this may be the result of more wide-spread motor neuron degeneration and atrophy in the *Ercc1*$^{d/-}$ muscles. This is in contrast to natural ageing where faster myofibre types are reportedly more susceptible to denervation and damage (Larsson & Edström 1986; Rowan et al. 2011). Additionally, myofibre size appeared to be reduced in the *Ercc1*$^{d/-}$ *Soleus* compared to that in old and geriatric animals, significantly so in the faster myofibre types. As hypertrophy is a key feature determining muscle growth, this finding is consistent with the overall stunted size of *Ercc1*$^{d/-}$ animals. Moreover, as previously discussed, it could be suggested that the naturally-aged animals are experiencing a shift towards maintenance, away from growth, as a survival response with the onset and development of sarcopenia. However, this survival response appears to be further amplified in the severe *Ercc1*$^{d/-}$ model of premature ageing. This could further suggest that the severity of the DNA damage accumulation has caused a large majority of regulation of signalling pathways to default towards apoptosis, autophagy and necrosis.

Out of the physiological parameters measured in the *Ercc1*$^{d/-}$ *Soleus*, that arguably mimic characteristics observed in natural ageing include oxidative capacity, ROS production and antioxidant

Taryn Morash

activity. In contrast, features that appear to occur to a more extreme degree than in natural ageing, include evidence of myofibre atrophy and greatly reduced muscle weight, myofibre CSA, capillary density, collagen thickness and DGC component, dystrophin expression. Whereas, a feature that seems to display an alternative trend to that noted in natural ageing was MHC composition, exhibiting an overall faster phenotype in the *Ercc1*$^{d/-}$ *Soleus*. Capillary density, collagen thickness and also dystrophin levels were reduced in the *Ercc1*$^{d/-}$ *Soleus* however, these are trends that are arguably less surprising when the reduced myofibre size is also considered. This therefore suggests that blood supply and basement membrane collagen IV and dystrophin content are 'scaled-down' proportionately to serve the smaller *Ercc1*$^{d/-}$ myofibre. In conclusion, the *Soleus* muscle profile developed in the *Ercc1*$^{d/-}$ progeric model, shares a number of characteristics with the onset and progression of sarcopenia in natural ageing. In contrast, the severity of the DNA damage accumulation ultimately results in some seemingly amplified features that far exceed those observed in natural ageing. These would potentially continue to surpass those levels experienced by the most moribund naturally-aged animals, if allowed to survive to end-of-life. It can also be concluded that the *Ercc1*$^{d/-}$ mouse also demonstrated a distinct *Soleus* MHC myofibre composition which did not mimic the phenotype shift that is well-documented in natural ageing. Overall, these characteristics of the *Ercc1*$^{d/-}$ *Soleus* drive the notion that the *Ercc1*$^{d/-}$ model is one displaying features of 'super-ageing', from a skeletal muscle aspect.

Taryn Morash

Chapter 5

Investigation into the therapeutic effects of conditioned media on satellite cell number and mechanisms of function during natural ageing and in the *Ercc1$^{d/-}$* model of progeria

Taryn Morash

Introduction

It has been previously established in the literature that there are notable changes that occur to satellite cell (SC) number and function with age. It is well-reported that SCs exhibit a reduction in proliferation and self-renewal, thereby leading to a depleted stem cell pool, with age (Collins et al. 2007; Shefer et al. 2006). Stem cell exhaustion is one of the hallmarks of ageing, along with increased cellular senescence (López-otín et al. 2013). Studies have established that SCs experience 'geroconversion' and enter an irreversible state of senescence, leading to these declines in SC number attributed to a reduction in proliferative capacity (Sousa-Victor et al. 2014; García-Prat et al. 2016). Colleagues have previously reported a reduction in aged SC migration speeds, alterations in amoeboid-based motility through abnormal bleb dynamics, as well as a delayed activation and emergence of aged SCs (Collins-Hooper et al. 2012). SC activation and subsequent emergence, is known to occur upon myofibre injury or damage, or induced in this study by isolating single myofibres, within the initial 24 hours (Collins-Hooper et al. 2012; Zammit et al. 2004). Hereafter, SCs proliferate and migrate along myofibres, while MyoD and Myf5 co-expression demonstrates commitment to a myogenic lineage by 48 hours (Zammit 2002; Cornelison & Wold 1997; Cooper et al. 1999). As important steps in the process of skeletal muscle myofibre regeneration, any declines in the function of these underlying features, impact on the potential for efficient and effective repair and have therefore, been implicated in muscular dystrophies as well as sarcopenia (Collins-Hooper et al. 2012; Gutmann & Carlson 1976; Schultz & Lipton 1982; Yin et al. 2013). To analyse and document the characteristics of SC function, parameters were measured at a cellular level in order to develop a more detailed skeletal muscle profile for both natural ageing and the $Ercc1^{d/-}$ progeria model.

Importantly, findings reported by Johnny Huard and colleagues, indicated the therapeutic potential of the secretome of young stem/progenitor cells, in the ability to restore the dysfunction demonstrated by aged and progeric stem cells, regarding proliferation and differentiation processes (Lavasani et al. 2012). These findings are an extension to the landmark studies reported by Conboy and colleagues that saw similar rejuvenating effects in aged SC proliferative and differentiation potential, from circulating factors in young serum, using a heterochronic (young/old) parabiosis system (Conboy et al. 2003; Conboy et al. 2005). Using these reported findings as a platform, a series of experiments were conducted in order to investigate the effects of our human adipose-derived mesenchymal stem cell (hADMSC) conditioned media (CM) on key mechanisms of skeletal muscle satellite cell regeneration in both natural ageing, as well as in the $Ercc1^{d/-}$ progeria model. As previously described, the $Ercc1^{d/-}$ mouse has been reported to demonstrate segmental age-associated functional decline and some of these features have been classified based on the rate that these symptoms are acquired, relative to natural ageing (Dollé et al. 2011). Lavasani and colleagues

Taryn Morash

reported defective proliferation and differentiation potential in *Ercc1$^{d/-}$* muscle-derived progenitor cells isolated and cultured *in vitro* (Lavasani et al. 2012). However, these aspects of SC activity have yet to be fully characterised, alongside the other vital mechanisms of SC function (such as emergence and migration), within the single myofibre microenvironment. The aim of this series of experiments was to investigate the mechanisms underpinning SC activity, which are well-known to undergo age-associated deterioration during sarcopenia, in the *Ercc1$^{d/-}$* model of progeria. Additionally, the suitability of the *Ercc1$^{d/-}$* progeric mouse, as a model of accelerated natural muscle ageing at a cellular level, can be assessed. Lastly, as with the naturally-aged experimentation, the therapeutic potential of ADMSC CM was investigated utilising these well-known parameters of cellular regenerative decline.

Taryn Morash

Results

Conditioned media reversed the abnormally advanced emergence trend observed in naturally aged satellite cells

In order to visualise the locations of SCs during the process of emergence, an immunocytochemical protocol was used to determine the positions of SCs (identified by Pax7 expression), relative to the basal lamina (indicated by laminin expression) (Collins-Hooper et al. 2012; Otto et al. 2011). Initially, it was observed that at T0, the point of single myofibre isolation, the majority of SCs were present beneath the basal lamina layer ('IN'), for the young (98.8%), old PBS (97.1%) and old CM (97.2%) conditions, compared to those beginning to emerge ('50%' or 'partially emerged') or those having emerged, residing on the outside surface of single myofibres ('OUT') (p = <0.001, respectively) (Figure 5.1 A, B, C, D) . There were no significant differences observed between cohorts in the percentage of SCs 'IN', '50%' emerged or 'OUT' at T0. By T24 however, 58.2% of young SCs remained in a sub-basal position, significantly more than those fully emerged (29.4%) and those that were undergoing emergence (12.4%), at that time (p = <0.01 and <0.001, respectively) (Figure 5.1 E, F, G, H). Interestingly, in the old age cohort at T24, fewer SCs remained beneath the surface layer (18.1%) compared to those that had emerged (51.3%) (p = <0.05) and the remaining 30.6% of cells that were in the process of emerging. Although, as observed with young control SCs, CM treatment in old age resulted in a larger percentage of cells yet to emerge (51.4%) compared to the 20.6% undergoing emergence (p = <0.05), with the remaining 28% of SCs having completely emerged. Moreover, analysis between age and treatment groups further indicates these findings, that there was a substantially smaller proportion of SCs under the basement membrane compared to young and Old CM-treated cultures (p = <0.01, respectively). The proportion of SCs 50% and fully emerged were not statistically different when compared between age and treatment.

Taryn Morash
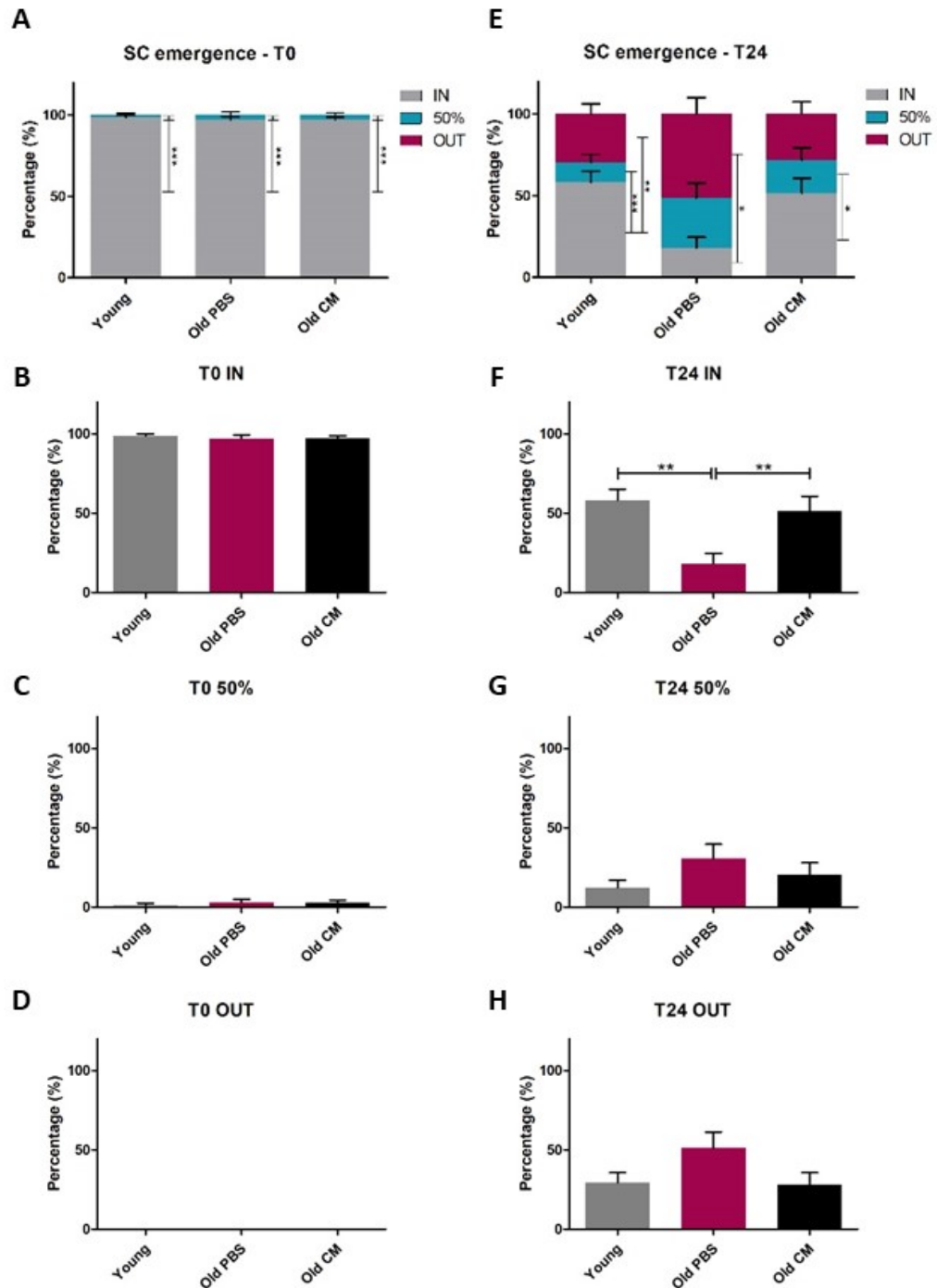
Figure 5.1 Conditioned media reversed the abnormally advanced emergence trend observed in naturally aged satellite cells. **(A-D)** The analysis of SCs positioning relative to the basal lamina, as quantified by proportion of cells 'IN' (inside/under), '50%' (in the process of emerging) and 'OUT' (outside/over), at T0, concomitant with SC activation and subsequent emergence. **(E-H)** An abnormal proportion of aged SCs were undergoing or has successfully emerged at T24. This pattern appeared to be reversed by CM. *p<0.05, **p<0.01, ***p<0.001, One-way ANOVA with Tukey post hoc testing.

Taryn Morash

Conditioned media greatly increased satellite cell migration speeds in old age

SC migration speeds have previously been shown to decrease with age (Collins-Hooper et al. 2012). However, it is currently unknown whether the underlying mechanisms regulating cell migration can be influenced by components maintained by CM treatment. Migrating SCs on myofibres were monitored from T24 to T48, at 10x magnification using time-lapse microscopy and average speeds were calculated for each age and treatment group. Firstly, it was noted that cell migration speeds, despite being slightly reduced from young (45.2μm/h) to adult (38.3μm/h) ages and then increasing again in old (42.8μm/h) and geriatric (47.9μm/h) ages, these fluctuations were not statistically significant (Figure 5.2 A). Remarkably however, despite SC migration speeds remaining constant with age, CM treatment considerably increased the velocities of aged SCs, when compared to both the adult and old age control groups (p = <0.05) (Figure 5.2 A).

Satellite cells adopt a rounded morphology on both adult and aged single myofibres

Cellular characteristics such as the morphologies adopted by cells analysed can provide basic indications as to which of the two methods of cell migration SCs were utilising at the point of single myofibre fixation. These two mechanisms of motility include the more traditionally reported lamellipodia-mediated traction whereas the more recently established blebbing or amoeboid-based method, defined in SC movement during the process of muscle regeneration, is shown to be associated with an increased velocity (Otto et al. 2011). An elongated (mesenchymal) cellular appearance, suggests migration via the former, lamellipodia-driven mechanism and on the other hand, a more rounded morphology, indicates that a SC may be utilising the latter, the amoeboid bleb-based mechanism. Single myofibres fixed and analysed at T48 using an immunofluorescence protocol to identify the organisation of alpha smooth muscle actin (SMA), paired with an antibody against myogenic marker MyoD, to detect the SCs and classify the frequencies that 'round' or 'elongated' morphologies were adopted. It was noted that SCs at both young and old age (with and without CM treatment), took on a more rounded morphology, compared to those more elongated (p = <0.001, respectively) (Figure 5.2 B). However, there was a slightly reduced proportion of SCs observed adopting a round morphology at old age (93.7%) and again with CM treatment (85.2%), when compared to 100% of young SCs (Figure 5.2 C). This was therefore accompanied by a corresponding increased percentage of elongated cells (6.3 and 14.8%, respectively), although these differences were statistically not significant (Figure 5.2 D). Thus, the majority of SCs observed on both adult and aged myofibres (with and without CM) adopted a more rounded form.

Taryn Morash
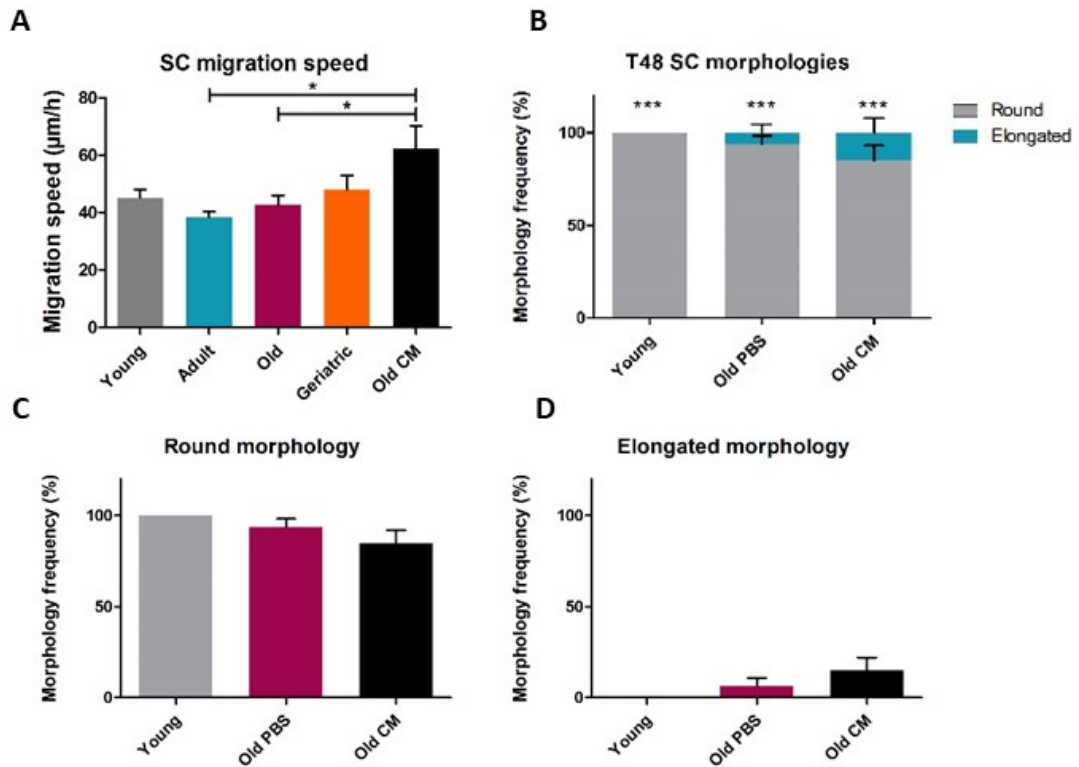
Figure 5.2 Conditioned media greatly increased satellite cell migration speeds in old age. **(A)** SC migration speeds determined for young (3 months), adult (6 months), old (24 months), geriatric (27-30 months) and old CM-treated myofibre conditions. **(B)** The majority of young, old and old CM-treated SCs were observed adopting a round form. Significance indicated between round and elongated morphologies ***$p<0.001$ **(C)** The proportion of rounded cells was no different between cohorts **(D)** The proportion of elongated cells was no different between cohorts. *$p<0.05$, ***$p<0.001$, **(A, C, D)** One-way ANOVA with Tukey post hoc testing. **(B)** Individual student's t-tests.

Conditioned media did not enhance the diminished proliferative potential of aged satellite cells

SC proliferation has been shown to be diminished with increasing age and has also been associated with increased cellular senescence and apoptosis and an overall depleted stem cell pool (Collins 2006; Collins et al. 2007; Schultz & Lipton 1982; Collins-Hooper et al. 2012; García-Prat et al. 2016; Sousa-Victor et al. 2014; Wang et al. 2014; Shefer et al. 2006). The dysfunction underlying this reduction in SC proliferative capacity in ageing however, was remarkably restored through experimentation exploring rejuvenating properties as part of a paracrine effect (Conboy et al. 2003; Conboy et al. 2005; Lavasani et al. 2012). Thus, it remains to be seen whether the ADMSC CM used in

Taryn Morash

the current study, contains similar regulatory potential in enhancing the proliferative capacity of aged SCs.

Pax7, the SC marker of quiescence, was used in immunocytochemical protocols on single myofibre cultures fixed at the earlier time-points (T0 and T24), whereas at T48, MyoD, a myogenic marker expressed later in the SC differentiation pathway, was used to identify individual or groups of SCs along myofibres over time to monitor proliferation. Average cells per myofibre were quantified, as well as the number of sites or events (clusters), that cells appeared along myofibres. The size of these clusters (number of cells per cluster) were additionally analysed. Firstly, it was noted that young SC populations at T0 had an average of 2.1 cells per myofibre which subsequently almost doubled by T24 to 4.8 cells (Figure 5.3 A). Following this, from T24 to 48, further proliferation resulted in more than double the number of cells within this time to an average of 11.6 (p = <0.001). Secondly, this was not the case in aged conditions (with and without CM treatment) (Figure 5.3 A). Despite a consistent T0 starting average number of cells to that of young myofibres, initial proliferation within the first 24 hours was not evident. By T48, the average number of cells had risen to 4.3, a significant increase to those observed at T0 (p = <0.05), but statistically no different to T24. Moreover, SC numbers did not change significantly from those present at T0, in the 48-hour culture duration in old age with CM treatment (Figure 5.3 A).

Analysis of SC clusters or events along the myofibres showed an increase in young SC clusters from T0 to 24, from an average of 1.8 to 4 clusters and to 5.5 at T48 (p = <0.05, respectively and p = <0.001 between T0 and 48) (Figure 5.3 B). In old age, the number of SC clusters did not change in the initial 24 hours of culture, but subsequently, increased from 1.8 to 3.3 cell clusters from T24 to 48 (p = <0.05) (Figure 5.3 B). As observed previously with the average cells per myofibre in old age with CM treatment, similarly, the number of clusters did not change during the 48 hours of culture. Furthermore, the number of cells per cluster (cluster size) increased only in the young SC population, doubling from single cell events at T0 and 24 time-points to clusters containing 2 cells at T48 (p = <0.001, respectively). In contrast, old SC populations (with or without CM treatment), were observed as single cells throughout the 48-hour culture period (Figure 5.3 C).

When this data was analysed between age and treatment groups, it was noted that there were no discernible differences in the number of cells or clusters per myofibre and cluster size remained constant, at T0 (Figure 5.3 D, E, F). By T24 however, following the initial proliferation previously described in young SC populations, the number of cells per myofibre was significantly greater than those present in old PBS and CM conditions (p = <0.001 and <0.05, respectively) (Figure 5.3 G). This increase in the young SC population was also evident when the number of clusters per myofibre at T24

Taryn Morash

were compared to those in the old PBS and CM cohorts (p = <0.001 and <0.01, respectively) (Figure 5.3 H). There were no observed differences in cluster size between age and treatment groups at T24 (Figure 5.3 I). Lastly, following the further population doubling seen from T24 to 48, the number of cells per myofibre at T48 were greatly increased in young SCs when compared to old PBS and old CM conditions (p = <0.05 and <0.01, respectively) (Figure 5.3 J). An observed decreased number of clusters per myofibre between young and old age and again with CM treatment, were statistically not significant (Figure 5.3 K). However, the cluster sizes quantified in old age (with and without CM treatment) at T48 were notably reduced when compared to those in young SCs (p = <0.05 and <0.01, respectively) (Figure 5.3 L). Therefore, the number of SCs and cell clusters were greatly reduced on aged myofibres and CM did not show any additional effects on these parameters at old age.

Taryn Morash
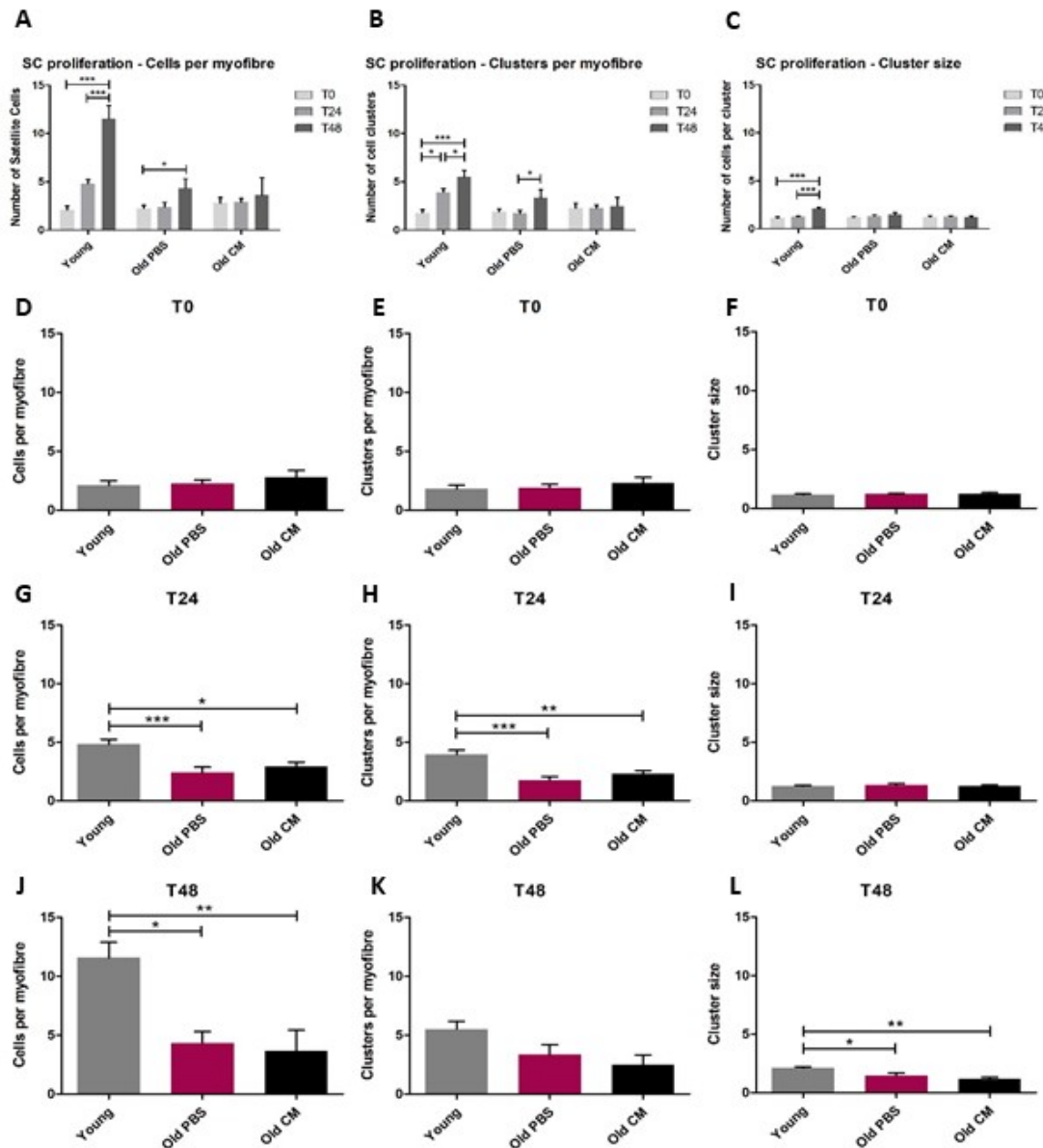
Figure 5.3 Conditioned media did not enhance the diminished proliferative potential of aged satellite cells **(A-C)** SC proliferation recorded as cells per myofibre, clusters per myofibre and cluster size. **(D-F)** Very few cells were present on myofibres at T0, in all three conditions, young, old and old CM **(G-I)** By T24, young SCs had proliferated, whereas old SCs had not. **(J-L)** By 48, young SCs had continued to proliferate further, while old SCs increased in quantity slightly, CM treatment appeared to perturb this, already diminished capacity. *p<0.05, **p<0.01, ***p<0.001, One-way ANOVA with Tukey post hoc testing.

Conditioned media advanced satellite cell emergence in the $Ercc1^{d/-}$ model of progeria

The essential underlying mechanisms of SC reparative function, emergence, migration, proliferation and differentiation, were subsequently characterised in the progeric $Ercc1^{d/-}$ murine model. As before with the natural ageing experimentation, SCs, following activation through single myofibre isolation at T0, emergence from the original sub-basal location was analysed using an immunocytochemical protocol for Pax7 and laminin, between T20 and 24 time-points. At T20, the majority of SCs remained inside the basal lamina layer in both the control (+/+) (78.5%) and $Ercc1^{d/-}$ (d/-) (86.5%) vehicle-treated (PBS) conditions, relative to both those cell populations 50% and fully emerged (p = <0.001, respectively) (Figure 5.4 A). Additionally, there was an increased proportion of cells undergoing emergence (16.4%) in the control PBS condition, compared to those fully emerged (5.2%), at the T20 culture point (p = <0.05) (Figure 5.4 A). Examination of the $Ercc1^{d/-}$ CM-treated condition however, showed no statistical differences and therefore indicated that there were equal proportions of SCs that remained beneath the basal lamina layer, that had emerged half-way and those that had fully emerged by T20 (Figure 5.4 A).

Moreover, when exploring this result further between cohorts, it was noted that there were distinctly fewer SCs positioned at a sub-basal location in the $Ercc1^{d/-}$ CM condition (42.9%), compared to the $Ercc1^{d/-}$ PBS (86.5%) and control PBS (78.5%) (p = <0.001 and <0.01, respectively) (Figure 5.4 B). There were no statistical differences in the percentage of cells that were 50% emerged at T20, between the control PBS, $Ercc1^{d/-}$ PBS and $Ercc1^{d/-}$ CM cohorts, 16.4, 12.5 and 19.6%, respectively (Figure 5.4 C). Consequently, the proportion of SCs of the $Ercc1^{d/-}$ CM cohort (37.5%) were shown to have fully emerged at this earlier time-point, remarkably increased relative to the control PBS and $Ercc1^{d/-}$ PBS (p = <0.001, respectively) (Figure 5.4 D).

By T24, the majority of SCs were still yet to fully emerge in both the control PBS and $Ercc1^{d/-}$ PBS cultures (p = <0.001) (Figure 5.4 E). Whereas, the majority of $Ercc1^{d/-}$ CM SCs had fully emerged

Taryn Morash

(54.6%, p = <0.001, relative to those half-way emerged), with only 36.5% at a sub-basal position (Figure 5.4 E). This trend was further evident when comparing the positions of SCs between cohorts, similarly to those described at T20. The proportion of SCs that were residing under the basement membrane at T24 were greatly reduced in the $Ercc1^{d/-}$ CM condition, relative to control PBS and $Ercc1^{d/-}$ PBS (p = <0.01, respectively) (Figure 5.4 F). As with the earlier time-point (T20), the percentages of cells undergoing emergence were statistically no different between groups (Figure 5.4 G). However, there was a greatly increased proportion of $Ercc1^{d/-}$ CM SCs fully emerged by T24, when compared to control PBS and $Ercc1^{d/-}$ PBS (p = <0.001 and <0.01, respectively) (Figure 5.4 H). The effect of CM treatment in the control animals on SC emergence was investigated. At T20, the results indicated no discernible differences in the proportions of SCs that were undergoing emergence, those that had fully emerged or those residing interior to the basal lamina (Figure 5.4 i). CM treatment in the controls by T24 however, indicated a 50% reduction in SCs yet to emerge and a remarkable corresponding increase in the proportion of SCs fully emerged, relative to the control PBS (p = <0.001, respectively) (Figure 5.4 ii).

167

Taryn Morash
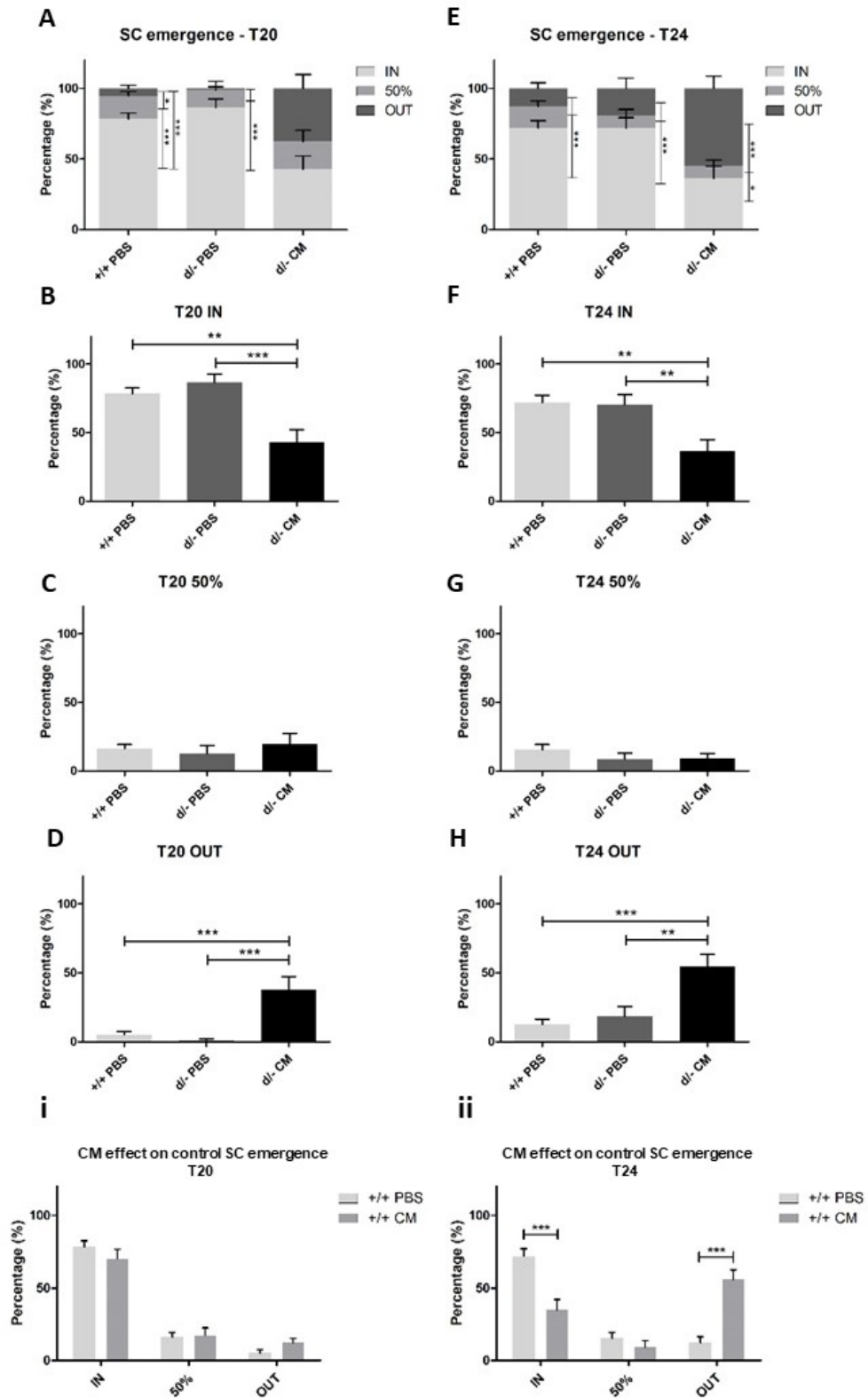
Figure 5.4 Conditioned media advanced satellite cell emergence in the *Ercc1*$^{d/-}$ model of progeria. The analysis of SCs positioning relative to the basal lamina, as quantified by proportion of cells 'IN' (inside/under), '50%' (in the process of emerging) and 'OUT' (outside/over). **(A-D)** By T20, a large proportion of *Ercc1*$^{d/-}$ SCs treated with CM had emerged in an advanced fashion. **(E-H)** By T24, this

Taryn Morash

advanced emergence trend had continued. **(i)** At T20, CM treatment did not influence emergence of the control SCs. **(ii)** By T24, however, control CM SCs has also emerged at a more advanced rate compared to control SCs. *p<0.05, **p<0.01, ***p<0.001, **(A-H)** One-way ANOVA with Tukey post hoc testing. **(i, ii)** Individual student's t-tests.

Increased *Ercc1*$^{d/-}$ satellite cell migration speeds were returned to control velocities with conditioned media treatment

SC migration speeds were also determined for each treatment group as part of the progeric *Ercc1*$^{d/-}$ investigation. Time-lapse microscopy was used to capture SC movement and behaviour from T24 and 48 time-points following SC activation, initiated at the point of single myofibre isolation (T0). The results showed that while the average SC migration speed recorded in the control PBS was 48.3μm/h, the progeric *Ercc1*$^{d/-}$ PBS SCs travelled at a remarkably faster rate of 63.3μm/h (p = <0.01) (Figure 5.5 A). Contrastingly, CM treatment reduced the average speed of motility of *Ercc1*$^{d/-}$ SCs to 52.7μm/h (p = <0.05), therefore, returning to a rate, although slightly quicker than that of the control PBS SCs, statistically no different to control PBS (Figure 5.5 A). CM treatment in the control animals however, had no discernible effects on SC migration speed (Figure 5.5 B).

Ercc1$^{d/-}$ satellite cells display the distinctive rounded morphology

Furthermore, information regarding morphology frequencies and basic indications as to the methods of SC motility along myofibres in each condition, was gathered in the *Ercc1*$^{d/-}$ experimentation, as per the protocol carried out for the natural ageing series. For example, 'round' or 'elongated' SC morphologies were visualised and classified using immunocytochemistry of single myofibres fixed at T48 to detect MyoD/SMA expression. As seen in the young and natural-aged SCs, the predominant morphologies adopted for migration along myofibres in each control and *Ercc1*$^{d/-}$ condition (PBS and CM) were those more rounded (p = <0.001, respectively) (Figure 5.5 C). The SC morphology frequencies, when compared between cohorts, indicated a slight reduction in the proportion of round cells, from 98% in control PBS and *Ercc1*$^{d/-}$ PBS to 90%, in the *Ercc1*$^{d/-}$ CM-treated condition (Figure 5.5 C, D). As well as a corresponding increase in those with an elongated form in *Ercc1*$^{d/-}$ CM SCs, however these observed differences were statistically not significant (Figure 5.5 C, E). Moreover, CM treatment had no effect in altering the morphologies adopted by control SCs.

Taryn Morash
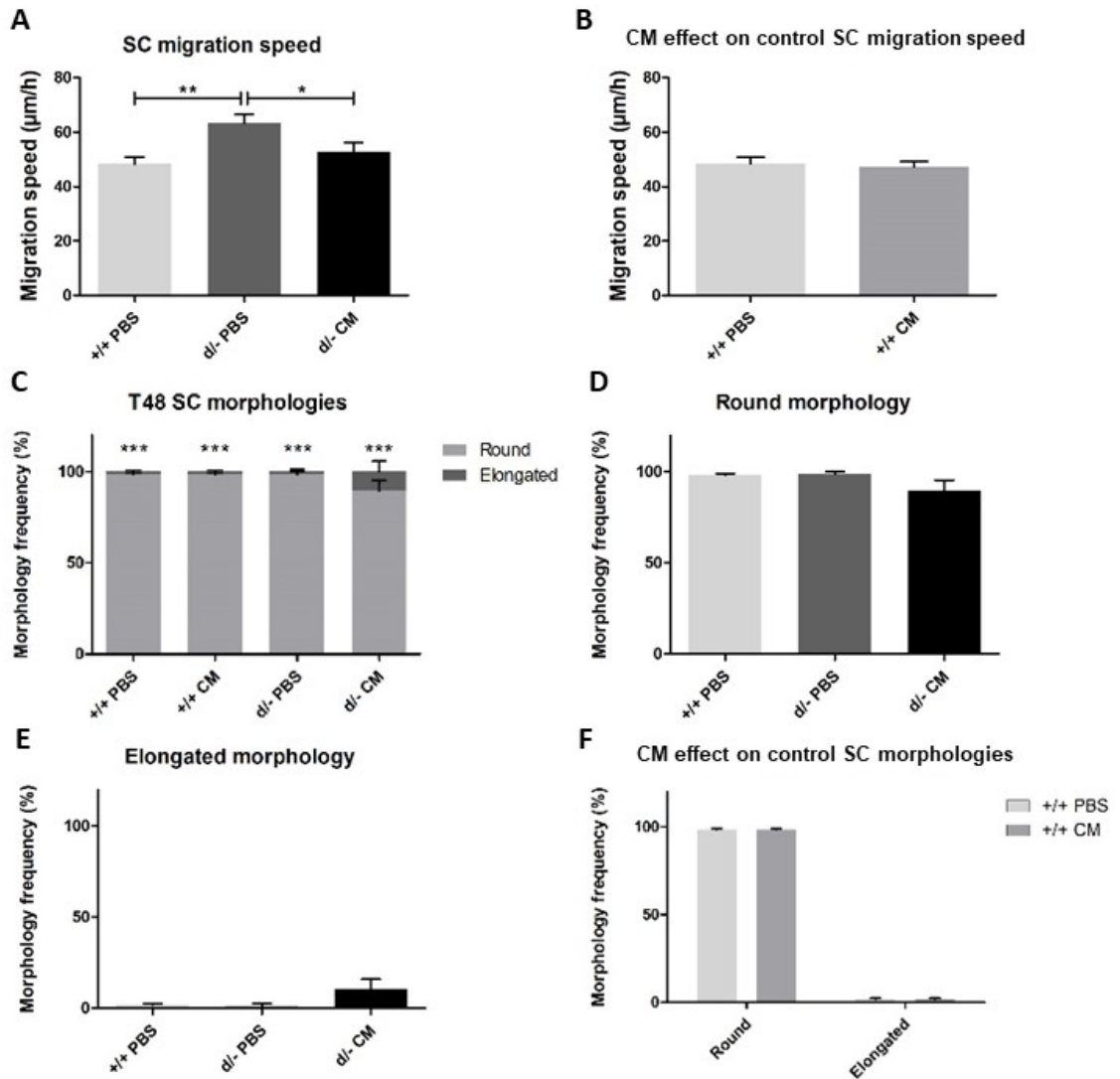
Figure 5.5 Increased *Ercc1$^{d/-}$* satellite cell migration speeds were returned to control velocities with conditioned media treatment **(A)** *Ercc1$^{d/-}$* SCs demonstrated a remarkably increased rate of migration however, CM appeared to reverse this to a control SC speed **(B)** CM did not influence control SC velocity. **(C-E)** *Ercc1$^{d/-}$* SCs adopted a characteristic rounded morphology and CM did not have any significant effect on cell shape. **(C)** Significance represented between round and elongated morphologies ***$p<0.001$. **(F)** CM also did not influence the control SC morphology.*$p<0.05$, **$p<0.01$, ***$p<0.001$, **(A, D, E)** One-way ANOVA with Tukey post hoc testing. **(B, C, F)** Individual student's t-tests.

Taryn Morash

The diminished *Ercc1$^{d/-}$* satellite cell number and proliferative capacity could not be restored by conditioned media

As in the naturally-aged series of experiments, immunofluorescent identification of Pax7 and MyoD was used at fixation points (T0, 24 and 48) to monitor SC proliferation, another key component process in muscle repair. In addition, during the series of analyses to investigate those differences in the progeric model, myofibres were also fixed at a later time-point after 72 hours culture following myofibre isolation (T72) to extend the time frame in which proliferation could be examined. Firstly, quantification of the number of cells per myofibre revealed that in the control SC populations, the largest increases in SC numbers occurred after the initial 24 hours of culture, from 4 - 6 cells at T0 and T24, to 13 - 14 cells at T48 and T72 (p = <0.001, respectively) (Figure 5.6 A). CM treatment in control animals showed a similar trend, with increased SC numbers from T0 and 24 to 48 (p = <0.01) and again to 19 cells at T72 (p = <0.001) (Figure 5.6 A). SC numbers in the *Ercc1$^{d/-}$* conditions also remained consistent in the first 24 hours of culture (T0 - 24) however average number of 2 cells per myofibre was observed at these early time points (Figure 5.6 A). Increased SC numbers were seen by T48 and 72 (4 – 4.5 cells per myofibre, respectively) in the *Ercc1$^{d/-}$* PBS control cultures (statistically significant at T72 only, p = <0.05) (Figure 5.6 A). CM treatment in progeric animals resulted in SC numbers peaking at T48, increasing from an average of less than 2 cells per myofibre at T0 to 4 cells at T48 (p = <0.05) and remaining consistent with no further proliferation noted between T48 and 72 (Figure 5.6 A). Furthermore, the number of clusters per myofibre increased from T24 (5.3 clusters), peaking at T48 (9 clusters) in the control groups (p = <0.01, respectively) (Figure 5.6 B). Subsequently, cluster numbers were decreased in the control PBS between 48 and 72 hours culture to 5.5 clusters (p = <0.01) (Figure 5.6 B). Meanwhile, with CM treatment control SC cluster numbers remained consistent at T72 with those counted at T48 (8 – 9 clusters), significantly more than T24 (p = <0.05). SC cluster numbers in the progeric myofibre cultures (with and without CM treatment) however, did not change notably over the 72-hour culture period (approximately 3 clusters per myofibre) (Figure 5.6 B). Moreover, average SC cluster sizes increased in control myofibre cultures (with and without CM treatment) significantly from 1 – 1.5 cells per cluster, at the earlier time-points (T24 and T48), to 2.5 cells at T72 (p = <0.001, respectively) (Figure 5.6 C). Additionally, the number of cells per cluster in the *Ercc1$^{d/-}$* PBS condition doubled from single cells to clusters of 2 cells between T24 and 72 (p = <0.01, respectively) (Figure 5.6 C).

Analysis of SC proliferation between cohorts showed that at each time-point (T0, 24, 48 and 72) the number of SCs per myofibre were significantly greater in the control PBS cultures compared to the *Ercc1$^{d/-}$* PBS and *Ercc1$^{d/-}$* CM conditions (p = <0.001, respectively) (Figure 5.6 D-G). A similar trend was observed with an increased number of clusters per myofibre in the control PBS at T24, 48 and 72

Taryn Morash

culture points (p = <0.001, respectively) (Figure 5.6 H-J). Contrastingly, cluster sizes were significantly larger in *Ercc1$^{d/-}$* CM SC populations at T24, relative to those in the control and *Ercc1$^{d/-}$* PBS cultures (p = <0.01, respectively) (Figure 5.6 K). By T48 however, there were no statistical differences in cluster size between the groups (Figure 5.6 L). Furthermore, *Ercc1$^{d/-}$* CM average cluster sizes were notably reduced from 2.5 cells per cluster to 1.7 cells at T72 (p = <0.05) (Figure 5.6 M). Lastly, CM treatment in control animals resulted in no discernible differences in the number of SCs per myofibre when compared to those without CM (Figure 5.6 i). Subsequently, CM however showed an increased number of clusters per myofibre at T72 compared to the control PBS (p = <0.05) but there were no differences observed in cluster size at any of the time-points (Figure 5.6 ii, iii).

Taryn Morash
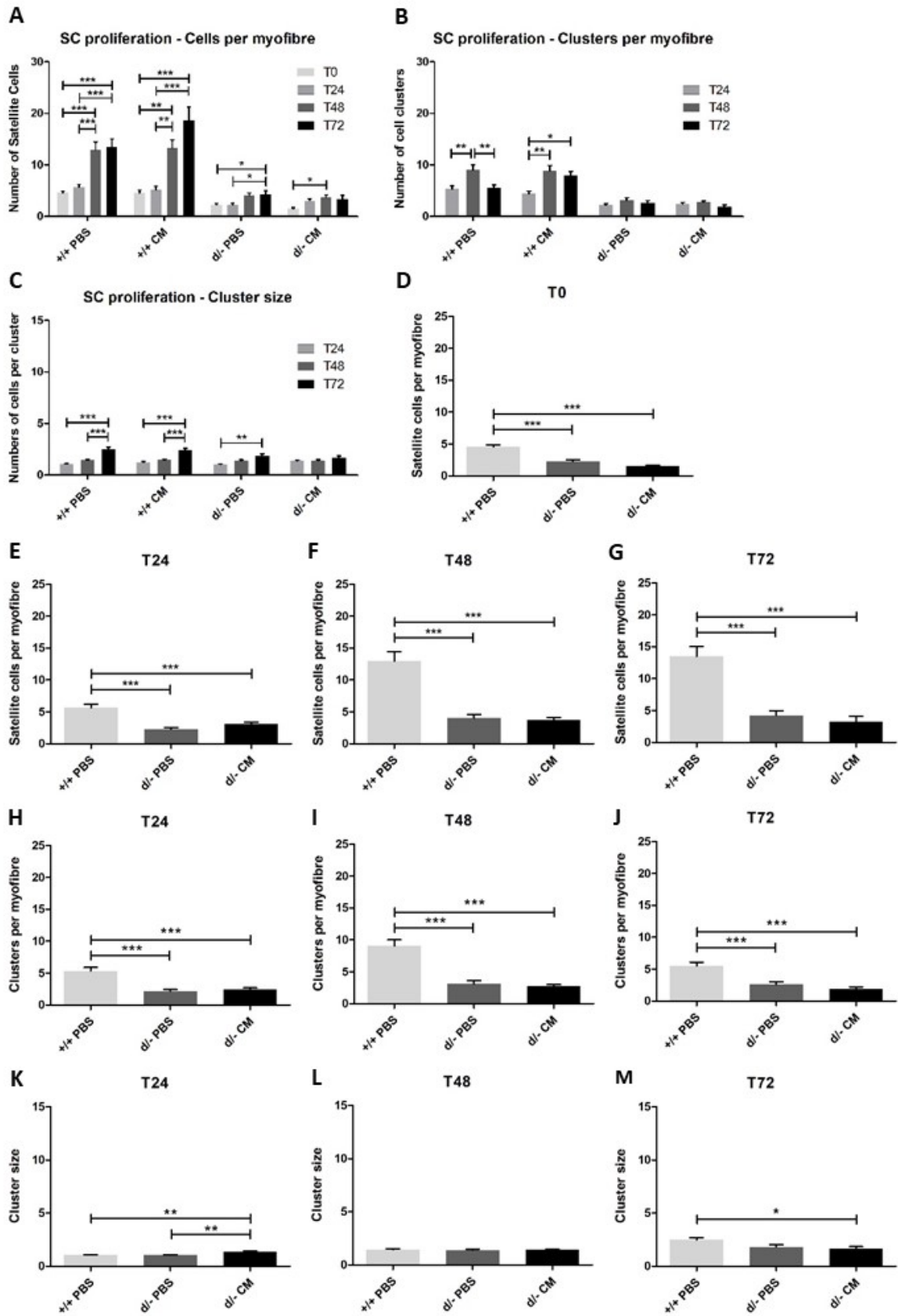
Figure 5.6 The diminished *Ercc1*^{*d/-*} satellite cell number and proliferative capacity could not be restored by conditioned media.

Taryn Morash
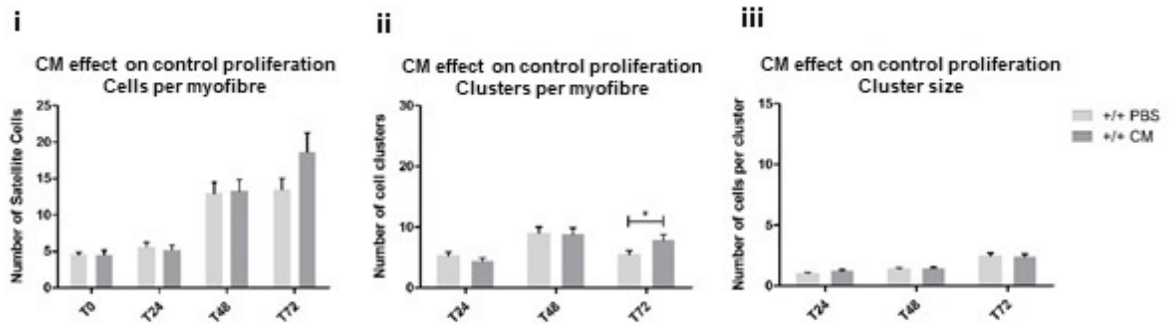
Figure 5.6 Continued. The diminished *Ercc1*$^{d/-}$ satellite cell number and proliferative capacity could not be restored by conditioned media **(A-C)** SC proliferation recorded as cells per myofibre, clusters per myofibre and cluster size. **(D-G)** *Ercc1*$^{d/-}$ SCs demonstrated a severely diminished proliferative capacity, the number of SCs per myofibre was unchanged during the 72-hour culture period. **(H-J)** A similar trend was noted with the number of clusters per myofibre. CM treatment did not influence *Ercc1*$^{d/-}$ SC proliferative potential. **(K-M)** SCs were observed primarily as single cells in each culture condition, CM treatment appeared to alter *Ercc1*$^{d/-}$ cluster sizes **(i, ii, iii)** CM treatment showed a slight increase in control SCs (non-significant) and clusters (*$p<0.05$) per myofibre. *$p<0.05$, **$p<0.01$, ***$p<0.001$, **(A-M)** One-way ANOVA with Tukey post hoc testing. **(i, ii, iii)** Individual student's t-tests.

Ercc1$^{d/-}$ satellite cells exhibited a normal commitment to myogenic differentiation and conditioned media delayed myogenin expression

To investigate the differentiation potential *Ercc1*$^{d/-}$ SCs, myofibres were cultured and fixed at T24, 48 and 72 following isolation and immunocytochemical protocols carried out to detect Pax7, MyoD (T24 and 48) and myogenin (T72). In order to examine any differences in SC myogenic differentiation in the *Ercc1*$^{d/-}$ progeric model, as well as to determine the effects of CM treatment on this parameter, the control and *Ercc1*$^{d/-}$ SC populations (PBS- and CM-treated) were compared. Firstly, it was observed that at T24 the SC populations of all four cohorts predominantly co-expressed both Pax7 and MyoD 'double' (ranging from 84 to 94%), significantly more than either marker expressed singly (*p* = <0.001, respectively) (Figure 5.7 A). Additionally, *Ercc1*$^{d/-}$ CM SCs showed increased expression of Pax7 individually (17%), relative to that of MyoD only (1%) (*p* = <0.05) (Figure 5.7 A). At T48, similarly, the majority of SCs continued to co-express Pax7 and MyoD (86 to 99%), compared to either alone (*p* = <0.001, respectively) (Figure 5.7 B). However by T72, when analysing Pax7 and myogenin expression, a greater proportion of SCs in the control PBS and *Ercc1*$^{d/-}$ PBS conditions were

Taryn Morash

myogenin-positive only (69 and 84%, respectively), significantly more than those expressing Pax7 only or double (p = <0.001, respectively) (Figure 5.7 C).

With CM treatment, control SCs showed significantly greater expression of Pax7 and myogenin individually than combined (p = <0.001, respectively) (Figure 5.7 C). Statistical analysis of the $Ercc1^{d/-}$ CM SCs, indicated that neither Pax7, myogenin alone nor double expression, comprised the largest proportion (Figure 5.7 C). Furthermore, when comparing the differences in myogenic marker expression between groups at the three time-points it was noted that there were no statistically significant variations in Pax7, MyoD individual or double expression at T24 (Figure 5.7 D, E, F). This was also the trend observed at T48 where proportions of SC populations expressing the myogenic markers were consistent between cohorts (Figure 5.7 G, H, I). At T72, despite a slightly increased proportion of $Ercc1^{d/-}$ CM SCs recorded expressing Pax7, relative to the control PBS and $Ercc1^{d/-}$ PBS, these differences were statistically not significant (Figure 5.7 J). Double expression of both Pax7 and myogenin however in the CM-treated $Ercc1^{d/-}$ SCs, was notably greater when compared to the $Ercc1^{d/-}$ PBS (p = <0.05) (Figure 5.7 K). Additionally, myogenin expression alone in the $Ercc1^{d/-}$ CM SC population at T72 was distinctly less than the $Ercc1^{d/-}$ control (p = <0.01) (Figure 5.7 L). CM treatment in control animals also indicated that at T24 there were no discernible differences in the proportions of SCs expressing Pax7, MyoD or both (Figure 5.7 i). At T48, CM increased the percentage SCs co-expressing both myogenic markers, from 86 to 99% (p = <0.001) (Figure 5.7 ii). Moreover, CM treatment showed that a greater proportion of SCs continued to express Pax7 by T72, as well as a corresponding decrease in the population of myogenin-positive SCs (p = <0.01, respectively) (Figure 5.7 iii).

Taryn Morash
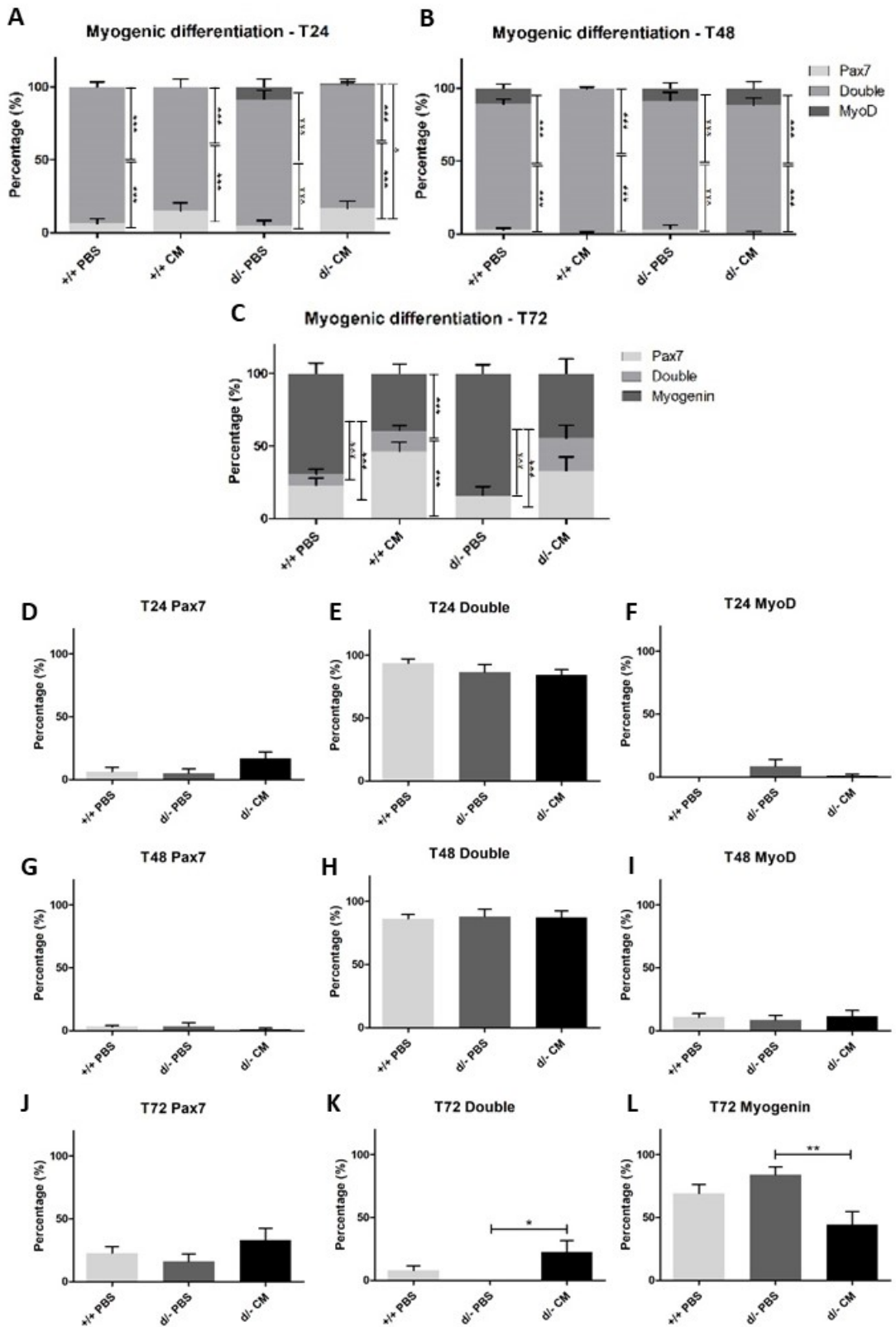
Figure 5.7 *Ercc1*^{d/-} satellite cells exhibited a normal commitment to myogenic differentiation and conditioned media delayed myogenin expression.
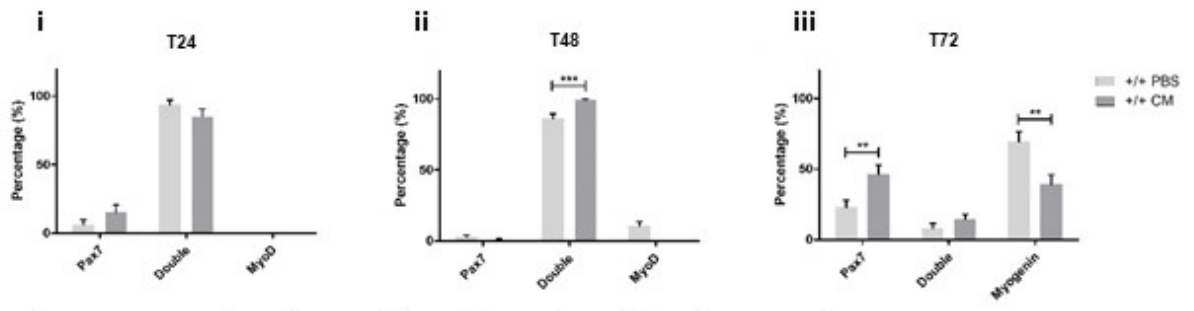
Figure 5.7 Continued. *Ercc1*$^{d/-}$ satellite cells exhibited a normal commitment to myogenic differentiation and conditioned media delayed myogenin expression. **(A-C)** Myogenic differentiation expression at T24, T48 (Pax7, MyoD), and T72 (Pax7, myogenin). **(D-F)** T24 expression of Pax7, Double and MyoD between cohorts. **(G-I)** T48 expression of Pax7, Double and MyoD between cohorts. **(J-L)** T72 expression of Pax7, Double and MyoD between cohorts. **(i, ii, iii)** Effect of CM on control SC differentiation *p<0.05, **p<0.01, ***p<0.001, **(A-L)** One-way ANOVA with Tukey post hoc testing. **(i, ii, iii)** Individual student's t-tests.

Characteristics of *Ercc1*$^{d/-}$ satellite cell function exhibit a 'super ageing' phenotype compared to natural ageing

Importantly, an objective of the current study is to establish the suitability of the *Ercc1*$^{d/-}$ mouse as a model of natural ageing, for use in potential future sarcopenia intervention approaches. Therefore, the parameters measured at a cellular level, to characterise SC number and function, can be compared to those findings reported in the natural ageing series of experiments. The first finding indicated that a large proportion of *Ercc1*$^{d/-}$ SCs, approximately 70%, were delayed in their emergence from their sub-laminal position at T24 compared to 18% of old SCs (p = <0.001) (Figure 5.8 A). Correspondingly, therefore, larger proportions of old SCs were either in the process of emerging, or had fully emerged by T24, relative to *Ercc1*$^{d/-}$ SCs (p = <0.05, respectively) (Figure 5.8 B, C). In regards to the average speed of SC migration, it was observed that *Ercc1*$^{d/-}$ SCs migrated faster (63.3μm/h) than both old (42.8μm/h) and geriatric (47.9μm/h) SCs (Figure 5.8 D). However, this increase was statistically significant relative to the old SC speeds only (p = <0.001). When comparing the morphologies assumed by *Ercc1*$^{d/-}$ SCs to those seen in old age, while the majority of SCs were rounded in shape, 98 and 94% respectively, statistically there were no differences between the groups when the morphologies were analysed individually (Figure 5.8 E, F). Moreover, the number of cells and clusters per myofibre were consistent between naturally-aged and *Ercc1*$^{d/-}$ myofibre cultures. Old SC cluster sizes were slightly increased relative to *Ercc1*$^{d/-}$ sizes at T24 (p = <0.05) (Figure 5.8 G, H, I).

Taryn Morash
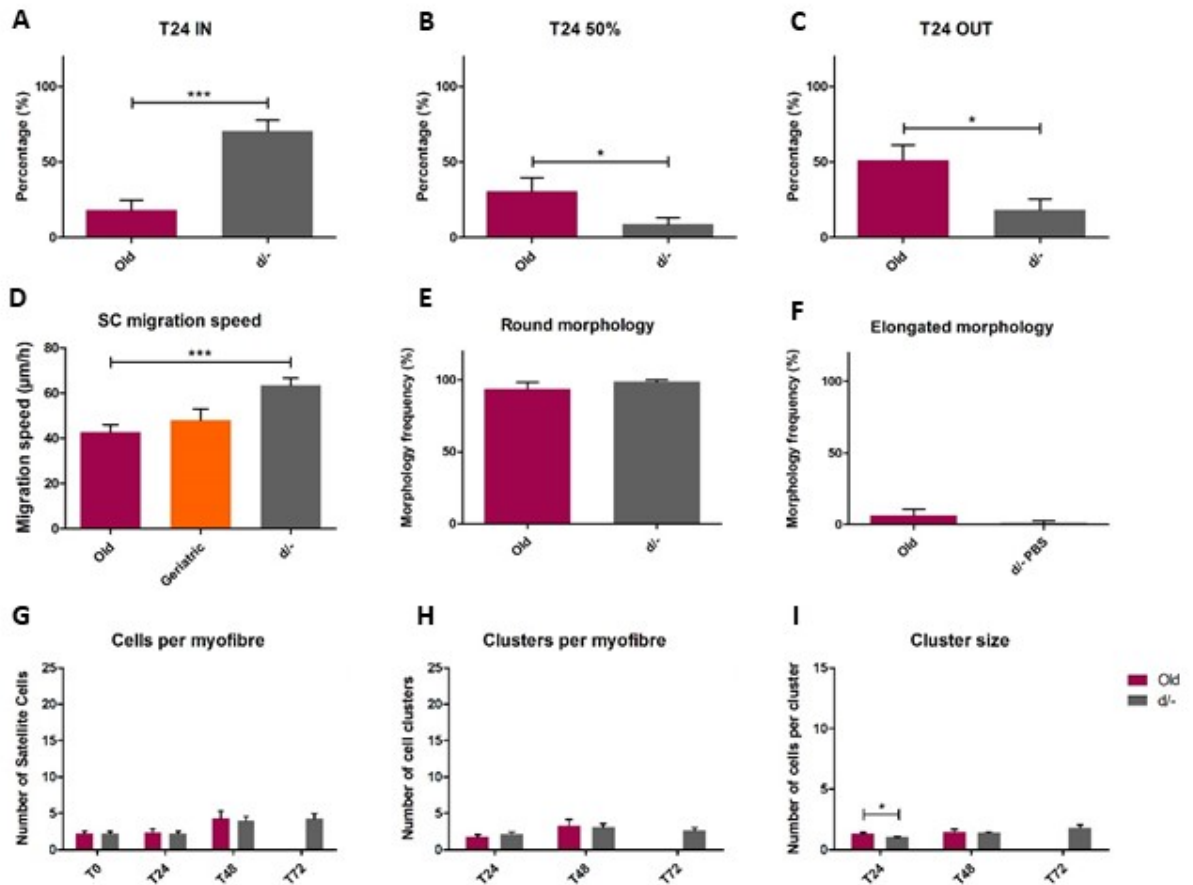
Figure 5.8 Characteristics of *Ercc1$^{d/-}$* satellite cell function exhibit a 'super ageing' phenotype compared to natural ageing. **(A-C)** *Ercc1$^{d/-}$* SC showed a delayed emergence compared to naturally-aged SCs. Indicated by the percentage of SCs observed inside/under the basal lamina ('IN'), partially emerged ('50%') and those positioned on the outer membrane of the basal lamina having fully emerged ('OUT'). **(D)** *Ercc1$^{d/-}$* SCs migrated at faster velocities compared to old and geriatric SCs. **(E-F)** Both aged and *Ercc1$^{d/-}$* SCs adopted a round morphology. **(G-I)** Both aged and *Ercc1$^{d/-}$* SCs demonstrated a diminished proliferative capacity *$p < 0.05$, ***$p < 0.001$, **(D)** One-way ANOVA with Tukey post hoc testing. **(A-C, E-I)** Individual student's t-tests.

Taryn Morash

Discussion

Mammalian skeletal muscle in adulthood is a stable postmitotic tissue, which under normal conditions, requires only periodic fusion of the resident stem cells, satellite cells (SCs), in response to daily wear and tear, to compensate for overall muscle turnover. However, upon injury skeletal muscle maintains a remarkable ability to regenerate damaged myofibres. The degeneration and subsequent regeneration process is highly regulated at molecular, cellular and tissue levels and results in renewal of contractile units, that are fully innervated and vascularised. This process is dependent on SCs and the intrinsic factors that govern the underlying mechanisms of their regenerative function, as well as the interactions with the muscle stem cell microenvironment (niche) through extrinsic factors. SCs remain quiescent beneath the basal lamina until activated in response to damage or injury. Following activation, SCs proceed to emerge from their sub-laminal position to the myofibre surface, where they migrate, proliferate, differentiate and subsequently fuse to maintain existing myofibres or comprise newly formed myofibres. The declines in skeletal muscle regenerative potential with age are consistently attributed to reductions in SC number and function. In 1976, Gutmann and Carlson observed that aged skeletal muscle maintains the ability to regenerate however, the rate of regeneration is reduced with age (Gutmann & Carlson 1976). Research into this notion has since continued and has revealed fewer SCs in aged muscle, reduced myogenic progression and differentiation as well as increased SC apoptosis (Collins et al. 2007). Schultz and Lipton reported that SCs isolated from the EDL and *Soleus* muscles of aged rats, showed a diminished capacity for generating progeny and that initiation of this activity was delayed, indicating overall compromised SC activation and proliferation (Schultz & Lipton 1982). However, Collins and colleagues also reported that despite the overall SC depletion in old age, a minority of the SC population generated large clusters of progeny as well as a distinct population of differentiated cells. This finding indicated that this small proportion of the ageing SC pool could regenerate muscle as effectively as observed in the larger SC populations of young myofibres, but could explain the overall reduced rate of regenerative associated with old age (Collins et al. 2007). Additionally, colleagues have previously established that aged murine SCs demonstrate delayed activation, emergence and differentiation, as well as a decreased rate of migration and alterations to the amoeboid-based form of motility associated with abnormal bleb dynamics (Collins-Hooper et al. 2012). Therefore, it is evident that age-related declines in regenerative function and regulation impacts each aspect of SC activity. This suggests that research into potential therapeutic strategies may be required to analyse and target each of the underlying mechanisms compromised during ageing.

Taryn Morash

In recent decades, research has focused on SCs and their niche, in order to better understand the interactions between them and to develop therapeutic approaches. These approaches aim to target the dysregulation and dysfunction implicated in physiological and pathological conditions, such as those reported in sarcopenia and muscular dystrophies, where regenerative capacity is compromised. A number of strategies so far, have concentrated on stem or progenitor cell transplantation and rely on donor cell integration, differentiation and engraftment into damaged or impaired tissue (Péault et al. 2007; Satoh et al. 1993; Lafreniere et al. 2004). Myoblasts, bone marrow stem cells (BMSCs), mesangioblasts, pericytes, embryonic stem (ES) cells and induced Pluripotent Stem (iPS) cells are among the cell types examined regarding their potential to carry out myogenic regeneration as forms of cell-based therapy (Yin et al. 2013). However, these approaches have resulted in limited success and although stem cells are often associated with measurable features of amelioration in pathology, donor cells experience high levels of rapid cell death, initiate an immune response and show minimal intramuscular migration and incorporation (Satoh et al. 1993; Lafreniere et al. 2004; Péault et al. 2007; Partridge 2000; Briggs & Morgan 2013). For these reasons, alternative strategies have moved away from the concept of whole cell-based approaches and instead have fuelled research into the notion that stem cells mediate tissue renewal and overall enhancement through factors released as a paracrine effect. In ageing muscle this concept was developed further through a series of heterochronic parabiosis experiments conducted by Conboy, Rando and colleagues. These experiments demonstrated that systemic factors circulating in the vasculature of young mice had rejuvenating effects in aged mice (Conboy et al. 2005). Notably, one mechanism that this was believed to be achieved was through modification of the Notch signalling pathway, up-regulation of which is known to diminish with age (Conboy & Rando 2002). Therefore, it was concluded that factors present in the young serum enhanced the proliferative and overall regenerative capacity of aged SCs (Conboy et al. 2005). Additionally, in the *Ercc1$^{d/-}$* model of premature ageing utilised in the present project, a landmark study conducted by Lavasani and colleagues concluded similarly, that 'secreted factors' from young control muscle stem/progenitor cells introduced intraperitoneally into progeric mice extended lifespan and improved regenerative function (Lavasani et al. 2012). As before, limited engraftment into host muscles was noted and beneficial effects such as improved proliferation, differentiation as well as indications of neo-vascularisation were evident even where transplanted donor cells were not detected, further suggesting a paracrine effect.

These findings were used as a basis in the formation of the following hypotheses which subsequently, directed investigation at a cellular level through the current series of experiments. The first hypothesis builds on what is reported in the literature and investigates the notion that the

Taryn Morash

decline in regenerative function observed in natural ageing, is attributed to deterioration of mechanisms intrinsic to the ageing skeletal muscle satellite cell. Secondly, extending this body of work into the $Ercc1^{d/-}$ experimentation, similarly, the mechanisms of SC function were investigated in order to document the characteristics of skeletal muscle regenerative function in the progeric model. Importantly, this work aims to further our knowledge of these processes in a murine model that is continuing to display features that could be described as 'super-ageing'. The third hypothesis is that the regenerative capacity is enhanced in skeletal muscle of aged mice treated with ADMSC CM. Finally, as in natural ageing, the hypothesis that ADMSC CM treatment harbours therapeutic potential in the enhancement of SC regenerative function in $Ercc1^{d/-}$ mice was also examined. The platform therefore, for this work relies on the important landmark findings regarding the rejuvenating potential of secreted factors from stem cells. These beneficial properties are believed to function through therapeutic paracrine effects, rather than more traditional, whole stem cell-based approaches.

Characterisation of mechanisms of satellite cell numbers and function in natural ageing

The essential first step in the regenerative process following injury-induced activation is the emergence of SCs from their sub-laminal position to the myofibre surface. Otto and colleagues reported that SCs immediately after myofibre isolation (T0), were uniformly covered in the layer of laminin which constitutes a component of the plasma membrane (Otto et al. 2011). This finding was consistent with the emergence analysis carried out in the current study, where both young and old SCs were observed in their original quiescent location at T0. Following this and prior to the emergence of SCs, remodelling of the laminin layer takes place within the initial 18 hours of culture, at which time holes become visible. By 24 hours, the majority of SCs reportedly emerge via these holes and were observed positioned above intact laminin (Otto et al. 2011; Collins-Hooper et al. 2012). However, this characteristic was not the case with the young SCs in the present emergence analysis, as more than 50% of the total SCs remained beneath the basal lamina at T24. Whereas, the majority of old SCs had either fully emerged or were partially emerged by this time, which is therefore in keeping with what has been previously reported for young SCs, but does not follow trends described in old SC populations. For example, colleagues showed overall delayed emergence in aged SCs compared to young controls (Collins-Hooper et al. 2012). Reasons for these discrepancies are however, currently unknown. One explanation could be that the myofibre connective tissue, laminin, basal lamina and ECM components are more easily remodelled, allowing SCs to emerge at a more advanced rate compared to young SCs. Collagen IV was previously examined at the whole-muscle level and this indicated that collagen IV, found in the basement membrane of myofibres, was

Taryn Morash

thicker at older ages, significantly so at geriatric ages, for example. This therefore, would not support this notion as denser, more tightly cross-linked collagen associated with aged muscle, has been shown to impair SC regenerative function and provides a greater challenge for SCs to create holes to emerge through (Lacraz et al. 2015; Collins-Hooper et al. 2012; Alnaqeeb et al. 1984; Gao et al. 2008). A further explanation could be that slight growth factor fluctuations between batches of the chick embryo extract supplement of single fibre culture media, could result in varied responses from different cultures of single myofibres. As emergence is the first step of SC regenerative function, following activation, it could be argued that an advanced rate of SC emergence could also be indicative of an overall more efficient repair or myofibre turnover. However, this process of efficient renewal is highly reliant on the subsequent steps of SC regeneration, for example, migration, proliferation and differentiation. Thus, further mechanisms of SC function were also examined in the current series of experiments.

Another essential aspect of SC activity that was a much neglected feature of regeneration until relatively recently, is the necessity for SCs to migrate to the site of damage in order to carry out cellular tissue repair (Otto et al. 2011; Collins-Hooper et al. 2012). Therefore, SC migration was analysed and unlike the trends previously documented by colleagues, old SCs did not demonstrate a reduced migration speed compared to young controls (Collins-Hooper et al. 2012). Thus, this finding is surprising but even more so, was that the velocity at which SCs travelled at a geriatric age, was also statistically no different to those measured at all other ages. Marked declines at geriatric ages, associated with the progression of sarcopenia, reduced intrinsic regenerative and self-renewal potential, have been reported by others and is starting to highlight the importance of the dramatic deterioration that occurs between old and geriatric ages, in both animal and human subjects (Sousa-Victor et al. 2014). Analysis of the morphologies adopted by SCs at both young and old ages also indicated that 90 – 100% of the SCs were more rounded in shape. A more spherical morphology was noted to be positively correlated with the amoeboid/bleb-based form of cellular motility. Therefore, together the results suggest that the intrinsic regulatory mechanisms that mediate the migratory aspects of SC function, were not substantially influenced by ageing progression in the current study. Moreover, reductions in SC velocity in ageing, reported by Collins-Hooper and colleagues, were attributed to abnormal bleb dynamics, specifically evident from a prolonged bleb lifespan through delayed bleb extension and retraction phases (Collins-Hooper et al. 2012). Additionally, aged SCs were also shown to have reduced expression of cell-extracellular adhesion components, integrin α6, α7 and β1 (Collins-Hooper et al. 2012). These heterodimer glycoproteins are known to have high affinities for laminin in skeletal muscle and disruption of integrin adhesion has been linked with decreased SC migration speeds (Collins-Hooper et al. 2012; Siegel et al. 2009; Mayer 2003).

Taryn Morash

Therefore, it would be of interest to the present series of experiments, to further investigate the characteristics of old and geriatric SC bleb dynamics as well as integrin expression, to provide an explanation for the alternative trends in migration speed observed, relative to those previously stated in the literature.

Next, the proliferative capacity of aged SCs was analysed and in keeping with findings of others, proliferation in aged SC populations was diminished (Schultz & Lipton 1982; Collins et al. 2007; Collins-Hooper et al. 2012; Sousa-Victor et al. 2014; García-Prat et al. 2016). Although some evidence of proliferation was observed over the 48-hour culture period in aged SC populations, the total number of cells present at T24 and 48 were remarkably reduced compared to young SCs. Additionally, there is also indication of the delayed initiation of proliferation that Schultz and Lipton previously described (Schultz & Lipton 1982). This is evident by the apparent lag in increased SC number per myofibre at T48, equalling the average observed at the earlier T24 time-point in young populations. Moreover, it can potentially be surmised that the SCs initiating proliferation in old age within the 48-hour culture period analysed, are the minority population that Collins and colleagues described as the smaller proportion of total SCs that retain the proliferative capability into old age (Collins et al. 2007). Sousa-Victor and colleagues reported at a geriatric age, that SCs had lost the ability to maintain reversible quiescence and instead, entered an irreversible senescence, known as geroconversion (Sousa-Victor et al. 2014). This has been shown to occur through the derepression of p16^{INK4a}, a tumour suppressor gene that stalls cell cycle progression from G1 to S phase and therefore is considered a master regulator of senescence (Sousa-Victor et al. 2014; García-Prat et al. 2016). Regulatory mechanisms such as this function as DNA damage check-points in normal stem cell physiology to detect and initiate apoptotic clearance of damaged cells that exhibit features of dysfunctional control that occur during natural ageing progression. Therefore these otherwise protective mechanisms may be 'hijacked' and become inappropriately regulated, exacerbating further damage responses during age-associated DNA damage accumulation, similarly to dysregulation also observed in cancer (Sperka et al. 2012; García-Prat et al. 2016). Although, this feature was prominent at geriatric ages in the previously discussed study conducted by Sousa-Victor and colleagues, it would be of interest to the current project to investigate DNA damage check-point regulatory mechanisms, such as cell cycle arrest via p16^{INK4a} or other indications of cellular senescence, such as senescence-associated beta galactosidase (SA-β-gal). This could be used to establish if the reduction in proliferative potential observed in old SCs in the present study could be attributed to premature geroconversion to a senescent state. Another explanation for decreased SC number in old age could be the result of increased SC apoptosis reported by others in the field (Collins et al. 2007; Wang et al. 2014).

Taryn Morash

It should be noted that due to a lack of availability of aged myofibres during experimentation, it was not possible to examine myogenic differentiation of aged SCs. However, it has been previously reported that SCs demonstrate a delayed commitment to, as well as a reduced myogenic differentiation. Furthermore, it could be argued that the underlying regulatory mechanisms of SC proliferation were overall affected by ageing to a higher degree than the other aspects examined in the current series of experiments (emergence and migration). This could be indicative of age-related dysregulation impacting more detrimentally on signalling pathways mediating the balance between growth and maintenance, described previously as part of a survival response, evident in ageing progression. This therefore, could suggest a potential trade-off in the prioritisation of maintenance over growth regarding a compromised SC regenerative capacity, as those mechanisms required for proliferation would seemingly be dampened during this shift in resources with age. Despite observing superficially positive findings for aspects of SC regenerative function in the aged myofibre condition, such as advanced emergence and 'normal' SC migration observed in the current study. These, coupled with an observed reduction in SC number and progeny-generating capacity, as well as potentially impaired terminal myogenic differentiation (based on the findings of others), however, would still result in an overall reduced regenerative capacity. Therefore, an advanced pattern of SC emergence and maintenance of migration speed in old age, may serve as compensatory regulation in order to limit the impact of reduced SC number, proliferative capacity and reportedly impaired differentiation on the overall process of repair. Each aspect is essential in order to bring about successful and efficient muscle repair and diminished function of any of these mechanisms, either as a result of ageing or in disease, will have a detrimental effect. It is important that studies wishing to examine the SC regeneration process, for example in disease or ageing intervention research, analyse and target each aspect of SC function. As with the whole muscle studies, an appropriate model of accelerated age-related muscle decline is required, in order to conduct successful and efficient intervention studies examining these features of SC regenerative capacity.

Characterisation of mechanisms of satellite cell number and function in the $Ercc1^{d/-}$ progeric model

As SCs are known to be quiescent at T0 and emerge from their sub-laminal position in the latter hours of the initial 24 hours of single myofibre culture, this important window for emergence in early SC activity was more closely studied in the $Ercc1^{d/-}$ experimentation (Otto et al. 2011). In keeping with previous observations therefore, within this relatively short period of culture (4 hours), more SCs (control and $Ercc1^{d/-}$) had emerged. However, similarly to trends seen in the naturally-aged SC emergence analysis, these proportions were distinctly less than the control SCs reported to have emerged by T24 by colleagues previously (Otto et al. 2011; Collins-Hooper et al. 2012). Reasons for

Taryn Morash

these discrepancies, other than possible serum growth factor level variations, are currently unknown. Although an unknown degree of variation, if any at all, may be introduced with the C57BL/6/FVB hybrid genetic background the $Ercc1^{d/-}$ mutant is generated in, as the naturally-aged animals were C57BL/6 laboratory strains only. In addition, despite the aforementioned abnormally delayed emergence noted in control conditions, the findings indicate that mechanisms underlying SC emergence may not be profoundly affected in the $Ercc1^{d/-}$ model. This is because observed proportions of emerged SCs were not statistically different from those observed in the control myofibre cultures.

In keeping with what others have previously reported, almost 100% of the SCs analysed in both control and $Ercc1^{d/-}$ conditions, were observed with amoeboid/bleb characteristics (Otto et al. 2011; Collins-Hooper et al. 2012). Surprisingly, however, $Ercc1^{d/-}$ SCs were found to migrate along myofibres at a considerably faster rate compared to control cells. This finding is somewhat unexpected in a model of such extreme dysregulation, as it could be argued that a faster migration speed would also subsequently result in SCs reaching the lesion site faster, in order to carry out more efficient repair. As discussed in previous chapters, multiple factors, other than migration method, can influence cell motility and overall speed of movement. Characteristics both intrinsic and extrinsic to the cell can influence motility and a number of these are reported to become altered with age. For example, intrinsic regulation of well-known mediators of migration such as the finding that artificially inducing NO/HGF signalling in myofibre suspension cultures *in vitro*, has been associated with increasing motility of aged SC populations (Otto et al. 2011; Collins-Hooper et al. 2012). Additionally, smooth muscle actin concentrated at the plasma membrane of a forming bleb during the amoeboid method of migration indicates that changes in cytoskeletal organisation bring about bleb extensions and retractions. It has been suggested that an increased rate of extension and retraction results in an increased rate of movement and that this bleb lifespan is decreased in aged SCs (Otto et al. 2011; Collins-Hooper et al. 2012). External interactions via focal adhesion contacts, integrins and therefore, both cell to cell, as well as cell to ECM communications, have also been implicated in ageing, as discussed and like-wise regarding both the naturally-aged and $Ercc1^{d/-}$ SC experimentation, further analysis into these features is required.

Collagen, a major component of connective tissue, is shown to become thicker and more densely cross-linked with age, which not only impacts on overall muscle contractility but has been shown to interfere with cellular signalling (Kragstrup et al. 2011; Gao et al. 2008; Alnaqeeb et al. 1984). Additionally, an important finding within the field of cell biology and tissue engineering, is that stem cells respond to their microenvironment of niche by 'feeling' the elasticity of their substrate which then directs characteristics of cell behaviour including migration and differentiation (Engler et al.

Taryn Morash

2004; Engler et al. 2006). Although, when analysing the *Ercc1*^{d/-} *Soleus* at a whole tissue level, discussed in the previous chapters, it was noted that collagen IV thickness surrounding each myofibre was not statistically different between *Ercc1*^{d/-} and controls. However, this parameter does not indicate how densely cross-linked the collagen is and therefore cannot provide any insights into the substrate elasticity in the *Ercc1*^{d/-} model.

The efficiency of the regeneration process, as previously discussed, is heavily influenced by the other features of SC function, such as productive generation of progeny, as well as successful and efficient myogenic differentiation. Thus, critically, it was established that, although there was some evidence of proliferation during the 72-hour culture period, the number of *Ercc1*^{d/-} SCs per myofibre was drastically depleted at each time-point, including those quiescent at T0. This finding is therefore in keeping with what is reported in the literature in naturally-aged skeletal muscle, as well as what was observed in the previous series of experiments. This suggests that a large proportion of *Ercc1*^{d/-} SCs are failing to proliferate and instead are undergoing premature geroconversion. That is, cells are entering an accelerated irreversible state of senescence, a process that has been associated with naturally-aged geriatric SCs (Sousa-Victor et al. 2014; García-Prat et al. 2016). As the *Ercc1*^{d/-} model is one of accumulated DNA damage, it can be reasonably postulated that the cell cycle arrest mechanisms and those driving SC senescence are functioning both in response to the detection of high levels of DNA damage, but also to prevent any further damage as a protective mechanism. Further experimentation using the SA-β-gal assay can be used to confirm the proportion of SCs that have become senescent. Despite observing dramatically depleted *Ercc1*^{d/-} SC numbers and reduced proliferation, those cells that remained functional and did not undergo geroconversion, appeared to differentiate as successfully as the control SCs. This was evident by consistent proportions, relative to the control, of *Ercc1*^{d/-} SC expression of myogenic markers, MyoD (T24 and 48) and myogenin (T72), being observed. This is a somewhat unexpected finding as delayed lineage commitment and reduced myogenic differentiation were features previously reported to occur in naturally-aged SC populations (Collins-Hooper et al. 2012; Collins et al. 2007).

Importantly, as in the naturally-aged SC populations, proliferation appears to be the mechanism that is the most detrimentally affected in the regenerative process in *Ercc1*^{d/-} SC populations. It is proposed therefore, that SCs have undergone geroconversion, transforming from a quiescent state to senescence. In an otherwise depleted SC pool, the underlying regulation that normally promotes growth has defaulted to conserve resources as a survival response and shifted towards cellular maintenance. Thus, it would be of interest to better our understanding of this survival response beginning with investigation into the regulatory pathways involved in apoptosis and autophagy. For example, analysing components of these signalling pathways, could aid in determining the extent

Taryn Morash

that the reduction in SC numbers can be attributed to cell death and to indicate how biological materials are being recycled instead of newly synthesised. Other aspects of regenerative function in *Ercc1$^{d/-}$* SCs however, were either consistent with control SCs, as in the case of differentiation and emergence, or advanced as with speed of movement. Regulation of these features could therefore, be the result of compensatory regulation in attempts to limit the impact of declines in regenerative function caused primarily by a lack of SC progeny-generation. Therefore, exhibiting characteristics associated with altered mechanisms of skeletal muscle regenerative capacity, the *Ercc1$^{d/-}$* model demonstrates parallels to those declines in SC number and function observed in natural ageing progression. However, in a model of such severe dysfunction it is somewhat surprising that the other underlying mechanisms of SC activity were not more drastically affected, particularly differentiation. However, the *Ercc1$^{d/-}$* model of progeria has been described as 'segmental' in its deterioration, referring to some compartments, organs and tissues being more affected by the DNA damage accumulation than others (Dollé et al. 2011). These declines were then scored relative to natural ageing as 'normal', 'accelerated' or 'extreme'. In conclusion therefore, it could be argued that SC regenerative potential in *Ercc1$^{d/-}$* skeletal muscle mimics some features of natural ageing to a 'normal' extent, for example, reduced proliferative potential. However, there is evidence of dysregulation in the SC parameters discussed which show variability from aspects observed in natural ageing. For example, a large degree of abnormality was noted in emergence and migration characteristics in both *Ercc1$^{d/-}$* and aged SCs.

Investigating the effects of conditioned media treatment on satellite cell activity in natural ageing

The hypothesis that ADMSC CM treatment will enhance the function of the underlying mechanisms of SC regenerative activity in old age, was investigated. The initial finding indicated that CM treatment appeared to reverse the advanced pattern of SC emergence seen in old age, to that of the young control SCs. This therefore suggests that, despite emergence appearing abnormally delayed in young SCs, relative to previously reported findings of others, the advanced emergence of old SCs observed, may not necessarily be advantageous in the process of regeneration in aged SCs. However, this seems somewhat counterintuitive, as it could be surmised that the earlier SCs emerge to the myofibre surface, the earlier they are available to carry out cellular repair. Although, as previously mentioned, this notion is highly reliant on the functionality of the other aspects of SC activity, including migration, proliferation and differentiation. Nevertheless, this finding indicates that CM maintains properties that targeted and altered the regulation of intrinsic mechanisms that direct SC emergence.

Taryn Morash

Remarkably, CM treatment in old age also showed an increased SC migration speed compared to both the old and adult control SCs. This suggests that regulatory properties maintained within ADMSC CM can also mediate features of cell motility. Altered characteristics could include for example, modified bleb dynamics such as bleb number, size or lifespan, or other membrane adaptations, such as those regulating focal adhesion contacts or actin cytoskeletal organisation. As before, utilising what has been reported regarding the cellular processes targeted by the miRNA content of AFS CM, it could be reasonably postulated that broad signalling pathways such as those regulating cell communication, ECM organisation, cell adherence and motility, may also be targets of ADMSC content (Mellows et al. 2017). Further investigation into establishing the properties specific to CM generated from ADMSC is required. Importantly, CM treatment therefore, not only shows potential for adapting the regulation intrinsic to the SC population but introduced systemically, CM has adaptive regulatory effects universally within the local microenvironment, mediating somatic and stem cell interactions (Mellows et al. 2017).

Treatment with NO donors and HGF separately, has been shown to induce aged SCs to travel at speeds associated with young SCs (Collins-Hooper et al. 2012). Despite SC migration speeds remaining constant with age in the current study, CM treatment similarly enhanced migration speed and therefore, this previously reported finding, could indicate key signalling components that are regulated by factors within CM. Therefore, the NO/HGF signalling pathways would be an important avenue for further investigation into elucidating more specific properties of ADMSC CM. Along with analysis of SC migration speed in old age, colleagues have also previously used a mathematical model approach to study SC migration trajectories (Collins-Hooper et al. 2012). The outcome saw that young SCs adopt a migratory pattern that is described as a 'memoryless' random walk method and travel larger distances length-wise along myofibres. This pattern indicates that a cell's past movement does not have any bearing on the future directionality and that there is equal chance of taking a left or right turn. Whereas, this 'memoryless' feature appeared to be lost in ageing, where SCs were more likely to continue travelling in the direction it had been previously, whilst migrating overall shorter distances within a time frame (Collins-Hooper et al. 2012). This model would infer that older SCs would be less adaptable or plastic regarding their directionality in response to a damage stimuli and additionally, would take longer to arrive at the lesion site. This finding is important to take into consideration in the present study, as observed comparable velocities to younger ages, as well as increased speeds with CM treatment, in aged conditions, might not necessarily correlate with functional SC directionality. Indeed, an increased migration speed could be described as compensatory if in the instance that aged SC directionality is impaired. It would be of interest to mathematically model the migration of SCs treated with CM in old age in order to

Taryn Morash

establish if the observed increase in velocity is coupled with correction of the 'memoryless' feature of young SC motility. It is therefore important to consider that cell migration comprises multiple parameters beyond speed of movement, such as directionality, that can become altered with age impacting on overall SC regenerative efficacy.

A further finding of the present study was that SC proliferation was not enhanced with CM treatment in old age. Rather the opposing trend was observed at T48, where the number of SCs and cell clusters per myofibre were statistically no different to those present at earlier time-points with CM treatment. Whereas, there was evidence of proliferation over the culture duration in the old age control. This suggests that factors found in CM treatment may have negatively regulated proliferative pathways (such as Notch-mediated signalling) in old age, instead of having an overall rejuvenating effect as reported by others previously (Conboy et al. 2003; Conboy et al. 2005; Lavasani et al. 2012). However, findings such as this require further investigation into the properties of ADMSC CM, specifically. As any observed variation in effects could be attributed to the use of a therapeutically viable mesenchymal stem cell, this is an alternate stem cell type to those myogenic and haematopoietic in origin examined in the studies conducted by others (Conboy et al. 2003; Conboy et al. 2005; Lavasani et al. 2012). This is an important consideration as secreted factors are believed to vary between cell types. Overall, however, these findings suggest that regulatory properties harboured by CM could not enhance the proliferative potential of naturally-aged SCs. This could suggest that the proposed shift of resources with age, from mechanisms of growth to those that prioritise maintenance, may not be overcome by CM treatment intervention approaches to improve regenerative function (Garinis et al. 2008; Niedernhofer et al. 2006). Equally, the modulating regulatory effect of CM was unable to sufficiently combat the reduction in SC numbers in old age, as a result of increased apoptosis or geroconversion to a senescent state, for example. Interestingly, the *in vitro* assay used to test the efficacy of the CM generated from ADMSC cells demonstrates the protective effects of CM treatment against cellular senescence. This therefore could be explained by a number of scenarios, including but not limited to, the possibility that the aged SCs were not undergoing senescence. That, *in vivo* CM treatment in aged animals was unable to combat SC senescence. Or alternatively, that aged SCs were already experiencing SC geroconversion prior to CM administration beginning at 20 months of age. Hence, the equivalent 'protective' effect may be achieved with CM administration earlier in life (for example, in late adults, before the onset of ageing progression).

Taryn Morash

Investigating the effects of conditioned media treatment on satellite cell activity in the *Ercc1$^{d/-}$* model of progeria

Similarly to the naturally-aged series of experiments, the effects of CM treatment were also measured utilising the parameters underlying SC reparative function in *Ercc1$^{d/-}$* myofibre cultures. Remarkably, CM treatment appeared to advance SC emergence compared to the control PBS and *Ercc1$^{d/-}$* PBS at T20, which has resulted in the majority of SCs having become fully emerged by T24. Moreover, CM treatment in the control PBS had no effect on SC emergence at T20 however, as with *Ercc1$^{d/-}$* PBS, by T24 the majority of control CM cells had fully emerged. This indicates an overall advanced rate of emergence compared to control, that was also somewhat delayed relative to *Ercc1$^{d/-}$* CM SCs. Taken with what is already known about the emergence process, this therefore, could suggest that CM maintains factors that potentially regulate features of SC activation and response to damage stimuli, ECM and laminin remodelling and/or SC migration, in order to enable overall increased emergence efficiency (Otto et al. 2011; Collins-Hooper et al. 2012). Features such as the response to stimuli, cell communication, ECM organisation and cell motility were identified among the vast array of cellular processes that were targeted by miRNA present in AFS CM reported by our colleagues (Mellows et al. 2017). Despite utilising CM generated from an alternative stem cell type in the current project, it can be reasonably postulated that factors targeting aspects of cellular function similar to those identified in the AFS secretome, could also be released from ADMSCs.

Similarly to CM treatment in old age as previously discussed, CM also appeared to adapt regulation that directed changes in SC motility in *Ercc1$^{d/-}$* myofibre cultures. In contrast however, rather than increasing SC migration speeds as observed in naturally-aged SCs, CM treatment reduced *Ercc1$^{d/-}$* SC velocities to a control level. Furthermore, this could suggest that the greater *Ercc1$^{d/-}$* (PBS vehicle-treated control) SC migration speeds initially observed, were not beneficial or perhaps not fully functional in the process of *Ercc1$^{d/-}$* SC repair, possibly due to the aforementioned impairments in response to stimuli and directionality (Collins-Hooper et al. 2012). Additionally, as before with the naturally-aged experimentation, the regulatory mechanisms that underpin proliferation appear to be those most affected by age-related modifications and is a feature of SC function seemingly mimicked in the *Ercc1$^{d/-}$* model of progeria. Moreover, CM treatment in the *Ercc1$^{d/-}$* model was also seen to have the least influence on SC number and proliferative capacity. As before, this is believed to be due to the shift away from mechanisms controlling growth, which further suggests that the regulatory potential of CM is unable to impact on such as strong survival response.

Interestingly, regarding the final aspect of SC function analysed, CM appeared to perturb the progression of myogenic differentiation in a substantial proportion of both control and *Ercc1$^{d/-}$* SCs at T72. At this time-point in young SCs, the majority of SCs are reported to express myogenin, a late

Taryn Morash

myogenic marker indicating initiation of differentiation, which was consistent with the trends observed in control PBS and *Ercc1*$^{d/-}$ PBS SC populations in the present study (Grounds et al. 1992; Zammit et al. 2004; Zammit, Partridge, et al. 2006; Otto et al. 2011; Collins-Hooper et al. 2012). Importantly, it is known that SCs adopt divergent fates that is, once activated, SCs express both Pax7 and MyoD a transcription factor key to the initiation of myogenic commitment (Zammit et al. 2004; Grounds et al. 1992; Rudnicki et al. 1993). Hereafter, proliferating SCs downregulate Pax7 and continue along the myogenic lineage, subsequently expressing myogenin and differentiate (Yablonka-Reuveni & Rivera 1994; Zammit et al. 2004; Zammit, Relaix, et al. 2006). Contrastingly, other SCs seemingly withdraw from immediate myogenic differentiation and instead continue to express Pax7 but lose MyoD, entering a state of quiescence once more (Nagata et al. 2006; Zammit et al. 2004; Yablonka-Reuveni & Rivera 1994). The majority of SCs in all conditions at T24 and 48 were observed co-expressing both Pax7 and MyoD. Interestingly, evident from the larger proportion of cells still expressing Pax7 only at T72 however, it is difficult to say whether this subset is delayed in their lineage progression from MyoD to myogenin expression, or these cells are in the process of downregulating to a quiescent state. It would be important therefore to determine whether the Pax7^{+} proportion at T72 were also co-expressing MyoD. Nevertheless, these findings demonstrate that CM contains properties that delayed the activity of the key components driving progression of myogenic differentiation, in both the control and *Ercc1*$^{d/-}$ SCs. Indeed, over 20% of the miRNA present in AFS CM was shown to be those that targeted cell differentiation (Mellows et al. 2017). Therefore, this result in the current study suggests that CM generated from ADMSCs could contain similar regulatory potential, regarding the control of SC myogenic differentiation. However, this could indicate a potentially negative effect of CM treatment whereby, SC regenerative capacity is further compromised through delayed myogenic differentiation. Although, in the instance that this subset of SCs were withdrawing from myogenic lineage progression, it could be argued that CM treatment was acting on these regulatory mechanisms to promote conservation of the quiescent SC pool. Further investigations into these trends however, are required in order to provide a better understanding of this regulation.

CM treatment in the *Ercc1*$^{d/-}$ model therefore, was shown to initiate an advanced rate of SC emergence, normalise the accelerated SC migration speed observed in *Ercc1*$^{d/-}$ control SCs and surprisingly, delay myogenic lineage progression. Overall, these results suggest that ADMSC CM harbours regulatory potential regarding the underlying mechanisms of these features of SC activity. Moreover, it is unclear the extent of the CM therapeutic effects, as some of these altered mechanisms appear to be unexpected and possibly counterintuitive. For example, the slowed SC migration speed, although, as discussed, this could highlight further migratory defects, such as

Taryn Morash

directionality and response to damage stimuli. Nevertheless, these findings seem to indicate a large degree of dysregulation underpinning $Ercc1^{d/-}$ SC function. As with the naturally-aged SCs, proliferative capacity is the characteristic most perturbed in the process of SC regeneration in $Ercc1^{d/-}$ skeletal muscle. As described previously therefore, this could further suggest that regulation and resources have moved away from growth, in a shift concerned with cellular conservation and survival. Additionally, in a model associated with high rates of DNA damage accumulation, it is essential to protect genomic and cellular integrity. Thus, it can be reasoned that a mechanistic shut-down of proliferation, as well as a possible drive towards cellular senescence and apoptosis exemplifies protective action to prevent further dysregulation. Further investigation into the regulation of features such as senescence and apoptosis, is therefore, required to provide a more detailed understanding of this survival response in the $Ercc1^{d/-}$ model.

Overall, parallels can be drawn between the characteristic changes that occur in SC number and function in natural ageing and the $Ercc1^{d/-}$ progeric model. However, the concept of the $Ercc1^{d/-}$ mouse being a model of skeletal muscle 'super-ageing' is therefore, not only evident at a whole muscle level, but also at a cellular level, when analysing both the myofibre and the resident stem cell population. Therefore, the $Ercc1^{d/-}$ model can be confidently taken forward for use in future skeletal muscle ageing studies to research potential intervention approaches, wishing to better regenerative function. However, as also discussed previously at a tissue level, old SCs may not be old enough and it could be argued that those features observed at a geriatric age are more comparable and similar to characteristics of SC function seen in the $Ercc1^{d/-}$ progeric model. This further indicates that future experimentation should focus on CM administration in geriatric animals to directly compare to the effects of CM treatment in $Ercc1^{d/-}$ muscle.

Remarkably, however, these findings demonstrate the regulatory potential of ADMSC CM treatment. Moreover, this further indicates that, although properties harboured by CM altered mechanisms of SC regeneration, those signalling pathways that suggested such a strong shift towards cellular maintenance, were not additionally effected by CM. It could be subsequently postulated that CM supported this shift. Further investigation into the properties maintained by ADMSC CM and detail regarding the cellular processes and signalling pathways targeted by components of ADMSC CM, is required. This subsequently, can also be studied in conjunction with the findings of altered mechanisms of SC function presented in the current project, alongside additional aspects such as senescence, apoptosis and autophagy, to further define the result of CM treatment and how it may be having a regulatory effect.

Taryn Morash

Chapter 6

Skeletal muscle myofibres promote non-muscle stem cells and non-stem cells to adopt myogenic characteristics

Taryn Morash

Introduction

It has been established that skeletal muscle myofibres promote SCs to migrate utilising a distinctive amoeboid-based mechanism, which involves the frequent extension and retraction of membrane protrusions or 'blebs' (Otto et al. 2011; Collins-Hooper et al. 2012). Amoeboid-based migration is believed to develop traction through numerous blebs forming simple focal adhesions with the ECM, each creating small amounts of pull (Charras & Paluch 2008; Tozluoğlu et al. 2013). Bleb-based motility in SCs is shown to be the faster form of movement along myofibres, relative to the more traditionally-described lamellipodia-based method (Otto et al. 2011). However, until relatively recently, cell migration was a much neglected although, essential characteristic of SC repair.

Regulation of the Rac and Rho GTPase signalling pathways, that function antagonistically to one another, are known to mediate between the two mechanisms of migration (Sanz-Moreno et al. 2011). Rac activity and its downstream components control lamellipodia extension, whereas the Rho signalling pathway is responsible for plasma membrane blebbing and therefore, the amoeboid-based migration (Calvo et al. 2011; Charras & Paluch 2008; Sanz-Moreno et al. 2011). Importantly, it is unknown whether the underlying mechanisms of bleb-based motility are regulated by intrinsic properties of SCs, or stimulated by characteristics of the myofibre surface. Indeed, the myofibre matrix seemingly influences the mode of migration adopted by SCs, as it was previously noted that on plastic surfaces *in vitro*, SCs formed lamellipodia (Otto et al. 2011).

The physical properties of the microenvironment surface are not only believed to impact on mechanisms of migration, but have also been shown to direct lineage specification and therefore, the fate of stem cells. Engler and colleagues demonstrated that, by mimicking the physiologically-relevant matrix elasticities of brain, muscle or bone *in vitro*, human mesenchymal stem cells were induced towards neuronal, myogenic or osteogenic lineages, respectively (Engler et al. 2006). Furthermore, Gilbert and colleagues reported that altered surface stiffness, for example through fibrosis as a result of damage, dramatically perturbed the self-renewing capacity of SCs (Gilbert et al. 2010). Therefore, these findings are vital to the fields of stem cell therapy and tissue engineering, where culture conditions and tissue scaffolds can be tailored to the physiological elasticities, improving overall therapeutic success. Consideration of the physiological matrix elasticity and how these become altered in both ageing, injury and disease, can better optimise stem cell treatment within a specific tissue. Moreover, the so far largely limited success reported with the use of whole cell-based therapies, in replenishing damaged tissue in cases of injury and disease, can therefore in part, be attributed to a limited understanding or consideration of the tissue surface elasticity. Additionally, alterations to the skeletal muscle myofibre microenvironment or niche are known to

Taryn Morash

occur with increasing age which impact on overall contractility and force-generating capacity, as well as also reducing mechanotransduction signalling and SC regulation. For example, SC activity has been shown to be impaired due to an increased microenvironment stiffness linked with subsequent increases in ECM content and cross-linking (Lacraz et al. 2015; Kragstrup et al. 2011). Deposition of collagen, a main structural ECM component, as well as fat infiltration have also been shown to be greater in ageing muscle (Alnaqeeb et al. 1984; Lacraz et al. 2015; Kent-Braun et al. 2000; Baumgartner 2000; Taaffe et al. 2009). Other features such as collagen cross-linking and a build-up of advanced glycation end-product (AGE) cross-links are also believed to contribute to increased stiffness of myofibres observed in ageing (Zimmerman et al. 1993; Gosselin et al. 1998; Haus et al. 2007).

These findings taken together formed the knowledge basis for the following series of experiments. Importantly, building on the results from the experiments conducted and discussed in previous sections, the role of the myofibre microenvironment in directing SC activity was investigated. (**A**) It was hypothesised that the amoeboid-based migratory phenomenon demonstrated by skeletal muscle SCs, is directed predominantly by the myofibre surface (Otto et al. 2011; Collins-Hooper et al. 2012). (**B**) It is unknown whether the myofibre matrix similarly, could induce the bleb-based form of migration in non-muscle cells, as an alternative migratory option available to all stem cells. (**C**) The impact of the ageing myofibre microenvironment on the migratory and morphological characteristics of the non-muscle cells was examined. (**D**) The extent that alterations to SC activity can be attributed to physical features of the ageing myofibre, rather than changes intrinsic to the SC, was assessed. (**E**) The *in vitro* effects of CM treatment in our single myofibre culture set-up, were investigated and comparisons drawn between *in vitro* and *in vivo* CM treatment of the previous experimentation. (**F**) It was postulated that the same molecular mechanisms underpinned the regulation of amoeboid-based migration in each cell type examined. (**G**) It was proposed that the fate of, not only transplanted non-muscle stem cells, but also non-stem cells could be influenced by the myofibre surface.

As before, single myofibres were isolated from the EDL muscle of mice and cultured. Alternatively, however, myofibres were co-cultured with transplanted non-muscle stem and non-stem cells. Three well-defined stem cell populations used included human adipose-derived mesenchymal stem cells (ADMSC), dental pulp stem cells (DP) and amniotic fluid stem cells (AFS). These stem cell types have been extensively characterised for multipotency, are relatively easily cultured and are currently being developed as stem cell therapies for human diseases (Bajek et al. 2016; Condé-Green et al. 2016; Mead et al. 2016; Collart-Dutilleul et al. 2015; Zhang et al. 2006; Tajiri et al. 2014). The MDA-MB-231 breast cancer cell line (MDA) is a well-defined, highly invasive epithelial cancer cell line, chosen in the present study as a non-stem cell source that is extremely easy to cultivate. The MDA cell line is also

Taryn Morash

studied extensively in cancer metastasis, characterised by an invasive endothelial-like morphology in three-dimensional (3D) Matrigel culture (Chavez et al. 2010; Kenny et al. 2007; Harrell et al. 2014). AFS, DP and MDA cells were all GFP+ cell lines and therefore, were identified using an anti-GFP antibody. The ADMSC cells however, were identified using PKH26 membrane dye. Subsequently, migration of these transplanted cell types along myofibres was analysed using time-lapse microscopy and morphological features were visualised using immunocytochemistry protocols for alpha smooth muscle actin (SMA).

Taryn Morash

Results

The skeletal myofibre matrix influences non-muscle cellular morphologies

Firstly, the influence of the myofibre surface on the mechanisms underlying cell migration was characterised. Thus, cell morphologies of each cell type were compared on tissue culture plastic versus on myofibres. It was noted that, like the majority of SCs, ADMSC, AFS and DP stem cells cultured on plastic, displayed an elongated, flattened shape (p = <0.001) (Figure 6.1 A, C1-4). In contrast, approximately 80% of MDA cells were more rounded than elongated (p = <0.001) (Figure 6.1 A). These morphology profiles were subsequently compared to those displayed when the same cell types were situated on the myofibres surface. As previously reported, it was observed that all SCs assumed a rounded morphology (p = <0.001) (Figure 6.1 B). Once placed on myofibres, remarkably, the proportion of rounded morphologies were significantly higher in all of the other cell types examined (ADMSC, p = <0.01. AFS, DP, MDA, p = <0.001, respectively) (Figure 6.1 B, C5-8).
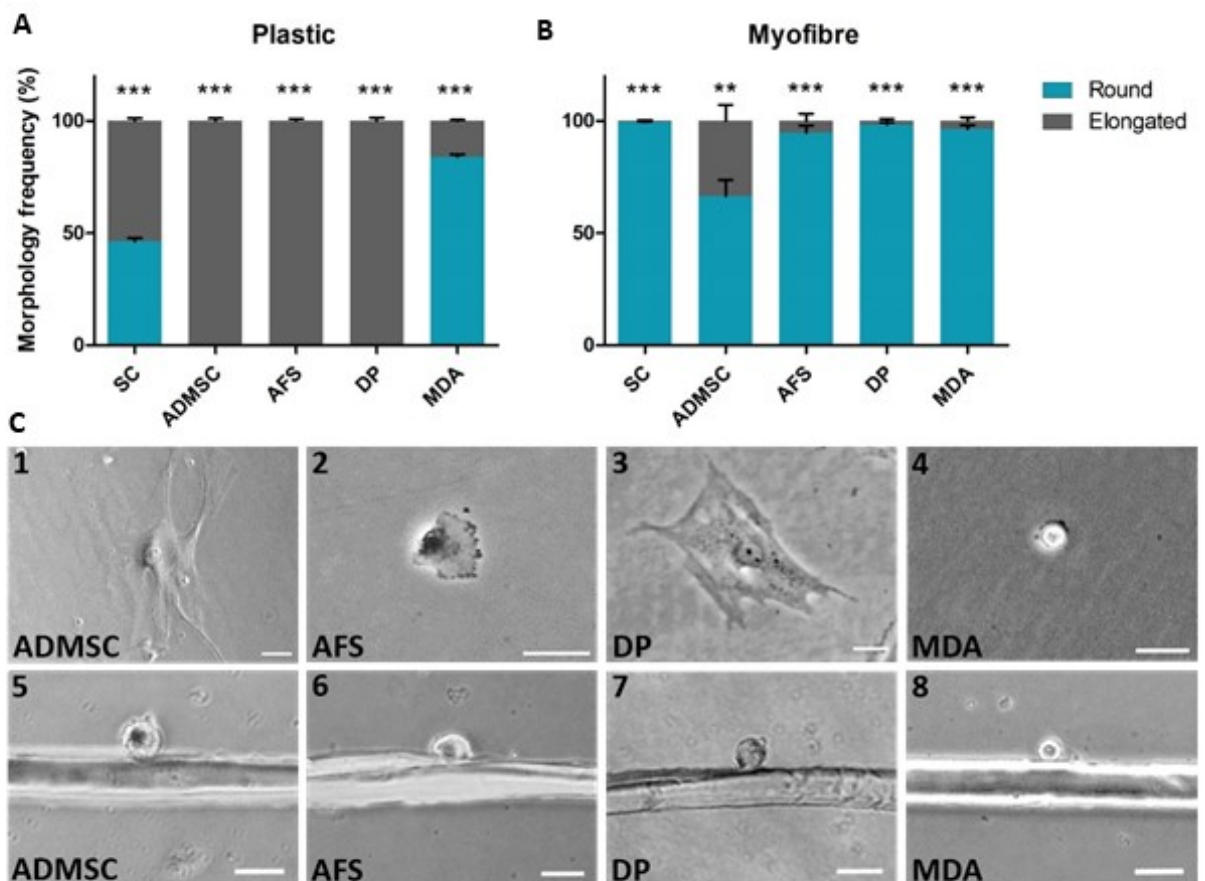
Figure 6.1 The skeletal myofibre matrix influences non-muscle cellular morphologies. **(A)** Frequencies of morphologies adopted by SCs, ADMSCs, AFS, DP, MDA on plastic. **(B)** Frequencies of morphologies adopted by SCs, ADMSCs, AFS, DP, MDA on myofibres. *Ercc1*$^{d/-}$ SCs migrated at faster velocities

Taryn Morash

compared to old and geriatric SCs. **(C)** Representative morphologies of non-muscle cells observed on plastic (1-4) and on myofibres (5-8). **p<0.01, ***p<0.001, Individual student's t-tests.

The skeletal muscle myofibre impacts on the migration speed of co-cultured non-muscle cells

Next, the influence of the matrix substrate on cell migration speed was explored. Firstly, it was observed that SCs travelled faster on myofibres, when compared to plastic (p = <0.001) (Figure 6.2 A). In fact, the SC migration speed on myofibres was double that recorded on plastic (approximately 40 and 20μm/h, respectively). In addition, the myofibre matrix also supported faster motility than that of a plastic surface, for both DP and MDA cells (p = <0.001) (Figure 6.2 A). In contrast, a significantly decreased migration speed was observed in ADMSC and AFS cells, on myofibres when compared to plastic (p = <0.01 and <0.001, respectively) (Figure 6.2 A). The migration speeds of the differing cell morphologies on myofibres, were compared. It was noted that migration speeds of ADMSC, DP and MDA cells were not affected by the shape of the cell (round v elongated). Surprisingly however, rounded AFS cells travelled at slower speeds on myofibres, (23μm/h), compared to those with an elongated form (32μm/h, p = <0.01) (Figure 6.2 B).
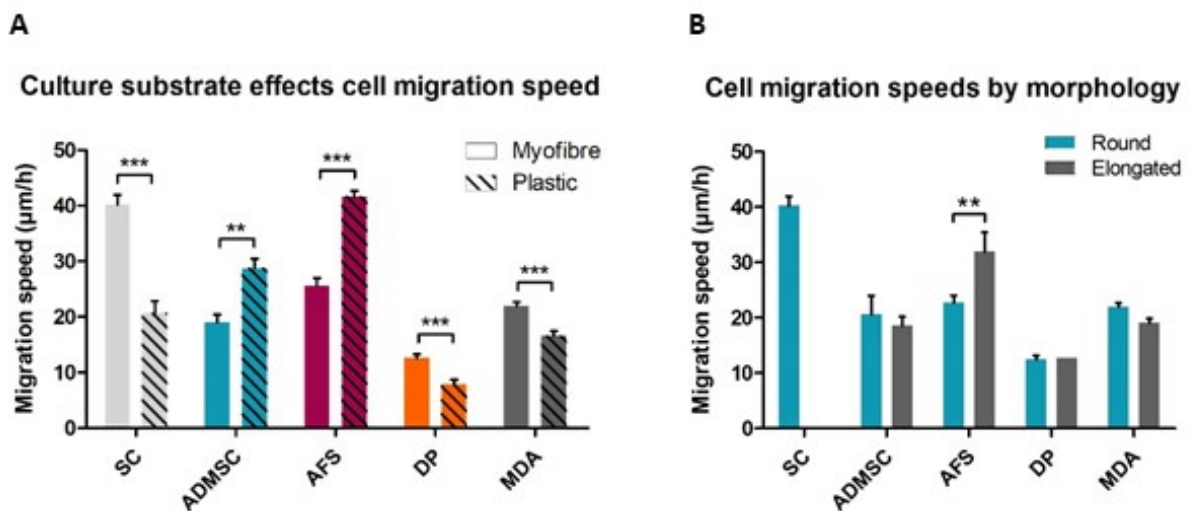
Figure 6.2 The skeletal muscle myofibre impacts on the migration speed of co-cultured non-muscle cells. **(A)** Cell migration speed comparison between plastic and myofibre substrates. **(B)** Migration speeds of differing morphologies of resident and non-muscle cells on myofibres. **p<0.01, ***p<0.001, Individual student's t-tests.

Taryn Morash

The effect of the ageing skeletal myofibre matrix and *in vitro* conditioned media treatment on non-muscle cellular morphologies

After establishing that the myofibre surface influenced the cellular morphologies adopted by transplanted non-muscle cells on young myofibres, similar analyses were conducted using aged (24 month-old) myofibres. Firstly, it was noted that, concurrent with the findings of young myofibres, for each cell type examined, the majority of cells adopted a rounded morphology on aged myofibres (ADMSC, p = <0.05. SC, AFS, DP, MDA p = <0.001, respectively) (Figure 6.3 A, B). CM treatment was then used alternatively *in vitro*, at the chosen concentration (1%), which demonstrated protection against cellular senescence during CM testing. Secondly, with CM treatment, as observed previously, the majority of cells in each cell type, were more rounded in shape in young myofibre cultures (p = <0.001) (Figure 6.3 C). Similarly, in aged myofibre cultures with CM treatment, the rounded form was the most frequently adopted morphology in SC, ADMSC, DP and MDA cell types (ADMSC, p = <0.01. SC, DP, MDA p = <0.001, respectively) (Figure 6.3 D). In contrast, for AFS cells, there was no statistical difference between the proportions of cells that took on more rounded or more elongated forms, in the aged CM-treated condition (Figure 6.3 D). The proportions of round cells were subsequently analysed in more detail between culture conditions, for each cell type examined (Figure 6.3 D). It was noted that neither the aged myofibre surface nor *in vitro* CM treatment influenced SC morphology (Figure 6.3 E). Additionally, there were no statistical differences in the proportion of rounded ADMSCs observed between conditions (Figure 6.3 F). The aged myofibre surface alone did not influence the shape of AFS cells (Figure 6.3 G). However, CM treatment in old myofibre cultures drastically reduced the percentage of AFS cells that adopted a round form, relative to the other conditions (p = <0.001 and <0.01) (Figure 6.3 G). Remarkably, the proportions of both DP and MDA cells that took on a rounded morphology were significantly decreased on aged myofibres, when compared to young (p = <0.05 and <0.001, respectively) (Figure 6.3 H, I). Moreover, CM treatment in aged cultures, subsequently increased the percentage of round DP cells observed to a proportion equivalent to young myofibres (p = <0.05) (Figure 6.3 H).

Taryn Morash
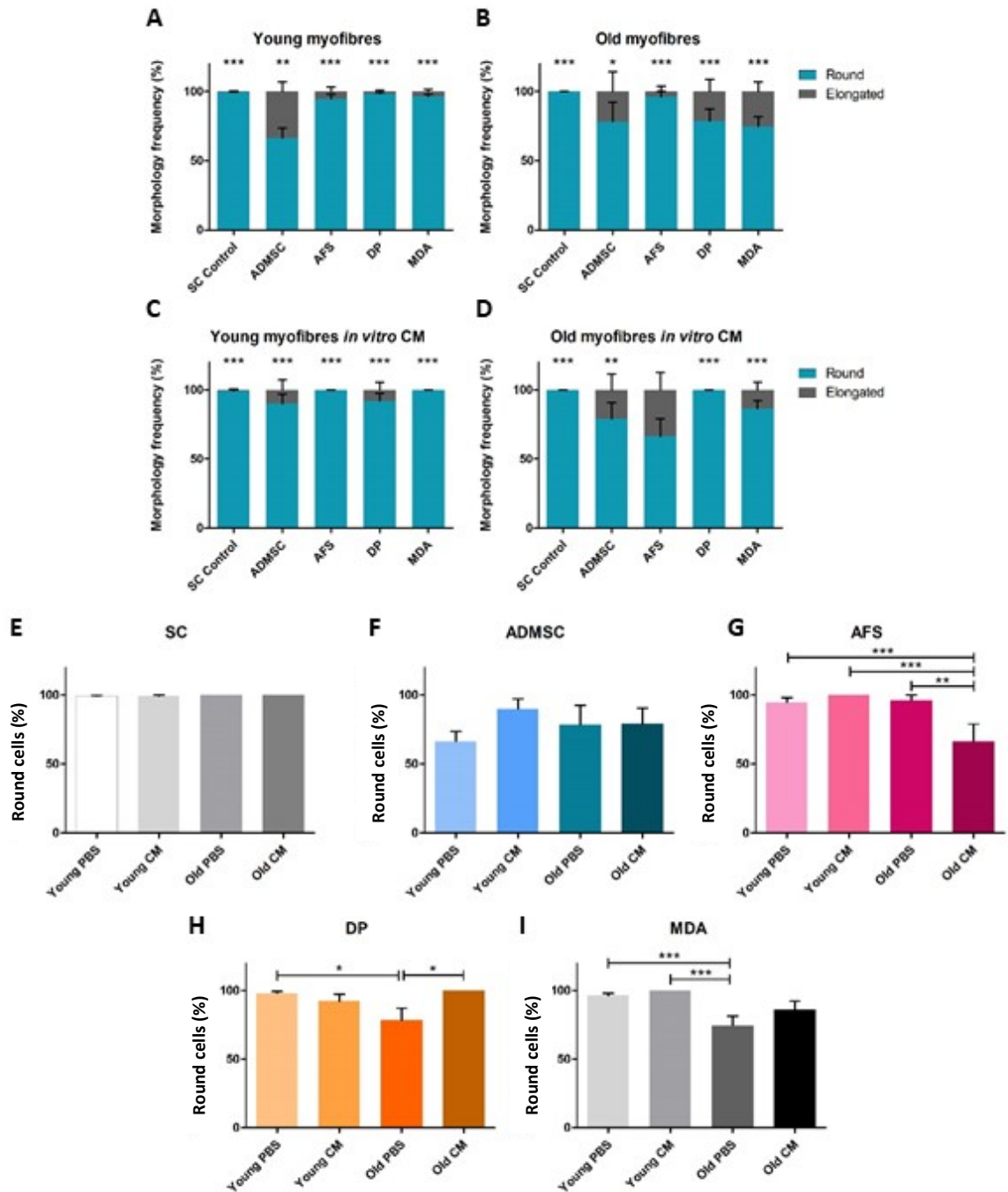
Figure 6.3 The effect of the ageing skeletal myofibre matrix and *in vitro* conditioned media treatment on non-muscle cellular morphologies. Frequencies of morphologies adopted by SCs, ADMSCs, AFS, DP, MDA on: **(A)** Young myofibres. **(B)** Old myofibres. **(C)** Young myofibres with *in vitro* CM. **(D)** Old myofibres with *in vitro* CM. Significance indicated between round and elongated forms. **(E-I)** Percentage of rounded cells observed of each cell type between culture conditions. *$p<0.05$, **$p<0.01$, ***$p<0.001$, **(A-D)** Individual student's t-tests. **(E-I)** One-way ANOVA with Tukey post hoc testing.

The effect of the ageing skeletal myofibre matrix and *in vitro* conditioned media treatment on the migration speeds of non-muscle cells

In the previous series of experiments, *in vivo* CM treatment resulted in altered cell migration speeds (increased in natural ageing, decreased in *Ercc1*$^{d/-}$). Thus, the regulatory effects of *in vitro* CM treatment on the speed of movement in the non-muscle cells, in young and aged myofibre culture conditions, was explored. Firstly, it was noted that, despite a slightly reduced average migration speed observed on aged myofibres, there were no statistical differences in SC velocities in any of the conditions (Figure 6.4 A). ADMSC migration speeds were significantly increased in aged myofibre cultures when compared to young (p = <0.001) (Figure 6.4 B). Additionally, CM treatment in young myofibre cultures also resulted in greater rates of ADMSC motility (p = <0.05) (Figure 6.4 B). Similarly to SCs, variations in AFS migration speeds between culture conditions, were statistically not significant (Figure 6.4 C). On the other hand, as observed with ADMSCs, CM treatment in young myofibre cultures increased the rate of motility of DP cells (p = <0.05) (Figure 6.4 D). Moreover, speed of movement was further drastically increased in DP cells co-cultured on the aged myofibre surface (p = <0.001). Strikingly however, CM treatment in aged myofibre cultures, returned DP migration speeds to those recorded when travelling along young myofibres (p = <0.05). Lastly, the age of the myofibre did not significantly influence the rate of motility of the transplanted MDA cells (Figure 6.4 E). However, remarkably, CM treatment in the aged myofibre condition greatly enhanced MDA migration speeds when compared to all other conditions (p = <0.01 and <0.001) (Figure 6.4 E).

Taryn Morash
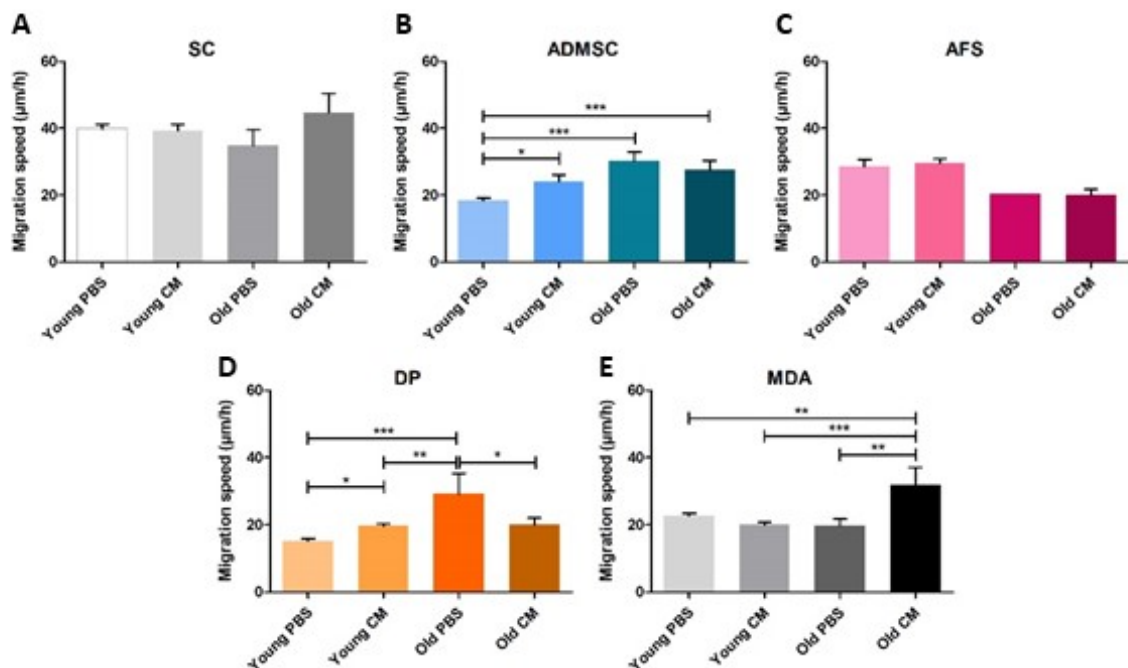
Figure 6.4 The effect of the ageing skeletal myofibre matrix and *in vitro* conditioned media treatment on the migration speeds of non-muscle cells. Cell migrations speeds of **(A)** SC, **(B)** ADMSC, **(C)** AFS, **(D)** DP, **(E)** MDA in different age and CM culture conditions. *p<0.05, **p<0.01, ***p<0.001, One-way ANOVA with Tukey post hoc testing.

Examining the activity of ROCK and Arp2/3 in the regulation of cell migration and morphologies

Next, the molecular mechanisms underpinning cell migration and morphology were investigated. It was proposed that the same regulatory signalling pathways that support efficient SC motility, also drives the amoeboid-based method of migration observed in all other cell types examined, when placed on myofibres. Importantly, colleagues have previously shown that ROCK activity was a key determinant of the rounded morphology and bleb-based migration in SCs (Collins-Hooper et al. 2012; Otto et al. 2011). Contrastingly, studies have demonstrated that the activity of the Arp2/3 complex is required for actin branching and organisation in the formation of lamellipodia (Bergert et al. 2012; Wu et al. 2012). Through the use of Y-27632 and CK666, well-known inhibitors of ROCK and Arp2/3, respectively, the effects of blocking the activity of each counter-acting signalling pathway separately, on cell migration speeds and morphology, were analysed (Krawetz et al. 2011; Hetrick et al. 2013; Bergert et al. 2012). As before, cell migration was analysed using time-lapse microscopy. Additionally, cell morphologies were visualised using an immunocytochemistry protocol to identify alpha smooth muscle actin (SMA) organisation within transplanted cells on myofibres. Firstly, it was observed that inhibiting ROCK did not affect SC migration speeds (Figure 6.5 A). Inhibiting ROCK decreased the rate of motility in ADMSC, AFS and MDA cells, when compared to the control cells (mock-treated with solvent only) (p = <0.001) (Figure 6.5 B). Like with the SCs, DP cells treated with the ROCK inhibitor however, showed no statistical difference in migration speeds, relative to control cells (Figure 6.5 B). Furthermore, inhibition of Arp2/3 activity significantly reduced the rate of motility of SCs and ADMSCs only (p = <0.001 and <0.05, respectively) (Figure 6.5 B). Following this, the influence of the inhibitors on cell morphology was also investigated. For all cell types, inhibition of ROCK resulted in the majority of cells adopting an elongated morphology (SC, ADMSC, DP, p = <0.001. MDA, p = <0.01. AFS, p = <0.05) (Figure 6.5 C). Whereas, Arp2/3 inhibition promoted almost 100% of cells of each cell type to take on a more rounded form (p = <0.001. SC CK666 data missing values) (Figure 6.5 C).

Taryn Morash
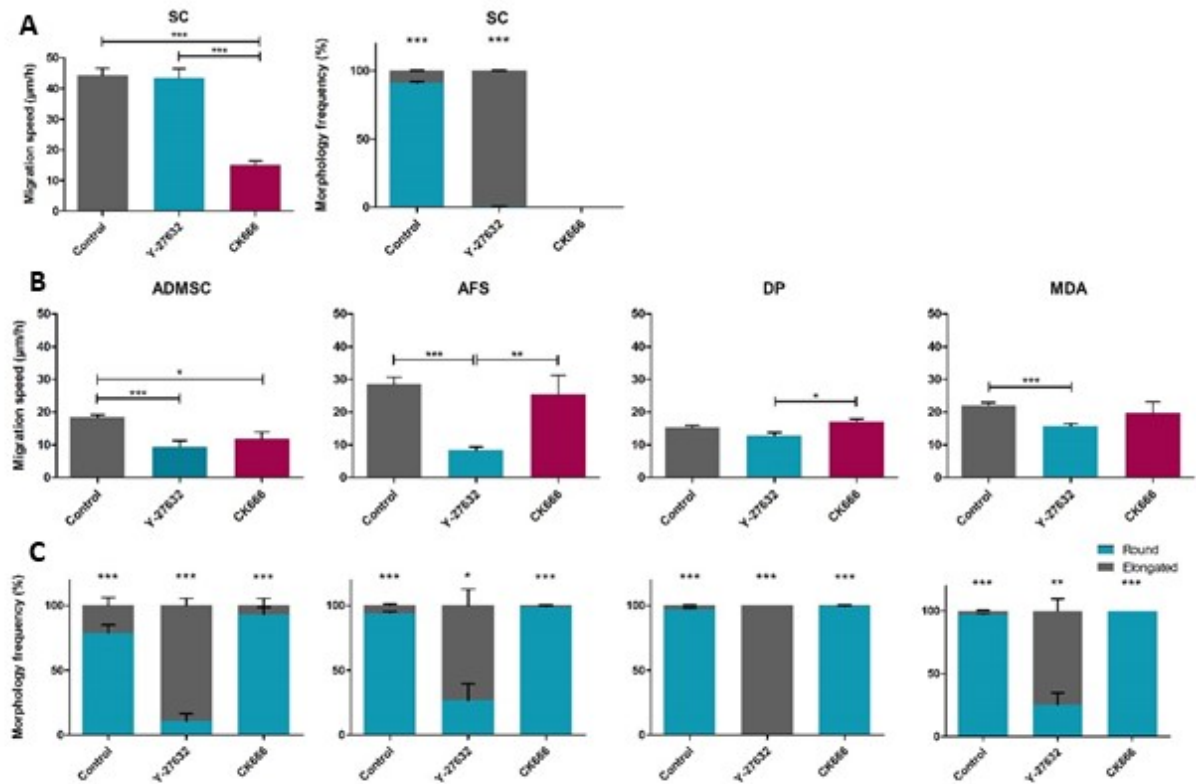
Figure 6.5 Examining the activity of ROCK and Arp2/3 in cell migration and morphologies. **(A)** Effect of inhibiting ROCK (Y-27632) and Arp2/3 (CK666) on resident SC migration and morphologies. **(B)** Effect of inhibiting ROCK (Y-27632) and Arp2/3 (CK666) on non-muscle cell migration on myofibres. **(C)** Effect of inhibiting ROCK (Y-27632) and Arp2/3 (CK666) on non-muscle cell morphology frequencies. Statistical differences indicated between proportion of rounded and elongated cell numbers. *p<0.05, **p<0.01, ***p<0.001, **(A-B)** One-way ANOVA with Tukey post hoc testing. **(A, C)** Individual student's t-tests.

Influence of ROCK and Arp2/3 on cell surface characteristics of non-muscle cells on myofibres

It is well-established that SCs utilise the amoeboid-like mechanism for movement along myofibres and characteristically, this form of motility employs an abundance of regular dynamic plasma membrane vesicle-like protrusions or blebs (Otto et al. 2011; Collins-Hooper et al. 2012; Charras & Paluch 2008). Thus, the non-muscle cells were examined for the presence of visible cell surface blebs using scanning electron microscopy (SEM). As treatment with the Y-27632 (ROCK) inhibitor resulted in an abundance of elongated cells on myofibres, as discussed, therefore there was an absence of cell surface blebs with all cell types (ADMSC, DP, MDA, *p* = <0.001., AFS, *p* = <0.01 SC) (Figure 6.6 i, A). In contrast, treatment with CK666 indicated a significant increase in the number of blebs present on the

Taryn Morash

surface of ADMSC, DP and MDA cells on myofibres, when compared to control cells (p = <0.05 and <0.001, SC CK666 data missing) (Figure 6.6 i, A). Following this, examination of the bleb dimensions, was subsequently conducted. It was noted that bleb dimensions were not affected to any great degree, compared between control and Arp2/3-inhibited cells, with the exception of an increase observed in the width of blebs on the surface of MDA cells treated with CK666 (p = <0.05) (Figure 6.6 ii, B).

Taryn Morash
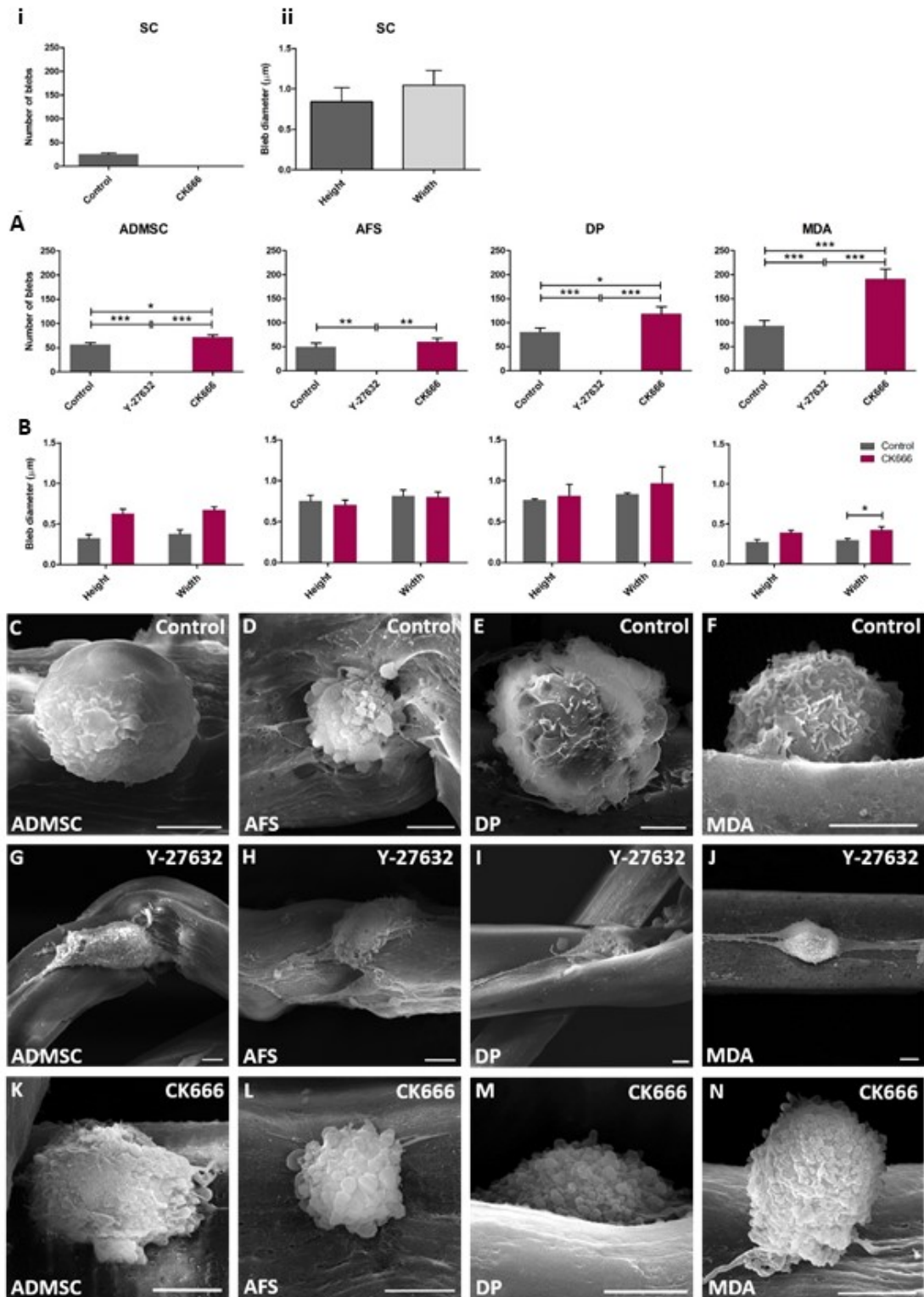
Figure 6.6 Influence of ROCK and Arp2/3 on cell surface characteristics of non-muscle cells on myofibres. Quantification of resident SC bleb numbers **(i)** Bleb dimensions **(ii)**. **(A)** Quantification of bleb numbers on non-muscle cells following ROCK (Y-27632) and Arp2/3 (CK666) inhibition; **(B)** Bleb dimensions. Scanning electron microscopy (SEM) images of transplanted cell types treated with

205

solvent only (C-F), ROCK inhibitor (G-J) and Arp2/3 inhibitor (K-N). Scale 5µm. *p<0.05, **p<0.01, ***p<0.001, **(A)** One-way ANOVA with Tukey post hoc testing. **(i-ii, B)** Individual student's t-tests.

The effect of the skeletal myofibre matrix on the proliferative capacity of non-muscle cells

The influence of the extrinsic physical properties of the myofibre surface, on the underlying mechanisms of proliferation remained to be examined. Young SCs following activation are shown to initiate rounds of cell division at approximately 24 hours, hereafter total numbers of SCs per myofibre are known to more than double by 48 hours of culture (Collins-Hooper et al. 2012; Zammit 2002). Proliferation of the transplanted ADMSC, AFS and MDA cells on the surface of single myofibres, was monitored at T14, 24 and 48 (Figure 6.7 A, B, C). Most notably however, the total number and cluster sizes of ADMSCs present on myofibres had significantly decreased by T48 (p = <0.05, respectively) (Figure 6.7 C). Additionally, proliferation was evident in the MDA population, with an observed increase in total cells per myofibre by T48, however this difference was not statistically significant (Figure 6.7 A). Although, contrastingly, the number of MDA clusters per myofibre was reduced between T14 and 24 (p = <0.05) (Figure 6.7 B). Moreover, the number of AFS cells fluctuated slightly but differences observed were statistically not significant.

Induction of MyoD expression in AFS and MDA cells after prolonged culture on myofibres

Myogenic lineage commitment and differentiation of SCs into myoblasts, the expression of MHC and fusion into mature myotubes, marks the essential final step in the process of SC-mediated skeletal muscle repair, maintenance and growth. Lastly, therefore, the myofibre matrix was examined regarding the potential to direct non-muscle cells towards a myogenic fate. As before, the GFP[+] non-muscle cells were seeded onto freshly isolated myofibres in order to profile the expression of MyoD, the marker of myogenic lineage commitment (Zammit et al. 2004). Resident SCs are known to express Pax7 on freshly isolated myofibres, whereas MyoD expression becomes detectable at approximately T24 (Zammit et al. 2004). Pax7 is subsequently, gradually down-regulated following 48 hours of culture, where cells continue along the myogenic differentiation pathway (Zammit et al. 2004; Zammit, Relaix, et al. 2006; Yablonka-Reuveni & Rivera 1994). None of the transplanted GFP[+] non-muscle cells examined (ADMSC, AFS and MDA), co-expressed Pax7 at the SC-relevant culture time-points (T14, 24 and 48), evident by the lack of 'Double' expression (Figure 6.7 D, E, F). MyoD expression was detected in more than 80% of the resident SCs after 24 hours of culture (Figure 6.8 A). Between 48 and 120 hours of culture, all SCs on myofibres expressed MyoD, which then

Taryn Morash

diminished by T240 (Figure 6.8 A). The non-muscle cell types were observed initially adopting rounded morphologies once transplanted onto myofibres, up until approximately T48, where cells took on one of two forms. ADMSC and DP cells were observed gradually elongating and outstretching lamellipodia protrusions, particularly around the myofibre circumference, resulting in myofibre constrictions (Figure 6.8 B, C). By T72, it was observed that no normal, healthy myofibres remained in the presence of both ADMSC and DP cells, with a large majority either curled into balls or hyper-contracted signifying myofibre damage. Contrastingly, AFS and MDA cells maintained a rounded morphology and myofibres remained healthier during prolonged culture. Remarkably, it was noted that by T240, approximately 50% of AFS and MDA cells robustly expressed MyoD (Figure 6.8 A, D, E).
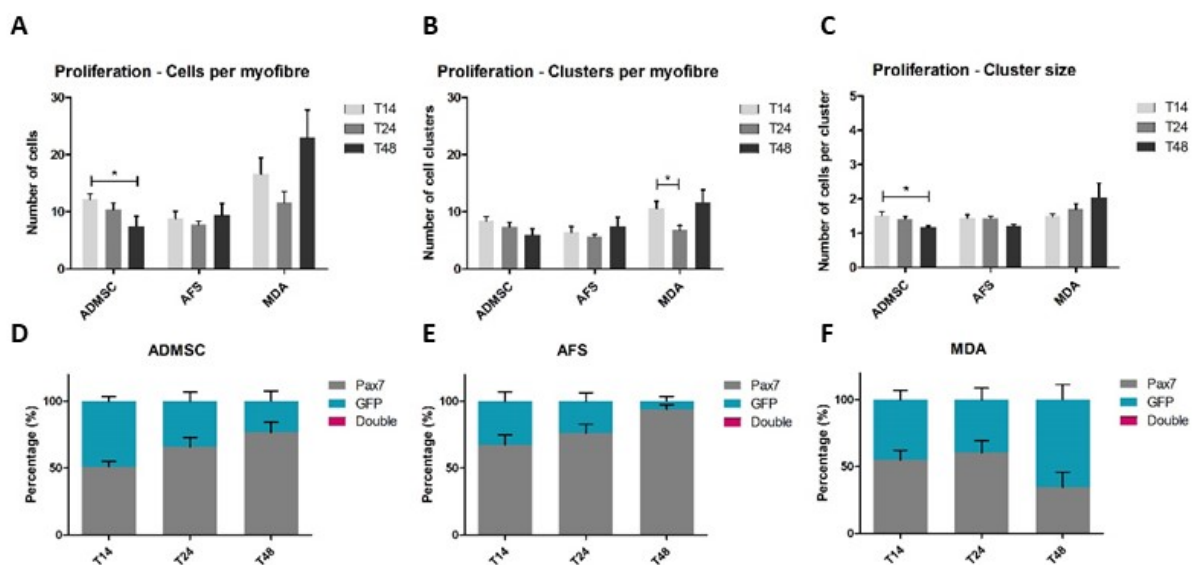
Figure 6.7 The effect of the skeletal myofibre matrix on the proliferative capacity of non-muscle cells. (A) Proliferation analysed as cells per myofibre. (B) Proliferation analysed as clusters per myofibre. (C) Proliferation analysed as cluster size. GFP+ (D) ADMSC (E) AFS (F) MDA do not co-express Pax7. *p<0.05, (A-F) One-way ANOVA with Tukey post hoc testing.

Next, the myogenic differentiation potential of the non-muscle cells was further investigated. As observed with SC in previous studies, following enzymatic dissociation from myofibres, the ability of cells to create myotube structures and therefore, myogenic differentiation, can be demonstrated (Zammit et al. 2004; Zammit, Relaix, et al. 2006). Most remarkably, AFS cells that had been dissociated from myofibres, fused to create elongated myotubes and this was further supported by the co-expression of GFP and MHC, a key component of the contractile property of muscle (Figure 6.8 F). In contrast however, MDA cells that had also previously been co-cultured for 240 hours on the myofibre surface and subsequently dissociated, failed to fuse and form myotubes and did not

207

Taryn Morash

express MHC (Figure 6.8 G). Alternatively, MDA cells proliferated profusely resulting in multiple cell layers. Quantification of the AFS cells that expressed MHC showed that approximately 8% of all AFS cells cultured, were positive for MHC and fused to form myotubes with an average of 1.5 nuclei (Figure 6.8 H, I). Importantly, characteristics of myogenic differentiation were not observed in MDA or AFS cells that had not previously been in contact with myofibres (Figure 6.9 A, B). SC positive controls expressed MHC and fused to form myotubes in culture (Figure 6.9 C).
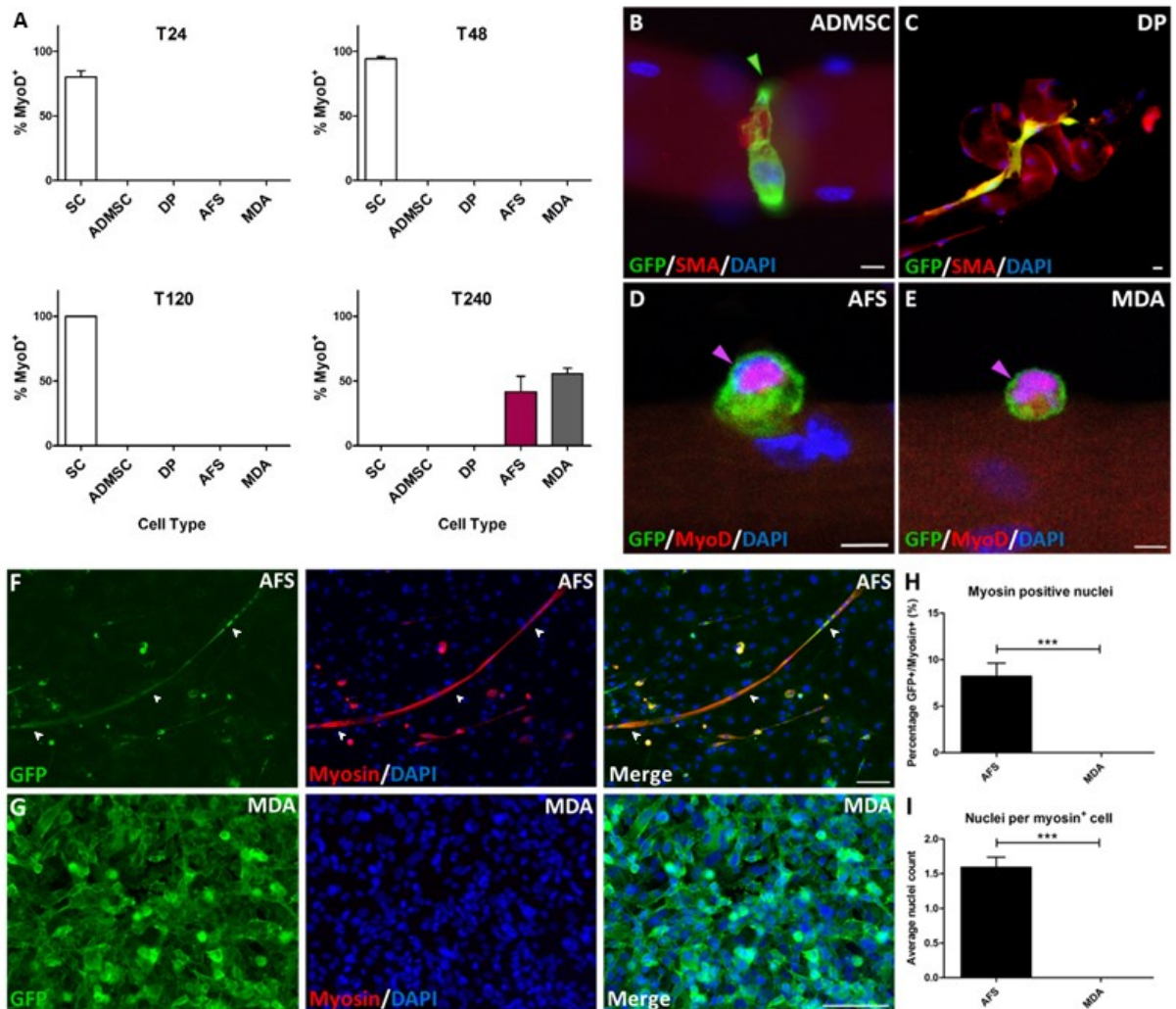
Figure 6.8 Induction of MyoD expression in AFS and MDA cells after prolonged culture on myofibres. **(A)** Temporal profiling of non-resident cells on myofibres for MyoD expression **(B)** ADMSC identified by GFP expression, constricting myofibres at T24. **(C)** DP cell distorting myofibres at T24. **(D)** AFS cell T240 showing nuclear expression of MyoD co-localising with DAPI (indicated by magenta arrow). **(E)** MDA cell at T240 showing nuclear expression of MyoD co-localising with DAPI (indicated by magenta arrow). **(F)** AFS cells, identified by GFP expression, co-localising with myosin, fused to form elongated myotube structures (arrowheads). **(G)** MDA cells co-cultured with myofibres failed to initiate myosin

Taryn Morash

expression. **(H)** Quantification of GFP+ cells expressing myosin. **(I)** Number of nuclei per cell GFP+ expressing myosin. Scale 10µm (B–E), and 100µm (F, G). *p<0.05, **(H-I)** Individual student's t-tests.
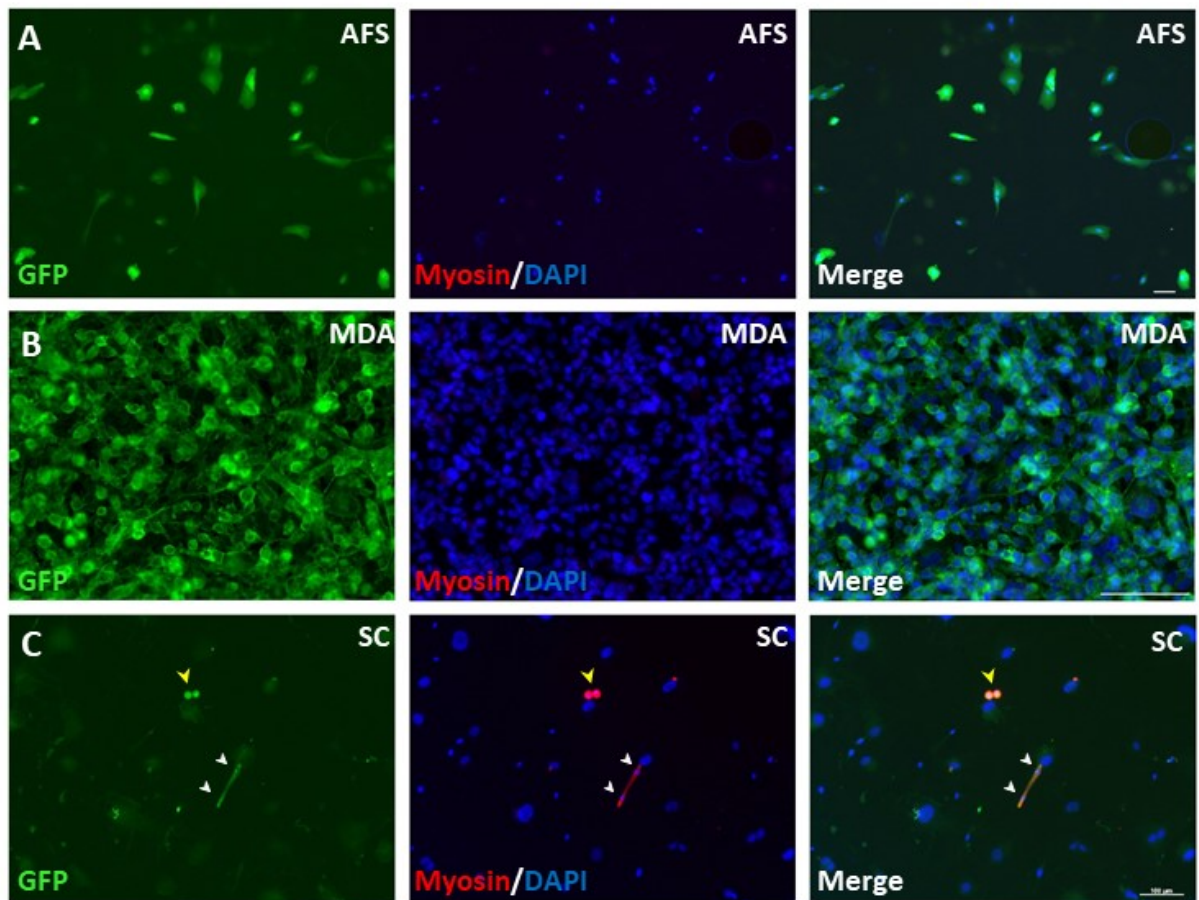
Figure 6.9 AFS and MDA cells that had not been in contact with the myofibre failed to express MHC and did not fuse **(A)** MHC- AFS cells, grown on glass cover slips in single myofibre culture media (SFCM), that had not previously been co-cultured with myofibres. **(B)** MHC- MDA cells, grown on glass cover slips in single myofibre culture media (SFCM), that had not previously been co-cultured with myofibres. **(C)** Dissociated SC positive control, cultured SCs on glass cover slips express MHC and fuse (white arrowheads). MHC+ SCs positioned side-by-side, aligning prior to fusion (yellow arrowhead). Scale 100µm.

Taryn Morash

Discussion

The importance of the physical properties of microenvironments is ever-increasingly becoming a focal point of much research. This is largely due to relatively unsuccessful use of whole stem cell approaches to enhance tissue regeneration (Yin et al. 2013). For example, including those that employ the use of pre-existing mechanisms of host tissues, through a paracrine effect such as stem cell-derived conditioned media (Conboy et al. 2005; Mellows et al. 2017). However, there remains huge clinical benefit for successful whole stem cell-based therapies.

Engler and colleagues altered the field of stem cell therapy, by showing that the elasticity or rigidity of a matrix has profound effects on the fate of stem cells (Engler et al. 2006). It was demonstrated that by artificially mimicking the physiologically-relevant matrix elasticities of the brain, muscle, or bone *in vitro*, human mesenchymal stem cells were directed towards neuronal, myogenic or osteogenic differentiation lineages, respectively (Engler et al. 2006). Additionally, increased myofibre stiffness with age and increased fibrosis following damage, has been shown to significantly impaired SC regenerative potential and self-renewing capacity (Gilbert et al. 2010; Lacraz et al. 2015). Colleagues have also previously demonstrated that the skeletal muscle myofibre promotes resident SCs to migrate utilising the distinctive amoeboid bleb-based mechanism (Otto et al. 2011). Therefore, this further highlights the importance of the matrix elasticity in altering mechanisms of SC function and further suggests how features such as cell migration, proliferation, self-renewal and differentiation are impacted in ageing, injury and disease.

It was established that all cell types, once introduced to the myofibre surface, similarly to the resident SC population, adopted a rounded morphology and migrated by the amoeboid-based form of motility. Additionally, all cell types developed cell surface blebs, as observed during bleb-mediated movement of SCs. Therefore, these findings demonstrate that these features are not unique intrinsic characteristics to SCs and instead, they are directed through contact with the myofibre (Morash et al. 2017). Others have previously reported that the amoeboid-based migratory method was the faster of the two forms of motility, demonstrated in SCs (Otto et al. 2011). However, it should be noted that, despite all non-muscle cell types taking on the bleb-mediated amoeboid mechanism, this was not always accompanied by an increase in velocity. Rapid amoeboid movement is dependent on rapid and frequent bleb extensions and retractions, whereby the full lifecycle of a bleb has been shown to total approximately 60 seconds (Otto et al. 2011). Furthermore, the bleb lifecycle is known to be prolonged in aged SC motility which has been linked to an observed reduction in SC velocities in ageing (Collins-Hooper et al. 2012). Therefore, one explanation for an apparent discordant finding of bleb-based migration, resulting in a slower rate of movement, in some of the non-muscle cell types

Taryn Morash

(ADMSC and AFS), could be that there is variation in the bleb dynamics between cell types. Furthermore, upon closer investigation, it does seem that the number of blebs per DP and MDA cell were slightly greater than those present on the surface on both ADMSCs and AFS cells. Moreover, rapid assembly and disassembly of simple focal adhesion structures between the cell and the matrix, has been proposed in the faster bleb-mediated motility (Nagano et al. 2012; Tozluoğlu et al. 2013; Charras & Paluch 2008). Therefore, it could be postulated that the regulation of the molecules required for efficient focal adhesion formation and deconstruction may be mismatched in some of these cell types. It could be further suggested that the focal adhesions and other contacts formed with the myofibre, vary between non-muscle cells and SCs. For example, primary SCs have been shown to express and interact with a wider range of integrins in the myofibre niche, compared to C2C12 and MM14 murine satellite cell/myoblast cell lines (LaFramboise et al. 2003). These cell lines are extensively studied alongside mouse primary SCs similarly, to examine their capacities to express MHC and differentiate to fuse and form myotubes *in vitro* (Yablonka-Reuveni 2011). However, even in such similar myoblast cell types, variation in features of cell to ECM communication and interaction have been identified. Thus, in four vastly different non-muscle cell types (including one non-stem cell, MDA), in the current series of experiments, the concept of differing developmental histories can be considered, regarding their altered interactions with the myofibre niche. Moreover, in muscle, this notion of developmental history has been well-defined, with respect to the divergent properties and regulation of muscle stem cells, responsible for maintaining muscle growth during late stages of embryogenesis and alternatively, carrying out post-natal growth and repair (McKinnell & Rudnicki 2005; Relaix et al. 2005). However, further analysis to determine whether these differences in migration speed between cell types can be attributed to variations in the bleb dynamics or focal adhesions, remains to be examined. It would be of interest to analyse FAK signalling pathway, as well as focal adhesion protein localisation in these different cell types on myofibres. Additionally, it could be hypothesised that differing integrin isoforms may be presented on these different cell types which may have differing affinities for the myofibre ECM components, therefore, integrin staining would aid in investigating these features.

A further finding of the current series of experiments was that, when comparing the cell morphologies adopted on aged myofibres to those observed on young myofibres, all cell types similarly took on a more rounded form. This result could therefore, suggest that despite the previous reports of myofibre stiffening with age, any potential alterations in myofibre substrate elasticity did not affect the cell morphologies observed in each cell type (Lacraz et al. 2015). Following this, *in vitro* CM treatment in both young and aged myofibre cultures was examined in each cell type. Firstly, it was observed that resident SC morphologies were not affected by myofibre age nor CM treatment.

Taryn Morash

This finding is therefore, in keeping with the previous series of naturally-aged SC experiments, which demonstrated that SC morphologies were unchanged in ageing and CM treatment *in vivo* was observed to have no additional effects on this feature. Notably however, CM treatment in aged myofibre cultures significantly reduced the proportion of round AFS cells. Additionally, the aged myofibre decreased the proportion of round DP and MDA cells, which appeared to be restored by CM treatment in the DP cells, but not in the MDA cells. This indicates that properties maintained by CM, could be counteracting the influence of the myofibre, in directing the signalling implicated in actin organisation and the overall structure of the cell, in the AFS and DP cell types. Subsequently, cell migration speeds were compared between young and aged myofibres, with and without *in vitro* CM treatment. Interestingly, despite *in vivo* CM treatment in the previous naturally-aged SC series of experiments, increasing aged SC migration speeds, this was not evident with *in vitro* CM. This therefore, could indicate potentially more potent effects of *in vivo* administration of CM treatment versus that added to myofibre cultures *in vitro*. Furthermore, ADMSC migration speeds appeared to be increased by CM treatment as well as by an aged myofibre. This was also observed in DP cells, with the exception that CM treatment in aged cultures reduced DP velocities to those comparable to young control cultures. Contrastingly, CM treatment in aged cultures significantly increased MDA migration speeds. These findings indicate that the aged myofibre surface induced a faster rate of motility in ADMSC and DP cells. As previously discussed, this could suggest that features such as focal adhesion contacts, as well as bleb dynamics were altered in these cell types whilst in contact with the aged myofibre substrate. Additionally, CM also appeared to regulate components of the underlying mechanisms regulating cell migration. Mellows and colleagues showed that a large proportion of the AFS CM contents targeted regulation of cell motility and actin organisation. Therefore, ADMSC-derived CM used in the current study could potentially harbour similar properties to result in the altered features of cell morphology and migration observed (Mellows et al. 2017). Overall, these findings indicate that alterations in the physical properties of aged myofibres, such as an increased substrate elasticity as previously reported, appeared to be detected by the non-muscle types and resulted in variances in cell morphologies adopted and speed of movement. Interestingly however, these alterations in cell behaviour were not elicited in resident SCs, to the degree that non-muscle cells were influenced. This therefore, could be explained by the previously mentioned concept of the differing developmental histories between SCs and non-muscle cells. Furthermore, this could indicate that SCs are perhaps more plastic in their behaviour, in order to cope with physical adaptations to their niche, for example as a result of ageing or damage, as opposed to non-muscle cells in a foreign microenvironment.

Taryn Morash

Despite observing varying profiles of migration speeds, importantly, it was shown that regulation of the same underlying molecular pathways are responsible for directing the cell morphologies of both SCs and non-muscle cells on myofibres (Morash et al. 2017). Previous work conducted by Marshall and colleagues has shown that the blebbing and lamellipodia-driven mechanisms are regulated by the antagonistic activity of Rho and Rac GTPase signalling, respectively (Sanz-Moreno et al. 2008; Sanz-Moreno & Marshall 2009). Rho activity is supported by downstream ROCK function to promote the formation of actin stress fibres and produce high levels of actomyosin contractility in amoeboid-based motility and simultaneously, inactivates Rac (Calvo et al. 2011; Sanz-Moreno et al. 2011; Sanz-Moreno & Marshall 2009). Rac alternatively, through downstream interactions with the WAVE2 and Arp2/3 complexes, drives actin filament formation and 'γ-branching' of lamellipodia protrusions (Eden et al. 2002; Goley et al. 2004; Soderling & Scott 2006; Sanz-Moreno et al. 2008; Wu et al. 2012). Therefore, in the current study, it was observed that the relationship between these two counteracting pathways is conserved in the three different stem cells and the non-stem cell types examined. Moreover, physical contact with the myofibre surface therefore, appears to be detected by the transplanted non-muscle cells, which in turn, elicits an intracellular response, altering the regulation of these intrinsic signalling mechanisms, resulting in the adoption of resident SC behaviour. An understanding of this feature in young, healthy myofibre cultures can be used to provide possible insights into the mechanisms and signalling components that may become dysregulated with age or during disease. Examination of the intrinsic regulation of the Rac/Rho pathways that determine cell morphology and migration in ageing SCs therefore, is required.

An additional finding of the present series of experiments was that proliferation, a further key component of SC activity, was influenced by the myofibre surface (Morash et al. 2017). Resident SCs following activation, are known to proliferate on myofibres after approximately 24 hours of culture and double in number by T48 (Zammit 2002; Collins-Hooper et al. 2012). This was somewhat the trend observed with the transplanted MDA cells on myofibres, which is in keeping with the reported population doubling time of MDA cells of approximately 27 hours (Limame et al. 2012). MDA cells are also well-known for being a highly aggressive, invasive breast cancer cell and a key feature underpinning cancer progression, is the ability to act outside normal control and 'hijack' mechanisms utilised in normal tissue homeostasis, in order to drive proliferation and growth (Chavez et al. 2010; Hanahan & Weinberg 2000). Therefore, unsurprisingly, MDA cells demonstrated a high degree of cell proliferation on myofibres, which may indeed occur regardless of physical microenvironmental characteristics. Contrastingly, AFS cells, despite having a reported population doubling time of 25-30 hours *in vitro*, were not induced to proliferate by the myofibre surface (Cananzi et al. 2009; Tsai et al. 2007). The number of ADMSCs on myofibres significantly declined over the 48-hour culture duration

Taryn Morash

which could indicate a lack of proliferative activity on this 'foreign' matrix. Furthermore, as previously discussed, the morphology of ADMSCs notably changed following extended culture on myofibres, gradually cells elongated and caused a large degree of myofibre constriction and overall death (hypercontraction) through lamellipodia extensions. Therefore, this could indicate not only an absence of ADMSC proliferation, but also increased myofibre loss in culture. Moreover, this finding could suggest a possible damaging characteristic of ADMSC interaction with myofibres *in vivo*. For example, an infiltration of fat tissue into muscle is believed to occur during DMD as well as ageing, and has been implicated in reduced SC function (Taaffe et al. 2009; Kragstrup et al. 2011; Hamrick et al. 2016). However, the findings of the present study suggest a more direct feature of ADMSCs that could lead to myofibre damage, that they can induce hypercontraction through myofibre contact as elongated morphologies. In fact, there were no healthy intact myofibres remaining following three days of ADMSC co-culture. Moreover, it was noted that myofibres co-cultured with AFS and MDA cells remained viable for a minimum of 10 days. To further examine the proposed injurious feature of ADMSC cells to the myofibre, staining for the localisation of non-muscle myosin (II) organisation in transplanted cells could give an indication as the tension applied to the myofibre surface through lamellipodia extension (Vicente-Manzanares et al. 2009). Additionally, recent studies have established myosin II as an essential cellular component necessary for ECM remodelling and matrix stiffening (Hindman et al. 2015; Engler et al. 2006). Therefore, this finding could suggest that transplanted ADMSCs exerted non-muscle myosin II-mediated tension, further remodelling the myofibre surface, causing overall stiffening, which in turn, induced ADMSCs to adapt to a more elongated morphology, eventually causing the myofibre to hypercontract.

The most remarkable finding of this series of experiments was that AFS and MDA cells, following 10 days of co-culture on the surface of myofibres, adopted not only myogenic features of cell migration, but also a myogenic fate, as evident by MyoD expression (Morash et al. 2017). Furthermore, strikingly, AFS cells then subsequently, following dissociation from myofibres, fused to form MHC[+] myotubes. Importantly, it was demonstrated that this state developed without first initiating Pax7 expression. Significantly, it is therefore surmised that these cell types are not utilising the molecular programme associated with normal myogenic development (Amthor et al. 1998). Instead, the expression of MyoD alone, in the absence of Pax7, in adult SCs, indicates that the only option is terminal differentiation and therefore, the potential of reverting to a stem cell state is lost (Zammit et al. 2004; Nagata et al. 2006; Yablonka-Reuveni & Rivera 1994). This feature suggests that, for future research and exploitation of these findings, AFS cells could only possibly be used to initiate repair of damaged tissue, rather than being able to rely of these cells in forming a reservoir, or replenishing exhausted SC stem cell pools, for future cycles of muscle regeneration. Overall, these

Taryn Morash

findings suggest that an alternative stem cell type (AFS), as well as a non-stem cell (MDA) demonstrated myogenic lineage commitment, evident through robust MyoD expression, at a relatively high frequency. These findings therefore imply that cells do not necessarily need to be stem cells to be induced towards a myogenic lineage. Thus, this work can be extended to explore other non-muscle, non-stem types that maintain a similar capacity to generate muscle cells for whole cell-based therapies in ageing, injury and disease. This would be beneficial, as current work into the therapeutic potential of alternative non-satellite cell types in trauma-induced muscle regeneration so far has shown varying success (Yin et al. 2013). However, one route currently being investigated is the use of embryonic stem (ES) cells and induced pluripotent stem (IPS) cell types, in determining their capacity to incorporate into the SC niche, express Pax7, undergo extensive self-renewal and engraft successfully into injured muscle (Chang et al. 2009; Mizuno et al. 2010). Although, the use of these cells is associated with issues related to both ethics and specialised isolation and culture techniques (Condic & Rao 2010; Medvedev et al. 2010). Therefore, achieving a similar effect of culturing alternative cell types and utilising the tissue matrix to almost 're-programme' the cells towards a myogenic fate, would be of great clinical value and merits further research.

Remarkably, these findings also revealed that AFS cells, but not the non-stem cell (MDA), were directed through contact with the muscle microenvironment to fuse and form MHC$^+$ myotubes, reinforcing the potential therapeutic value of AFS cells. In conclusion, the findings indicate the profound influence that the microenvironment or matrix has on regenerative processes, such as cell differentiation and fusion (Morash et al. 2017). Furthermore, this supports previous findings, that alterations to the microenvironment or niche with age, or during damage or disease, can have major implications in the regulation of cell behaviour during tissue repair, maintenance and homeostasis. Moreover, whole stem cell-based therapeutic approaches aimed to enhance tissue regeneration, can be better optimised with the physical features of the host microenvironment, matrix elasticity and cell to ECM interactions considered. For example, artificially engineered scaffolds and substrates *in vitro*, that mimic the physiological characteristics of damaged, diseased, fibrotic or aged tissues could be used to prime cultured cell populations prior to introduction into the host tissues. Numerous studies are currently exploring the use of animal-based, or completely artificial materials and scaffolds in the treatment of muscle pathologies. For example, studies utilising human decellularised skeletal muscle scaffolds that have been shown to maintain ECM architecture, are being conducted to examine muscle cell implantation and colonisation (Porzionato et al. 2015). In order to minimise the use of large numbers of small animals, in scaled-up experiments, larger scaffolds are therefore required. However, (commercial) bovine sources, used as an alternative to human constructs, would be more beneficial and ethical, in the generation of larger quantities of decellularised material.

Taryn Morash

Furthermore, recent advances in the tissue engineering field are moving partially, or completely away from the use of human/animal tissues and involve electrospun nanofibers or carbon nanotubes for use in skeletal muscle-based pathologies, where the potential for these scaffolds to promote myogenesis, are assessed (Manchineella et al. 2016; Kim et al. 2016). However, these matrices have yet to be investigated for their influence on the movement of SCs, to determine if cells adopt amoeboid-based migration, or whether the physical characteristics support myogenic lineage specification in non-muscle cells. Furthermore, the findings of the current study highlights the need for extended examination into the influence of decellularised muscle and artificial muscle-like materials on migratory and differentiation mechanisms. Much research in this field is focussed on developing an appropriate maximal decelluarisation technique, usually using detergents or enzymes, as source tissues are typically allogeneic or xenogeneic (Crapo et al. 2011). However, Perniconi and colleagues developed acellular murine TA scaffolds that preserved biochemical features including collagen, laminin and fibronectin and once implanted *in vivo*, to replace the whole host muscle, resulted in a pro-myogenic environment being established (Perniconi et al. 2011). Additionally, further characterisation of the key properties underpinning the myogenic specification of AFS and MDA cells, by the myofibre co-culture method utilised in the present study, is required. Lastly, the additional hypothesis that these cells can subsequently be used to promote muscle tissue regeneration, remains to be addressed. This could be examined through the development of GFP[+]/MyoD[+] AFS and MDA cells, using the co-culture technique described and injecting them into immunocompromised mice following cardiotoxin-induced muscle injury. Successful muscle regeneration would be evident in the supposed development of GFP[+] myofibres.

Taryn Morash

Chapter 7
General discussion

The main aim of this research project was to investigate the potential therapeutic effects of stem cell-derived conditioned media on the progression of sarcopenia. An experimental programme was conducted in order to address the following: (**A**) An extensive naturally-aged skeletal muscle profile, examining a broad range of parameters at molecular, cellular, tissue and whole organism levels was generated, to provide a basis for subsequent experimentation. (**B**) Features of skeletal muscle composition, function and regeneration were characterised in the novel use of the *Ercc1$^{d/-}$* murine model of progeria. The *Ercc1$^{d/-}$* skeletal muscle profile was subsequently examined in the capacity to mimic aspects of decline associated with sarcopenia in natural ageing. (**C**) The therapeutic potential of conditioned media (CM) treatment, generated from adipose-derived mesenchymal stem cells (ADMSC), was investigated in both naturally-aged and progeric skeletal muscle. (**D**) The importance of the skeletal muscle myofibre matrix in defining satellite cell (SC) regenerative function, as well as the influence of the myogenic microenvironment on the behaviour and fate of non-muscle cells, was explored.

Development of an ageing skeletal muscle profile and the therapeutic effects of conditioned media

The central hypothesis of this work was that conditioned media (CM) generated from adipose-derived mesenchymal stem cells (ADMSC), maintains regulatory properties that attenuate, delay or even prevent age-associated alterations in skeletal muscle composition and function. It has been well-established that skeletal muscle, along with all other tissues, undergoes time-dependent, progressive declines in genomic and cellular integrity and function (López-otín et al. 2013). This age-related deterioration of skeletal muscle is defined as sarcopenia, which broadly encompasses the loss of muscle mass, strength, quality and function (Demontis et al. 2013; Burton & Sumukadas 2010). Numerous other physiological, histochemical and biochemical alterations, have also been extensively reported in ageing human and animal studies. Additionally, comparisons made to assess the well-defined intrinsic and extrinsic alterations that occur in skeletal muscle between both human and rodents, indicate that mice and rats are close models of human sarcopenia (Demontis et al. 2013). For example, skeletal muscle is known to experience a loss of force-generating capacity, myofibre atrophy and a switch in myofibre composition, to comprise a larger proportion of those more slow twitch and oxidative in nature, among others, in both humans and rodents (Degens 2007; Larsson & Edström 1986; Ansved & Larsson 1989; Lexell et al. 1988; Alnaqeeb & Goldspink 1987; Rowan et al. 2011).

It was established that sarcopenia was evident, primarily at a geriatric age, in the naturally-aged mice of the current study, by the observed loss of muscle mass and reduced grip strength. Key

Taryn Morash

phenotypical characteristics, in keeping with what is established in the literature, included reduced total myofibre number, increased metabolic dysfunction, greater O_2^- ROS production, reduced oxidative capacity (*Soleus*) and evidence of a fast to slow MHC switch (*Soleus*). However, a decline in myofibre CSA, which is the general agreement, but highly variable among naturally-aged human and animal studies, was not noted in the present study (Klitgaard et al. 1989; Degens, Veerkamp, et al. 1993; Lexell et al. 1988). Furthermore, a switch in the reverse direction, instead from fast to an even faster type, was observed in the ageing EDL. The ageing skeletal muscle profile developed in the current study samples only a subset of key parameters in such as vast research field, in order to provide a broad basis for subsequent novel examination of the therapeutic 'anti-ageing' paracrine potential of ADMSC CM. Furthermore, these are the first reports, to our knowledge, of a broad assessment of the influence of (ADMSC-generated) CM, on the well-defined skeletal muscle characteristics, reported during the progression of sarcopenia.

As an alternative therapeutic approach to whole cell-based treatments in injury and disease, stem cell-derived CM is currently being explored. It has been established that key regulatory growth factors, such as VEGF, bFGF, TGF-β and HGF, as well as antioxidants, are among the released factors maintained by ADMSC CM that have shown beneficial effects in regeneration of dermal wounds (Kim et al. 2007; Kim et al. 2009). Furthermore, CM generated from AFS cells, utilising the same isolation method as the one used in the current study, produced a clinically-compliant CM rich in secreted factors, released under stressed conditions (Mellows et al. 2017). The AFS CM was also free from all other exogenous molecules and demonstrated enhanced muscular regenerative properties. Crucially, circulating secretory factors released from young/healthy donor cellular sources, saw rejuvenating effects once introduced into an aged microenvironment, impacting on the underlying mechanisms of muscle regeneration, to improve SC proliferation and differentiation (Conboy et al. 2005; Lavasani et al. 2012).

The findings at a tissue level, in the current project, indicated that firstly, the *Soleus* muscle was affected to a greater degree by the ageing process, compared to the EDL. This could potentially be explained by the slower twitch oxidative nature of the *Soleus* and that a switch to a slow phenotype characteristic of ageing, may be more readily 'achievable' in an already slow muscle (IIA to I), instead of a faster, more glycolytic muscle, EDL (IIB to IIX to IIA to I) (Schiaffino & Reggiani 2011). Secondly, the findings demonstrate that while CM treatment in aged animals did not appear to influence features of overall myofibre composition, such as myofibre number, size or types, there was some evidence for potential modification of signalling pathways involved in angiogenesis, oxidative metabolism, mitochondrial function, reduced ROS production/enhanced antioxidant activity, as well as ECM collagen organisation. Therefore, it could be hypothesised that growth factors promoting

Taryn Morash

angiogenesis, such as VEGF or bFGF, and collagen synthesis (procollagen I) in local dermal fibroblasts, previously observed to enhance skin regeneration after treatment with ADMSC CM, may be functioning similarly in ageing muscle in the present study (Kim et al. 2007; Kim et al. 2011). However, features of myofibre composition such as hypertrophy, a highly orchestrated mechanism driven by growth factor-mediated protein synthesis signalling, were not altered significantly by CM treatment. This is despite a proportion of CM content believed to be comprised of trophic factors, alongside the mRNA (lesser amounts) and miRNA (more abundant). This suggests that the regulation required to bring about these arguably quite major alterations to myofibre composition could be the result of more sustained modulation, as with repeated exercise. Whereas, CM may be sufficient to adapt cell to cell and cell to ECM communications, to bring about alterations to vascularisation, collagen synthesis/deposition, mitochondrial biogenesis and function, in a more transient manner. Whether an increased CM administration programme would be sufficient to alter these features of overall myofibre composition and muscle strength, therefore, remains unknown.

As noted by Mellows and colleagues, miRNA contents that target the cellular mechanisms that regulate vascularisation, may also be harboured by the CM generated in this project (Mellows et al. 2017). Moreover, the vast majority of the secreted miRNA from AFS CM, were established to target signalling pathways associated with metabolic processes. Therefore, it is reasonably postulated that ADMSC CM treatment could act similarly to drive changes in the regulation of mitochondrial biogenesis, abundance and function and enhancing antioxidant activity (Mellows et al. 2017). Thus, this pin-points two key areas to continue to explore further with ADMSC CM, the signalling pathways involved in the formation of new vasculature, as well as those relating to metabolism.

Despite observing an increase in (oxidative) type I myofibres in the aged *Soleus*, the oxidative capacity (SDH activity), was reduced in advanced old age which indicated potential metabolic dysfunction or impaired oxygen delivery. It has been established that there is overall capillary loss with age (Degens, Turek, et al. 1993). However, it was determined that there was no evidence for capillary loss with age in the present study. Although, this is just one aspect that could indicate impaired oxygen delivery, so it cannot be ruled out completely. It would be of interest to probe this line of enquiry further and assess features such as myoglobin or hypoxia inducible factor – 1 (HIF-1) expression, which would give a better understanding of the oxygen status, in future experimentation (Fitts et al. 1974; Ordway 2004).

Although there was no loss of capillaries observed, CM demonstrated pro-angiogenic effects in the aged *Soleus*. *VEGFa165* mRNA expression was increased with CM in the aged *Soleus*, when compared to a geriatric age only (it was unchanged to the old age control). This invites further investigation into

Taryn Morash

the explanation of overall increased capillary density observed with CM treatment. For example, the VEGF protein levels, VEGF receptors (VEGFR1 and VEGFR2), or the alternative growth factors that influence angiogenesis, such as FGF, as well as the VEGF content of the CM itself, have yet to be investigated in the present study (Cross & Claesson-Welsh 2001). Croley and colleagues showed that *VEGF* mRNA exercise-induced expression was 50% lower in aged *Vastus lateralis* muscle biopsies from women, compared to a young age (Croley et al. 2005). The VEGF protein was 35% lower at rest but there were no age-related differences in VEGFR expression. A similar mRNA and protein trend for VEGF, was then shown in aged men, although exercise increased VEGF mRNA and protein, independent of age group (Ryan et al. 2006). The laboratory mice in the present study remain relatively sedentary in their cages, so it can be reasoned that *VEGF* mRNA remains low, with very little fluctuation due to inactivity, with age as the main contributing factor to any changes. It would therefore, be of interest to test the VEGF response at mRNA and protein levels in aged mice, subjected to regular treadmill or running wheel exercises, with and without CM treatment. Wheel running exercise in mice for example, induced *VEGF* mRNA expression and protected VEGF protein levels against age-related decline skeletal muscle and this activity was mediated by PGC-1α and downstream AMPK activation (Leick et al. 2009). Additionally, treadmill exercise in mice was shown to induce brain mitochondrial biogenesis via PGC-1α, and neurogenesis via *VEGF* in the hippocampus, thereby exercise initiates angiogenesis systemically, benefitting the function of further compartments than just skeletal muscle (E et al. 2014). Future work will explore the angiogenesis signalling further, by examining other VEGF isoforms at protein and mRNA levels, VEGFR abundance, as well as FGF, as an alternative growth factor influence on vascularisation, in the aged *Soleus*. Interestingly, capillary densities were not affected in the aged EDL, this may not be overtly surprising considering the more glycolytic nature of the EDL and unaltered oxidative capacity, noted with age in this study.

Moreover, mitochondrial dysfunction is a defined hallmark of ageing and it was postulated that this feature could contribute to the mis-match between the increased type I myofibres and a decreased oxidative capacity, observed in the current research project (López-otín et al. 2013; Pieczenik & Neustadt 2007). This was further supported by an increased ROS production (DHE analysis) at geriatric ages. This finding in turn, lead to the examination of antioxidant SOD2 expression analysis which was unchanged with age. However importantly, this does not rule out insufficient antioxidant activity as a contributing factor to this finding, as further types of antioxidant would require exploration, at both mRNA and protein levels.

CM treatment reversed the decrease in oxidative capacity in aged *Soleus* muscles to levels higher than younger controls. This also could explain the requirement for an increased blood supply with

Taryn Morash

CM in old age, which seems to accompany this trend. It was established that CM reduced O_2^- ROS production (DHE) in old age and along with an unchanged SOD2 antioxidant expression, this raises questions regarding the mitochondrial function that are currently unidentified. Therefore, further study into the mechanisms that underpin mitochondrial biogenesis, abundance and overall function are required. For example, mitochondrial homeostasis is reportedly controlled by nuclear transcription regulators such as p53, PGC-1α, HIF1α, FOXO and SIRT1, SIRT6 and SIRT7 signalling pathways, as well as NAD+ availability, which is known to be depleted in ageing (Gibson & Kraus 2012; Fang et al. 2016). Future work will be to analyse these key mitochondrial regulators using qPCR analysis and also western blot protocols to get an overview of activity both at a molecular mRNA level but also post-translationally, to analyse protein function.

Additionally, O_2^- is just one of the ROS that can play a role in overall damage of DNA, mtDNA, lipids, proteins, oxidative phosphorylation enzymes for example, there are also many other free radicals that can do just as much damage if levels are not maintained by the range of antioxidant mechanisms. For example, initial superoxide damage has been shown to damage the active site of an enzyme involved in the Kreb's (TCA) cycle, exposing iron which then reacts with H_2O_2 to produce hydroxyl free radicals via Fenton's reactions (Vásquez-Vivar et al. 2000). Furthermore, glutathione peroxidase (GPX), an antioxidant enzyme that functions downstream of SOD2, is responsible for the detoxification of H_2O_2 to water (Pieczenik & Neustadt 2007). GPX and catalase, a further antioxidant, are known to increase with ageing and training in rat *Vastus lateralis* and *Soleus* muscles (Leeuwenburgh et al. 1994). These features and other free radicals, damage biological molecules and it is almost impossible to distinguish a specific damage to a specific oxidant (Vásquez-Vivar et al. 2000). Thus, it is reasoned that damage is dependent on the cell type, the biological target, as well as interactions with other free radicals and these may act in conjunction with other cytotoxic processes (Vásquez-Vivar et al. 2000; Olanow 1992). This taken together suggests that investigation conducted at a protein level, determining the activity of SOD2 and its key regulators, such as NF-κB and p53, would provide a better understanding of antioxidant function in aged *Soleus* and EDL muscles, with and without CM treatment. Moreover, analysis of the abundance and activity of other antioxidants, such as GPX, could also establish a more comprehensive view of which components associated with detoxification step, are potentially the most impaired. Therefore, this could aid in the identification of where the largest sources of free radical accumulation lie, which lead to the overall increased oxidative stress reported with age progression. Thus, potentially highlighting components most susceptible, reflected in the natural ageing process that could be therapeutically targeted.

Collagen IV thickness was shown to increase with age in the *Soleus* which is in keeping with what is reported in the literature (Marshall et al. 1989). A corresponding downregulation of collagen IV

Taryn Morash

mRNA expression with increasing age, indicated that at the molecular level, the thickening appeared to be modulated. However, this does also suggest that despite this downregulation, post-translational modifications appear to be having a more predominant effect, resulting in increased collagen deposition and/or a lack of degradation as an overall outcome, potentially highlighting an area of collagen signalling dysfunction with age. Interestingly, CM treatment in old age maintained collagen density at a thickness displayed in the adult muscle, thereby, attenuating the proposed post-translational dysfunction. As discussed, the AFS CM showed a large portion of the miRNA present targeted ECM organisation which may indicate the underlying regulatory mechanisms we can expect to identify in the ADMSC CM analyses (Mellows et al. 2017). Therefore, signalling pathways targeted may include those regulating collagen synthesis and degradation. Taken with the findings of a reduction in collagen thickness with CM treatment in the aged *Soleus*, it can be hypothesised that the signalling pathways targeted by CM components could include: downregulated Wnt-, TGF-β- and IGF-1-mediated collagen synthesis and deposition, reduced post-translational collagen and advanced glycation end-product (AGE) cross-linking and/or increased MMP-2 and MMP-9 activity (Kjær et al. 2009; Zimmerman et al. 1993; Haus et al. 2007; Bani et al. 2008).

Overall, the vast majority of key phenotypical features examined in the present study, were in agreement with what has already been established in the literature and therefore, were used as a basis for subsequent experimentation. ADMSC CM treatment in these naturally-aged animals saw beneficial regulatory effects of the vasculature, oxidative metabolism and collagen organisation and features of overall functionality, mass and composition were maintained into old age. Therefore, these findings indicate that CM attenuates the progression of some of the hallmarks of ageing mechanisms underlying decline, for example, mitochondrial dysfunction.

Characterisation of the skeletal muscle phenotype in the *Ercc1$^{d/-}$* murine model of progeria

The main objectives of this body of work aimed to (**A**) Characterise the phenotypical aspects of skeletal muscle in the *Ercc1$^{d/-}$* murine model of accelerated ageing (progeria). (**B**) As carried out in the previous series of naturally-aged experimentation, assessment of the therapeutic potential of ADMSC CM treatment was extended into this severe model of systemic DNA damage accumulation. (**C**) It was important to establish the suitability of this model, in mimicking those characteristic alterations that are well-defined in naturally-aged skeletal muscle with the progression of sarcopenia. It has been established that there is a requirement for a suitable mammalian model of accelerated ageing, in order to examine potential intervention approaches, in the amelioration of age-related symptoms of sarcopenia and other pathologies, observed in both animals and humans

Taryn Morash

(Demontis et al. 2013; De Waard et al. 2010; Lavasani et al. 2012). The main criticisms of utilising naturally-aged rodents for this purpose, is that there is an inability to perform large-scale genetic screens *in vivo*, as carried out in simple model organisms and due to the 2-3 year lifespan, efficiencies of intervention programmes are low and uneconomical, as rodent housing costs are high (Demontis et al. 2013).

It is well-known that in early (post-natal) growth phases, body mass increases rapidly and continues into adulthood and muscle hypertrophy, rather than hyperplasia, contributes the majority of this increase (Gokhin et al. 2008; White et al. 2010; Stickland 1981). The findings in the current series of experiments however, in keeping with what is known about the *Ercc1$^{d/-}$* mutant, indicated that progeric animals did not undergo this rapid growth and instead, displayed a small appearance (Weeda et al. 1997; De Waard et al. 2010; Dollé et al. 2006). *Ercc1$^{d/-}$* also displayed much lower hindlimb muscle weights and grip strength, indicative of an extreme model of dysfunction, both are key defining characteristics of sarcopenia.

It was shown that the *Ercc1$^{d/-}$* mice were severely stunted in their growth, which is attributed to the rapid DNA damage accumulation and further indicates a switch away from growth, where genomic and cellular maintenance is the priority (Weeda et al. 1997; De Waard et al. 2010; Niedernhofer et al. 2006; Garinis et al. 2008). Furthermore, this shift must happen early on in their post-natal growth, as muscles were half the weight of the controls. This finding therefore raises questions regarding the signalling pathways involved in this shift to maintenance, where it would be of interest to carry out qPCR analysis of the following in the musculature of the *Ercc1$^{d/-}$* mice, to determine AMPK expression, in response to metabolic stress and energy deprivation and the expected downstream downregulation of mTORC1, 4E-BP2, eIF2 and P70S6K1 via the TSC1/TSC2 complex (Baar 2006). Additionally, IGF-1 activity would also be expected to be downregulated, limiting protein synthesis, which also acts on downstream mTORC2 and AKT to activate FOXO (1 and 3), Atrogin-1 and MuRF1 (Milman et al. 2014; Bartke 2005; Niedernhofer et al. 2006; Garinis et al. 2008).

Myofibre loss was also evident in the *Ercc1$^{d/-}$* *Soleus* and as a diminished force-generating capacity with age, can be attributed to declines in myofibre number and/or myofibre size, it is suggested that grip strength was decreased, due to these reductions in the *Ercc1$^{d/-}$* mice (Alnaqeeb & Goldspink 1987; Larsson & Edström 1986). It was previously established that *Ercc1$^{d/-}$* animals experience motor neuron degeneration and a progressive loss of neuromuscular connectivity (De Waard et al. 2010). Therefore, this would support the reduction in myofibre number, as a result of denervation-induced atrophy. Importantly, it has been previously established that initial development of *Ercc1$^{d/-}$* mice was reportedly normal and it was noted that after this time, rapid DNA damage accumulation occurred

Taryn Morash

(Dollé et al. 2006). This indicates that early muscle development was unaffected and therefore, *Ercc1*[d/-] muscles are believed to comprise a full complement of myofibres at birth, and as in natural ageing, further implicating myofibre atrophy as a main contributing feature to reduced myofibre numbers (Glass 2005; Alnaqeeb & Goldspink 1987; Rowe & Goldspink 1969).

Furthermore, taken with the marked motor neuron degeneration known to take place in the *Ercc1*[d/-] mice, a lack of myofibre transition, suggests that the ability for surviving motor neurons to successfully re-innervate those denervated myofibres, may have also been affected, leading to further wide-spread, non-specific myofibre loss (Degens 2007; Lexell et al. 1986; Larsson et al. 1991). However, loss of contractile ability is not solely attributable to reduced myofibre number, composition and size. Other structural characteristics, such as collagen and AGE cross-linking, fat infiltration and ECM alterations, disrupted mechano-sensing, dysregulated protein homeostasis and post-translational modifications, for example impacting on myosin structure and cross-linking activity, among multiple others, lead to overall muscle weakening (Degens 2007; Lowe et al. 2001; Marshall et al. 1989; Haus et al. 2007; Hamrick et al. 2016).

Moreover, the findings of the study currently suggest, that along with the overall smaller size of the *Ercc1*[d/-] mice having a profound effect of muscle mass, myofibre atrophy may be the only other predominant cause of the dramatically reduced muscle mass. As further histological examination revealed that unexpectedly, the muscle composition, regarding characteristics of myofibre number, type, size and collagen density, were largely unchanged in the *Ercc1*[d/-] animals, relative to their young littermate controls. Skeletal muscle is known to be a large reservoir for amino acid storage in the body, with a large protein synthesis/degradation turnover, which also sustains protein synthesis in other tissues, while limited muscle mass is often associated with impaired responses to stress and chronic illness (Wolfe 2006). Therefore, it may be that this balance is tipped more strongly towards degradation, in *Ercc1*[d/-] animals where DNA damage accumulation will be leading to its chronic state of cellular stress (McWhir et al. 1993). In turn, this could impact on myofibrillar and other protein content degradation, potentially having a profound impact on the overall weight. This is further evidence for the notion that *Ercc1*[d/-] animals experience a default survival response, as well as this, loss of proteostasis is a well-defined hallmark of ageing which may further exacerbate the observed deterioration, of which future work will aim to determine, primarily utilising qPCR and western blot techniques (López-otín et al. 2013; García-Prat et al. 2016; McWhir et al. 1993).

A discrepancy remains however, as it was established that only the faster myofibre types, of which there are very few, as this analysis was carried out in the *Soleus*, appeared to showed a trend towards reduced CSAs. This result is more akin to that reported in the aged rat *Plantaris* (Degens,

Taryn Morash

Turek, et al. 1993). Myofibre CSA was unchanged in the slower type I and IIA myofibres. This finding however is in agreement with the trends noted previously in the naturally-aged series of experiments but overall, is not in keeping with the general agreement of a reduced CSA in natural ageing (Klitgaard et al. 1989; Lexell et al. 1988; Degens et al. 1993). However, Chai and colleagues saw a similar trend in geriatric (29 month old) *Soleus* muscles, where CSA was not significantly different to those at 3 months (Chai et al. 2011). Which arguably, is a more age-matched study to the naturally-aged geriatric mice of the present study, which experienced some of the most detrimental decline, such as reduced oxidative capacity and a dramatically increased ROS production in the *Soleus*. Additionally, there were no observed changes in collagen IV thickness measured histologically, nor collagen I mRNA expression suggesting that the decreased grip strength may not be attributable to altered collagen thickness. However, this does not take into account the potential impaired contractility, associated with collagen cross-linking, nor other ECM component stiffening such as AGE cross links (Zimmerman et al. 1993; Arnesen & Lawson 2006; Haus et al. 2007).

It was established that capillary density was reduced in the $Ercc1^{d/-}$ *Soleus*, suggesting that oxygen delivery may not be as efficient. This feature is in keeping with the loss of capillaries associated with natural ageing, but was not observed in the naturally-aged muscles of the current project (Degens et al. 1993). However, the reduction in capillary density did not impact on the overall oxidative capacity in the $Ercc1^{d/-}$ *Soleus*. It was also established that mitochondrial ROS production was slightly increased and SOD2 expression levels slightly decreased, somewhat indicating mitochondrial dysfunction, however these differences were not significant. Moreover, these findings seem surprising in a model that experiences high levels of oxidative stress, which would be expected to further exacerbate DNA and mtDNA damage and further compromise genomic integrity (McWhir et al. 1993; Pieczenik & Neustadt 2007).

An increased level of oxidative stress has been previously reported in the liver, kidney and brain in the *ERCC1*-deficient model (McWhir et al. 1993). Therefore, due to the nature of the model of insufficient NER, subsequent DNA damage accumulation and compromised nuclear and mitochondrial DNA integrity, it is suspected that other characteristics of mitochondrial dysfunction would also be evident, in addition to ROS and other free radical production. Moreover, regulation of numerous other components and processes are key to maintaining mitochondrial functionality, such as regulation of mitochondrial quantity and morphology, through efficient organelle biogenesis and fusion- and fission-mediated renewal (Terman & Brunk 2004; Frank et al. 2001; Powers et al. 2012). Emerging findings from our research group, currently indicate decreased mitochondrial density in $Ercc1^{d/-}$ muscles, both within the intermyofibrillar space, responsible for contractile energy production, as well as those lying just beneath the sarcolemma, implicated in ATP-dependent events

Taryn Morash

occurring at the membrane. Both sub-populations are reportedly compromised during muscle atrophy. The subsarcolemmal mitochondria are lost more readily during extended inactivity and also produce higher levels of ROS, whereas, those located more centralised within the myofibre are more susceptible to apoptotic stimuli induced by inactivity (Powers et al. 2012). Additionally, emerging evidence of mitochondrial swelling in $Ercc1^{d/-}$ muscle would also suggest dysfunction in those processes of morphological regulation of mitochondria during fusion and fission. Furthermore, increased mitochondrial fission, orchestrated via dynamin-related protein-1 (Drp1) for example, is elevated in myofibre atrophy and equally, fusion is also required for maintaining mtDNA stability and integrity. An imbalance or dysfunction in this process leads to abnormal mitochondrial morphologies as well as swelling and is highly linked to contractile deficit and denervation-induced myofibre atrophy (Powers et al. 2012). These features, among others discussed, are therefore postulated to be main contributing factors in the overall declines observed in the $Ercc1^{d/-}$ muscle. Although, interestingly, it was CM treatment that seemingly exacerbated ROS production in the $Ercc1^{d/-}$ Soleus, whereas, this provides a possible underlying cause. As mitochondrial dysfunction was also evident in the naturally-aged Soleus and EDL, these mechanisms of mitochondrial homeostasis and 'health', merit further investigation in both ageing and progeria, along with the assessment of any effects of CM treatment on these processes.

CM treatment in the $Ercc1^{d/-}$ Soleus

It was shown that with ADMSC CM treatment in the $Ercc1^{d/-}$ Soleus, as with the naturally-aged series of experiments, whole organism parameters such as body weight, grip strength and rotarod performance, as well as muscle weights and myofibre composition, CSA and oxidative capacity were not influenced. However, CM increased the proportion of type IIA myofibres, which could potentially indicate that CM prevented atrophy, or caused a myofibre switch to this faster, oxidative myofibre type. In both of these scenarios, alterations to motor neuron activity are inferred, as a prevention of myofibre loss in this myofibre type, would suggest that motor neuron degeneration may be reduced. Although possibly not sufficiently enough to maintain a full complement of myofibres, as total myofibre numbers were not significantly greater with CM treatment. Alternatively, a myofibre switch could indicate more successful re-innervation. However the reason for the switch to a faster phenotype remains unclear, as this kind of transition is often associated with disuse or muscle unloading. A recent study previously utilised an immunocytochemical protocol for bungarotoxin, to assess neuromuscular junction (NMJ) connectivity and showed that in naturally-aged geriatric animals, the percentage of fully denervated myofibres was drastically increased, in the EDL, but not in the Soleus (Chai et al. 2011). Interestingly, however, this could be a potential method to determine

Taryn Morash

the degree that motor neuron innervation is firstly diminished in $Ercc1^{d/-}$ muscles and potentially enhanced by CM treatment, if at all.

The other feature in the $Ercc1^{d/-}$ *Soleus* that appeared to be altered by ADMSC CM treatment, was an increased DHE intensity which indicated a higher level of O_2^- ROS production. This, as previously discussed, is seemingly counterintuitive for a potential therapy in a model of progeria, which would only exacerbate the damage through increased levels of oxidative stress. However, it is reasoned that CM treatment enhanced the rate of metabolism, using the 'faulty' machinery in the $Ercc1^{d/-}$ muscle and inadvertently, also increased O_2^- ROS generation, as a by-product of dysfunctional oxidative metabolism. Thus, as in the naturally-aged experimentation, ADMSC CM demonstrated that contents harboured could bring about alterations to features surrounding mitochondrial function, in agreement with the vast majority of targets identified in AFS CM (Mellows et al. 2017).

It was established that, despite the reduced muscle size and overall decreased grip strength reflecting features of sarcopenia, at this histological level, most other characteristics of myofibre composition, were not as dramatically affected in the $Ercc1^{d/-}$ *Soleus*. This however, is unexpected in a model of severe and rapid systemic decline. Although, as discussed, this could provide evidence for the initiation of a strong survival response, where resources are conserved to support protein maintenance. Therefore, it would be of great interest to explore the regulatory mechanisms of protein synthesis (IGF-1/PI3K/AKT/4E-BP) and degradation (FOXO/MuRF1/Atrogin-1), using both qPCR and western blot analysis, to provide a better understanding of this proposed shift.

It was found that the $Ercc1^{d/-}$ animals displayed characteristic parallels to the naturally-aged *Soleus* and these included oxidative capacity, ROS production and antioxidant activity, all features measured that reflect the metabolic status of the muscle. In contrast, those features that appeared to occur to a more extreme extent in the $Ercc1^{d/-}$ progeric *Soleus*, relative to natural ageing, encompassed a greater degree of myofibre atrophy, a dramatically reduced muscle weight, myofibre CSA, capillary density, collagen thickness and dystrophin expression. Therefore, the characteristics implicate altered myofibre composition and ECM components. Alternatively, it was established that the $Ercc1^{d/-}$ *Soleus* displayed an altogether distinctive MHC myofibre type composition, exhibiting an overall faster phenotype. While the $Ercc1^{d/-}$ *Soleus* was still a predominantly slow oxidative muscle, it contained significantly more type IIX and IIB myofibres than in natural ageing. As previously discussed, a transition in this direction, from slow to fast, is typically indicative of a more sedentary lifestyle through disuse. Measurements of rodent activity are frequently recorded utilising open field activity cage monitoring. For example, studies conducted in mice, have explored the effect of pre-clinical drugs in the *mdx* (DMD) mouse model on their activity, as well as in transgenic mice

Taryn Morash

modelling human inflammatory myopathies, such as autoimmune myositis (Spurney et al. 2009; Nagaraju et al. 2000). Therefore, activity cage monitoring would be a useful tool in determining the overall mobility of *Ercc1*$^{d/-}$ animals, compared to young control animals, as well as to naturally-aged activity. This provides general information regarding overall motility, distance travelled, high and low speed movement, rearing counts, among numerous other analyses. It is postulated that CM treatment improves overall mobility of the aged and progeric animals.

It was established that capillary density, collagen thickness and dystrophin expression were all reduced in the *Ercc1*$^{d/-}$ *Soleus*, however, this is unsurprising when the overall remarkably smaller muscle size is considered. Capillary density, collagen synthesis and structural membrane components are reportedly increased with compensatory hypertrophy, induced by exercise for example, in order to better serve the larger myofibre (Degens, Turek, et al. 1992; Yasuda et al. 1996; Yang et al. 1997; Kjær et al. 2009). Therefore, it is reasoned that smaller myofibres require a lower blood supply, basement membrane collagen IV and dystrophin content, 'scaled-down' proportionately to *Ercc1*$^{d/-}$ myofibre size.

In conclusion, the *Soleus* muscle profile, examining characteristics measured at a whole tissue level, reflects a number of features of sarcopenia observed in natural ageing. In contrast, however, the extreme nature of the *Ercc1*$^{d/-}$ mutant in the rapid accumulation of systemic DNA damage overall, results in some arguably amplified characteristics of decline. It is postulated that levels of deterioration in the *Ercc1*$^{d/-}$ mouse model would far exceed those of even the most moribund of naturally-aged animals, if enabled to survive to end-of-life. These findings show that, from an ageing skeletal muscle prospective, the amplified characteristics displayed as well as the strong switch to maintenance, establishes the *Ercc1*$^{d/-}$ mouse, as a 'super-ageing' model. Taken together, these findings potentially indicate that CM treatment efficacy may be distinctly different in progeria, compared to natural ageing, where seemingly beneficial alterations to the underlying regulatory mechanisms were observed and brought about pro-angiogenic, antioxidant and modified ECM effects in naturally-aged muscle. Whereas, comparatively, CM has had relatively little impact in the severe model of premature 'super-ageing'.

Investigation into the therapeutic effects of conditioned media on satellite cell number and mechanisms of function during natural ageing and in the *Ercc1*$^{d/-}$ model of progeria

The principle objective of this series of experimentation, extends the work carried out in the previous two chapters, to examine the potential beneficial paracrine-mediated regulatory effects of ADMSC CM on ageing skeletal muscle regenerative function. Subsequently, this experimental programme

Taryn Morash

was also carried out in the *Ercc1$^{d/-}$* progeric model to further explore its suitability as a natural ageing model at a cellular level. Importantly, therefore, investigation was conducted in order to assess the effects of ageing, with and without CM treatment, on the characteristics of the underlying mechanisms both intrinsic to the cell, as well as extrinsic interactions with the myofibre matrix.

It is well-established that the SC population experiences a decline in number and function with age and features of this trend are arguably attributable to changes in the intrinsic regulation of the cell itself or alternatively, alterations to the ageing skeletal muscle microenvironment or 'niche', or more likely, a combination of the two (Collins et al. 2007; Yin et al. 2013). Intrinsic features to the cell lead to a degree of heterogeneity in the population and these underpin the self-renewal, proliferative or myogenic differentiation potential of SCs. However, extrinsic signalling from numerous regulatory factors of the local myofibre and ECM niche, direct SCs to activate, emerge, migrate, proliferate and differentiate in response to muscle activity/exercise and crucially, following myofibre damage or injury.

In ageing muscle, SCs have been shown to activate and emerge in a delayed manner, as well as migrate via amoeboid-based motility, at a slower rate compared to young SCs (Collins-Hooper et al. 2012). However, the findings of the current study do not reflect these previously reported aspects of function, despite utilising the same analysis techniques and age-matched animals. Naturally-aged SCs in the present study alternatively, emerged at a seemingly advanced rate. However, young controls also did not reflect what has previously been reported, as young SCs showed an opposing delayed emergence. Furthermore, aged SCs in the current study did not parallel the delayed migration speed, previously reported by Collins-Hooper and colleagues (Collins-Hooper et al. 2012). It has been previously established that aged SCs demonstrated abnormal bleb dynamics, with a prolonged extension/retraction duration, which is believed to have had a detrimental effect on the rate of aged SC movement (Collins-Hooper et al. 2012). Thus, as migration speeds in aged SCs in the present study were unchanged to the young SCs, bleb dynamic measurements would provide a better understanding of this finding, as it could be hypothesised that bleb dynamics would appear statistically no different from the young controls.

Aged SCs did however, show a reduced proliferative capacity, which is in keeping with what has been reported extensively (Schultz & Lipton 1982; Collins et al. 2007; Collins-Hooper et al. 2012; Sousa-Victor et al. 2014; García-Prat et al. 2016). Therefore, these discrepancies suggest that intrinsically the underlying regulatory mechanisms of SC activity, particularly those that mediate emergence and migration, remain somewhat functional into old age. Perhaps with the exception of proliferative capacity, which infers greater intrinsic dysregulation with age and potentially, differentiation

Taryn Morash

capacity, which was untested in natural ageing, in the current series of experiments, but is extensively reported to diminish in aged SC populations. Moreover, this suggests that extrinsic signalling components may vary within our single myofibre experimental set-ups or depending on the dissection and single myofibre isolation, variation could be introduced. It is postulated that some components of the single myofibre culture media are ill defined. For example, varying levels of growth factors present in chick embryo extract as a media supplement. Indeed, any slight variability in culture conditions, could produce slightly different results, although in general, the method for single myofibre culture appears highly reproducible, so reasons behind these discrepancies remain unclear (Bischoff 1986b; Rosenblatt et al. 1995; Zammit 2002; Otto et al. 2011).

It was further established that ADMSC CM (*in vivo*) treatment, had seemingly beneficial effects on naturally-aged SC migration speeds as compared to all other age groups, rate of motility was drastically enhanced. Taken with what is known about the amoeboid/bleb-based migration method, continuation of this work will measure the CM effect on aged SC bleb dynamics (Collins-Hooper et al. 2012). As a prolonged bleb lifecycle was associated with a slower SC rate of movement, it could be postulated that the finding of a faster migration speed in aged SCs, would be supported by a more rapid bleb lifecycle. Furthermore, it has been shown that AFS CM harboured miRNA that are known to target and regulate cell motility (Mellows et al. 2017). Therefore, future work into elucidating the properties maintained by ADMSC CM utilised in the current study, may reveal similar regulatory components. However, it is reasoned that a faster migratory speed may not prove to be a beneficial property overall, if other aspects of motility are compromised, for example, directionality and appropriate response to stimuli (chemotaxis). Therefore, it would be of interest to test these features as future CM work, as directionality was demonstrated to be altered in aged SCs, using mathematical modelling, to show SCs adopted a 'memoryless' form of motility, which is believed to impact on the speed cells arrive at a lesion site for repair (Collins-Hooper et al. 2012). Continued work therefore, utilising mathematical modelling, could indicate if CM treatment is able to restore this defect in aged SCs. Additionally, Bischoff used a form of 'checkerboard' analysis, to create an *in vitro* gradient of a variety of growth factors and saw that SCs responded with positive chemotactic activity to HGF and TGF-β (Bischoff 1997). Furthermore, Johnstone and colleagues reported positive chemotactic activity in myoblasts treated with angiotensin II (Ang II), believed to function through actin organisation and MMP to initiate motility (Johnston et al. 2010). Therefore, future work investigating aged SCs response to stimuli to evoke motility (chemotaxis), would be of interest and these studies highlight potential factors and an analysis method that could be utilised.

Moreover, CM did not alter the other aspects of SC function in naturally-aged SCs, thus, emergence, morphologies and proliferation, were all shown to be largely unchanged by CM treatment.

Taryn Morash

Moreover, this could further suggest that the migratory feature of SC activity in old age, is reversible and more readily altered by extrinsic factor treatment. In contrast to the self-renewal, proliferative capacity which appears to be governed more strongly by the altered intrinsic properties that arise in aged SCs. Additionally, as this feature was restored in the studies conducted by Conboy and colleagues, but was not affected by the paracrine factors in CM in the present study, it could be postulated that the more constant delivery of rejuvenating factors in the serum via direct circulatory coupling was more influential in altering proliferative capacity, relative to the 8-week course of CM administration, once every 2 weeks. Therefore, more regular CM treatment may continue to observe potentially therapeutic effects on these currently unchanged SC processes.

In the $Ercc1^{d/-}$ SC populations however, along with a reduced proliferative capacity, in agreement with natural ageing trends, $Ercc1^{d/-}$ SCs migrated at a significantly increased rate, compared to the control SCs. As discussed previously, the ability to migrate at an advanced rate, to the lesion site, could be correlated with an expected faster rate of repair. However, it is reasoned that this would result in successful myofibre repair, only if firstly, the superficially positive effect on increased migration speed also comprises functional directionality and a response to damage stimuli and secondly, the subsequent SC mechanisms are fully functional (proliferation and differentiation). Therefore, additionally, it would be beneficial to also assess these features of migratory directionality in the $Ercc1^{d/-}$ SC population. $Ercc1^{d/-}$ SC morphologies were unchanged compared to controls. This indicated that both $Ercc1^{d/-}$ SC populations and the control SCs, were migrating using the amoeboid-based mechanism of motility, which is established as the preferred method adopted by SCs on myofibres (Otto et al. 2011). Surprisingly, however, the differentiation programme was not altered in the $Ercc1^{d/-}$ SCs. This does not reflect the findings of Lavasani and colleagues, who found that $Ercc1^{d/-}$ SC/progenitor cells exhibited reduced proliferative and differentiation capacity, both *in vitro* and *in vivo* (Lavasani et al. 2012). The reasons for this discrepancy are unknown, although it could be postulated that the *in vitro* system utilised in the current study, analyses SC function on the isolated single myofibre, as opposed to tissue culture plates used by Lavasani and colleagues. Thus, as it is known that the physical properties of the myofibre substrate, as well as the vast array of released signalling components, function to bring about alterations in regulation and subsequent behaviour of SCs, it can be suggested that the two culture methods would create variable results. However, this does not account for the reduced regenerative (proliferation and differentiation) effects seen in the $Ercc1^{d/-}$ muscles *in vivo*.

CM treatment in the $Ercc1^{d/-}$ animals resulted in a greater effect on the underlying mechanisms of SC function, compared to those underpinning the parameters measured at a tissue level, previously. Firstly, it was established that $Ercc1^{d/-}$ SCs were driven towards an advanced rate of emergence,

Taryn Morash

which is reasoned would be overall beneficial providing that as mentioned previously, the following SC processes function successfully to bring about repair. Interestingly, the decreased migration speed with CM treatment could indicate that indeed, the faster speed noted in $Ercc1^{d/-}$ control SCs may have been overall dysfunctional and CM treatment appears to have normalised this feature to those in the (+/+) control SCs. Further exploration into the directionality as well as bleb extension/retraction times, as previously mentioned would provide a better understanding of this finding. It is hypothesised that $Ercc1^{d/-}$ SCs, similarly to naturally-aged SCs, experience altered directionality and bleb dynamics leading to the findings of altered migration speeds, in this series of experiments. Moreover, as seen in the naturally-aged SCs, CM failed to increase proliferative capacity. This further implicates intrinsic mechanistic dysfunction impacting to a greater degree on this characteristic of SC activity. Furthermore, this provides further evidence that a strong survival response, driving regulation away from proliferation and growth, is evident at this cellular level in the $Ercc1^{d/-}$ model, thus sharing this feature with naturally-aged SCs. Moreover, it suggests that this intrinsic dysregulation may not be so easily overridden by CM treatment. Lastly, myogenic differentiation was shown to be delayed with CM treatment in both $Ercc1^{d/-}$ and the control SCs, with a larger proportion of cells maintaining Pax7, the maker of quiescence. It is reasoned that this would overall negatively impact regenerative ability, as a smaller proportion of the SC population progressed to express myogenin, towards terminal differentiation. However, as stem cell exhaustion is a key feature of ageing and the SC pool is known to become depleted with advancing age, this delay could indicate a proportion of the SC population that are down-regulating MyoD between T48 and 72 to revert back to a state of quiescence (Shefer et al. 2006; Nagata et al. 2006).

Overall, the underlying features of SC activity were observed to be variable in both natural ageing and progeric myofibre cultures, with a diminished proliferative capacity, common to both, as evidence of dysfunction. However, these findings provide a platform for further investigation into the effects of CM *in vivo* for example, in an acute injury model (cardiotoxin) and will determine how these alterations noted in the present study, impact on overall regenerative function in natural ageing and progeria.

Skeletal muscle myofibres promote non-muscle stem cells and non-stem cells to adopt myogenic characteristics

The hypotheses for this work focused on the central role of the myofibre microenvironment in determining the key features underlying SC function. It has been established that SCs migrate along myofibres utilising a distinctive amoeboid-based mechanism (Otto et al. 2011; Collins-Hooper et al. 2012). It was also postulated that the amoeboid-based mechanism of motility is a migratory option

Taryn Morash

available to all stem cells, not just SCs and that this characteristic is induced by contact with the myofibre surface.

Firstly, it was established that non-muscle stem cells (ADMSC, AFS and DP) and a non-stem cell (MDA) adopted a rounded morphology and migrated by the amoeboid-based form of motility and exhibited cell surface blebs. This finding demonstrates that these characteristics are not unique to the SC but instead, directed by the myofibre surface (Morash et al. 2017). Non-muscle myosin II has been established as a key component that exerts force through focal adhesion contacts, in order to sense matrix elasticity (Engler et al. 2006). Therefore, this could provide a mechanism in which the transplanted cell types are able to sense the myofibre elasticity and respond, by altering intrinsic regulation of cell motility. Furthermore, it was established that the key regulatory mechanisms directing methods of cell motility, Rac and Rho GTPase signalling were responsible for directing morphology in both SCs and non-muscle cells, indicating that this pathway is conserved in the differing cell types. Importantly, it was shown that despite all cells adopting the blebbing form of motility, it was not always accompanied by a faster migration speed (Morash et al. 2017). Bleb dynamics measurements have shown that aged SCs experience a prolonged bleb lifecycle and this is believed to be one of the contributing factors to an overall decreased migration speed (Collins-Hooper et al. 2012). Therefore, bleb dynamics measurements in the non-muscle cell types could provide a better understanding of this induced form of motility and the effect on the different cell speeds. It was also suggested that assembly and disassembly of focal adhesion contact apparatus, could also influence the speed at which these different cells travel (Nagano et al. 2012; Tozluoğlu et al. 2013; Charras & Paluch 2008). Furthermore, it is reported that the majority of the cell to ECM contact is maintained via the interaction of myofibre transmembrane receptors, as well as laminin, which is the predominant cell-adhesive protein found in the basement membrane (Mayer 2003). Staining the myofibre/non-muscle cell co-cultures for antibodies against laminin and integrin isoforms, could indicate how these cells are forming attachments with the myofibre and migrating. α7β1 integrin is the major integrin receptor located in skeletal muscle (α5β1 α6β1 are also present) which binds to laminin, facilitating SC motility, however there a multiple isoform variations (18 α and 8 β, with 24 different dimers) which results in variable substrate affinities (Mayer 2003; Siegel et al. 2009). It is known that SCs remodel their niche, in order to emerge and migrate to the lesion site. This is mediated mainly through the synthesis and secretion of MMP-2 and MMP-9 by SCs, that target collagen IV and laminin (Guérin & Holland 1995). With four differing cell types used in the present study, it could be reasoned that some cell types would have a higher affinity with the myofibre and remodel the ECM more effectively, relative to others. Additionally, future work would evaluate these adhesion and cell to ECM interactions to further understand the differences in the

Taryn Morash

different cell type response in speed, to the myofibre substrate, in both young and aged myofibre cultures.

A further finding was that similarly to observations on young myofibres, all cell types adopted a more rounded morphology on aged myofibres (Morash et al. 2017). This could indicate therefore, that despite the myofibre stiffening with age and the cells sensing this change in elasticity, it was not sufficient to affect the rounded morphology adopted, in any of the conditions. Importantly, SC morphologies nor migration speed, were altered on the aged myofibre, which could indicate a higher adaptability in the resident niche, compared to the non-muscle cells, all of which were affected by the age of the myofibre, in either the morphology adopted or migration speed, or both. Interestingly, all of the non-muscle cell types, but not the SC, showed evidence of regulatory effects of *in vitro* CM on morphology or migration, or both which further supports the higher plasticity of SC to cope with alterations in their own niche. It would be of interest to explore this plasticity in reverse by transplanting freshly isolated SCs into a non-muscle microenvironment, in order to examine migration, proliferation and differentiation potential. This could be achieved by utilising explant cultures, for those similar in origin of the cell types used in the current study. For example, dentin and umbilical cord matrix, which are both known to be a source of growth factors, similar to skeletal muscle including, FGF, IGF, TGF-β and VEGF, among others (Sloan et al. 2000; La Rocca et al. 2009). Although, there would be some technical concerns to address as far as visualising transplanted SC migration using a time-lapse microscope as a denser explant tissue for example, would not be easily viewable. As what makes single myofibre culture so feasible, is due to the translucency of the myofibres enables tracking of single cells. However, GFP[+] tracking using fluorescent time-lapse confocal microscopy could circumvent the issue.

Taken together, the findings of this study, highlight the importance of the myofibre microenvironment in regulating features of SC function, as well as the influence on the behaviour and fate of non-muscle cells. This series of experiments also indicates that SCs demonstrate a level of plasticity in response to changes within their niche and by taking physical features of the microenvironment into account, in ageing, injury and disease for example, stem cell therapies can potentially be better tailored to the host tissue for greater engraftment success. This work provides a basis for a wealth of future studies in the fields of stem cell and tissue engineering research.

Taryn Morash

Future work

Single myofibre experimentation

It would be of interest to the current study to continue this line of work by collecting the culture media and characterising the properties released from the myofibres in our single myofibre culture, from young and old ages, as well as that secreted from *Ercc1$^{d/-}$* progeric myofibres. It has been established that numerous growth factors are released from the SCs, as well as the myofibre ECM, that direct not only SC activity, but also many other interstitial cells, including fibroblasts, cells that constitute the vasculature and immune system, motor neurons, as well as adipocytes, for example. Common regulatory factors include HGF, bFGF, VEGF, IGF, Nitric oxide (NO), Delta/Jagged (Notch signalling) and it is widely-reported that changes in the regulation via these components alters with age (Yin et al. 2013). For example, Notch signalling has shown to be diminished in aged muscle which directly impacts on regenerative function as SC proliferation and cell fate determination, are reduced (Conboy et al. 2003; Brack et al. 2007). However, Conboy and colleagues subsequently, showed that exposure to circulatory factors in young serum, restored Notch signalling in aged animals and enhanced SC regenerative function (Conboy et al. 2003; Conboy et al. 2005). Importantly, this indicates that dysfunctional reparative regulation in aged SCs is reversible. Additionally, this raises further questions concerning the target of the rejuvenating factors present in young serum, whether alterations in underlying mechanisms are achieved by targeting the SCs, or the myofibre ECM, or both. Further experimentation therefore, could include the generation of conditioned media from myofibre cultures, as well as isolated SC cultures from young and old animals and test the regenerative potential, via a paracrine effect. Firstly, by treating an acute (Naja pallida) cardiotoxin (CTX) injury model *in vivo*, in the *Tibialis anterior* (TA) and analysing the percentage of regenerative myofibres within 3 and 6 days post-injury, as well as the pro-angiogenic and macrophage infiltration activity, with each developed CM, as previously observed with AFS CM (Mellows et al. 2017). Secondly, the different CM could be used along with the senescence assay, utilised to test the efficacy of the ADMSC CM in the present study, to assess the potential of myofibre/SC-released paracrine effects in the protection against senescence. Other *in vitro* assays are currently being developed to test CM by colleagues and include a fibroblast migration/wound closure assay, to examine regulatory impact on migration, as well as differentiation assays to examine adipo-, osteo- and chondrogenic lineage specification.

Moreover, it is established that the skeletal muscle myofibre substrate and surrounding ECM becomes stiffer with age and this has been attributed to the increased deposition and enzymatic cross-linking of ECM components by interstitial cells such as fibroblasts (Marshall et al. 1989;

Taryn Morash

Zimmerman et al. 1993; Haus et al. 2007). This not only impacts on overall muscle contractility, but is also believed to alter SC to ECM interactions (Garg & Boppart 2016; Lacraz et al. 2015). The work in this chapter studied the features of resident SC function and behaviour in young and old conditions. It would therefore be of interest to further clarify whether these alterations in SC activity originate predominantly with the age-related changes in the SC, or the ageing myofibre microenvironment. This could be achieved through the separate dissociation of the resident young and aged SC populations from their myofibres and subsequently heterochronically co-culture young SCs with old myofibre and old SCs with young myofibres and repeat SC analyses as carried out in this series of experimentation. Although, it has been established that the myofibre is able to heavily influence non-muscle cells to adopt SC characteristics (ADMSC, AFS, DP, MDA) and direct towards a myogenic lineage and fuse to form myotubes (AFS) (Morash et al. 2017). Thus, this finding indicates that the physical properties of the myofibre surface are able to elicit remarkable alterations in transplanted cells and therefore provides evidence that the myofibre plays a defining role in cellular activity.

Further investigations into the ECM could explain the observation of reduced grip strength in both naturally-aged and progeric animals. As glycation-related cross-linking of intramuscular connective tissue, has been implicated in altered force-generating capacity with age. It would be of interest to investigate this feature further in both naturally-aged and $Ercc1^{d/-}$ muscle. Ramamurthy and Larsson used an anti-AGE immunofluorescence confocal microscopy protocol to identify intracellular and sarcolemmal protein glycation (Ramamurthy & Larsson 2013). It was found that myosin is also glycated, in both type I and type II myofibres, of young and aged rat *Soleus* and EDL muscles. Additionally, the greatest concentration of AGEs were located intracellularly in the aged *Soleus*. Moreover, generation of irreversible AGEs, is believed to be mediated by free radical oxidation, of which production is well-defined in mitochondrial dysfunction with age (Avigad et al. 1996; Pieczenik & Neustadt 2007). Continued work in the current study will examine the accumulation of AGEs in the *Soleus* and EDL muscles of naturally-aged and $Ercc1^{d/-}$ animals, with and without *in vivo* ADMSC CM treatment. It is postulated that CM will prevent the build-up of age-associated AGEs.

$Ercc1^{d/-}$ progeric and natural ageing experimentation

In order to use the findings of the current study and extend both the naturally-aged and progeric experimentation forward, it will be essential to examine the overall regenerative capacity of the $Ercc1^{d/-}$ model at a tissue level, utilising the CTX induced-injury model, comparatively the same will be carried out in naturally-aged animals. Following the same protocol as that carried out by Mellows and colleagues, the ability of $Ercc1^{d/-}$ SCs to carry out the renewal of whole, fully functional, innervated and vascularised contractile myofibres will be assessed and compared to that of naturally-

Taryn Morash

aged tissue. Histologically, CD31 analysis, as carried out in previous chapters will identify capillarisation. F4/80 staining for macrophages, responsible for the phagocytosis of dead myofibre contents and cellular debris, will indicate the initiation and extent of an inflammatory response. Embryonic myosin (MHC-3) staining along with the presence of centrally-located nuclei will identify those myofibres that are undergoing regeneration (Mellows et al. 2017). A further hypothesis that will in turn, be investigated is that ADMSC CM treatment will enhance the regenerative capacity of the $Ercc1^{d/-}$ and naturally-aged muscle following CTX injury. In this experimentation, TA muscles will be primed with ADMSC CM, administered via the tail vein, prior to intramuscular (IM) CTX injections (Mellows et al. 2017).

Furthermore, extended investigations in both the naturally-aged and $Ercc1^{d/-}$ progeric experimentation, would include more comprehensive functional testing. It is essential that force-generating capacity be assessed for comparison between natural ageing and progeria. It is hypothesised that the 'super-ageing' features of the $Ercc1^{d/-}$ mice would lead to a reduced maximal isometric tetanic force compared to young controls and naturally-aged muscles. A second hypothesis would be that ADMSC CM enhances maximal tetanic force in naturally-aged and $Ercc1^{d/-}$ muscles. This could be achieved by measuring the maximal isometric tetanic force of limb musculature and recording this relative to muscle weight and CSA, using an isometric force transducer (Degens & Alway 2003). Similarly, muscle fatigue could also be measured in this way and these features would provide a more detailed understanding of whether the strength exerted by the $Ercc1^{d/-}$ muscles, is proportionate to its reduced size. It has been established that in naturally-aged rat $Plantaris$ muscles, following compensatory hypertrophy, the lowest tetanic force was that exerted by 25-month old muscles and was highest in those at 13-months old (Degens et al. 1993). Similarly, the mass and maximal tetanic force diminished by approximately 30% between the ages of 9 and 26 months (Degens & Alway 2003). Further investigation could measure the maximal tetanic force and fatigue of treadmill-trained $Ercc1^{d/-}$ and naturally-aged muscles in order to characterise and compare the hypertrophic response to endurance training in the $Ercc1^{d/-}$ model. These experiments can also encompass cohorts treated with ADMSC CM in $vivo$ as in the current study, to test any therapeutic effects of CM on functionality with age and in progeria.

As the $Ercc1^{d/-}$ model has demonstrated a severely reduced muscle mass, it would be of interest to test not only the ability of the $Ercc1^{d/-}$ musculature to undergo hypertrophy 'naturally', following high levels of exercise training, or surgically, to induce compensatory hypertrophy, but pharmacologically. This can be achieved through the inhibition of the negative regulators of skeletal muscle growth, including myostatin, by using a soluble form of the Activin type IIB receptor (sActRIIB). Treatment of normal and mdx mice has demonstrated rapid muscle growth and increases in absolute maximal

Taryn Morash

force, of the EDL and *Soleus* and therefore, the myostatin/activin signalling pathway has been identified as a potential therapeutic target in combating sarcopenia in old age (Relizani et al. 2014).

Properties of conditioned media

Although, the current study demonstrates that ADMSC CM harbours properties impacting on various characteristics of ageing skeletal muscle, the focus of these analyses was not to determine specific regulatory components. However, by characterising the features that are altered by CM treatment, in the current study, the first insights into its therapeutic potential in ageing and progeria, are assessed. Therefore, the most immediate future work for the continuation of project will be to determine the specific content of ADMSC CM, defining the signalling mechanisms and their broad cellular process targets. Microarray analysis, as carried out by colleagues with the AFS CM, to determine the mechanistic properties of the ADMSC CM would begin with isolating the extracellular vesicle (EV) fraction, forming the two distinct types of CM, the whole CM (as used in this study) and just the isolated EV fraction, through ultracentrifugation. This is because colleagues and others have observed distinct differences in the contents of each fraction (Mellows et al. 2017; Le Bihan et al. 2012). Alternatively to qPCR and western blot analysis, of specific pathway components, global analyses of interest to determine the properties of ADMSC CM would include Luminex multi-analyte profiling (MAP) technology to screen CM for cytokines and growth factors (Oliver et al. 1998). Gel-free nano-flow LC-MS/MS analysis and 2-dimensional gel electrophoresis (2DGE) and LC-MS/MS analysis. Additionally, computational sieving following RNA or protein identification can be a useful tool to predict reliable subcellular localisation of protein content, as well as bioinformatics approach in the evaluation of specific functional profiles of secreted factors (Le Bihan et al. 2012). Additionally, as EVs are membrane-bound vesicles, these can be stained using a fluorescent cell linker (PKH26) and used in a cell culture assay, to visualise the cellular uptake of ADMSC EVs (Mellows et al. 2017).

Cell transplantation future experimentation

Based on the findings of the non-muscle cell transplantation series of experimentation, a future investigation would involve the transplantation of the non-muscle cells types onto the single myofibres of the *Ercc1*$^{d/-}$ progeric mouse, in order to assess the extrinsic and physical properties of the progeric 'super-ageing' model, with and without CM treatment, to compare to both the naturally-aged cell transplantation experiment, as well as young findings. Taken with the findings of the previous experimentation, it is postulated that the physical myofibre environment will be further altered in the *Ercc1*$^{d/-}$ muscle and therefore, cell to ECM communications will be further affected, in turn, impacting on observed cell behaviour. Furthermore, it is hypothesised that the *Ercc1*$^{d/-}$ myofibres matrix, may not elicit the same proliferative capacity and myogenic specification of

Taryn Morash

transplanted cells as these characteristics were most affected in resident SC populations, observed in this study.

One of the most remarkable findings of the current study was that a non-muscle stem cell (AFS) and a non-stem cell (MDA) were induced towards a myogenic lineage (MyoD$^+$) through contact with the myofibre surface and strikingly, the AFS cells went on to fuse to produce MHC$^+$ myotubes. Importantly, this finding opens up further avenues of experimentation, particularly in the fields of stem cell therapy and tissue engineering for the treatment of human injury and disease, as well as age-related decline. Additionally, this highlights the clinical potential of AFS cells to be more extensively researched for these applications but does not rule out the continuation to test more non-muscle cell types for similar properties in a myofibre set-up.

Firstly, these findings indicate that cells can be more successfully cultured *in vitro* by initially priming them to the relevant physiological elasticities, prior to administration into damaged tissues (Engler et al. 2004). It was shown that introduction of mesenchymal stem cells into a stiffening fibrotic infarct region in the heart resulted in cellular expression of myocyte markers. However, differentiation was halted and cells failed to assemble functional contractile apparatuses (Shake et al. 2002). Additionally, myoblast cultures are known to undergo fusion to form myotubes which can be observed *in vitro* (Bischoff & Holtzer 1970). However, contractile actin/myosin striations were evident only in the myotube cultures mimicking the passive stiffness typical of normal muscle (Young's modulus, *E* ~12 kPa) (Engler et al. 2004). On substrates with much softer or stiffer elasticities, for example on surfaces akin to soft fibroblast cell layers or those representing stiffened dystrophic muscle, myotubes did not become striated. Thus, these findings indicate that there is a seemingly narrow window of optimum substrate elasticity that will therefore support successful, functional myogenic differentiation (Engler et al. 2004). Therefore, in understanding the specific physiological state and elasticity of the tissue matrix *in vivo*, culture conditions can be customised to that specific tissue, whilst taking into account features such as fibrosis or differences in age, so that stem cell introduction and processes of repair are more successful. However, further work would be required in order to assess the effects of the well-defined complications of a lack of diffuse migration away from the point of administration and high levels of rapid cell death (Briggs & Morgan 2013; Yin et al. 2013; Péault et al. 2007). Although, with the cells having first been primed to the tissue conditions, the expectation would be that the occurrence of these complications would be less. Alternatively, 3-dimensional (3D) scaffold matrices either allogeneic, xenogeneic in origin or artificially-generated from biomaterials or moving away from these approaches to used synthetic constructs (Perniconi et al. 2011; Crapo et al. 2011; Porzionato et al. 2015; Carnio et al. 2011; Manchineella et al. 2016). Carnio and colleagues created a 3D collagen porous scaffold seeded with

Taryn Morash

WT myogenic precursor cells and implanted this into the TA muscles of normal and *mdx* mice. It was shown that scaffold-delivered precursors exhibited lower apoptosis, higher proliferation and yielded better dystrophin restoration that contralateral intramuscular injections of precursor cells (Carnio et al. 2011). Future work could examine the engraftment potential of AFS and other stem cells, primed *in vitro* to the physiological elasticity of muscle (~12 kPa), using decellularisation techniques on myofibre or whole tissue scaffolds. Similarly, taken with the other findings of this work, the importance of the microenvironment on cellular reparative function and the evidence that CM treatment can alter features of the ECM having a predominant effect over suspected intrinsic regulation. Primed whole stem cell-based approaches, along with ADMSC or AFS-generated CM as a combination treatment, could act to also prime the microenvironment of the injury/disease site. This is reasoned through the recent findings that AFS CM harboured miRNA and other molecules, that were found to function on the already existing signalling machinery, in not just the resident stem cell populations to carry out regeneration within the tissue, but on the cells of the supporting tissue (Mellows et al. 2017).

Key to the contractility of muscle cells is excitation-contraction (EC) coupling. This is the physiological mechanism which involves the transformation of an electrical signal sensed by the dihydropyridine receptor (DHPR) located on the transverse tubules (T tubules), into a chemical gradient, through Ca^{2+} increase by activation of the ryanodine receptor (RyR) located on the sarcoplasmic reticulum (SR). Investigation into the ultrastructural, biochemical and cellular properties of EC has been studied using isolated single myofibres however, more recent success has arisen from the use of immortalised myoblast cultures from human muscle biopsies (Ravenscroft et al. 2007; Calderón et al. 2009; Rokach et al. 2013). Rokach and colleagues have characterised the EC machinery using an immortalised human muscle cell line to demonstrate that the cells retain expression of essential mRNA and protein components of EC apparatus including CSQ, SERCA (1 and 2), $Ca_v1.1$, RyR1 and DHPR (Rokach et al. 2013). Next, they determined the cellular localisation, using super resolution structured illumination microscopy (3D-SIM), of these proteins, as EC functionality is highly-dependent on the organisation in the T tubules (DHPR) and terminal cisternae of the SR (RyR). Finally, they confirmed that these human myoblast cells displayed a normal response to membrane de-polarisation using voltage/patch-clamping to measure Ca^{2+} release. This work presents the methodology key to examining the physiological mechanism of EC, which defines functional differentiation of an immortalised cell line into myotubes. This methodology will be used in future experimentation of the present study, to apply to the MHC[+] AFS myotube cultures following co-culture on the myofibre surface. This can be used to determine the presence of the vital EC component organisation and Ca^{2+} release, in AFS myotube cultures and thereby, will potentially re-

Taryn Morash

define these originally non-muscle cells, as 'functional' muscle cells. A further extension to this work would then follow to test the regenerative and engraftment potential of the AFS cells, directed by the myofibre to a myogenic lineage. This can be achieved with transplantation into immunodeficient mice lacking competition from resident SCs/myoblasts, which is also a common method carried out to test novel immortal SC lines and in myoblast transplantation experiments using mdx null mice (Muses et al. 2011; Cooper et al. 2001; Huard et al. 1994).

Taryn Morash

Summary

This is the first report, to my knowledge, that characterises the skeletal muscle phenotype in a novel use of the $Ercc1^{d/-}$ mutant model of progeria. I show that the growth of $Ercc1^{d/-}$ hindlimb musculature is stunted and the muscles are supported by fewer capillaries per myofibre, while almost all other parameters analysed, remained proportionate and unchanged to the control. Furthermore, with the novel use of CM treatment in the $Ercc1^{d/-}$ animals however, unlike in the naturally-aged *Soleus*, CM had very little effect, indicating a slight shift to a faster myofibre phenotype, with an increase in type IIA myofibres. I report here that rather counterintuitively, for a potential treatment against age-related decline, an increase in O_2^- ROS production was further exacerbated by CM treatment. I reason that this may be indicative of an enhanced rate of oxidative metabolism targeted by CM properties, in a model where metabolic machinery is 'faulty'. Importantly, these findings indicate that CM treatment has a lower efficacy in altering myofibre composition and function in the $Ercc1^{d/-}$ *Soleus* muscle, compared to natural ageing. This suggests that in this model of severe DNA damage accumulation, CM may not be a beneficial therapeutic approach. However, these findings also provide a platform for future studies into alternative CM approaches, for example, investigating more frequent CM delivery, alternative stem cell sources of CM, or the exploration of engineering EVs to be used as a therapeutic drug-delivery system. Alternative research focused on preventing muscle wasting, could for example, involve the inhibition of Myostatin using a soluble activin type IIB receptor, to induce muscle growth in the $Ercc1^{d/-}$ determine their capacity for muscle hypertrophy and examine the effects on composition and contractile function.

At a cellular level, in naturally-aged SC populations I report that seemingly beneficial effects of CM on rate of motility, as an underlying mechanism of SC regenerative function and cellular turnover. Suggesting that the migratory characteristic of SC activity may be more readily altered by extrinsic factor treatment, than the other aspects of function. I show that $Ercc1^{d/-}$ SC populations, migrated at a faster rate whereas CM treatment normalised this faster migration speed. I reason that a faster rate may not necessarily be indicative of improved regenerative function in this model or even in natural ageing, as other components such as bleb dynamics, ECM communication and SC measures of directionality could also be influencing this behaviour. In naturally-aged and $Ercc1^{d/-}$ SC populations, proliferative capacity is reduced, akin with previous studies and I show that ADMSC CM (*in vivo*) treatment, was not able to restore this function. Furthermore, unlike the general agreement of previous studies in natural ageing, I report that $Ercc1^{d/-}$ SC differentiation potential is normal. Whereas, I show that CM treatment resulted in the maintenance of Pax7 expression in a large proportion of SCs, thereby delaying or reducing the progression to terminal differentiation.

Taryn Morash

I report a comparison between the underlying mechanisms of function in both $Ercc1^{d/-}$ and naturally-aged SCs. I show that the $Ercc1^{d/-}$ SC emergence trend is much more indicative of that which occurs in young healthy SCs, as there was a discrepancy in the (advancement of) emergence in aged SCs in the present study, compared to others where this feature was delayed. I report that the increase in $Ercc1^{d/-}$ SC migration is significantly greater than old SCs but not geriatric SCs. Furthermore, I report that SC $Ercc1^{d/-}$ morphology and proliferation mimicked natural ageing. These findings suggest that $Ercc1^{d/-}$ and naturally-aged SC behaviour is variable when directly compared and further work is required to understand the discrepancies between the opposing effects of CM on SC migration. Although, it should be noted that there are both intrinsic and extrinsic components governing these results and further work is required to study the differences in physical properties of the $Ercc1^{d/-}$ and naturally-aged myofibre, as well as the local signalling components of each. However, importantly, for SC self-renewal and proliferation, both $Ercc1^{d/-}$ and naturally-aged SCs show a reduced potential, thus, the $Ercc1^{d/-}$ model does hold some potential for further work into enhancing this aspect of SC function. Overall, I reason that while the impacts on SC function in both natural ageing and progeria appeared variable, dysfunction of one or more of the underlying mechanisms would lead to altered regenerative effects. However, this work provides a basis for further studies examining $Ercc1^{d/-}$ and aged SC function as well as CM treatment, *in vivo* using an induced injury model, for example, cardiotoxin. This will provide a better understanding of how the alterations to the mechanisms shown here, are impacting overall regenerative function.

Furthermore, the importance of the skeletal muscle myofibre microenvironment in determining key features underlying SC function, was established. I show here that it is the myofibre surface that directs SC amoeboid-based form of motility. Furthermore, all non-muscle cell types, once in contact with the myofibre, adopt a rounded morphology and migrated by the bleb-based mechanism. Thus, demonstrating that these features are not unique intrinsic characteristics of SCs and are mediated through contact with the myofibre and are not always accompanied by an increase in velocity.

It is shown that while all cell types adopted a rounded morphology on aged myofibres, resident SCs demonstrated a higher level of adaptability to the aged environment than the transplanted non-muscle cells. Additionally, SC morphology and migration speeds were not affected by age nor CM treatment. Whereas, all non-muscle cells indicated variations in morphology and speed with age and or CM. This indicates that there may be intrinsic differences between the SCs and non-muscle cells, within the myofibre microenvironment, that determines their response to the combination of physical properties of the matrix, as well as exogenous signalling, for example, mediated by a CM paracrine effect. I also show that there could be more potent effects of *in vivo* administration of CM treatment in comparison to its addition to myofibre cultures *in vitro*, an important feature for the

Taryn Morash

development of CM as a therapeutic treatment. Furthermore, I show that the same underlying molecular pathways are responsible for directing the cell morphologies of both SCs and non-muscle cells on myofibres.

Most remarkably, I show that a non-muscle stem cell (AFS) and a non-stem cell (MDA), following 10 days co-culture on the surface of myofibres, adopted a myogenic fate. Importantly, I also show that AFS cells, but not the non-stem cell (MDA), were directed through contact with the muscle microenvironment, to fuse and form MHC$^+$ myotubes. This reinforces the therapeutic potential of AFS cells and highlights the importance of the tissue matrix in the success of whole stem cell-based and tissue engineering-based therapies. Further work will aim to determine whether co-cultured myogenic AFS cells present aspects of functional excitation-contraction coupling, challenging the current thinking of what can broadly be defined as muscle.

This study has provided an extensive investigation into the effects of ADMSC CM on key physiological, histochemical, morphometric and biochemical alterations associated with the onset and progression of sarcopenia in naturally-aged and progeric mice. I show here that, at a whole organism and tissue level, while CM treatment in aged animals did not appear to influence overall characteristic alterations to muscle function, as measured by grip strength and myofibre composition, such as myofibre number, size or MHC types, well-defined in sarcopenia, in neither the *Soleus*, nor the EDL. CM treatment did, however, demonstrate beneficial regulatory effects in mediating the signalling involved with the enhancement of angiogenesis and oxidative metabolism, while reducing O_2^- ROS production and collagen thickness, which importantly, appears to attenuate any further decline. These alterations observed can instead be considered as key to the support and maintenance of healthy ageing skeletal muscle and the slowing down of age-associated deterioration. This could also facilitate improved overall fitness and health as the observed beneficial effects are unlikely to impact on skeletal muscle alone, but are hypothesised to improve function tissue-wide due to the systemic administration of CM. For example, increased angiogenesis in the brain, would result in enhanced neurotrophic factor networks therefore, maintaining neuron health and cognitive function into old age. Thus, these global benefits of CM in ageing individuals involve the systemic regulation of mechanisms underpinning the nine hallmarks of ageing, such as mediation of mitochondrial function and oxidative stress, energy and nutrient sensing and delivery, prevention of cellular senescence and stem cell exhaustion, enhanced cell to cell and cell to ECM communication, into advancing age, postulated to delay overall deterioration.

Furthermore, I report a comparison between both *Ercc1$^{d/-}$* and naturally-aged *Soleus* muscle phenotypes. Indicative of a strong shift of resources away from growth and protein synthesis,

Taryn Morash

towards maintenance and preservation of genomic and cellular integrity. I show that the *Ercc1*$^{d/-}$ model is one of 'super-ageing'. Thus, far exceeding levels of deterioration reached in 'normal' ageing, such as a greatly reduced muscle mass, myofibre atrophy, myofibre CSA, capillary density, collagen IV thickness and dystrophin expression. However, in such an acute model of tissue-wide DNA damage accumulation, these mice demonstrate that remarkably, through this switch to maintenance, they have initiated a programme of slowing down the progression of deterioration, concerned with preserving survival as a priority. Therefore, the 'super-ageing' description encompasses the ability of the *Ercc1*$^{d/-}$ mice to launch this survival programme, functioning above and delaying the natural progression of age-associated decline. This model therefore, can be used to provide insights into the regulation behind this 'super-ageing' maintenance programme, including those pathways associated with prolonged longevity, such as IGF-1, to investigate further in human ageing. For example, the genetic and stochastic events that lead to overall natural systemic deterioration in humans, also appears to be mediated more successfully in a subset of the elderly population that live a prolonged lifespan, including centenarians (over 100 years old) and supercentenarians (over 110 years old). Thus, it could be reasoned that these extremely aged individuals maintain the ability, through factors relating to genetics and/or lifestyle, to deploy a similar survival response, enabling the systemic slowing of natural ageing progression.

Taryn Morash

References

Afanas'ev, I., 2010. Signaling and Damaging Functions of Free Radicals in Aging-Free Radical Theory, Hormesis, and TOR. *Aging and disease*, 1, pp.75–88.

Ahn, J., Sanz-Moreno, V. & Marshall, C.J., 2012. The metastasis gene NEDD9 product acts through integrin β3 and Src to promote mesenchymal motility and inhibit amoeboid motility. *Journal of cell science*, 125(Pt 7), pp.1814–26.

Aiello, A. et al., 2017. Nutrient sensing pathways as therapeutic targets for healthy ageing. *Expert Opinion on Therapeutic Targets*, 21(4), pp.371–380.

Alberts, B. et al., 2008. *Molecular Biology Of The Cell* 5th ed., New York: Garland Science.

Allen, D.L. et al., 2001. Cardiac and skeletal muscle adaptations to voluntary wheel running in the mouse. *Journal of applied physiology (Bethesda, Md. : 1985)*, 90(5), pp.1900–1908.

Allen, R.E. et al., 1995. Hepatocyte growth factor activates quiescent skeletal muscle satellite cells in vitro. *Journal of cellular physiology*, 165(2), pp.307–12.

Allen, R.E. & Boxhorn, L.K., 1989. Regulation of skeletal muscle satellite cell proliferation and differentiation by transforming growth factor-beta, insulin-like growth factor I, and fibroblast growth factor. *Journal of cellular physiology*, 138(2), pp.311–315.

Alnaqeeb, M. a & Goldspink, G., 1987. Changes in fibre type, number and diameter in developing and ageing skeletal muscle. *Journal of anatomy*, 153(1962), pp.31–45.

Alnaqeeb, M. a, Al Zaid, N.S. & Goldspink, G., 1984. Connective tissue changes and physical properties of developing and ageing skeletal muscle. *Journal of anatomy*, 139 (Pt 4, pp.677–689.

Alway, S.E. et al., 1996. Muscle torque in young and older untrained and endurance-trained men. *Journal of Gerontology: Biological Sciences*, 51A(3), pp.B195–B201.

Amthor, H. et al., 1998. The importance of timing differentiation during limb muscle development. *Current biology : CB*, 8(11), pp.642–652.

Andersen, P. & Henriksson, J., 1977. Training Induced Changes in the Subgroups of Human Type II Skeletal Muscle Fibres. *Acta Physiologica Scandinavica*, 99(1), pp.123–125.

Ansved, T. & Larsson, L., 1989. Effects of ageing on enzyme-histochemical, morphometrical and contractile properties of the soleus muscle in the rat. *Journal of the Neurological Sciences*, 93(1), pp.105–124.

Ardoin, S.P., Shanahan, J.C. & Pisetsky, D.S., 2007. The role of microparticles in inflammation and thrombosis. *Scandinavian Journal of Immunology*, 66, pp.159–165.

Ariano, M. a, Armstrong, R.B. & Edgerton, V.R., 1973. Hindlimb muscle fiber populations of five mammals. *The journal of histochemistry and cytochemistry : official journal of the Histochemistry Society*, 21(1), pp.51–55.

Taryn Morash

Armstrong, R.B. et al., 1987. Distribution of blood flow in muscles of miniature swine during exercise. *Journal of Applied Physiology Bethesda Md 1985*, 62(3), pp.1285–1298.

Armstrong, R.B. et al., 1982. Distribution of fiber types in locomotory muscles of dogs. *American Journal of Anatomy*, 163(1), pp.87–98.

Armstrong, R.B. & Phelps, R.O., 1984. Muscle fiber type composition of the rat hindlimb. *American Journal of Anatomy*, 171(3), pp.259–272.

Arnesen, S.M. & Lawson, M.A., 2006. Age-related changes in focal adhesions lead to altered cell behavior in tendon fibroblasts. *Mechanisms of Ageing and Development*, 127(9), pp.726–732.

Artavanis-Tsakonas, S., Rand, M.D. & Lake, R.J., 1999. Notch signaling: cell fate control and signal integration in development. *Science (New York, N.Y.)*, 284(5415), pp.770–776.

Asakura, A., Rudnicki, M.A. & Komaki, M., 2001. Muscle satellite cells are multipotential stem cells that exhibit myogenic, osteogenic, and adipogenic differentiation. *Differentiation*, 68(4–5), pp.245–253.

Avigad, G., Kniep, A. & Bailin, G., 1996. Reaction of rabbit skeletal myosin with D-glucose 6-phosphate. *Biochem Mol Biol Int*, 40(2), pp.273–284.

Baar, K. et al., 2002. Adaptations of skeletal muscle to exercise: rapid increase in the transcriptional coactivator PGC-1. *The FASEB journal : official publication of the Federation of American Societies for Experimental Biology*, 16(14), pp.1879–86.

Baar, K., 2006. Training for endurance and strength: Lessons from cell signaling. In *Medicine and Science in Sports and Exercise*. pp. 1939–1944.

Baglio, S.R., Pegtel, D.M. & Baldini, N., 2012. Mesenchymal stem cell secreted vesicles provide novel opportunities in (stem) cell-free therapy. *Frontiers in Physiology*, 3 SEP(September), pp.1–11.

Bajek, A. et al., 2016. Adipose-Derived Stem Cells as a Tool in Cell-Based Therapies. *Archivum Immunologiae et Therapiae Experimentalis*, 64(6), pp.443–454.

Bani, C. et al., 2008. Pattern of metalloprotease activity and myofiber regeneration in skeletal muscles of mdx mice. *Muscle and Nerve*, 37(5), pp.583–592.

Bark, T.H. et al., 1998. Increased protein synthesis after acute IGF-I or insulin infusion is localized to muscle in mice. *The American journal of physiology*, 275(17), pp.E118–E123.

Barnouin, Y. et al., 2017. Coupling between skeletal muscle fiber size and capillarization is maintained during healthy aging. *Journal of Cachexia, Sarcopenia and Muscle*, 8(4), pp.647–659.

Barns, M. et al., 2014. Molecular analyses provide insight into mechanisms underlying sarcopenia and myofibre denervation in old skeletal muscles of mice. *The international journal of biochemistry & cell biology*, 53, pp.174–85.

Bartke, A., 2005. Role of the growth hormone/insulin-like growth factor system in mammalian aging. *Endocrinology*, 146(9), pp.3718–3723.

Bartoli, M. & Richard, I., 2005. Calpains in muscle wasting. *International Journal of Biochemistry and Cell*

Taryn Morash

Biology, 37(10 SPEC. ISS.), pp.2115–2133.

Barton-Davis, E.R., Shoturma, D.I. & Sweeney, H.L., 1999. Contribution of satellite cells to IGF-I induced hypertrophy of skeletal muscle. In *Acta Physiologica Scandinavica*. pp. 301–305.

Bassel-Duby, R. & Olson, E.N., 2006. Signaling Pathways in Skeletal Muscle Remodeling. *Annual Review of Biochemistry*, 75(1), pp.19–37.

Baumgartner, R.N., 2000. Body composition in healthy aging. *Ann N Y Acad Sci*, 904, pp.437–448.

Baumgartner, R.N. et al., 1998. Epidemiology of sarcopenia among the elderly in New Mexico. *American journal of epidemiology*, 147(8), pp.755–63.

Beauchamp, J.R. et al., 2000. Expression of CD34 and Myf5 defines the majority of quiescent adult skeletal muscle satellite cells. *Journal of Cell Biology*, 151, pp.1221–1233.

Bechet, D. et al., 2005. Lysosomal proteolysis in skeletal muscle. *International Journal of Biochemistry and Cell Biology*, 37(10 SPEC. ISS.), pp.2098–2114.

Beckman, K.B. & Ames, B.N., 1998. The free radical theory of aging matures. *Physiological reviews*, 78(2), pp.547–581.

Bell, M.A. & Ball, M.J., 1990. Neuritic plaques and vessels of visual cortex in aging and Alzheimer's dementia. *Neurobiology of Aging*, 11(4), pp.359–370.

Ben-Yair, R., 2005. Lineage analysis of the avian dermomyotome sheet reveals the existence of single cells with both dermal and muscle progenitor fates. *Development*, 132(4), pp.689–701.

Bergert, M. et al., 2012. Cell mechanics control rapid transitions between blebs and lamellipodia during migration. *Proceedings of the National Academy of Sciences*, 109(36), pp.14434–14439.

Bernstein, C. et al., 2013. Epigenetic field defects in progression to cancer. *World journal of gastrointestinal oncology*, 5, pp.43–9.

Bertolotto, A. et al., 1983. Laminin and fibronectin distribution in normal and pathological human muscle. *Journal of the neurological sciences*, 60(3), pp.377–82.

Bhang, S.H. et al., 2014. Efficacious and clinically relevant conditioned medium of human adipose-derived stem cells for therapeutic angiogenesis. *Molecular therapy : the journal of the American Society of Gene Therapy*, 22(4), pp.862–72.

Le Bihan, M.-C. et al., 2012. In-depth analysis of the secretome identifies three major independent secretory pathways in differentiating human myoblasts. *Journal of proteomics*, 77, pp.344–56.

Bischoff, R., 1986a. A satellite cell mitogen from crushed adult muscle. *Developmental Biology*, 115(1), pp.140–147.

Bischoff, R., 1997. Chemotaxis of skeletal muscle satellite cells. *Developmental dynamics : an official publication of the American Association of Anatomists*, 208(4), pp.505–15.

Bischoff, R., 1990. Interaction between satellite cells and skeletal muscle fibers. *Development (Cambridge, England)*, 109, pp.943–952.

Taryn Morash

Bischoff, R., 1986b. Proliferation of muscle satellite cells on intact myofibers in culture. *Developmental Biology*, 115(1), pp.129–139.

Bischoff, R., 1975. Regeneration of single skeletal muscle fibers in vitro. *The Anatomical Record*, 182(2), pp.215–235.

Bischoff, R., 2004. *Satellite and stem cells in muscle regeneration* Myology Vo. C. Engel, A.G., Franzini-Armstrong, ed., New York: McGraw- Hill.

Bischoff, R. & Holtzer, H., 1970. Inhibition of myoblast fusion after one round of dna synthesis in 5-bromodeoxyuridine. *Journal of Cell Biology*, 44(1), pp.134–150.

Bjorksten, J. & Tenhu, H., 1990. The crosslinking theory of aging--added evidence. *Experimental gerontology*, 25(2), pp.91–5.

Bjornson, C.R.R. et al., 2012. Notch signaling is necessary to maintain quiescence in adult muscle stem cells. *Stem Cells*, 30(2), pp.232–242.

Boa, B.C.S. et al., 2017. Exercise effects on perivascular adipose tissue: Endocrine and paracrine determinants of vascular function. *British Journal of Pharmacology*.

Borgesius, N.Z. et al., 2011. Accelerated age-related cognitive decline and neurodegeneration, caused by deficient DNA repair. *The Journal of neuroscience : the official journal of the Society for Neuroscience*, 31(35), pp.12543–12553.

Brack, A.S. et al., 2008. A Temporal Switch from Notch to Wnt Signaling in Muscle Stem Cells Is Necessary for Normal Adult Myogenesis. *Cell Stem Cell*, 2(1), pp.50–59.

Brack, A.S. et al., 2007. Increased Wnt signaling during aging alters muscle stem cell fate and increases fibrosis. *Science (New York, N.Y.)*, 317(5839), pp.807–10.

Briggs, D. & Morgan, J.E., 2013. Recent progress in satellite cell/myoblast engraftment - Relevance for therapy. *FEBS Journal*, 280, pp.4281–4293.

Brodal, P., 2010. *The Central Nervous System*, Oxford University Press.

Brooks, S. V & Faulkner, J.A., 1991. Maximum and sustained power of extensor digitorum longus muscles from young, adult, and old mice. *J Gerontol*, 46(1), pp.B28-33.

Bruusgaard, J.C., Liestøl, K. & Gundersen, K., 2006. Distribution of myonuclei and microtubules in live muscle fibers of young, middle-aged, and old mice. *Journal of Applied Physiology*, 100(6), pp.2024–2030.

Bryant, R.A. & Nix, D.P., 2012. *Acute & Chronic Wounds: Current Management Concepts* R. A. Bryant & D. P. Nix, eds., Elsevier Health Sciences.

Bua, E. a et al., 2002. Mitochondrial abnormalities are more frequent in muscles undergoing sarcopenia. *Journal of applied physiology (Bethesda, Md. : 1985)*, 92(February 2002), pp.2617–2624.

Buller, A.J., Eccles, J.C. & Eccles, R.M., 1960. Differentiation of Fast and Slow Muscles in the Cat Hind Limb. *J. Physiol*, 150, pp.399–416.

Taryn Morash

Burke, R.E. et al., 1973. Physiological types and histochemical profiles in motor units of the cat gastrocnemius. *The Journal of physiology*, 234(3), pp.723–748.

Burke, R.E., Levine, D.N. & Zajac, F.E., 1971. Mammalian motor units: physiological-histochemical correlation in three types in cat gastrocnemius. *Science (New York, N.Y.)*, 174(4010), pp.709–12.

Burkin, D.J. & Kaufman, S.J., 1999. The alpha7beta1 integrin in muscle development and disease. *Cell Tissue Res*, 296(1), pp.183–190.

Burtner, C.R. & Kennedy, B.K., 2010. Progeria syndromes and ageing: what is the connection? *Nature reviews. Molecular cell biology*, 11(8), pp.567–78.

Burton, L.A. & Sumukadas, D., 2010. Optimal management of sarcopenia. *Clinical interventions in aging*, 5, pp.217–28.

Bustelo, X.R., Sauzeau, V. & Berenjeno, I.M., 2007. GTP-binding proteins of the Rho/Rac family: regulation, effectors and functions in vivo. *BioEssays : news and reviews in molecular, cellular and developmental biology*, 29(4), pp.356–70.

Butala, P. et al., 2012. Zmpste24-/- mouse model for senescent wound healing research. *Plastic and reconstructive surgery*, 130(6), p.788e–798e.

Caiozzo, V.J., Baker, M.J. & Baldwin, K.M., 1998. Novel transitions in MHC isoforms: separate and combined effects of thyroid hormone and mechanical unloading. *J Appl Physiol*, 85(8750–7587), pp.2237–2248.

Calderón, J.C. et al., 2009. Different fibre populations distinguished by their calcium transient characteristics in enzymatically dissociated murine flexor digitorum brevis and soleus muscles. *Journal of Muscle Research and Cell Motility*, 30(3–4), pp.125–137.

Calvo, F. et al., 2011. RasGRF suppresses Cdc42-mediated tumour cell movement, cytoskeletal dynamics and transformation. *Nature cell biology*, 13(7), pp.819–26.

Campbell, N.A., 2008. *Biology* 8th ed., San Francisco: Pearson.

Camussi, G. et al., 2010. Exosomes/microvesicles as a mechanism of cell-to-cell communication. *Kidney international*, 78(9), pp.838–848.

Cananzi, M., Atala, A. & De Coppi, P., 2009. Stem cells derived from amniotic fluid: new potentials in regenerative medicine. *Reproductive BioMedicine Online*, 18, pp.17–27.

Candas, D. & Li, J.J., 2014. MnSOD in Oxidative Stress Response-Potential Regulation *via* Mitochondrial Protein Influx. *Antioxidants & Redox Signaling*, 20(10), pp.1599–1617.

Cantinieaux, D. et al., 2013. Conditioned medium from bone marrow-derived mesenchymal stem cells improves recovery after spinal cord injury in rats: an original strategy to avoid cell transplantation. *PloS one*, 8(8), p.e69515.

Caplan, A.I., 2007. Adult mesenchymal stem cells for tissue engineering versus regenerative medicine. *Journal of cellular physiology*, 213(2), pp.341–7.

Taryn Morash

Carlson, B.M. et al., 2001. Skeletal muscle regeneration in very old rats. *The journals of gerontology. Series A, Biological sciences and medical sciences*, 56(5), pp.B224–B233.

Carlson, B.M. & Faulkner, J.A., 1989. Muscle transplantation between young and old rats: age of host determines recovery. *The American journal of physiology*, 256(6 Pt 1), pp.C1262-6.

Carmeli, E. et al., 2004. Matrix metalloproteinases and skeletal muscle: A brief review. *Muscle & Nerve*, 29(2), pp.191–197.

Carnio, S. et al., 2011. Three-dimensional porous scaffold allows long-term wild-type cell delivery in dystrophic muscle. *Journal of Tissue Engineering and Regenerative Medicine*, 5(1), pp.1–10.

Cartee, G.D. et al., 1996. Growth hormone supplementation increases skeletal muscle mass of old male Fischer 344/brown Norway rats. *The journals of gerontology. Series A, Biological sciences and medical sciences*, 51(3), pp.B214-9.

Cesari, M. et al., 2006. Frailty syndrome and skeletal muscle: Results from the Invecchiare in Chianti study. *American Journal of Clinical Nutrition*, 83(5), pp.1142–1148.

Chai, R.J. et al., 2011. Striking denervation of neuromuscular junctions without lumbar motoneuron loss in geriatric mouse muscle. *PloS one*, 6(12), p.e28090.

Chang, C.-P. et al., 2013. Hypoxic preconditioning enhances the therapeutic potential of the secretome from cultured human mesenchymal stem cells in experimental traumatic brain injury. *Clinical science (London, England : 1979)*, 124(3), pp.165–76.

Chang, H. et al., 2009. Generation of transplantable, functional satellite-like cells from mouse embryonic stem cells. *FASEB journal : official publication of the Federation of American Societies for Experimental Biology*, 23(6), pp.1907–19.

Chardin, P., 1988. The ras superfamily proteins. *Biochimie*, 70(7), pp.865–8.

Charras, G. & Paluch, E., 2008. Blebs lead the way: how to migrate without lamellipodia. *Nature Reviews Molecular Cell Biology*, 9(9), pp.730–736.

Charras, G.T. et al., 2005. Non-equilibration of hydrostatic pressure in blebbing cells. *Nature*, 435(7040), pp.365–9.

Chavez, K.J., Garimella, S. V. & Lipkowitz, S., 2010. Triple negative breast cancer cell lines: One tool in the search for better treatment of triple negative breast cancer. *Breast Disease*, 32(1–2), pp.35–48.

Cheung, T.H. et al., 2012. Maintenance of muscle stem-cell quiescence by microRNA-489. *Nature*, 482(7386), pp.524–528.

Cheung, T.H. & Rando, T. a, 2013. Molecular regulation of stem cell quiescence. *Nature reviews. Molecular cell biology*, 14(June), pp.329–40.

Chin, E.R. et al., 1998. A calcineurin-dependent transcriptional pathway controls skeletal muscle fiber type. *Genes & development*, 12(16), pp.2499–509.

Cho, Y.J. et al., 2012. Therapeutic effects of human adipose stem cell-conditioned medium on stroke.

Taryn Morash

Journal of neuroscience research, 90(9), pp.1794–802.

Christopoulos, D. et al., 1989. Pathogenesis of venous ulceration in relation to the calf muscle pump function. *Surgery*, 106(5), pp.829–35.

Clark, R.K., 2005. *Anatomy and Physiology: Understanding the Human Body*, Jones & Bartlett Learning.

Clement, R.S., Carter, P.M. & Kipke, D.R., 2002. Measuring the electrical stapedius reflex with stapedius muscle electromyogram recordings. *Annals of Biomedical Engineering*, 30(2), pp.169–179.

Coelho, P. et al., 2017. Adipocyte Secretome Increases Radioresistance of Malignant Melanocytes by Improving Cell Survival and Decreasing Oxidative Status. *RADIATION RESEARCH Radiat. Res*, 187(187), pp.0–0.

Collart-Dutilleul, P.-Y. et al., 2015. Allogenic banking of dental pulp stem cells for innovative therapeutics. *World journal of stem cells*, 7(7), pp.1010–21.

Collins-Hooper, H. et al., 2012. Age-related changes in speed and mechanism of adult skeletal muscle stem cell migration. *Stem Cells*, 30(44), pp.1182–1195.

Collins, C.A. et al., 2007. A population of myogenic stem cells that survives skeletal muscle aging. *Stem cells (Dayton, Ohio)*, 25(4), pp.885–94.

Collins, C.A., 2006. Satellite cell self-renewal. *Current Opinion in Pharmacology*, 6(3), pp.301–306.

Conboy, I.M. et al., 2003. Notch-mediated restoration of regenerative potential to aged muscle. *Science (New York, N.Y.)*, 302(November), pp.1575–1577.

Conboy, I.M. et al., 2005. Rejuvenation of aged progenitor cells by exposure to a young systemic environment. *Nature*, 433(February), pp.760–764.

Conboy, I.M. & Rando, T.A., 2002. The regulation of Notch signaling controls satellite cell activation and cell fate determination in postnatal myogenesis. *Developmental cell*, 3(3), pp.397–409.

Conboy, M.J., Conboy, I.M. & Rando, T.A., 2013. Heterochronic parabiosis: historical perspective and methodological considerations for studies of aging and longevity. *Aging cell*, 12(3), pp.525–30.

Condé-Green, A. et al., 2016. Fat Grafting and Adipose-Derived Regenerative Cells in Burn Wound Healing and Scarring. *Plastic and Reconstructive Surgery*, 137(1), pp.302–312.

Condic, M.L. & Rao, M., 2010. Alternative sources of pluripotent stem cells: ethical and scientific issues revisited. *Stem cells and development*, 19(8), pp.1121–9.

Cooper, R.N. et al., 2001. A New Immunodeficient Mouse Model for Human Myoblast Transplantation. *Human Gene Therapy*, 12(7), pp.823–831.

Cooper, R.N. et al., 1999. In vivo satellite cell activation via Myf5 and MyoD in regenerating mouse skeletal muscle. *Journal of cell science*, 112 (Pt 1, pp.2895–2901.

De Coppi, P. et al., 2006. Rosiglitazone modifies the adipogenic potential of human muscle satellite cells. *Diabetologia*, 49(8), pp.1962–73.

Taryn Morash

Cornelison, D.D. & Wold, B.J., 1997. Single-cell analysis of regulatory gene expression in quiescent and activated mouse skeletal muscle satellite cells. *Developmental biology*, 191(2), pp.270–283.

Crapo, P.M., Gilbert, T.W. & Badylak, S.F., 2011. An overview of tissue and whole organ decellularization processes. *Biomaterials*, 32(12), pp.3233–3243.

Croley, A.N. et al., 2005. Lower capillarization, VEGF protein, and VEGF mRNA response to acute exercise in the vastus lateralis muscle of aged vs. young women. *Journal of applied physiology (Bethesda, Md. : 1985)*, 99(5), pp.1872–9.

Cross, M.J. & Claesson-Welsh, L., 2001. FGF and VEGF function in angiogenesis: Signalling pathways, biological responses and therapeutic inhibition. *Trends in Pharmacological Sciences*, 22(4), pp.201–207.

Davies, K.J.A. et al., 1982. Free radicals and tissue damage produced by exercise. *Biochemical and Biophysical Research Communications*, 107(4), pp.1198–1205.

Degens, H., 2007. Age-related skeletal muscle dysfunction: Causes and mechanisms. In *Journal of Musculoskeletal Neuronal Interactions*. pp. 246–252.

Degens, H., Turek, Z., et al., 1993. Capillarisation and fibre types in hypertrophied m. plantaris in rats of various ages. *Respiration Physiology*, 94(2), pp.217–226.

Degens, H., Veerkamp, J.H., et al., 1993. Metabolic capacity, fibre type area and capillarization of rat plantaris muscle. Effects of age, overload and training and relationship with fatigue resistance. *International Journal of Biochemistry*, 25(8), pp.1141–1148.

Degens, H. et al., 1992. The relationship between capillarisation and fibre types during compensatory hypertrophy of the plantaris muscle in the rat. *Journal of anatomy*, 180 (Pt 3, pp.455–63.

Degens, H. & Alway, S.E., 2003. Skeletal muscle function and hypertrophy are diminished in old age. *Muscle and Nerve*, 27(3), pp.339–347.

Degens, H., Turek, Z. & Binkhorst, R.A., 1993. Compensatory hypertrophy and training effects on the functioning of ageing rat M. plantaris. *Mechanisms of Ageing and Development*, 66(3), pp.299–311.

Delp, M.D. & Duan, C., 1996. Composition and size of type I, IIA, IID/X, and IIB fibers and citrate synthase activity of rat muscle. *Journal of applied physiology (Bethesda, Md. : 1985)*, 80(1), pp.261–270.

Demontis, F. et al., 2013. Mechanisms of skeletal muscle aging: insights from Drosophila and mammalian models. *Disease models & mechanisms*, 6, pp.1339–52.

DeNardi, C., 1993. Type 2X-myosin heavy chain is coded by a muscle fiber type-specific and developmentally regulated gene. *The Journal of Cell Biology*, 123(4), pp.823–835.

Dimri, G.P. et al., 1995. A biomarker that identifies senescent human cells in culture and in aging skin in vivo. *Proceedings of the National Academy of Sciences of the United States of America*, 92(20), pp.9363–7.

Doherty, T.J., 2003. Invited review: Aging and sarcopenia. *Journal of applied physiology (Bethesda, Md. : 1985)*, 95(4), pp.1717–27.

Taryn Morash

Dollé, M.E.T. et al., 2011. Broad segmental progeroid changes in short-lived Ercc1(-/Δ7) mice. *Pathobiology of aging & age related diseases*, 1.

Dollé, M.E.T. et al., 2006. Increased genomic instability is not a prerequisite for shortened lifespan in DNA repair deficient mice. *Mutation Research - Fundamental and Molecular Mechanisms of Mutagenesis*, 596, pp.22–35.

Domenighetti, A.A. et al., 2014. Loss of FHL1 induces an age-dependent skeletal muscle myopathy associated with myofibrillar and intermyofibrillar disorganization in mice. *Human Molecular Genetics*, 23(1), pp.209–225.

Duan, Y. et al., 2017. Metabolic control of myofibers: promising therapeutic target for obesity and type 2 diabetes. *Obesity Reviews*, 18(6), pp.647–659.

Dupont-Versteegden, E.E., 2005. Apoptosis in muscle atrophy: Relevance to sarcopenia. *Experimental Gerontology*, 40(6), pp.473–481.

Dupont-Versteegden, E.E., 2006. Apoptosis in skeletal muscle and its relevance to atrophy. *World Journal of Gastroenterology*, 12(46), pp.7463–7466.

E, L., Burns, J.M. & Swerdlow, R.H., 2014. Effect of high-intensity exercise on aged mouse brain mitochondria, neurogenesis, and inflammation. *Neurobiology of aging*, 35(11), pp.2574–2583.

Eden, S. et al., 2002. Mechanism of regulation of WAVE1-induced actin nucleation by Rac1 and Nck. *Nature*, 418(6899), pp.790–3.

Egerman, M.A. et al., 2015. GDF11 Increases with Age and Inhibits Skeletal Muscle Regeneration. *Cell Metabolism*, 22(1), pp.164–174.

Elashry, M.I. et al., 2017. The effect of caloric restriction on the forelimb skeletal muscle fibers of the hypertrophic myostatin null mice. *Acta Histochemica*.

Engler, A.J. et al., 2006. Matrix Elasticity Directs Stem Cell Lineage Specification. *Cell*, 126, pp.677–689.

Engler, A.J. et al., 2004. Myotubes differentiate optimally on substrates with tissue-like stiffness: Pathological implications for soft or stiff microenvironments. *Journal of Cell Biology*, 166(6), pp.877–887.

Engvall, E. et al., 1990. Distribution and isolation of four laminin variants; tissue restricted distribution of heterotrimers assembled from five different subunits. *Cell regulation*, 1(10), pp.731–40.

Faber, R.M. et al., 2014. Myofiber branching rather than myofiber hyperplasia contributes to muscle hypertrophy in mdx mice. *Skeletal Muscle*, 4(1), p.10.

Fahlstrom, A. et al., 2011. Behavioral changes in aging female C57BL/6 mice. *Neurobiology of aging*, 32(10), pp.1868–1880.

Fang, E.F. et al., 2014. Defective mitophagy in XPA via PARP-1 hyperactivation and NAD +/SIRT1 reduction. *Cell*, 157(4), pp.882–896.

Fang, E.F. et al., 2016. Nuclear DNA damage signalling to mitochondria in ageing. *Nature Reviews*

Taryn Morash

Molecular Cell Biology, 17(5), pp.308–321.

Faulkner, J.A. & Brooks, S. V, 1995. Muscle fatigue in old animals. Unique aspects of fatigue in elderly humans. *Advances in experimental medicine and biology*, 384, pp.471–80.

Feng, Z. et al., 2005. The coordinate regulation of the p53 and mTOR pathways in cells. *Proceedings of the National Academy of Sciences*, 102(23), pp.8204–8209.

Ferreira, R. et al., 2010. Subsarcolemmal and intermyofibrillar mitochondria proteome differences disclose functional specializations in skeletal muscle. *Proteomics*, 10(17), pp.3142–3154.

Fitts, R.H., Nagle, F.J. & Cassens, R.G., 1974. The adaptation of myoglobin with age and training and its relationship to the three fiber types of skeletal muscle in miniature pig. *European Journal of Applied Physiology and Occupational Physiology*, 33(4), pp.275–284.

Floss, T., Arnold, H.H. & Braun, T., 1997. A role for FGF-6 in skeletal muscle regeneration. *Genes and Development*, 11(16), pp.2040–2051.

Frank, S. et al., 2001. The Role of Dynamin-Related Protein 1, a Mediator of Mitochondrial Fission, in Apoptosis. *Developmental Cell*, 1(4), pp.515–525.

Franz, T. et al., 1993. The Splotch mutation interferes with muscle development in the limbs. *Anatomy and Embryology*, 187(2), pp.153–160.

Frontera, W.R. et al., 2008. Muscle fiber size and function in elderly humans: a longitudinal study. *Journal of applied physiology (Bethesda, Md. : 1985)*, 105(2), pp.637–42.

Frontera, W.R. & Ochala, J., 2015. Skeletal Muscle: A Brief Review of Structure and Function. *Calcified Tissue International*, 96(3), pp.183–195.

Fuentes, I., Cobos, a R. & Segade, L. a, 1998. Muscle fibre types and their distribution in the biceps and triceps brachii of the rat and rabbit. *Journal of anatomy*, 192 (Pt 2, pp.203–210.

Funk, W.D., Ouellette, M. & Wright, W.E., 1991. Molecular biology of myogenic regulatory factors. *Molecular biology & medicine*, 8(2), pp.185–95.

Gallagher, D. et al., 2009. Adipose tissue distribution is different in type 2 diabetes. *The American journal of clinical nutrition*, 89(3), pp.807–14.

Gao, Y. et al., 2008. Age-related changes in the mechanical properties of the epimysium in skeletal muscles of rats. *Journal of Biomechanics*, 41(2), pp.465–469.

Garber, K., 2016. No longer going to waste. *Nature Biotechnology*, 34(5), pp.458–461.

García-Prat, L. et al., 2016. Autophagy maintains stemness by preventing senescence. *Nature*, 529(7584), pp.37–42.

Garcia-Roves, P.M. et al., 2008. Gain-of-function R225Q mutation in AMP-activated protein kinase γ3 subunit increases mitochondrial biogenesis in glycolytic skeletal muscle. *Journal of Biological Chemistry*, 283(51), pp.35724–35734.

Garg, A., Peshock, R.M. & Fleckenstein, J.L., 1999. Adipose tissue distribution pattern in patients with

Taryn Morash

familial partial lipodystrophy (Dunnigan variety). *The Journal of clinical endocrinology and metabolism*, 84, pp.170–174.

Garg, K. & Boppart, M.D., 2016. Influence of Exercise and Aging on Extracellular Matrix Composition in the Skeletal Muscle Stem Cell Niche. *Journal of applied physiology (Bethesda, Md. : 1985)*, p.jap.00594.2016.

Garinis, G.A. et al., 2008. DNA damage and ageing: new-age ideas for an age-old problem. *Nature cell biology*, 10(11), pp.1241–1247.

Gibson, B.A. & Kraus, W.L., 2012. New insights into the molecular and cellular functions of poly(ADP-ribose) and PARPs. *Nature Reviews Molecular Cell Biology*, 13(7), pp.411–424.

Gilbert, L. et al., 2002. Expression of the osteoblast differentiation factor RUNX2 (Cbfa1/AML3/Pebp2alpha A) is inhibited by tumor necrosis factor-alpha. *The Journal of biological chemistry*, 277(4), pp.2695–701.

Gilbert, P.M. et al., 2010. Substrate Elasticity Regulates Skeletal Muscle Stem Cell Self-Renewal in Culture. *Science*, 329(5995), pp.1078–1081.

Gilbert, P.M. et al., 2010. Substrate elasticity regulates skeletal muscle stem cell self-renewal in culture. *Science (New York, N.Y.)*, 329(2010), pp.1078–1081.

Gladyshev, T. V. & Gladyshev, V.N., 2016. A Disease or Not a Disease? Aging As a Pathology. *Trends in Molecular Medicine*, 22(12), pp.995–996.

Glass, D.J., 2005. Skeletal muscle hypertrophy and atrophy signaling pathways. *Int J Biochem Cell Biol*, 37(10), pp.1974–84.

Glatt, V. et al., 2007. Age-Related Changes in Trabecular Architecture Differ in Female and Male C57BL/6J Mice. *Journal of Bone and Mineral Research*, 22(8), pp.1197–1207.

Gokhin, D.S. et al., 2008. Quantitative analysis of neonatal skeletal muscle functional improvement in the mouse. *The Journal of experimental biology*, 211(Pt 6), pp.837–43.

Golding, J.P. et al., 2007. Skeletal muscle stem cells express anti-apoptotic ErbB receptors during activation from quiescence. *Experimental Cell Research*, 313(2), pp.341–356.

Goldspink, G., 1999. Changes in muscle mass and phenotype and the expression of autocrine and systemic growth factors by muscle in response to stretch and overload. *Journal of anatomy*, 194 (Pt 3, pp.323–34.

Goley, E.D. et al., 2004. Critical conformational changes in the Arp2/3 complex are induced by nucleotide and nucleation promoting factor. *Molecular cell*, 16(2), pp.269–79.

Gomez-Cabrera, M.-C. et al., 2005. Decreasing xanthine oxidase-mediated oxidative stress prevents useful cellular adaptations to exercise in rats. *The Journal of Physiology*, 567(1), pp.113–120.

Gosselin, L.E. et al., 1998. Effect of exercise training on passive stiffness in locomotor skeletal muscle: role of extracellular matrix. *Journal of applied physiology (Bethesda, Md. : 1985)*, 85(3), pp.1011–1016.

Taryn Morash

Goulding, M., Lumsden, A. & Paquette, a J., 1994. Regulation of Pax-3 expression in the dermomyotome and its role in muscle development. *Development (Cambridge, England)*, 120(4), pp.957–971.

Goulding, M.D. et al., 1991. Pax-3, a novel murine DNA binding protein expressed during early neurogenesis. *The EMBO journal*, 10(5), pp.1135–47.

Green, H.J. et al., 1979. Fiber composition, fiber size and enzyme activities in vastus lateralis of elite athletes involved in high intensity exercise. *European Journal of Applied Physiology and Occupational Physiology*, 41(2), pp.109–117.

Green, K., Brand, M.D. & Murphy, M.P., 2004. Prevention of Mitochondrial Oxidative Damage As A Therapeutic Strategy in Diabetes. In *Diabetes*.

Grimby, G. et al., 1984. Is there a change in relative muscle fibre composition with age? *Clinical Physiology*, 4(2), pp.189–194.

Groen, B.B.L. et al., 2014. Skeletal muscle capillary density and microvascular function are compromised with aging and type 2 diabetes. *Journal of Applied Physiology*, 116(8), pp.998–1005.

Gros, J. et al., 2005. A common somitic origin for embryonic muscle progenitors and satellite cells. *Nature*, 435(7044), pp.954–958.

Grounds, M.D. et al., 1992. Identification of skeletal muscle precursor cells in vivo by use of MyoD1 and myogenin probes. *Cell & Tissue Research*, 267(1), pp.99–104.

Grounds, M.D., 2014. Therapies for sarcopenia and regeneration of old skeletal muscles: more a case of old tissue architecture than old stem cells. *Bioarchitecture*, 4(3), pp.81–87.

Guérin, C.W. & Holland, P.C., 1995. Synthesis and secretion of matrix-degrading metalloproteases by human skeletal muscle satellite cells. *Developmental dynamics : an official publication of the American Association of Anatomists*, 202(1), pp.91–99.

Gulati, A.K., Reddi, A.H. & Zalewski, A.A., 1982. Distribution of fibronectin in normal and regenerating skeletal muscle. *The Anatomical record*, 204(3), pp.175–83.

Gullberg, D., Tiger, C.F. & Velling, T., 1999. Laminins during muscle development and in muscular dystrophies. *Cellular and molecular life sciences : CMLS*, 56(5–6), pp.442–60.

Gundersen, K., 2011. Excitation-transcription coupling in skeletal muscle: The molecular pathways of exercise. *Biological Reviews*, 86(3), pp.564–600.

Gutmann, E. & Carlson, B.M., 1976. Regeneration and transplantation of muscles in old rats and between young and old rats. *Life Sciences*, 18(1), pp.109–114.

von Haehling, S., Morley, J.E. & Anker, S.D., 2010. An overview of sarcopenia: facts and numbers on prevalence and clinical impact. *Journal of cachexia, sarcopenia and muscle*, 1(2), pp.129–133.

Hagege, A.A. et al., 2001. Regeneration of the myocardium: a new role in the treatment of ischemic heart disease? *Hypertension*, 38(6), pp.1413–1415.

Halloran, B.P. et al., 2002. Changes in bone structure and mass with advancing age in the male C57BL/6J

Taryn Morash

mouse. *Journal of bone and mineral research : the official journal of the American Society for Bone and Mineral Research*, 17(6), pp.1044–50.

Hämäläinen, N. & Pette, D., 1993. The histochemical profiles of fast fiber types IIB, IID, and IIA in skeletal muscles of mouse, rat, and rabbit. *The journal of histochemistry and cytochemistry : official journal of the Histochemistry Society*, 41(5), pp.733–743.

Hamrick, M.W., McGee-Lawrence, M.E. & Frechette, D.M., 2016. Fatty Infiltration of Skeletal Muscle: Mechanisms and Comparisons with Bone Marrow Adiposity. *Frontiers in Endocrinology*, 7.

Hanahan, D. & Weinberg, R.A., 2000. The hallmarks of cancer. *Cell*, 100(1), pp.57–70.

Harman, D., 1956. Aging: a theory based on free radical and radiation chemistry. *Journal of gerontology*, 11(3), pp.298–300.

Harrell, J.C. et al., 2014. Endothelial-like properties of claudin-low breast cancer cells promote tumor vascular permeability and metastasis. *Clinical and Experimental Metastasis*, 31(1), pp.33–45.

Haus, J.M. et al., 2007. Collagen , cross-linking , and advanced glycation end products in aging human skeletal muscle. *Journal of applied physiology (Bethesda, Md. : 1985)*, 47306(6), pp.2068–2076.

Hauschka, P. V, 1986. Osteocalcin: the vitamin K-dependent Ca2+-binding protein of bone matrix. *Haemostasis*, 16(3–4), pp.258–72.

Hetrick, B. et al., 2013. Small molecules CK-666 and CK-869 inhibit actin-related protein 2/3 complex by blocking an activating conformational change. *Chemistry and Biology*, 20(5), pp.701–712.

Hickey, M.S. et al., 1995. Skeletal muscle fiber composition is related to adiposity and in vitro glucose transport rate in humans. *The American journal of physiology*, 268(3 Pt 1), pp.E453–E457.

Hindman, B. et al., 2015. Non-muscle myosin II isoforms have different functions in matrix rearrangement by MDA-MB-231 cells. *PLoS ONE*, 10(7).

Hitachi, K. & Tsuchida, K., 2014. Role of microRNAs in skeletal muscle hypertrophy. *Frontiers in Physiology*, 4 JAN.

Hoeijmakers, J.H.J., 2009. DNA damage, aging, and cancer. *The New England journal of medicine*, 361(15), pp.1475–85.

Holloszy, J.O., 1967. Biochemical Adaptations in Muscle. *The Journal of biological chemistry*, 242(9), pp.2278–2282.

Höök, P. et al., 1999. In vitro motility speed of slow myosin extracted from single soleus fibres from young and old rats. *Journal of Physiology*, 520(2), pp.463–471.

Horton, M.J. et al., 2001. Abundant expression of myosin heavy-chain IIB RNA in a subset of human masseter muscle fibres. *Archives of Oral Biology*, 46(11), pp.1039–1050.

Huard, J. et al., 1994. High efficiency of muscle regeneration after human myoblast clone transplantation in SCID mice. *Journal of Clinical Investigation*, 93(2), pp.586–599.

Hulbert, A.J. et al., 2007. Life and death: metabolic rate, membrane composition, and life span of animals.

Taryn Morash

Physiological reviews, 87(4), pp.1175–213.

Hussain, S.P. et al., 2004. p53-Induced Up-Regulation of MnSOD and GPx but not Catalase Increases Oxidative Stress and Apoptosis. *Cancer Research*, 64(7), pp.2350–2356.

Inbar, O., Kaiser, P. & Tesch, P., 1981. Relationships between Leg Muscle Fiber Type Distribution and Leg Exercise Performance. *International Journal of Sports Medicine*, 2(3), pp.154–159.

Inoue, T. et al., 2013. Stem cells from human exfoliated deciduous tooth-derived conditioned medium enhance recovery of focal cerebral ischemia in rats. *Tissue engineering. Part A*, 19(1–2), pp.24–9.

Itahana, K., Campisi, J. & Dimri, G.P., 2007. Methods to detect biomarkers of cellular senescence: the senescence-associated beta-galactosidase assay. *Methods in molecular biology (Clifton, N.J.)*, 371, pp.21–31.

Jaffe, A.B. & Hall, A., 2005. Rho GTPases: biochemistry and biology. *Annual review of cell and developmental biology*, 21, pp.247–69.

Janssen, I. et al., 2000. Skeletal muscle mass and distribution in 468 men and women aged 18–88 yr. *Journal of Applied Physiology*, 89(1), pp.81–88.

Janssen, I. et al., 2004. The Healthcare Costs of Sarcopenia in the United States. *Journal of the American Geriatrics Society*, 52(1), pp.80–85.

Jaweed, M.M., Herbison, G.J. & Ditunno, J.F., 1977. Myosin ATPase activity after strengthening exercise. *Journal of Anatomy*, 124(Pt 2), pp.371–81.

Jenkins, D.D. et al., 2003. Tissue engineering and regenerative medicine. *Clinics in Plastic Surgery*, 30(4), pp.581–588.

Ji, L.L. et al., 2004. Acute exercise activates nuclear factor (NF)-{kappa}B signaling pathway in rat skeletal muscle. *The FASEB Journal*, 18(13), pp.1499–1506.

Jiang, Y. et al., 2015. Aged-related changes in body composition and association between body composition with bone mass density by body mass index in Chinese Han men over 50-year-old. *PLoS ONE*, 10(6).

Johnson, M.A. et al., 1973. Data on the distribution of fibre types in thirty-six human muscles. An autopsy study. *Journal of the Neurological Sciences*, 18(1), pp.111–129.

Johnston, A.P.W. et al., 2010. Regulation of muscle satellite cell activation and chemotaxis by angiotensin II. *PloS one*, 5(12), p.e15212.

Karnati, S. et al., 2013. Mammalian SOD2 is exclusively located in mitochondria and not present in peroxisomes. *Histochemistry and Cell Biology*, 140(2), pp.105–117.

Kassar-Duchossoy, L. et al., 2005. Pax3/Pax7 mark a novel population of primitive myogenic cells during development. *Genes and Development*, 19(12), pp.1426–1431.

Kästner, S. et al., 2000. Gene expression patterns of the fibroblast growth factors and their receptors during myogenesis of rat satellite cells. *The journal of histochemistry and cytochemistry : official*

Taryn Morash

journal of the Histochemistry Society, 48(8), pp.1079–1096.

Kenny, P.A. et al., 2007. The morphologies of breast cancer cell lines in three-dimensional assays correlate with their profiles of gene expression. *Molecular Oncology*, 1(1), pp.84–96.

Kent-Braun, J.A., Ng, A. V & Young, K., 2000. Skeletal muscle contractile and noncontractile components in young and older women and men. *Journal of applied physiology (Bethesda, Md. : 1985)*, 88(2), pp.662–8.

Kherif, S. et al., 1999. Expression of matrix metalloproteinases 2 and 9 in regenerating skeletal muscle: a study in experimentally injured and mdx muscles. *Developmental biology*, 205, pp.158–170.

Kim, J.-H. et al., 2011. Adipose-derived stem cells as a new therapeutic modality for ageing skin. *Experimental Dermatology*, 20(5), pp.383–387.

Kim, J.Y. et al., 2010. Human cord blood-derived endothelial progenitor cells and their conditioned media exhibit therapeutic equivalence for diabetic wound healing. *Cell transplantation*, 19(12), pp.1635–44.

Kim, S.H. et al., 2016. Bio-inspired, Moisture-Powered Hybrid Carbon Nanotube Yarn Muscles. *Scientific Reports*, 6(1), p.23016.

Kim, W.-S. et al., 2007. Wound healing effect of adipose-derived stem cells: A critical role of secretory factors on human dermal fibroblasts. *Journal of Dermatological Science*, 48(1), pp.15–24.

Kim, W.-S., Park, B.-S. & Sung, J.-H., 2009. The wound-healing and antioxidant effects of adipose-derived stem cells. *Expert opinion on biological therapy*, 9(7), pp.879–87.

Kim, W.K. et al., 2014. Secretome analysis of human oligodendrocytes derived from neural stem cells. *PloS one*, 9(1), p.e84292.

Kinnaird, T. et al., 2004. Marrow-derived stromal cells express genes encoding a broad spectrum of arteriogenic cytokines and promote in vitro and in vivo arteriogenesis through paracrine mechanisms. *Circulation research*, 94(5), pp.678–85.

Kjær, M. et al., 2009. From mechanical loading to collagen synthesis, structural changes and function in human tendon. *Scandinavian Journal of Medicine and Science in Sports*, 19(4), pp.500–510.

Klitgaard, H., Bergman, O., et al., 1990. Co-existence of myosin heavy chain I and IIa isoforms in human skeletal muscle fibres with endurance training. *Pflugers Arch*, 416, pp.470–472.

Klitgaard, H., Mantoni, M., et al., 1990. Function, morphology and protein expression of ageing skeletal muscle: a cross-sectional study of elderly men with different training backgrounds. *Acta Physiologica Scandinavica*, 140(1), pp.41–54.

Klitgaard, H. et al., 1989. Morphological and biochemical changes in old rat muscles: effect of increased use. *J Appl Physiol*, 67(4), pp.1409–1417.

Kosek, D.J., 2006. Efficacy of 3 days/wk resistance training on myofiber hypertrophy and myogenic mechanisms in young vs. older adults. *Journal of Applied Physiology*, 101(2), pp.531–544.

Taryn Morash

Koskelo, E.K., Saarinen, U.M. & Siimes, M.A., 1990. Skeletal muscle wasting and protein-energy malnutrition in children with a newly diagnosed acute leukemia. *Cancer*, 66(2), pp.373–376.

Kovanen, V., 2002. Intramuscular extracellular matrix: complex environment of muscle cells. *Exercise and sport sciences reviews*, 30(1), pp.20–25.

Kragstrup, T.W., Kjaer, M. & Mackey, a L., 2011. Structural, biochemical, cellular, and functional changes in skeletal muscle extracellular matrix with aging. *Scandinavian journal of medicine & science in sports*, 21, pp.749–57.

Krawetz, R.J. et al., 2011. Inhibition of Rho kinase regulates specification of early differentiation events in P19 embryonal carcinoma stem cells. *PLoS ONE*, 6(11).

Lacraz, G. et al., 2015. Increased stiffness in aged skeletal muscle impairs muscle progenitor cell proliferative activity. *PLoS ONE*, 10(8).

LaFramboise, W.A. et al., 2003. Effect of muscle origin and phenotype on satellite cell muscle-specific gene expression. *Journal of Molecular and Cellular Cardiology*, 35(10), pp.1307–1318.

Lafreniere, J.F. et al., 2004. Growth factors improve the in vivo migration of human skeletal myoblasts by modulating their endogenous proteolytic activity. *Transplantation*, 77(11), pp.1741–1747.

Lariviere, R.C. & Julien, J.-P., 2004. Functions of intermediate filaments in neuronal development and disease. *Journal of neurobiology*, 58(1), pp.131–48.

Larsson, L. et al., 1991. Effects of age on physiological, immunohistochemical and biochemical properties of fast-twitch single motor units in the rat. *The Journal of physiology*, 443, pp.257–75.

Larsson, L. & Ansved, T., 1995. Effects of ageing on the motor unit. *Progress in neurobiology*, 45(5), pp.397–458.

Larsson, L. & Edström, L., 1986. Effects of age on enzyme-histochemical fibre spectra and contractile properties of fast- and slow-twitch skeletal muscles in the rat. *Journal of the Neurological Sciences*, 76(1), pp.69–89.

Lavasani, M. et al., 2012. Muscle-derived stem/progenitor cell dysfunction limits healthspan and lifespan in a murine progeria model. *Nature Communications*, 3, p.608.

Lee, S.W. et al., 2004. Regulation of muscle protein degradation: coordinated control of apoptotic and ubiquitin-proteasome systems by phosphatidylinositol 3 kinase. *Journal of the American Society of Nephrology : JASN*, 15(6), pp.1537–1545.

Leeuwenburgh, C. et al., 2005. Age-related differences in apoptosis with disuse atrophy in soleus muscle. *American journal of physiology. Regulatory, integrative and comparative physiology*, 288(5), pp.R1288-96.

Leeuwenburgh, C. et al., 1994. Aging and exercise training in skeletal muscle: responses of glutathione and antioxidant enzyme systems. *The American journal of physiology*, 267(2 Pt 2), pp.R439–R445.

Lefaucheur, J.P. et al., 1996. Angiogenic and inflammatory responses following skeletal muscle injury are altered by immune neutralization of endogenous basic fibroblast growth factor, insulin-like growth

Taryn Morash

factor-1 and transforming growth factor-beta 1. *Journal of neuroimmunology*, 70(1), pp.37–44.

Leick, L. et al., 2009. PGC-1alpha mediates exercise-induced skeletal muscle VEGF expression in mice. *American journal of physiology. Endocrinology and metabolism*, 297(1), pp.E92-103.

Lessard-Beaudoin, M. et al., 2015. Characterization of age-associated changes in peripheral organ and brain region weights in C57BL/6 mice. *Experimental Gerontology*, 63, pp.27–34.

Lexell, J., 1997. Evidence for nervous system degeneration with advancing age. *The Journal of nutrition*, 127(5 Suppl), p.1011S–1013S.

Lexell, J., Downham, D. & Sjöström, M., 1986. Distribution of different fibre types in human skeletal muscles. *Journal of the Neurological Sciences*, 72(2–3), pp.211–222.

Lexell, J., Taylor, C.C. & Sjöström, M., 1988. What is the cause of the ageing atrophy?. Total number, size and proportion of different fiber types studied in whole vastus lateralis muscle from 15- to 83-year-old men. *Journal of the Neurological Sciences*, 84(2–3), pp.275–294.

Li, H., 2014. Sirtuin 1 (SIRT1) and Oxidative Stress. In I. Laher, ed. *Systems Biology of Free Radicals and Antioxidants*. Berlin, Heidelberg: Springer Berlin Heidelberg, pp. 417–435.

Li, X. et al., 1996. Thyroid hormone effects on contractility and myosin composition of soleus muscle and single fibres from young and old rats. *The Journal of physiology*, 494(Pt 2), pp.555–67.

Light, N. & Champion, A.E., 1984. Characterization of muscle epimysium, perimysium and endomysium collagens. *Biochem. J*, 219, pp.1017–1026.

Limame, R. et al., 2012. Comparative Analysis of Dynamic Cell Viability, Migration and Invasion Assessments by Novel Real-Time Technology and Classic Endpoint Assays. *PLoS ONE*, 7(10).

Lin, J. et al., 2002. Transcriptional co-activator PGC-1α drives the formation of slow-twitch muscle fibres. *Nature*, 418(6899), pp.797–801.

Liu, B. et al., 2013. Defective ATM-Kap-1-mediated chromatin remodeling impairs DNA repair and accelerates senescence in progeria mouse model. *Aging cell*, 12(2), pp.316–8.

Loffredo, F.S. et al., 2013. Growth differentiation factor 11 is a circulating factor that reverses age-related cardiac hypertrophy. *Cell*, 153(4), pp.828–39.

Lomo, T., Westgaard, R.H. & Dahl, H.A., 1974. Contractile Properties of Muscle: Control by Pattern of Muscle Activity in the Rat. *Proceedings of the Royal Society B: Biological Sciences*, 187(1086), pp.99–103.

López-otín, C. et al., 2013. The Hallmarks of Aging. , 153(6), pp.1194–1217.

Lord, C.J. & Ashworth, A., 2012. The DNA damage response and cancer therapy. *Nature*, 481(7381), pp.287–94.

Lowe, D. a et al., 2001. Electron paramagnetic resonance reveals age-related myosin structural changes in rat skeletal muscle fibers. *American journal of physiology. Cell physiology*, 280(3), pp.C540-7.

Lowe, D. a & Alway, S.E., 2002. Animal models for inducing muscle hypertrophy: are they relevant for

Taryn Morash

clinical applications in humans? *The Journal of orthopaedic and sports physical therapy*, 32(2), pp.36–43.

Lowey, S., Waller, G.S. & Trybus, K.M., 1993. Function of skeletal muscle myosin heavy and light chain isoforms by an in vitro motility assay. *The Journal of biological chemistry*, 268(27), pp.20414–8.

Lynch, G.S., Schertzer, J.D. & Ryall, J.G., 2007. Therapeutic approaches for muscle wasting disorders. *Pharmacology and Therapeutics*, 113(3), pp.461–487.

Machida, S. & Booth, F.W., 2004. Insulin-like growth factor 1 and muscle growth: implication for satellite cell proliferation. *The Proceedings of the Nutrition Society*, 63, pp.337–340.

MacIntosh, B.R., Gardiner, P.F. & McComas, A.J., 2006. *Skeletal muscle: form and function* 2nd illust., Champaign.

Madaule, P. & Axel, R., 1985. A novel ras-related gene family. *Cell*, 41(1), pp.31–40.

Mammucari, C. et al., 2007. FoxO3 Controls Autophagy in Skeletal Muscle In Vivo. *Cell Metabolism*, 6(6), pp.458–471.

Manchineella, S. et al., 2016. Pigmented Silk Nanofibrous Composite for Skeletal Muscle Tissue Engineering. *Advanced Healthcare Materials*, 5(10), pp.1222–1232.

Mansouri, A., Hallonet, M. & Gruss, P., 1996. Pax genes and their roles in cell differentiation and development. *Current Opinion in Cell Biology*, 8(6), pp.851–857.

Marino, D.J., 2012. Age-specific absolute and relative organ weight distributions for B6C3F1 mice. *J Toxicol Environ Health A*, 75(2), pp.76–99.

Marshall, P.A., Williams, P.E. & Goldspink, G., 1989. Accumulation of collagen and altered fiber-type ratios as indicators of abnormal muscle gene expression in the mdx dystrophic mouse. *Muscle & nerve*, 12(7), pp.528–37.

Marshall, P.A., Williams, P.E. & Goldspink, G., 1989. Accumulation of collagen and altered fiber-type ratios as indicators of abnormal muscle gene expression in the mdx dystrophic mouse. *Muscle & Nerve*, 12(7), pp.528–537.

Martin, J.E. & Sheaff, M.T., 2007. The pathology of ageing: concepts and mechanisms. *The Journal of pathology*, 211(2), pp.111–3.

Mathivanan, S., Ji, H. & Simpson, R.J., 2010. Exosomes: extracellular organelles important in intercellular communication. *Journal of proteomics*, 73(10), pp.1907–20.

Mathiyalagan, P. et al., 2017. Angiogenic Mechanisms of Human CD34+ Stem Cell Exosomes in the Repair of Ischemic Hindlimb. *Circulation Research*, 120(9), pp.1466–1476.

Mauro, A., 1961. Satellite cell of skeletal musle fibers. *The Journal of Cell Biology*, 9(2), pp.493–495.

Mayer, U., 2003. Integrins: Redundant or important players in skeletal muscle? *Journal of Biological Chemistry*, 278(17), pp.14587–14590.

McKinnell, I.W. & Rudnicki, M. a, 2005. Developmental biology: one source for muscle. *Nature*, 435,

Taryn Morash

pp.898–899.

McWhir, J. et al., 1993. Mice with DNA repair gene (ERCC-1) deficiency have elevated levels of p53, liver nuclear abnormalities and die before weaning. *Nature genetics*, 5(3), pp.217–24.

Mead, B. et al., 2016. Dental Pulp Stem Cells: A Novel Cell Therapy for Retinal and Central Nervous System Repair. *Stem cells (Dayton, Ohio)*, pp.61–67.

Medvedev, S.P., Shevchenko, A.I. & Zakian, S.M., 2010. Induced Pluripotent Stem Cells: Problems and Advantages when Applying them in Regenerative Medicine. *Acta naturae*, 2(2), pp.18–28.

Mehlen, P. & Puisieux, A., 2006. Metastasis: a question of life or death. *Nature Reviews Cancer*, 6(6), pp.449–458.

Meissner, M.H. et al., 2012. Early thrombus removal strategies for acute deep venous thrombosis: clinical practice guidelines of the Society for Vascular Surgery and the American Venous Forum. *Journal of vascular surgery*, 55(5), pp.1449–62.

Melis, J.P.M. et al., 2013. Aging on a different scale--chronological versus pathology-related aging. *Aging*, 5(10), pp.782–8.

Mellows, B. et al., 2017. Protein and molecular characterisation of a clinically compliant amniotic fluid stem cell derived extracellular vesicle fraction capable of accelerating muscle regeneration through the enhancement of angiogenesis. *Stem Cells and Development*, p.scd.2017.0089.

Millau, J.F., Bastien, N. & Drouin, R., 2009. P53 transcriptional activities: A general overview and some thoughts. *Mutation Research - Reviews in Mutation Research*, 681(2–3), pp.118–133.

Miller, K.J. et al., 2000. Hepatocyte growth factor affects satellite cell activation and differentiation in regenerating skeletal muscle. *American journal of physiology. Cell physiology*, 278(1), pp.C174–C181.

Milman, S. et al., 2014. Low insulin-like growth factor-1 level predicts survival in humans with exceptional longevity. *Aging Cell*, 13(4), pp.769–771.

Mizuno, Y. et al., 2010. Generation of skeletal muscle stem/progenitor cells from murine induced pluripotent stem cells. *The FASEB journal : official publication of the Federation of American Societies for Experimental Biology*, 24(7), pp.2245–2253.

Morash, T. et al., 2017. Mammalian Skeletal Muscle Fibres Promote Non-Muscle Stem Cells and Non-Stem Cells to Adopt Myogenic Characteristics. *Fibers*, 5(1), p.5.

Mouchiroud, L. et al., 2013. XThe NAD+/sirtuin pathway modulates longevity through activation of mitochondrial UPR and FOXO signaling. *Cell*, 154(2).

Murphy, T. & Thuret, S., 2015. The systemic milieu as a mediator of dietary influence on stem cell function during ageing. *Ageing research reviews*, 19, pp.53–64.

Musarò, a et al., 1999. IGF-1 induces skeletal myocyte hypertrophy through calcineurin in association with GATA-2 and NF-ATc1. *Nature*, 400(6744), pp.581–585.

Muses, S., Morgan, J.E. & Wells, D.J., 2011. A new extensively characterised conditionally immortal muscle

Taryn Morash

cell-line for investigating therapeutic strategies in muscular dystrophies. *PLoS ONE*, 6(9).

Nagano, M. et al., 2012. Turnover of focal adhesions and cancer cell migration. *International Journal of Cell Biology*.

Nagaraju, K. et al., 2000. Conditional up-regulation of MHC class I in skeletal muscle leads to self-sustaining autoimmune myositis and myositis-specific autoantibodies. *Proceedings of the National Academy of Sciences*, 97(16), pp.9209–9214.

Nagata, Y. et al., 2006. Sphingomyelin levels in the plasma membrane correlate with the activation state of muscle satellite cells. *The journal of histochemistry and cytochemistry : official journal of the Histochemistry Society*, 54(4), pp.375–384.

Nelson, J., 2008. *Structure and function in cell signalling*, Hoboken, NJ.: John Wiley & Sons, Chichester, England.

Niedernhofer, L.J. et al., 2006. A new progeroid syndrome reveals that genotoxic stress suppresses the somatotroph axis. *Nature*, 444(December), pp.1038–1043.

Nishimura, T. et al., 2008. Inhibition of matrix metalloproteinases suppresses the migration of skeletal muscle cells. *Journal of Muscle Research and Cell Motility*, 29(1), pp.37–44.

Nwoye, L. & Mommaerts, W.F.H.M., 1981. The effects of thyroid status on some properties of rat fast-twitch muscle. *Journal of Muscle Research and Cell Motility*, 2(3), pp.307–320.

Olanow, C.W., 1992. An introduction to the free radical hypothesis in Parkinson's disease. *Annals of Neurology*, 32(1 S), pp.S2–S9.

Oliver, K.G., Kettman, J.R. & Fulton, R.J., 1998. Multiplexed analysis of human cytokines by use of the flowmetrix system. In *Clinical Chemistry*. pp. 2057–2060.

Omairi, S. et al., 2016. Enhanced exercise and regenerative capacity in a mouse model that violates size constraints of oxidative muscle fibres. *eLife*, 5(AUGUST).

Ordway, G.A., 2004. Myoglobin: an essential hemoprotein in striated muscle. *Journal of Experimental Biology*, 207(20), pp.3441–3446.

Orford, K.W. & Scadden, D.T., 2008. Deconstructing stem cell self-renewal: genetic insights into cell-cycle regulation. *Nature reviews. Genetics*, 9(2), pp.115–28.

Orgel, J.P.R.O. et al., 2006. Microfibrillar structure of type I collagen in situ. *Proceedings of the National Academy of Sciences*, 103(24), pp.9001–9005.

Otto, A. et al., 2011. Adult skeletal muscle stem cell migration is mediated by a blebbing/amoeboid mechanism. *Rejuvenation research*, 14(3), pp.249–60.

Otto, A. et al., 2008. Canonical Wnt signalling induces satellite-cell proliferation during adult skeletal muscle regeneration. *Journal of cell science*, 121, pp.2939–2950.

Otto, A., Schmidt, C. & Patel, K., 2006. Pax3 and Pax7 expression and regulation in the avian embryo. *Anatomy and Embryology*, 211(4), pp.293–310.

Taryn Morash

Paddon-Jones, D. & Rasmussen, B.B., 2009. Dietary protein recommendations and the prevention of sarcopenia. *Current opinion in clinical nutrition and metabolic care*, 12(1), pp.86–90.

Pan, B.T. & Johnstone, R.M., 1983. Fate of the transferrin receptor during maturation of sheep reticulocytes in vitro: selective externalization of the receptor. *Cell*, 33(3), pp.967–78.

Partridge, T., 2000. The current status of myoblast transfer. *Neurological sciences : official journal of the Italian Neurological Society and of the Italian Society of Clinical Neurophysiology*, 21(5 Suppl), pp.S939-42.

Paterson, H.F. et al., 1990. Microinjection of recombinant p21rho induces rapid changes in cell morphology. *The Journal of cell biology*, 111(3), pp.1001–7.

Pawitan, J.A., 2014. Prospect of stem cell conditioned medium in regenerative medicine. *BioMed research international*, 2014, p.965849.

Péault, B. et al., 2007. Stem and progenitor cells in skeletal muscle development, maintenance, and therapy. *Molecular therapy : the journal of the American Society of Gene Therapy*, 15(5), pp.867–77.

Pedersen, B.K., 2009. The diseasome of physical inactivity - and the role of myokines in muscle-fat cross talk. *The Journal of Physiology*, 587(23), pp.5559–5568.

Perniconi, B. et al., 2011. The pro-myogenic environment provided by whole organ scale acellular scaffolds from skeletal muscle. *Biomaterials*, 32(31), pp.7870–7882.

Peter, J.B. et al., 1972. Metabolic Profiles of Three Fiber Types of Skeletal Muscle in Guinea Pigs and Rabbits. *Biochemistry*, 11(14), pp.2627–2633.

Pette, D. & Staron, R.S., 1990. Cellular and molecular diversities of mammalian skeletal muscle fibers. *Reviews of physiology, biochemistry and pharmacology*, 116, pp.1–76.

Pette, D. & Staron, R.S., 1997. Mammalian skeletal muscle fiber type transitions. *International review of cytology*, 170, pp.143–223.

Pette, D. & Staron, R.S., 2000. Myosin isoforms, muscle fiber types, and transitions. *Microscopy research and technique*, 50(6), pp.500–9.

Pette, D. & Vrbova, G., 1985. Neural control of phenotypic expression in mammalian muscle fibers. *Muscle & nerve*, 8(8), pp.676–689.

Philippou, A. et al., 2007. Type I insulin-like growth factor receptor signaling in skeletal muscle regeneration and hypertrophy. *Journal of Musculoskeletal Neuronal Interactions*, 7(3), pp.208–218.

Pieczenik, S.R. & Neustadt, J., 2007. Mitochondrial dysfunction and molecular pathways of disease. *Experimental and Molecular Pathology*, 83(1), pp.84–92.

Pocock, G. & Richards, C.D., 2006. *Human physiology: the basis of medicine* 3rd ed., Oxford: Oxford University Press.

Pogozelski, A.R. et al., 2009. p38γ mitogen-activated protein kinase is a key regulator in skeletal muscle metabolic adaptation in mice. *PLoS ONE*, 4(11).

Taryn Morash

Pollard, T.D., Earnshaw, W.C. & Lippincott-Schwartz, J., 2007. *Cell Biology* 2nd ed., Philadelphia, PA, USA: Saunders Elsevier Inc.

Porzionato, A. et al., 2015. Decellularized human skeletal muscle as biologic scaffold for reconstructive surgery. *International Journal of Molecular Sciences*, 16(7), pp.14808–14831.

Potthoff, M.J. et al., 2007. Histone deacetylase degradation and MEF2 activation promote the formation of slow-twitch myofibers. *Journal of Clinical Investigation*, 117(9), pp.2459–2467.

Powers, S.K. et al., 2012. Mitochondrial signaling contributes to disuse muscle atrophy. *AJP: Endocrinology and Metabolism*, 303(1), pp.E31–E39.

Prince, F.P., Hikida, R.S. & Hagerman, F.C., 1976. Human muscle fiber types in power lifters, distance runners and untrained subjects. *Pflügers Archiv European Journal of Physiology*, 363(1), pp.19–26.

Ramamurthy, B. & Larsson, L., 2013. Detection of an aging-related increase in advanced glycation end products in fast- and slow-twitch skeletal muscles in the rat. *Biogerontology*, 14(3), pp.293–301.

Ravenscroft, G. et al., 2007. Dissociated flexor digitorum brevis myofiber culture system - A more mature muscle culture system. *Cell Motility and the Cytoskeleton*, 64(10), pp.727–738.

Relaix, F. et al., 2005. A Pax3/Pax7-dependent population of skeletal muscle progenitor cells. *Nature*, 435(7044), pp.948–953.

Relaix, F. et al., 2006. Pax3 and Pax7 have distinct and overlapping functions in adult muscle progenitor cells. *Journal of Cell Biology*, 172(1), pp.91–102.

Relizani, K. et al., 2014. Blockade of ActRIIB Signaling Triggers Muscle Fatigability and Metabolic Myopathy. *Molecular Therapy*, 22(8), pp.1423–1433.

Rice, K.M. et al., 2007. Load-induced focal adhesion mechanotransduction is altered with aging in the Fischer 344/NNiaHSd x Brown Norway/BiNia rat aorta. *Biogerontology*, 8(3), pp.257–67.

Ridley, A.J., 2001. Rho family proteins: coordinating cell responses. *Trends in cell biology*, 11(12), pp.471–7.

Ridley, A.J. et al., 1992. The small GTP-binding protein rac regulates growth factor-induced membrane ruffling. *Cell*, 70(3), pp.401–10.

Ridley, A.J. & Hall, A., 1994. Signal transduction pathways regulating Rho-mediated stress fibre formation: requirement for a tyrosine kinase. *The EMBO journal*, 13(11), pp.2600–10.

Ridley, A.J. & Hall, A., 1992. The small GTP-binding protein rho regulates the assembly of focal adhesions and actin stress fibers in response to growth factors. *Cell*, 70(3), pp.389–99.

Riggs, B.L. et al., 1981. Differential changes in bone mineral density of the appendicular and axial skeleton with aging. Relationship to spinal osteoporosis. *Journal of Clinical Investigation*, 67(2), pp.328–335.

Rittweger, J. et al., 2004. Is muscle power output a key factor in the age-related decline in physical performance? A comparison of muscle cross section, chair-rising test and jumping power. *Clinical Physiology and Functional Imaging*, 24(6), pp.335–340.

Taryn Morash

La Rocca, G. et al., 2009. Isolation and characterization of Oct-4+/HLA-G+ mesenchymal stem cells from human umbilical cord matrix: Differentiation potential and detection of new markers. *Histochemistry and Cell Biology*, 131(2), pp.267–282.

Röckl, K.S.C. et al., 2007. Skeletal muscle adaptation to exercise training: AMP-activated protein kinase mediates muscle fiber type shift. *Diabetes*, 56(8), pp.2062–2069.

Rockwood, K. et al., 2005. A global clinical measure of fitness and frailty in elderly people. *CMAJ*, 173(5), pp.489–495.

Rogers, M. a & Evans, W.J., 1993. Changes in skeletal muscle with aging: effects of exercise training. *Exercise and sport sciences reviews*, 21, pp.65–102.

Rokach, O. et al., 2013. Establishment of a human skeletal muscle-derived cell line: biochemical, cellular and electrophysiological characterization. *The Biochemical journal*, 455(2), pp.169–77.

Rollo, C.D., 2010. Aging and the Mammalian regulatory triumvirate. *Aging and disease*, 1(2), pp.105–38.

Roman, W.J. et al., 1993. Adaptations in the elbow flexors of elderly males after heavy-resistance training. *Journal of applied physiology*, 74(2), pp.750–754.

Rose, M.R., 1991. Evolutionary biology of aging. *American Journal of Human Genetics*, 1990.

Rosenblatt, J.D. et al., 1995. Culturing satellite cells from living single muscle fiber explants. *In Vitro Cellular & Developmental Biology - Animal: Journal of the Society for In Vitro Biology*, 31(10), pp.773–779.

Rowan, S.L. et al., 2011. Accumulation of severely atrophic myofibers marks the acceleration of sarcopenia in slow and fast twitch muscles. *Experimental Gerontology*, 46(8), pp.660–669.

Rowan, S.L. et al., 2012. Denervation causes fiber atrophy and myosin heavy chain co-expression in senescent skeletal muscle. *PLoS ONE*, 7(1).

Rowe, R.W. & Goldspink, G., 1969. Muscle fibre growth in five different muscles in both sexes of mice. II. Dystrophic mice. *Journal of anatomy*, 104(Pt 3), pp.531–538.

Rowe, R.W.D., 1981. Morphology of perimysial and endomysial connective tissue in skeletal muscle. *Tissue and Cell*, 13(4), pp.681–690.

Rudnicki, M.A. et al., 1993. MyoD or Myf-5 is required for the formation of skeletal muscle. *Cell*, 75(7), pp.1351–1359.

Russell, A.P. et al., 2003. Endurance Training in Humans Leads to Fiber Type-Specific Increases in Levels of Peroxisome Proliferator-Activated Receptor-γ Coactivator-1 and Peroxisome Proliferator-Activated Receptor-α in Skeletal Muscle. *Diabetes*, 52(12), pp.2874–2881.

Rutishauser, U., 1984. Developmental biology of a neural cell adhesion molecule. *Nature*, 310(5978), pp.549–54.

Ryan, M.J. et al., 2008. Aging-dependent regulation of antioxidant enzymes and redox status in chronically loaded rat dorsiflexor muscles. *J Gerontol A Biol Sci Med Sci*, 63(10), pp.1015–1026.

Taryn Morash

Ryan, N.A. et al., 2006. Lower skeletal muscle capillarization and VEGF expression in aged vs. young men. *Journal of applied physiology (Bethesda, Md. : 1985)*, 100(1), pp.178–85.

Salmons, S. & Vrbová, G., 1969. The influence of activity on some contractile characteristics of mammalian fast and slow muscles. *The Journal of physiology*, 201(3), pp.535–49.

Salvatore, D. et al., 2013. Thyroid hormones and skeletal muscle—new insights and potential implications. *Nature Reviews Endocrinology*, 10(4), pp.206–214.

Sandri, M. et al., 2004. Foxo transcription factors induce the atrophy-related ubiquitin ligase atrogin-1 and cause skeletal muscle atrophy. *Cell*, 117(3), pp.399–412.

Sanes, J.R., 2003. The basement membrane/basal lamina of skeletal muscle. *Journal of Biological Chemistry*, 278(15), pp.12601–12604.

Sanz-Moreno, V. et al., 2008. Rac Activation and Inactivation Control Plasticity of Tumor Cell Movement. *Cell*, 135(3), pp.510–523.

Sanz-Moreno, V. et al., 2011. ROCK and JAK1 signaling cooperate to control actomyosin contractility in tumor cells and stroma. *Cancer cell*, 20(2), pp.229–45.

Sanz-Moreno, V. & Marshall, C.J., 2009. Rho-GTPase signaling drives melanoma cell plasticity. *Cell Cycle*, 8(10), pp.1484–1487.

Satoh, A. et al., 1993. Use of fluorescent latex microspheres (FLMs) to follow the fate of transplanted myoblasts. *The journal of histochemistry and cytochemistry : official journal of the Histochemistry Society*, 41(10), pp.1579–1582.

Scheibye-Knudsen, M. et al., 2014. A high-fat diet and NAD+ activate sirt1 to rescue premature aging in cockayne syndrome. *Cell Metabolism*, 20(5), pp.840–855.

Schiaffino, S. et al., 1989. Three myosin heavy chain isoforms in type 2 skeletal muscle fibres. *Journal of muscle research and cell motility*, 10(3), pp.197–205.

Schiaffino, S. & Reggiani, C., 2011. Fiber types in mammalian skeletal muscles. *Physiological reviews*, 91(4), pp.1447–531.

Schiaffino, S. & Reggiani, C., 1996. Molecular diversity of myofibrillar proteins: Gene regulation and functional significance. *Physiol Rev*, 76(2), pp.371–423.

Schultz, E. & Lipton, B.H., 1982. Skeletal muscle satellite cells: Changes in proliferation potential as a function of age. *Mechanisms of Ageing and Development*, 20(4), pp.377–383.

Schwartz, L.M., 2008. Atrophy and programmed cell death of skeletal muscle. *Cell Death and Differentiation*, 15(7), pp.1163–1169.

Seale, P. et al., 2000. Pax7 is required for the specification of myogenic satellite cells. *Cell*, 102(6), pp.777–86.

Seifter, J., Sloane, D. & Ratner, A., 2005. *Concepts in Medical Physiology*, Lippincott Williams & Wilkins.

Sell, D. & Monnier, V., 1989. Structure elucidation of a senescence cross-link from human extracellular

Taryn Morash

matrix. Implication of pentoses in the aging process. *J. Biol. Chem.*, 264(36), pp.21597–21602.

Serradj, N. & Jamon, M., 2007. Age-related changes in the motricity of the inbred mice strains 129/sv and C57BL/6j. *Behavioural Brain Research*, 177(1), pp.80–89.

Shake, J.G. et al., 2002. Mesenchymal stem cell implantation in a swine myocardial infarct model: Engraftment and functional effects. *Annals of Thoracic Surgery*, 73(6), pp.1919–1926.

Shefer, G. et al., 2006. Satellite-cell pool size does matter: defining the myogenic potency of aging skeletal muscle. *Developmental biology*, 294(1), pp.50–66.

Siegel, A. & Sapru, H.N., 2010. *Essential Neuroscience*, Lippincott Williams & Wilkins.

Siegel, A.L. et al., 2009. 3D timelapse analysis of muscle satellite cell motility. *Stem Cells*, 27(10), pp.2527–2538.

Siegel, A.L. et al., 2009. 3D timelapse analysis of muscle satellite cell motility. *Stem cells (Dayton, Ohio)*, 27(10), pp.2527–38.

Sinha, M. et al., 2014. Restoring systemic GDF11 levels reverses age-related dysfunction in mouse skeletal muscle. *Science (New York, N.Y.)*, 344(6184), pp.649–52.

Sloan, A.J. et al., 2000. Transforming growth factor-beta isoform expression in mature human healthy and carious molar teeth. *The Histochemical journal*, 32(4), pp.247–252.

Small, J.V. et al., 2002. The lamellipodium: where motility begins. *Trends in cell biology*, 12(3), pp.112–20.

Smerdu, V. et al., 1994. Type IIx myosin heavy chain transcripts are expressed in type IIb fibers of human skeletal muscle. *The American journal of physiology*, 267(6 Pt 1), pp.C1723–C1728.

Snijders, T., Verdijk, L.B. & van Loon, L.J.C., 2009. The impact of sarcopenia and exercise training on skeletal muscle satellite cells. *Ageing Research Reviews*, 8, pp.328–338.

Snow, M.H., 1977a. Myogenic cell formation in regenerating rat skeletal muscle injured by mincing. I. A fine structural study. *Anat Rec*, 188(2), pp.181–199.

Snow, M.H., 1977. Myogenic cell formation in regenerating rat skeletal muscle injured by mincing II. An autoradiographic study. *The Anatomical Record*, 188(2), pp.201–217.

Snow, M.H., 1977b. The effects of aging on satellite cells in skeletal muscles of mice and rats. *Cell and tissue research*, 185(3), pp.399–408.

Soderling, S.H. & Scott, J.D., 2006. WAVE signalling: from biochemistry to biology. *Biochemical Society transactions*, 34(Pt 1), pp.73–6.

Song, W.K. et al., 1992. H36-alpha7 Is a Novel Integrin Alpha-Chain That Is Developmentally Regulated During Skeletal Myogenesis. *J Cell Biol*, 117(3).

Sonntag, W.E. et al., 1997. Decreases in cerebral microvasculature with age are associated with the decline in growth hormone and insulin-like growth factor 1. *Endocrinology*, 138, pp.3515–3520.

Sousa-Victor, P. et al., 2014. Geriatric muscle stem cells switch reversible quiescence into senescence.

Taryn Morash

Nature, 506, pp.316–21.

Sperka, T., Wang, J. & Rudolph, K.L., 2012. DNA damage checkpoints in stem cells, ageing and cancer. *Nature Reviews Molecular Cell Biology*, 13(9), pp.579–590.

Spindler, S.R., 2005. Rapid and reversible induction of the longevity, anticancer and genomic effects of caloric restriction. *Mechanisms of Ageing and Development*, 126(9 SPEC. ISS.), pp.960–966.

Spurney, C.F. et al., 2009. Preclinical drug trials in the mdx mouse: Assessment of reliable and sensitive outcome measures. *Muscle and Nerve*, 39(5), pp.591–602.

Staron, R.S. et al., 1984. Human skeletal muscle fiber type adaptability to various workloads. *The journal of histochemistry and cytochemistry : official journal of the Histochemistry Society*, 32, pp.146–152.

Stevenson, E.J. et al., 2003. Global analysis of gene expression patterns during disuse atrophy in rat skeletal muscle. *The Journal of physiology*, 551(Pt 1), pp.33–48.

Stickland, N.C., 1981. Muscle development in the human fetus as exemplified by m. sartorius: a quantitative study. *Journal of anatomy*, 132(Pt 4), pp.557–79.

Sullivan, K.E. et al., 2014. Extracellular matrix remodeling following myocardial infarction influences the therapeutic potential of mesenchymal stem cells. *Stem cell research & therapy*, 5(1), p.14.

Suzman, R. (National I. on A. & Beard, J. (World H.O., 2011. Global Health and Aging. *National Institute of Health*, pp.1–26. Available at: http://www.who.int/ageing/publications/global_health.pdf.

Suzuki, A., 1995. Differences in distribution of myofiber types between the supraspinatus and infraspinatus muscles of sheep. *The Anatomical Record*, 242(4), pp.483–490.

Taaffe, D.R. et al., 2009. Alterations in muscle attenuation following detraining and retraining in resistance-trained older adults. *Gerontology*, 55(2), pp.217–223.

Tajbakhsh, S. et al., 1997. Redefining the genetic hierarchies controlling skeletal myogenesis: Pax-3 and Myf-5 act upstream of MyoD. *Cell*, 89(1), pp.127–138.

Tajiri, N. et al., 2014. Therapeutic outcomes of transplantation of amniotic fluid-derived stem cells in experimental ischemic stroke. *Frontiers in Cellular Neuroscience*, 8.

Takahashi, M. et al., 1995. Direct measurement of crosslinks, pyridinoline, deoxypyridinoline, and pentosidine, in the hydrolysate of tissues using high-performance liquid chromatography. *Analytical biochemistry*, 232(2), pp.158–62.

Takemura, A. et al., 2017. Unloading-induced atrophy and decreased oxidative capacity of the soleus muscle in rats are reversed by pre- and postconditioning with mild hyperbaric oxygen. *Physiological Reports*, 5(14), p.e13353.

Tamaki, T. et al., 2005. Functional recovery of damaged skeletal muscle through synchronized vasculogenesis, myogenesis, and neurogenesis by muscle-derived stem cells. *Circulation*, 112(18), pp.2857–66.

Tamaki, T. et al., 2007. Synchronized reconstitution of muscle fibers, peripheral nerves and blood vessels

Taryn Morash

by murine skeletal muscle-derived CD34(-)/45 (-) cells. *Histochemistry and cell biology*, 128(4), pp.349–60.

Tapscott, S.J., 2005. The circuitry of a master switch: Myod and the regulation of skeletal muscle gene transcription. *Development*, 132(12), pp.2685–2695.

Tatsumi, R. et al., 1998. HGF/SF is present in normal adult skeletal muscle and is capable of activating satellite cells. *Developmental biology*, 194(1), pp.114–128.

Terman, A. & Brunk, U.T., 2004. Myocyte aging and mitochondrial turnover. *Experimental Gerontology*, 39(5), pp.701–705.

Tinevez, J.-Y. et al., 2009. Role of cortical tension in bleb growth. *Proceedings of the National Academy of Sciences of the United States of America*, 106(44), pp.18581–6.

Totonelli, G. et al., 2012. A rat decellularized small bowel scaffold that preserves villus-crypt architecture for intestinal regeneration. *Biomaterials*, 33(12), pp.3401–10.

Tozluoğlu, M., Tournier, A.L., et al., 2013. Matrix geometry determines optimal cancer cell migration strategy and modulates response to interventions. *Nature Cell Biology*, 15(7), pp.751–762.

Tozluoğlu, M., Tournier, A.L., et al., 2013. Matrix geometry determines optimal cancer cell migration strategy and modulates response to interventions. *Nature cell biology*, 15(7), pp.751–62.

Treisman, J., Harris, E. & Desplan, C., 1991. The paired box encodes a second DNA-binding domain in the Paired homeo domain protein. *Genes and Development*, 5(4), pp.594–604.

Trensz, F. et al., 2010. A muscle resident cell population promotes fibrosis in hindlimb skeletal muscles of mdx mice through the Wnt canonical pathway. *American journal of physiology. Cell physiology*, 299(5), pp.C939–C947.

Tsai, M.-S. et al., 2007. Functional network analysis of the transcriptomes of mesenchymal stem cells derived from amniotic fluid, amniotic membrane, cord blood, and bone marrow. *Stem cells (Dayton, Ohio)*, 25(10), pp.2511–23.

Turturro, A. et al., 1999. Growth curves and survival characteristics of the animals used in the Biomarkers of Aging Program. *The journals of gerontology. Series A, Biological sciences and medical sciences*, 54(11), pp.B492–B501.

Tyson, R.A. et al., 2014. How blebs and pseudopods cooperate during chemotaxis. *Proceedings of the National Academy of Sciences of the United States of America*, 111(32), pp.11703–8.

Vásquez-Vivar, J., Kalyanaraman, B. & Kennedy, M.C., 2000. Mitochondrial aconitase is a source of hydroxyl radical. An electron spin resonance investigation. *Journal of Biological Chemistry*, 275(19), pp.14064–14069.

Velloso, C.P., 2008. Regulation of muscle mass by growth hormone and IGF-I. *British Journal of Pharmacology*, 154(3), pp.557–568.

Vettor, R. et al., 2009. The origin of intermuscular adipose tissue and its pathophysiological implications. *American journal of physiology. Endocrinology and metabolism*, 297(5), pp.E987-98.

Taryn Morash

Vicente-Manzanares, M. et al., 2009. Non-muscle myosin II takes centre stage in cell adhesion and migration. *Nature Reviews Molecular Cell Biology*, 10(11), pp.778–790.

De Waard, M.C. et al., 2010. Age-related motor neuron degeneration in DNA repair-deficient Ercc1 mice. *Acta Neuropathologica*, 120, pp.461–475.

Wang, H. et al., 2014. Apoptosis in capillary endothelial cells in ageing skeletal muscle. *Aging Cell*, 13(2), pp.254–262.

Wang, L.C. & Kernell, D., 2001. Fibre type regionalisation in lower hindlimb muscles of rabbit, rat and mouse: a comparative study. *Journal of anatomy*, 199(Pt 6), pp.631–643.

Weeda, G. et al., 1997. Disruption of mouse ERCC1 results in a novel repair syndrome with growth failure, nuclear abnormalities and senescence. *Current biology : CB*, 7, pp.427–439.

Wei, Y.H. et al., 1998. Oxidative damage and mutation to mitochondrial DNA and age-dependent decline of mitochondrial respiratory function. *Annals of the New York Academy of Sciences*, 854, pp.155–170.

Weintraub, H. et al., 1989. Activation of muscle-specific genes in pigment, nerve, fat, liver, and fibroblast cell lines by forced expression of MyoD. *Proceedings of the National Academy of Sciences of the United States of America*, 86(14), pp.5434–8.

Weissman, I.L., 2000. Stem cells: units of development, units of regeneration, and units in evolution. *Cell*, 100(1), pp.157–68.

Welle, S., Totterman, S. & Thornton, C., 1996. Effect of Age on Muscle Hypertrophy Induced by Resistance Training. *The Journals of Gerontology Series A: Biological Sciences and Medical Sciences*, 51A(6), pp.M270–M275.

White, R.B. et al., 2010. Dynamics of muscle fibre growth during postnatal mouse development. *BMC developmental biology*, 10, p.21.

Wolfe, R.R., 2006. The underappreciated role of muscle in health and disease. *American Journal of Clinical Nutrition*, 84(3), pp.475–482.

Wood, L.K. et al., 2014. Intrinsic stiffness of extracellular matrix increases with age in skeletal muscles of mice. *Journal of Applied Physiology*, 117(4), pp.363–369.

Woodley, D.T. et al., 1983. Interactions of basement membrane components. *Biochimica et biophysica acta*, 761(3), pp.278–83.

Wu, C. et al., 2012. Arp2/3 is critical for lamellipodia and response to extracellular matrix cues but is dispensable for chemotaxis. *Cell*, 148(5), pp.973–987.

Yablonka-Reuveni, Z., 2011. The skeletal muscle satellite cell: still young and fascinating at 50. *The journal of histochemistry and cytochemistry : official journal of the Histochemistry Society*, 59(12), pp.1041–59.

Yablonka-Reuveni, Z. & Rivera, a J., 1994. Temporal expression of regulatory and structural muscle proteins during myogenesis of satellite cells on isolated adult rat fibers. *Developmental biology*,

Taryn Morash

164(2), pp.588–603.

Yan, Z. et al., 2011. Regulation of exercise-induced fiber type transformation, mitochondrial biogenesis, and angiogenesis in skeletal muscle. *Journal of Applied Physiology*, 110(1), pp.264–274.

Yang, H. et al., 1997. Changes in muscle fibre type, muscle mass and IGF-I gene expression in rabbit skeletal muscle subjected to stretch. *Journal of anatomy*, 190(Pt 4), pp.613–22.

Yasuda, T. et al., 1996. Regulation of extracellular matrix by mechanical stress in rat glomerular mesangial cells. *The Journal of clinical investigation*, 98(9), pp.1991–2000.

Yin, H., Price, F. & Rudnicki, M.A., 2013. Satellite cells and the muscle stem cell niche. *Physiological reviews*, 93(1), pp.23–67.

Yoshida, K. & Soldati, T., 2006. Dissection of amoeboid movement into two mechanically distinct modes. *Journal of cell science*, 119(Pt 18), pp.3833–44.

Young, S.G., Fong, L.G. & Michaelis, S., 2005. Prelamin A, Zmpste24, misshapen cell nuclei, and progeria-- new evidence suggesting that protein farnesylation could be important for disease pathogenesis. *Journal of lipid research*, 46(12), pp.2531–58.

Zammit, P., 2002. Kinetics of Myoblast Proliferation Show That Resident Satellite Cells Are Competent to Fully Regenerate Skeletal Muscle Fibers. *Experimental Cell Research*, 281(1), pp.39–49.

Zammit, P.S. et al., 2004. Muscle satellite cells adopt divergent fates: A mechanism for self-renewal? *Journal of Cell Biology*, 166(3), pp.347–357.

Zammit, P.S., Relaix, F., et al., 2006. Pax7 and myogenic progression in skeletal muscle satellite cells. *Journal of cell science*, 119(Pt 9), pp.1824–32.

Zammit, P.S., Partridge, T.A. & Yablonka-Reuveni, Z., 2006. The skeletal muscle satellite cell: the stem cell that came in from the cold. *The journal of histochemistry and cytochemistry : official journal of the Histochemistry Society*, 54(11), pp.1177–91.

Zhang, W. et al., 2006. Multilineage differentiation potential of stem cells derived from human dental pulp after cryopreservation. *Tissue engineering*, 12, pp.2813–2823.

Zimmerman, S.D. et al., 1993. Age and training alter collagen characteristics in fast- and slow-twitch rat limb muscle. *Journal of applied physiology (Bethesda, Md. : 1985)*, 75, pp.1670–1674.

Taryn Morash

Appendices

Taryn Morash

Appendix 1 - Materials

Mouse lines

The animals used were healthy wild-type mice (Strain: C57BL/6JOla/Hsd), young (3-4 month old), adult (6 month old), old (24 month old) and geriatric (27-30 month old). Young and adult mice were obtained from Charles River. The naturally-aged (24 month old) and geriatric (27-30 month old) mice and muscle tissues were generously provided by Dr. Paul Potter of the Medical Research Council (MRC) Harwell, Oxford, United Kingdom, as part of the Shared Ageing Research Models (ShARM) facility. Small breeding populations of heterozygous ERCC1 knockout mice (+/-) as well as ERCC1 delta mutants (d/+) on FVB and C57BL/6 backgrounds were generously provided by Professor Jan Hoeijmakers of the Department of Genetics, Erasmus University Medical Centre, Rotterdam, the Netherlands.

Cell lines

Human adipose-derived stem cells (hADMSC or ADMSC)

StemPro® Human Adipose–Derived Stem Cells (Life Technologies 510070), lot number 2117 obtained from a 49 year-old female donor.

Human amniotic fluid stem cells (AFS)

Amniotic fluid stem cells, lentivirus-transduced with GFP, were generously provided by Professor Paolo De Coppi, Centre for Stem Cells and Regenerative Medicine, Institute for Child Health, University College London (UCL), United Kingdom. These cells were obtained from second trimester amniotic fluid, are human in origin and selected by FACS for c-Kit (CD117) expression.

Rat dental pulp stem cells (DP)

DP cells (GFP) were isolated in-house from SD-Tg(CAG-EGFP)CZ-004OS6 rats.

MDA-MB-231 breast adenocarcinoma cell line (MDA)

MDA-MB-231 adenocarcinoma cells were kindly gifted by Professor Philip Dash, University of Reading, United Kingdom. MDA-MB-231 cells had been permanently transfected using a PB CAG myr GFP transposon and a PB HYPBASE transposase, to overexpress a membrane-tagged GFP. The original sample having been obtained from an adenocarcinoma, pleural effusion metastatic site in a 51 year old female with breast cancer.

Human Foetal Lung Fibroblast Cells (IMR-90)

Human foetal lung IMR-90 fibroblast cells were generously donated from Dr. Debacq-Chainiaux, Namur University, Belgium. These cells were used at 50% of Hayflick limit, 27 - 32 population doublings.

Culture media

Collagenase digestion

2mg/mL type-1 collagenase solution (Sigma C0130), Dulbecco modified Eagle medium (DMEM) (Gibco, Thermo Fisher Scientific 31966-021).

Taryn Morash

Single fibre culture medium (SFCM)

Dulbecco modified Eagle medium (DMEM) (Gibco, Thermo Fisher Scientific 31966-021), 10% horse serum (Gibco, Thermo Fisher Scientific 16050-122), 0.5% chick embryo extract (in-house preparation), 1% penicillin streptomycin (100X) (Invitrogen, Thermo Fisher Scientific 15240-062).

Single fibre culture medium adapted for long-term culture (LT-SFCM)

Dulbecco modified Eagle medium (DMEM) (Gibco, Thermo Fisher Scientific 31966-021), 10% horse serum (Gibco, Thermo Fisher Scientific 16050-122), 5% chick embryo extract (in-house preparation), 1% penicillin streptomycin (100X) (Invitrogen, Thermo Fisher Scientific 15240-062).

Amniotic fluid stem (AFS) cell media

Minimum Essential Medium, alpha modifications (α-MEM) (Gibco, Thermo Fisher Scientific 32561-037), 20% Chang B/C media supplement (Irvine Scientific T101-019), 15% foetal bovine serum (FBS) (Gibco, Thermo Fisher Scientific 10270-106), 1% L-glutamine supplement (Invitrogen, Thermo Fisher Scientific 25030-024), 1% penicillin streptomycin (100X) (Invitrogen, Thermo Fisher Scientific 15240-062).

Adipose-derived mesenchymal stem cell (ADMSC) media

MesenPro RS™ medium (Gibco, Thermo Fisher Scientific 12746-012) supplemented with 1% penicillin streptomycin (100X) (Invitrogen, Thermo Fisher Scientific 15240-062)

MDA-MB-231 (MDA breast cancer cell line) media

DMEM (Gibco 31966-021), 10% FBS (Gibco, Thermo Fisher Scientific 10270-106), 1% L-glutamine (Invitrogen, Thermo Fisher Scientific 25030-024), 1% penicillin streptomycin (100X) (Invitrogen, Thermo Fisher Scientific 15240-062).

Dental pulp (DP) stem cell media

Minimum Essential Medium, alpha modifications (α-MEM) (Gibco, Thermo Fisher Scientific 32561-037), 20% FBS (Gibco, Thermo Fisher Scientific 10270-106), 1% L-glutamine (Invitrogen, Thermo Fisher Scientific 25030-024), 1% penicillin-streptomycin (100X) (Invitrogen, Thermo Fisher Scientific 15240-062), 100mM L-ascorbic acid (Sigma-Aldrich A8960).

IMR-90 lung fibroblast media

Minimum Essential Medium, alpha modifications (α-MEM) (Gibco, Thermo Fisher Scientific 32561-037), 10% FBS (Gibco, Thermo Fisher Scientific 10270-106), 1% penicillin-streptomycin (100X) (Invitrogen, Thermo Fisher Scientific 15240-062)

Myogenic differentiation media

DMEM (Gibco, Thermo Fisher Scientific 31966-021), 2% horse serum (Gibco, Thermo Fisher Scientific 16050-122), 1% penicillin-streptomycin (100X) (Invitrogen, Thermo Fisher Scientific 15240-062).

Mesenchymal Stem Cell Chondrogenic Differentiation Media

StemPro® Osteocyte/Chondrocyte basal medium (Life Technologies, Thermo Fisher Scientific A10069-01), StemPro® Chondrogenesis Supplement (Life Technologies, Thermo Fisher Scientific A10064-01).

Mesenchymal Stem Cell Osteogenic Differentiation Media

Taryn Morash

StemPro® Osteocyte/Chondrocyte basal medium (Life Technologies, Thermo Fisher Scientific A10069-01), StemPro® Osteogenesis Supplement (Life Technologies, Thermo Fisher Scientific A10066-01).

Mesenchymal Stem Cell Adipogenic Differentiation Media

StemPro® Adipogenesis basal medium (Life Technologies, Thermo Fisher Scientific A10410-01), StemPro® Adipogenesis Supplement (Life Technologies, Thermo Fisher Scientific A10065-01).

Freezing media

90% FBS (Gibco, Thermo Fisher Scientific 10270-106), 10% Dimethyl sulfoxide (DMSO) (BDH Chemicals 103234L).

1 x PBS solution for cell culture

1 PBS tablet (Oxoid BR0014G) per 100mL distilled water.

Fixation medium

Fixation medium (Universal)

4% paraformaldehyde (w/v) (Sigma Aldrich P6148) in 1 x PBS solution.

Fixation medium for stress-induced cellular senescence assay

0.2% glutaraldehyde (Sigma Aldrich G5882), 2% paraformaldehyde (Sigma Aldrich P6148) in 1 x PBS solution.

Histological staining

Stress induced cellular senescence staining solution

5mM sodium phosphate solution pH 6.0, 5mM potassium ferricyanide, 5mM potassium ferrocyanide, 125mM sodium chloride, 50mM magnesium chloride, 2.5mg/mL X-gal.

NBT stock solution

100mM phosphate buffer pH 7.6, 6.5ng/mL potassium cyanide (Thermo Fisher Scientific 1059938), 0.185mg/mL EDTA (Sigma Aldrich E5134), 1mg/mL nitroblue tetrazolium (Sigma Aldrich 74032).

SDH incubation medium

500mM sodium succinate stock (Sigma Aldrich S2378) (0.1mL/1mL NBT stock), phenazine methosulphate (Sigma Aldrich P9625) (0.35mg/1mL NBT stock).

DHE incubation medium

Dihydroethidium (DHE) (Sigma-Aldrich D7008) 20mg/mL made up in DMSO stock, used at 1:2000 dilution in wash buffer.

Histology acidic alcohol solution

0.1% hydrochloric acid in 70% ethanol

Oil Red O stock solution

0.5g Oil Red O (Sigma Aldrich 0O625), 200mL isopropyl alcohol, incubated at 56°C for 1 hour, cooled for 20 minutes at room temperature. Stable for 6 months.

Taryn Morash

Oil Red O working solution

4 parts water to 6 parts oil red O stock solution, incubated for 10 minutes at room temperature and filtered through a 0.2μM filter. Stable for 2 hours.

Alizarin Red S working solution

1mg/mL Alizarin Red S stain (Sigma-Aldrich A5533) made up in dH2O, adjusted to pH 5.5 with ammonium hydroxide (Sigma-Aldrich 320145).

Alcian blue working solution

0.1mg/mL Alcian blue (Sigma-Aldrich A5268) made up in ethanol/acetic acid (6:4).

Immunocytochemistry

Permeability buffer

20mM Hepes, 300mM sucrose, 50mM NaCl, 0.5% Triton X100, 3mM MgCl2, 0.05% sodium azide.

Wash buffer

5% FBS (Gibco, Thermo Fisher Scientific 10270-106), 200mg sodium azide, 0.05% Triton X-100, 500mL phosphate buffered saline (PBS) (in-house preparation).

Fluorescent mounting media

Mounting media containing 2.5μg/mL 4',6-diamidino-2-phenylindole (DAPI) (DakoCytomation; DAKO Corp, Carpinteria, Calif).

Taryn Morash

Appendix 2 – Antibodies

Primary antibodies

Antibody	Source	Working dilution	Supplier	Catalogue No.
Pan MHC A4.1025	Mouse	Neat	Developmental Studies Hybridoma Bank (DSHB)	-
MHC isoform Type I A4.840 IgM	Mouse	Neat	Developmental Studies Hybridoma Bank (DSHB)	-
MHC isoform Type IIA A4.74 IgG	Mouse	Neat	Developmental Studies Hybridoma Bank (DSHB)	-
MHC isoform Type IIB BF-F3 IgM	Mouse	Neat	Developmental Studies Hybridoma Bank (DSHB)	-
Pax7	Mouse	1:1	Developmental Studies Hybridoma Bank (DSHB)	-
MyoD M-318	Rabbit	1:200	Santa Cruz Biotechnology	SC-760
Myogenin	Rabbit	1:200	Santa Cruz Biotechnology	SC-576
Laminin	Rabbit	1:100	Sigma-Aldrich	L9393
(Alpha) Smooth Muscle Actin (SMA)	Mouse	1:300	Sigma-Aldrich	A2547
Green Fluorescent Protein (GFP) (Biotin)	Goat	1:200	Abcam	AB6658
CD31	Rat	1:150	Bio-Rad	MCA2388
Collagen IV	Rabbit	1:500	Abcam	AB6586

Secondary antibodies

Antibody	Source	Working dilution	Supplier	Catalogue No.
Alexa fluor 488 IgG (anti-mouse)	Goat	1:200	Invitrogen	A-11029
Alexa fluor 488 IgG (anti-rabbit)	Goat	1:200	Invitrogen	A-11034
Alexa fluor 594 IgG (anti-mouse)	Goat	1:200	Invitrogen	A-11032
Alexa fluor 594 IgG (anti-rabbit)	Goat	1:200	Invitrogen	A-11037
Alexa fluor 488 Streptavidin	Goat	1:200	Invitrogen	S-11223
Alexa fluor 633 IgM (anti-mouse)	Goat	1:200	Invitrogen	A-21046
HRP (anti-rat)	Rabbit	1:200	Abcam	AB6734

Taryn Morash

Appendix 3 – Primers and PCR reagents

ERCC1 genotyping polymerase chain reaction (PCR) primers

Primer	Sequence
ERCC1d exon7	AGCCGACCTCCTTATGGAAA (forward for mutant allele)
ERCC1d intron7	ACAGATGCTGAGGGCAGACT (reverse for mutant allele)
ERCC1d neo	TCGCCTTCTTGACGAGTTCT
ERCC1d 3'utr	CTAGGTGGCAGCAGGTCATC

ERCC1 genotyping PCR reagents

Taq DNA Polymerase with Standard Taq Buffer (New England Biolabs M0273). Deoxynucleotide Triphosphates (dNTPs) (Promega, dATP U1205, dCTP U1225, dGTP U1215, dTTP U1235). 100bp DNA ladder (Promega G2101). SYBR™ Safe DNA Gel Stain (Thermo Fisher Scientific S33102)

Quantitative real-time polymerase chain reaction (qPCR) primers

Primer	Forward 3'	Reverse 5'
Beta sarcoglycan	GGACCGGCTCCATAAGACTG	GATGACGGCCAGGATAAACAG
Collagen Ia	TAAGGGTCCCCAATGGTGAGA	GGGTCCCTCGACTCCTACAT
Collagen IVa	GGCCCCAAAGGTGTTGATG	CAGGTAAGCCGTTAAATCCAGG
Dystrophin	ACTCAGCCACCCAAAGACTG	TGTCTGGATAAGTGGTAGCAACA
HPRT	GCTCGAGATGTCATGAAGGAGAT	AAAGAACTTATAGCCCCCCTTGA
SOD2	AGGAGAGTTGCTGGAGGCTA	CTGTAAGCGACCTTGCTCCT
VEGFa 165	TGC AGG CTG CTG TAA CGA TG	GAA CAA GGC TCA CAG TGA TTT TCT

Quantitative polymerase chain reaction (qPCR) kits and reagents

RNeasy® Mini Kit (Qiagen 74104). RNase-Free DNase Set (Qiagen 79254). RevertAid H Minus First Strand cDNA Synthesis Kit (Thermo Fisher Scientific K1631). SYBR® Green PCR Master Mix (Thermo Fisher Scientific 4309155).

Taryn Morash

Appendix 4 – Publication

Taryn Morash

Article

Mammalian Skeletal Muscle Fibres Promote Non-Muscle Stem Cells and Non-Stem Cells to Adopt Myogenic Characteristics

Taryn Morash [1], Henry Collins-Hooper [1], Robert Mitchell [1] and Ketan Patel [1,2,*]

[1] School of Biological Sciences, University of Reading, Reading RG5 4EW, UK;
t.m.morash@pgr.reading.ac.uk (T.M.); henry.collins-hooper@uk.lockton.com (H.C.-H.);
r.mitchell@reading.ac.uk (R.M.)

[2] Freiburg Institute for Advanced Studies (FRIAS), University of Freiburg, Freiburg 79104, Germany

* Correspondence: ketan.patel@reading.ac.uk; Tel.: +44-118-378-8079

Abstract: Skeletal muscle fibres are unique cells in large animals, often composed of thousands of post-mitotic nuclei. Following skeletal muscle damage, resident stem cells, called satellite cells, commit to myogenic differentiation and migrate to carry out repair. Satellite stem cells migrate on muscle fibres through amoeboid movement, which relies on dynamic cell membrane extension and retraction (blebbing). It is not known whether blebbing is due to the intrinsic properties of satellite cells, or induced by features of the myofibre surface. Here, we determined the influence of the muscle fibre matrix on two important features of muscle regeneration: the ability to migrate and to differentiate down a myogenic lineage. We show that the muscle fibre is able to induce amoeboid movement in non-muscle stem cells and non-stem cells. Secondly, we show that prolonged co-culture on myofibres caused amniotic fluid stem cells and breast cancer cells to express MyoD, a key myogenic determinant. Finally, we show that amniotic fluid stem cells co-cultured on myofibres are able to fuse and make myotubes that express Myosin Heavy Chain.

Keywords: stem cell; muscle; myofibre; adipose-derived stem cell; dental pulp; amniotic fluid stem cells; reprogramming; migration; amoeboid

1. Introduction

Skeletal muscle is imbued with a stem cell resident population called satellite cells (SC), which have a huge capacity to regenerate damaged tissue [1]. Transplantation of a single muscle fibre containing a few SC is able to generate tens of thousands of cells in a matter of weeks [1]. SC also have remarkable migratory properties, demonstrated by their ability to move from undamaged muscles, into areas that require repair [2,3]. However, in a disease context, the ability of SC to promote repair is severely hampered, for a number of reasons. Firstly, it is believed that repeated rounds of degeneration/regeneration, leads to an exhaustion of the stem cell pool [4]. Secondly, the development of a fibrotic and adipogenic environment impacts on not only SC differentiation, but also on their ability to migrate [5]. A number of studies have demonstrated the importance of migration in the muscle repair process. Clinical interventions based on myoblast injections have failed, since cells are rarely dispersed more than 200 μm from the site of application [6–8]. Therefore, there is an unmet need to generate cells with the appropriate ability to migrate, thus facilitating clinical skeletal muscle generation.

We have previously shown that skeletal muscle fibres promote SC to migrate, using a distinctive amoeboid-based mechanism in which cells extend and retract numerous membrane protrusions,

often one tenth of the diameter of the cells, within a couple of minutes [9,10]. Amoeboid-based migration is thought to develop simple focal adhesions (reviewed by [11]), and is believed to generate traction through multiple blebs, all of which generate small amounts of pull [12]. The matrix appears to be the defining factor governing how SC migrate, since placing them on plastic surfaces results in the formation of lamellipodia [10].

The surface matrix not only governs the mechanism of migration, but also directs the fate of stem cells. Engler and colleagues showed that the matrix elasticity directed the specification of stem cells into either neural, myogenic, or osteogenic lineages [13]. They demonstrated that the stiffness, over two orders of magnitude (ranging from 1 to 100 kPa), regulated the differentiation of human mesenchymal stem cells, into either neurons, skeletal muscle, or bone [13]. Subsequent work showed that changes in tissue stiffness (induced, for example, through fibrosis) had a major impact on the self-renewing properties of SC [14].

Our previous work has shown that SC adopted amoeboid-based migration when positioned on muscle fibres. However, it is not known whether this property is solely due to features of SC, or those of the muscle fibre. Secondly, it is not known whether the amoeboid-based migration is an option available to all stem cells, or even somatic cells, when they encounter the muscle fibre matrix. Lastly, it remains to be determined whether the surface of a muscle fibre could influence the fate of, not only stem cells, but also non-stem cells.

In this study, we examined the impact of the muscle fibre matrix on, firstly, the migratory properties and, secondly, the ability to promote a myogenic fate on three well-defined stem cell populations, as well as one non-stem cell line. We chose adipose-derived mesenchymal stem cells (ADMSC), dental pulp stem cells (DP), and amniotic fluid stem cells (AFS) for our investigation, as these have been extensively characterised for multi-potency, are relatively easy to culture, and are in advanced stages of development as therapeutic agents for human diseases [15–19]. The MDA-MB-231 breast cancer line (MDA) was chosen as a non-stem cell source as it is extremely easy to propagate and is well characterised. Here, we show that all three of the stem cell lines and the one non-stem cell line, migrated by the mesenchymal mechanism on plastic. However, once they were seeded on mouse muscle fibres, they adopted amoeboid-based migration. We also show that all of the cells which adopted amoeboid-based migration were underpinned by the same molecular mechanisms; ROCK (Rho-associated protein kinase) activity promoted blebbing, whereas Arp2/3 inhibited blebbing. Most remarkably, we show that simple contact of AFS and MDA at the surface of a muscle fibre was sufficient for cells to induce the expression of the key myogenic determinant, MyoD. Finally, we show that AFS cells grown on myofibres are able to form myotubes.

2. Material and Methods

2.1. Ethical Approval

The experiments were performed under a project license from the United Kingdom (UK) Home Office, in agreement with the Animals (Scientific Procedures) Act 1986.

2.2. Animal Maintenance

Healthy male wild-type C57BL/6 mice (3–5 month-old) were maintained in accordance with the Animals (Scientific Procedures) Act 1986 (UK), and were approved by the University of Reading in the Biological Resource Unit of Reading University. Mice were housed under standard environmental conditions (20–22 °C, 12–12 h light–dark cycle), and were provided with food (standard pelleted diet) and water *ad libitum*.

2.3. Cell Lines and Cultures

Cells transplanted onto mouse myofibres were identified using GFP-labelled cells. Human adipose-derived mesenchymal stem cells (ADMSC) (Life Technologies 510070, Carlsbad, CA, USA) were grown in MesenPro RS™ medium, supplemented with 1% penicillin streptomycin (Thermo Fisher

Scientific, Carlsbad, CA, USA). Human amniotic fluid stem cells (AFS) (GFP[+]) (Gift from Prof. Paolo De Coppi, University College London) were grown in Minimum Essential Medium (alpha modification) (α-MEM), 15% foetal bovine serum (FBS), 1% L-glutamine, and 1% penicillin streptomycin (Thermo Fisher Scientific) supplemented with 20% Chang B/C media (Irvine Scientific, Santa Ana, CA, USA). Rat dental pulp stem cells (DP) (GFP[+]; Isolated from SD-Tg(CAG-EGFP)CZ-004OS6 rats) (Gift from Professor Bing Song, Cardiff, UK) [20] were cultivated in α-MEM, 20% FBS, 1% L-glutamine, 1% penicillin-streptomycin (Thermo Fisher Scientific), and 100 mM L-ascorbic acid (Sigma-Aldrich, Saint Louis, MO, USA). A MDA-MB-231 (GFP[+]) breast adenocarcinoma cell line (MDA) (Gift from Prof. P. Dash, University of Reading) was cultivated in DMEM containing GlutaMAX, supplemented with 10% FBS, 1% L-glutamine, and 1% penicillin streptomycin (Thermo Fisher Scientific).

2.4. Single Myofibre Isolation and Culture

Animals were humanely sacrificed via Schedule 1 killing and myofibres were isolated from the *Extensor digitorum longus* (EDL) muscle of the hindlimb, as previously described [21,22]. Briefly, the EDL was carefully dissected and myofibres were dissociated with 0.2% type I collagenase in Dulbecco's modified Eagle medium (DMEM) at 37 °C in 5% CO_2. Using tapered glass pipettes, individual myofibres were liberated and placed into a suspension culture with single fibre culture medium (SFCM) consisting of DMEM containing GlutaMAXm supplemented with 10% horse serum, 1% penicillin/streptomycin, and 5% chick embryo extract, and were incubated at 37 °C in 5% CO_2. Cultures consisted of myofibres which had been isolated from three to nine animals, and were combined in order to maintain consistency and homogeneity among experimental conditions. Experimental time-zero (T0) began at the point of myofibre isolation. A total of 250,000 cells of each cell type were seeded into separate single myofibre suspension cultures for 2 h (T0–T2), at 37 °C in 5% CO_2, allowing for cell-myofibre adherence. At T2, myofibres (with non-muscle cells attached) were transferred to new culture wells with fresh SFCM.

2.5. Cytoskeletal Inhibitor Preparation

The ROCK inhibitor Y-27632 (Abcam 120129, Cambridge, UK) was used at a concentration of 10 μg/mL. The Arp2/3 inhibitor CK666 (Abcam 141231) was used at 150 μM. The required concentrations of inhibitors were made up in SFCM.

2.6. Time-Lapse Microscopy

Myofibre cultures were examined using phase-contrast microscopy with time-lapse capabilities, as previously described [9], but with the following differences: time-lapse video was captured at 10× magnification, at a rate of one frame per 15 min over a 12-h period (T2–T14), prior to endogenous satellite stem cell emergence and proliferation [23].

2.7. Myotube Formation

Myofibres were cultured with or without transplanted non-muscle cell types, at 37 °C in 5% CO_2 for up to 10 days (T240), and the fresh media (SFCM) was changed every three days. Cells were dissociated from myofibres with TrypLE™ Select Enzyme (Thermo Fisher Scientific), seeded onto cell culture-treated glass cover slips, and grown in cell-specific (AFS or MDA) growth medium (GM). Once confluent, GM was exchanged for a myogenic differentiation medium consisting of DMEM with GlutaMAX, containing 2% horse serum and 1% penicillin/streptomycin (Thermo Fisher Scientific), and this was cultured for up to 14 days before fixation in 4% paraformaldehyde (PFA) in phosphate buffered saline (PBS) for 15 min, after which it was stored in PBS.

2.8. Immunocytochemistry

Immunocytochemistry protocols for examining resident and transplanted non-muscle cells on single myofibres were carried out as described previously [23]. Briefly, myofibres (or cell/ myotube

cultures) were fixed in 4% paraformaldehyde in phosphate buffered saline (PBS) (PFA) for 10 min, and were washed three times in PBS before permeabilisation in a buffer solution, consisting of 20 mM HEPES, 300 mM sucrose, 50 mM NaCl, 3 mM $MgCl_2$, 0.5% Triton X-100, and 0.05% sodium azide (pH 7), at 4 °C for 15 min. Following this, non-specific binding was blocked using a wash buffer with 5% FBS, in PBS containing 0.01% Triton X-100 and 200 mg sodium azide, for 30 min at room temperature. The primary antibodies used in this study included: polyclonal rabbit anti-MyoD (Santa Cruz Biotechnology, Dallas, TX, USA), sc-760, 1:200), monoclonal mouse anti-actin (alpha smooth muscle) (Sigma-Aldrich, A2547, 1:200), polyclonal goat anti-green fluorescent protein (GFP) (biotin) (Abcam, ab6658, 1:200), and monoclonal mouse anti-Myosin Heavy Chain (MHC) (Developmental Studies Hybridoma Bank (DSHB) clone A4.1025, 1:1). Primary antibodies were visualised using the following secondary antibodies: Alexa Fluor goat anti-mouse 488 (Invitrogen, Carlsbad, CA, USA, A11029), Alexa Fluor goat anti-mouse 594 (Invitrogen, A11032), Alexa Fluor goat anti-rabbit 594 (Invitrogen, A11037), and Alexa Fluor 488 Streptavidin (Molecular Probes, Carlsbad, CA, USA, S-11223). Secondary antibodies were used at a scale of 1:200. To visualise non-GFP hADMSCs, a PKH26 red fluorescent membrane labelling kit was used, according to the manufacturer's instructions (Sigma-Aldrich, PKH26GL). Myofibres were mounted in fluorescent mounting medium (DAKO) containing 5 μg/mL 4′,6-diamidino-2-phenylindole-(DAPI) for nuclear visualisation.

2.9. Fluorescence Microscopy

Mounted myofibres were visualised using a Zeiss AxioImager fluorescent microscope and images were captured using an Axiocam digital camera system, before being analysed using Axiovision image analysis software (version 4.9.1) (Carl Zeiss AG, Oberkochen, Germany).

2.10. Scanning Electron Microscopy

Scanning electron microscopy (SEM) of single myofibres was carried out as previously described [9]. Briefly, single myofibres were fixed in 4% PFA/PBS for 10 min and dehydrated through a series of 15-min ethanol incubations (30%, 50%, 70%, 80%, 90%, and 100% ethanol solutions). Following this, myofibres were transferred to a critical point drier (Balzers CPD 030) (Oerlikon Balzers, Balzers, Liechtenstein) and further dehydrated using liquid carbon dioxide. Using micro forceps, dried myofibres were transferred to SEM sample stubs, and were gold-coated using an Edwards S150B sputter-coater (HHV, Crawley, UK), before being visualised using an FEI 600F SEM (FEI, Hillsboro, OR, USA) and supporting analysis software for image generation.

2.11. Image and Movie Analysis

All image analysis was carried out using the freeware package ImageJ (version 1.4.3) (Bethesda, MA, USA). Individual resident and non-muscle cells were manually tracked using the MTrackJ plugin. Bleb numbers and dimensions were quantified manually on SEM images of cells, using the cell counter and length measurement tools. Blebs were counted across the visible extent of the cell surface in each SEM image [9]. Measurements consisted of the bleb height from the individual point of protrusion, outwards from the cell surface to the boundary of each single bleb, as well as the measurement across each bleb to obtain the width. Cell morphology analysis of resident satellite cells and non-muscle cell types on myofibres, as well as an investigation into the effects of differing inhibitor treatments and the capacity for myogenic differentiation of non-muscle cells into myotubes, were all manually assessed using quantification of live images through the Zeiss Axio Imager microscope (Carl Zeiss AG, Oberkochen, Germany)and Axiovision digital camera system (Carl Zeiss AG, Oberkochen, Germany). The percentage of myotubes produced by non-muscle cells, was quantified as the number of nuclei located within myosin-positive cell structures, as a proportion of the total nuclei.

2.12. Statistical Analysis

Statistical analysis was performed using Student's *t*-tests, unless otherwise indicated, with significance levels of * $p < 0.05$, ** $p < 0.01$, and *** $p < 0.001$, using GraphPad Prism statistical software (Version 6) (La Jolla, CA, USA). All data are presented as mean $\pm$ standard error of the mean.

3. Results

Skeletal muscle stem cells display three interesting properties when examined on muscle fibres, their native surface: (1) cells are round in shape rather than flat, with a broad leading edge; (2) migrate at very high speeds; and (3) readily activate along the skeletal muscle differentiation pathway. Here, we examined whether these properties are due to a feature of the muscle fibre, or intrinsic to the SC.

Firstly, we characterised the influence of the matrix on the mechanisms used for cell migration. To that end, we compared the cell morphology of the differing cells on plastic versus muscle fibres. Our results show that, like most SC, ADMSC, AFS, and DP stem cells on plastic, took on a flattened elongated form (mesenchymal) (Figure 1(A, C1–C3)). In contrast to this, the majority of MDA cells were rounded (Figure 1(A, C4)). We then compared this profile to the same cells on the surface of a muscle fibre. As previously described, we found that all SC assumed a rounded morphology (Figure 1B) [10]. Surprisingly, there was a significant increase in the proportion of rounded morphologies in all of the other cell types examined, when they were juxtapositioned on muscle fibres (Figure 1(B, C5–C8)). These results show that the rounded morphology adopted by muscle stem cells, are not a unique intrinsic feature. Instead, all cells tested, either stem or non-stem, assume this form when they encounter the surface of a muscle fibre.
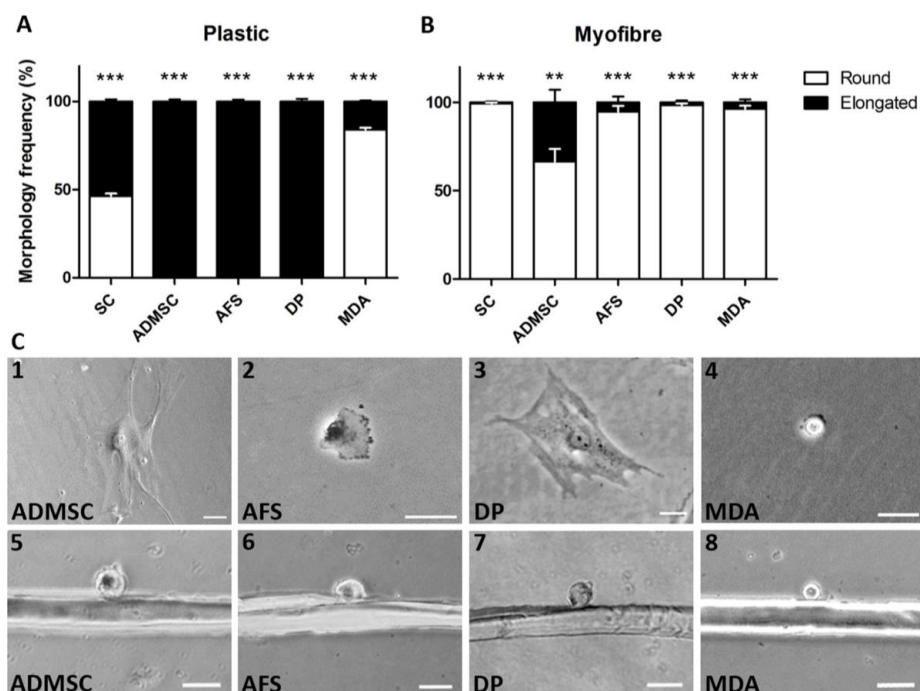

Figure 1. The skeletal myofibre matrix influences non-muscle cellular morphologies. (**A**) Frequencies of morphologies adopted by satellite cells (SC, *n* = 21 cells examined), adipose-derived mesenchymal stem cells (ADMSC, *n* = 52), amniotic fluid stem cells (AFS, *n* = 32), dental pulp stem cells (DP, *n* = 26) and MDA-MB-231 breast cancer cells (MDA, *n* = 31), on plastic; (**B**) Cell morphologies displayed by SC (*n* = 45 myofibres examined), ADMSC (*n* = 34), AFS (*n* = 35), DP (*n* = 26), and MDA (*n* = 43), on myofibres; (**C**) Representative morphologies of non-muscle cells observed on plastic (**1–4**) and on myofibres (**5–8**). Scale 50 μm. Individual Student's *t*-tests showed statistical significance between 'Round' and 'Elongated' morphologies in each cell type, ** $p < 0.01$, *** $p < 0.001$.

Next, we examined the influence of the matrix on cell migration speed, having previously shown that SC on muscle fibres travelled at high velocities, when compared to their movement on plastic [9,10]. In this study, we demonstrated that SC on myofibres moved at a higher speed than on plastic, thus reproducing our previous findings (Figure 2A) [10]. The ability of the myofibre surface to support faster movement than that of a plastic surface, was also found with DP and MDA (Figure 2A). In contrast, ADMSC and AFS cells showed a significant decrease in migration speed on muscle fibres, when compared to plastic (Figure 2A). Next, we examined the migration speeds of the differing cell morphologies on muscle fibres. We found that for ADMSC, DP, and MDA cells, migration speed was not influenced by the structure of the cell (Figure 2B). Surprisingly, we found that rounded AFS cells on muscle fibres moved slower than those with elongated characteristics (Figure 2B).
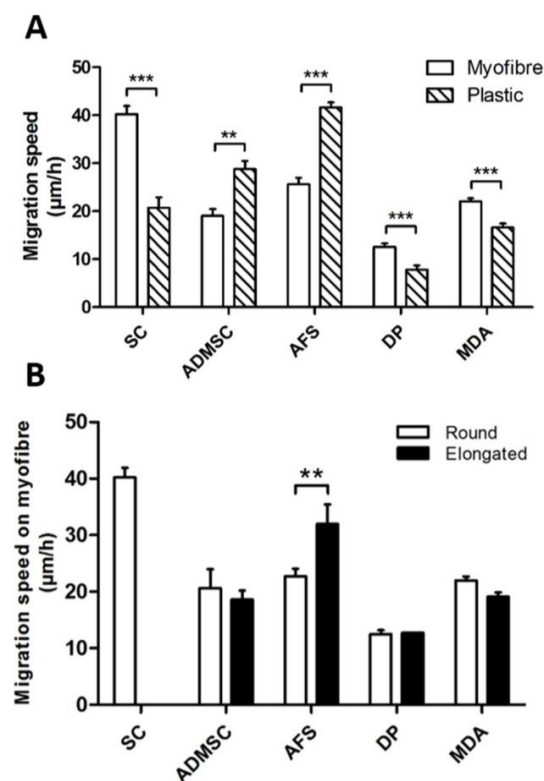

Figure 2. The skeletal muscle myofibre impacts on the migration speed of co-cultured non-muscle cells. (**A**) Cell migration speed comparison between plastic and myofibre substrates; (**B**) Migration speeds of differing morphologies of resident and non-muscle cells on myofibres. In all conditions $n \geq 15$ myofibres examined. Individual Student's *t*-tests, ** $p < 0.01$, *** $p < 0.001$.

We have previously shown that the activity of ROCK was a key determinant of the rounded/blebbing satellite cell morphology, when placed on muscle fibres [9,10]. In contrast, much work has shown that the leading edge of mesenchymal cells required the activity of Arp2/3, in order to promote the formation of lamellipodia [24]. Here, we examined the consequences of inhibiting ROCK and Arp2/3 with their specific inhibitors, Y-27632 and CK666, respectively, on cell migration velocity and morphology [25,26]. We found that inhibiting ROCK decreased the migratory speed of all cells examined, when compared to mock treated cells (solvent only) (Figure 3A). In contrast, inhibiting Arp2/3 activity only decreased the migration speed of ADMSCs (Figure 3A). We also examined the influence of the inhibitors on cell morphology. For all cell types, we found that inhibition of ROCK promoted the abundance of elongated cells, whereas CK666 increased the proportion of rounded cells (Figure 3B). These results show that molecular mechanisms regulating migration, are conserved in a diverse group of cells.
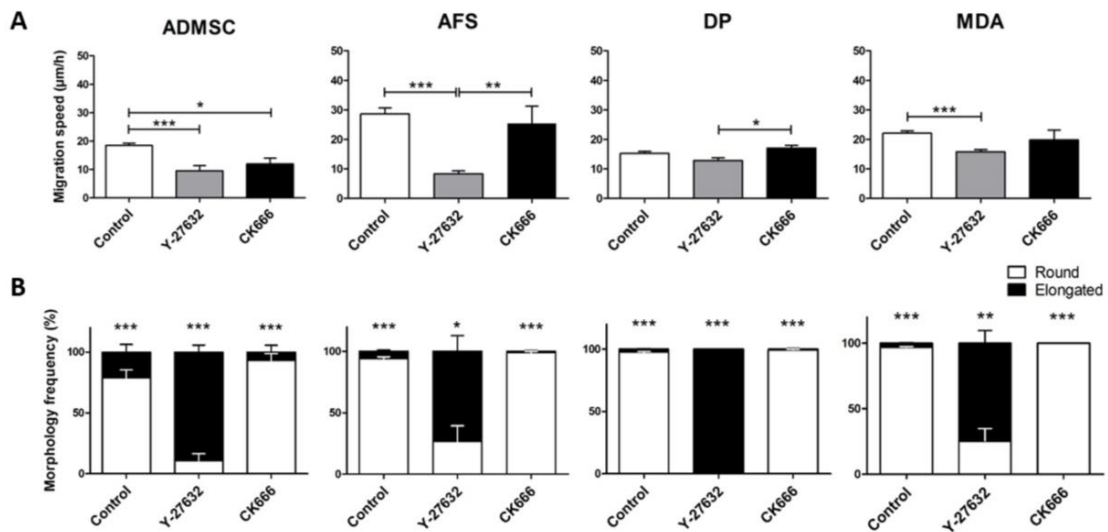
Figure 3. Examining the activity of ROCK and Arp2/3 in cell migration and morphologies. (**A**) Effect of inhibiting ROCK (Y-27632) and Arp2/3 (CK666) on cell migration on muscle myofibres; (**B**) Effect of inhibiting ROCK (Y-27632) and Arp2/3 (CK666) on cell morphology frequencies. In all conditions $n \geq 15$ myofibres examined. One-way ANOVA (**A**), individual Student's *t*-tests (**B**), * $p < 0.05$, ** $p < 0.01$, *** $p < 0.001$. In (**B**) statistical differences indicated between proportion of rounded and elongated cell numbers.

Next, we examined non-muscle stem cells for the presence of blebs, a key feature of amoeboid migration. We have previously shown that SC on myofibres use the amoeboid mechanism for cell movement, which manifests as a huge number of highly dynamic plasma membrane protrusions [10]. We found that, in all cell types examined, decreasing the Arp2/3 activity resulted in an increase in the number of blebs on the surface of cells located on muscle fibres (Figure 4A, C–F and K–N). However, the dimensions of the blebs in terms of their heights and widths, were not affected to any great degree, with Arp2/3 inhibition increasing only the width of blebs on the surface of MDA cells (Figure 4B). As previously demonstrated, inhibiting ROCK resulted in elongated cells that did not contain any blebs (Figure 4A,G–J).

These results show that the mechanisms underpinning blebbing are highly conserved, with ROCK activity responsible for maintaining a rounded profile and Arp2/3 controlling lamellipodia formation.
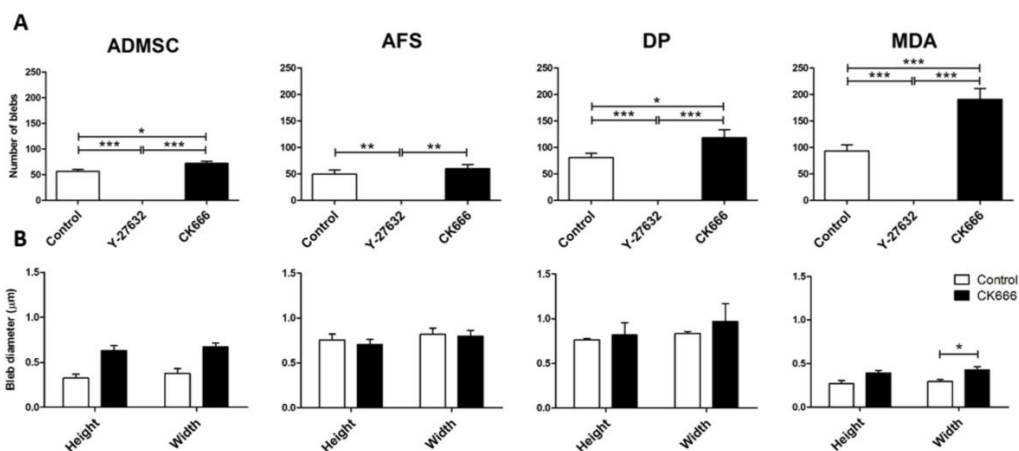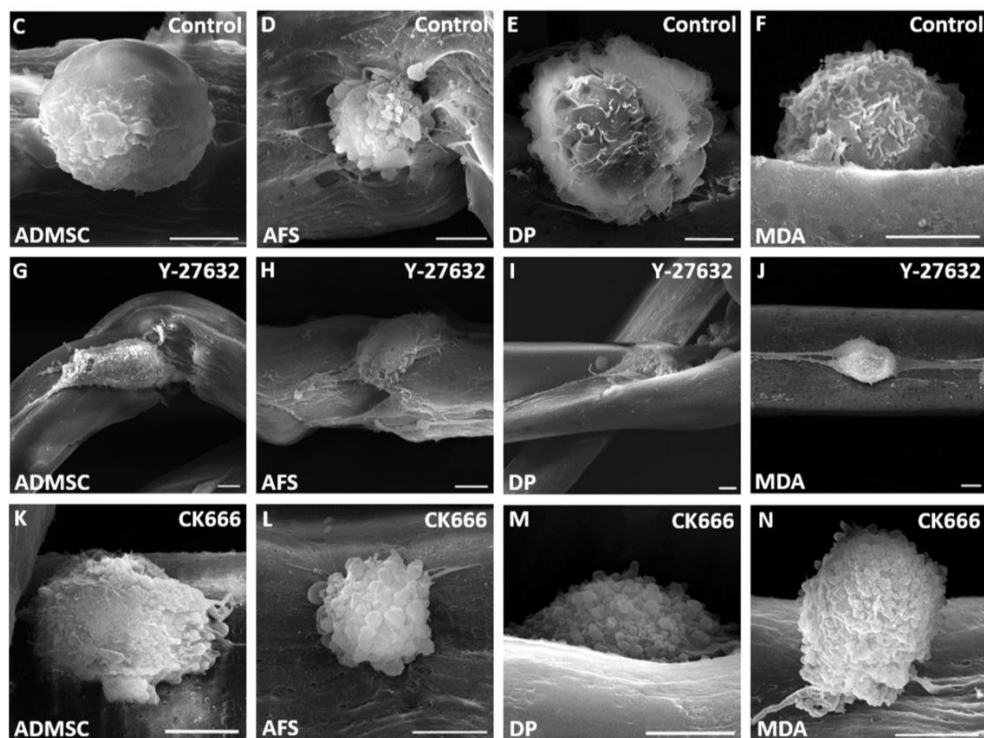

Figure 4. *Cont*.

Figure 4. Influence of ROCK and Arp2/3 on cell surface characteristics of non-muscle cells on myofibres. (**A**) Quantification of bleb numbers on non-muscle cells following ROCK (Y-27632) and Arp2/3 (CK666) inhibition; (**B**) Bleb dimensions. Scanning electron microscopy (SEM) images of the transplanted cell types treated with solvent only (**C**–**F**), ROCK inhibitor (**G**–**J**) and Arp2/3 inhibitor (**K**–**N**). Scale 5 μm. 6 cells examined per condition. One-way ANOVA (**A**), individual Student's *t*-tests (**B**), * $p < 0.05$, ** $p < 0.01$, *** $p < 0.001$.

Finally, we examined whether the myofibre surface encourages cells to adopt a myogenic fate. To that end, we seeded GFP$^+$ non-muscle stem cells, as well as GFP$^+$ MDA cells, onto freshly isolated muscle fibres, and profiled the expression of markers for muscle precursors (Pax7), committed muscle cells (MyoD), and differentiating muscle cells (Myogenin) [23]. Resident SC (non-GFP) expressed Pax7 on freshly isolated cells and continued to do so until 48 h, after which its presence gradually decreased, which is in agreement with previous studies [23,27]. MyoD is not expressed in freshly isolated SC, but is known to become detectable 24 h after activation [23]. Our data, in concordance with the literature, showed that MyoD was present in over 80% of cases after 24 h of culture (Figure 5A). Between 48 and 120 h of culture, all SC on myofibres expressed MyoD, which then decreased by 240 h, which has previously been shown to be replaced by the expression of Myogenin (Figure 5A) [23].

None of the non-muscle cells expressed Pax7 at any time point up to 240 h of culture. Non-muscle stem cells initially adopted rounded morphologies, up to approximately 48 h after seeding on freshly isolated fibres, but then took on one of two morphologies. ADMSC and DP cells gradually elongated, especially around the circumference of the fibres, and thereafter caused constrictions (Figure 5B,C). By 72 h, there were no normal elongated fibres in the presence of ADMSC and DP cells, with the vast majority either curled into balls or hyper-contracted, both of which signify myofibre damage.

In contrast, AFS and MDA maintained a rounded morphology and proliferated profusely (Figure 5D,E). Of significance was the finding that by 240 h, approximately 50% of AFS and MDA cells robustly expressed MyoD.

To investigate further, the myogenic differentiation potential of the non-muscle cells, as observed with dissociated SC in previous studies [23], and their ability to form myotube structures following enzymatic dissociation from the myofibres, was determined. Our results showed that AFS cells that had

been dissociated from myofibres, fused to create elongated myotubes, indicated by myotube formation with the co-expression of GFP$^+$ and MHC, a key to the contractile protein of muscle (Figure 5F). However, MDA cells that had also been detached from myofibres after 240 h of culture, failed to express MHC, and showed no fusion events. Instead, they proliferated, producing multiple cell layers (Figure 5H). Approximately 8% of all the AFS cells expressed MHC (Figure 5H) and formed cells with 1.5 nuclei (Figure 5I). Notably, no myogenic differentiation characteristics were observed in MDA or AFS cells, which had not previously been in contact with myofibres.

These results show that the myofibre surface is unable to promote the expression of a marker of muscle precursor cells (Pax7). However, prolonged culture of one stem cell (AFS) and remarkably, one somatic cancer cell (MDA), resulted in the robust expression of a marker of committed muscle cells, MyoD. Additionally, AFS cells cultured for prolonged periods with isolated myofibres, are able to form myotubes.
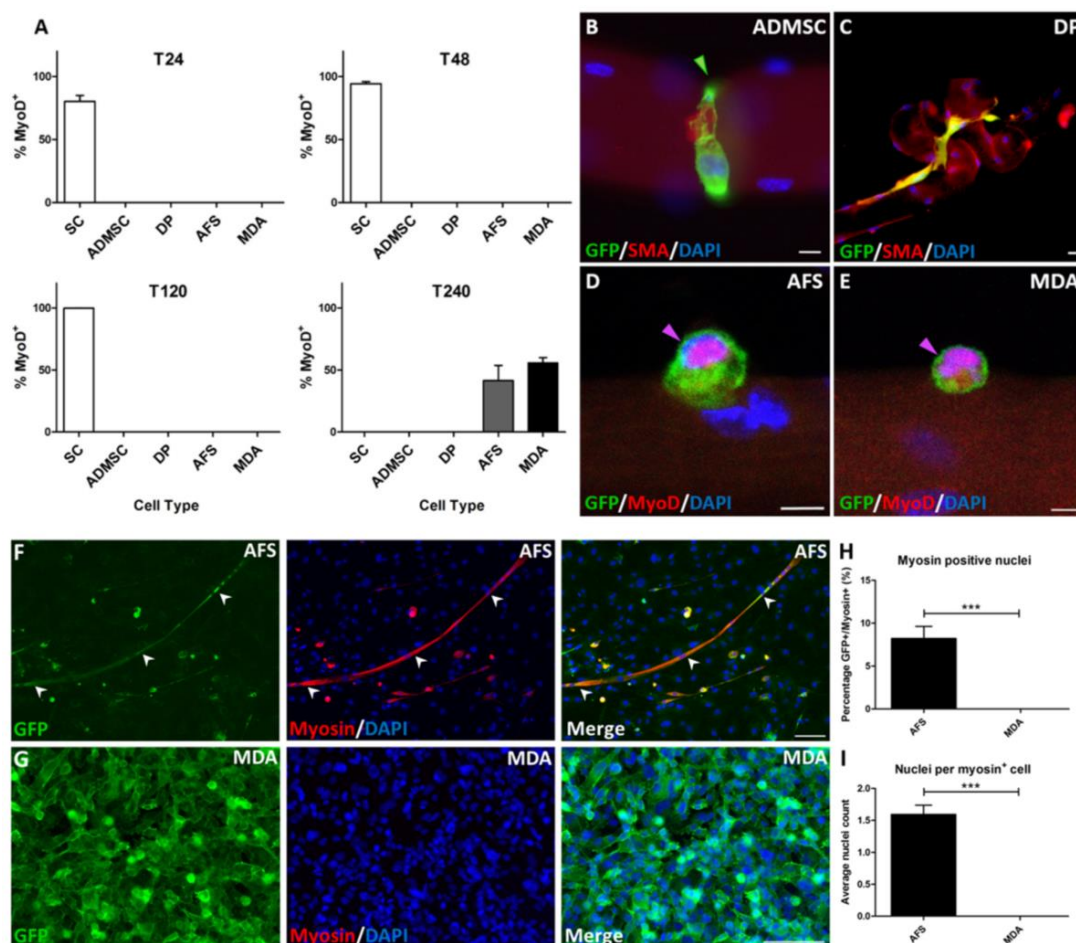

Figure 5. Induction of MyoD expression in AFS and MDA cells after prolonged culture on mouse myofibres. (**A**) Temporal profiling of non-resident cells on myofibres for MyoD expression; (**B**) ADMSC identified by GFP expression, constricting myofibre at T24; (**C**) DP cell distorting myofibre at T24; (**D**) AFS cell at T240 showing nuclear expression of MyoD co-localising with DAPI (indicated by magenta arrow); (**E**) MDA cell at T240 showing nuclear expression of MyoD co-localising with DAPI (indicated by magenta arrow); (**F**) AFS cells, identified by GFP expression, co-localising with myosin, fused to form elongated myotube structures (arrowheads); (**G**) MDA cells co-cultured with myofibres failed to initiate myosin expression; (**H**) Quantification of GFP$^+$ cells expressing myosin; (**I**) Number of nuclei per cell GFP$^+$ expressing myosin. Scale 10 μm (**B**–**E**), and 100 μm (**F**, **H**). In (**A**–**E**), $n \geq 12$ myofibres examined.

4. Discussion

The development of a source of muscle cells has huge clinical implications. Muscle is lost in a large number of diseases such as Duchenne Muscular Dystrophy and Spinal Muscular Atrophy, but is also a societal problem, as wasting occurs in a large proportion of the elderly who suffer from a condition called sarcopenia [28]. Therefore, any means of generating muscle would potentially be of great therapeutic value.

Previous work has shown that matrix elasticity has profound effects on cell fate, with stiff surfaces promoting the formation of bone, medium stiffness inducing muscle, and soft surfaces allowing the formation of neural tissues [13]. Here, we investigated the effect of the muscle fibre surface on stem cell migration and differentiation. We have previously shown that the muscle fibre supports a distinct form of movement, called amoeboid-based migration. Here, we show that three stem cell types, and one non-stem cell line, adopted amoeboid-based migration when seeded onto muscle fibres. Furthermore, they developed blebs, which made them essentially indistinguishable from resident stem cells. However, it is noteworthy that an adoption of amoeboid-based migration for non-muscle cells was not always accompanied by an increase in migration speed. It was previously proposed that rapid movement based on bleb-based migration, was partly due to the simplicity of the focal adhesions between the cells and the matrix, with less time being needed to assemble and disassemble these structures [29]. However, our results show that blebbing does not always result in increased migration, possibly due to a mis-match in the molecules needed for effective focal adhesion formation. We suggest that non-muscle cells and satellite cells form different focal adhesions with the muscle fibre, possibly linked to their developmental history. The concept of developmental history regulating cell behaviour is well mapped in muscle, where it even segregates the properties of muscle stem cells [29]. Despite differing profiles of migration speeds, we show that the cell morphology adopted by non-muscle cells on fibres is regulated by the same molecular pathways. Elegant work by the Marshall lab have shown that blebbing and lamellipodia-based mechanisms, act in an antagonistic fashion with Rho, through ROCK supporting the former, and Rac, via WAVE2, promoting the latter [30]. Here, we show that this relationship was conserved in the three differing stem cells and the one non-stem cell.

Our work sheds new light on a possible injurious role of ADMSC in chronic muscle degeneration/regeneration. Accumulation of fat tissue is a key feature of this condition, for example, in Duchenne Muscular Dystrophy, and is believed to hinder the activity of SC. [31,32]. However, our work reveals a more direct property of ADMSC that would contribute to muscle pathology, based on our finding that they induce fibre hyper-contraction. We were unable to find any live muscle fibres that had been co-cultured with ADMSC after three days in culture. In contrast, the fibres with the presence of other cells (e.g., AFS) are viable for a minimum of 10 days. Therefore, unregulated activity of ADMSC may contribute to muscle pathology by inducing myofibre death.

The most intriguing aspect of our work is the finding that AFS and MDA cells adopted a myogenic fate, as assessed by MyoD expression, and that AFS cells tfuse into MHC$^+$ myotubes. Importantly, we found that they developed this state without having first induced the expression of Pax7. This is significant, as it implies that the cells are not deploying a molecular programme that is used during normal development [33]. The expression of MyoD, but not Pax7, in adult cells has been interpreted to indicate a state in which the only option is terminal differentiation, without a possibility of reverting to a stem cell state [23]. This has major implications for future exploitation of our findings, as they could only be used to carry out immediate repair of damaged tissue, but the cells themselves could not be a reservoir for future rounds of muscle regeneration.

One major outcome of our work is that it shows that there is no necessity for using stem cells in order to generate muscle cells. Stem cells are associated with issues related to ethics and specialised isolation techniques [34]. However, we have shown that a rapidly growing non-muscle stem cell can be converted at relatively highly frequency into cells that express MyoD. Importantly, as an extension to this key finding, further investigation into the myogenic differentiation potential revealed that AFS cells, but not the non-stem cell, were directed through the exposure to the muscle environment, to form

myotube structures, reinforcing the potential therapeutic value of AFS cells. Therefore, we have further established the influence that the microenvironment or matrix has on regenerative processes, such as cell differentiation and fusion.

There are two major issues that we will resolve in future experiments, to determine the full potential of our finding. Firstly, it would be ideal to minimise the use of a large number of small animals for scale-up as a source of muscle matrix. To that end, we envisage using de-cellularised muscle from bigger (commercial) species (bovine), which can be generated in large quantities [35]. A number of advances have recently been made in creating materials often involving electrospinning, that direct either a partial or complete move away from man/animal tissues for use in muscle-based pathologies [36]. Many of the artificial materials support the differentiation and fusion of muscle stem cells, into ordered myotubes [37]. However, none, to our knowledge, have investigated the movement of SC in these matrixes, nor whether they occur in an amoeboid manner, let alone if their physical properties support myogenic conversion of non-muscle cells. Investigating migratory mechanisms and myogenic reprogramming by de-cellularised muscle and artificial muscle-like materials, will be the focus of our future investigations.

Secondly, it will be essential to characterise the key properties of myogenic cells induced by the co-culture method deployed here. To that end, it will be necessary to determine whether these cells can promote muscle regeneration. We will address this line of investigation by developing GFP-labelled MyoD$^+$ cells from both AFS and MDA, and injecting them into immunocompromised mice which have undergone cardiotoxin-induced muscle degeneration, before assessing the development of GFP$^+$ muscle fibres [38].

5. Conclusions

We show that the muscle fibre matrix is able to promote non-muscle cell movement based on amoeboid-based migration. Both non-muscle stem cells and non-stem cells are amenable to myofibre-based reprogramming of migration mechanisms. We also show that cell fate is reprogrammable by the muscle fibre matrix, resulting in a robust expression of the myogenic marker MyoD, in both AFS and MDA cells. Moreover, we demonstrate a greater myogenic differentiation capability of AFS cells, following dissociation from the myofibre matrix, leading to myosin expression and myotube formation.

Author Contributions: "K.P. conceived and designed the experiments; T.M., H.C.-H. and R.M. performed the experiments; T.M., R.M. and K.P. analyzed the data; K.P. wrote the paper." Authorship must be limited to those who have contributed substantially to the work reported.

Conflicts of Interest: The authors declare no conflict of interest.

References

1. Collins, C.A.; Olsen, I.; Zammit, P.S.; Heslop, L.; Petrie, A.; Partridge, T.A.; Morgan, J.E. Stem cell function, self-renewal, and behavioral heterogeneity of cells from the adult muscle satellite cell niche. *Cell* **2005**, *122*, 289–301. [CrossRef] [PubMed]

2. Watt, D.J.; Karasinski, J.; Moss, J.; England, M.A. Migration of muscle cells. *Nature* **1994**, *368*, 406–407. [CrossRef] [PubMed]

3. Watt, D.J.; Morgan, J.E.; Clifford, M.A.; Partridge, T.A. The movement of muscle precursor cells between adjacent regenerating muscles in the mouse. *Anat. Embryol. (Berl.)* **1987**, *175*, 527–536. [CrossRef] [PubMed]

4. Sacco, A.; Mourkioti, F.; Tran, R.; Choi, J.; Llewellyn, M.; Kraft, P.; Shkreli, M.; Delp, S.; Pomerantz, J.H.; Artandi, S.E.; et al. Short telomeres and stem cell exhaustion model duchenne muscular dystrophy in mdx/mTR mice. *Cell* **2010**, *143*, 1059–1071. [CrossRef] [PubMed]

5. Mu, X.; Urso, M.L.; Murray, K.; Fu, F.; Li, Y. Relaxin regulates MMP expression and promotes satellite cell mobilization during muscle healing in both young and aged mice. *Am. J. Pathol.* **2010**, *177*, 2399–2410. [CrossRef] [PubMed]

6. Peault, B.; Rudnicki, M.; Torrente, Y.; Cossu, G.; Tremblay, J.P.; Partridge, T.; Gussoni, E.; Kunkel, L.M.; Huard, J. Stem and progenitor cells in skeletal muscle development, maintenance, and therapy. *Mol. Ther.* **2007**, *15*, 867–877. [CrossRef] [PubMed]

7. Lafreniere, J.F.; Mills, P.; Tremblay, J.P.; El Fahime, E. Growth factors improve the in vivo migration of human skeletal myoblasts by modulating their endogenous proteolytic activity. *Transplantation* **2004**, *77*, 1741–1747. [CrossRef] [PubMed]

8. Satoh, A.; Huard, J.; Labrecque, C.; Tremblay, J.P. Use of fluorescent latex microspheres (flms) to follow the fate of transplanted myoblasts. *J. Histochem. Cytochem.* **1993**, *41*, 1579–1582. [CrossRef] [PubMed]

9. Collins-Hooper, H.; Woolley, T.E.; Dyson, L.; Patel, A.; Potter, P.; Baker, R.E.; Gaffney, E.A.; Maini, P.K.; Dash, P.R.; Patel, K. Age-related changes in speed and mechanism of adult skeletal muscle stem cell migration. *Stem Cells* **2012**, *30*, 1182–1195. [CrossRef] [PubMed]

10. Otto, A.; Collins-Hooper, H.; Patel, A.; Dash, P.R.; Patel, K. Adult skeletal muscle stem cell migration is mediated by a blebbing/amoeboid mechanism. *Rejuvenation Res.* **2011**, *14*, 249–260. [CrossRef] [PubMed]

11. Charras, G.; Paluch, E. Blebs lead the way: How to migrate without lamellipodia. *Nat. Rev. Mol. Cell Biol.* **2008**, *9*, 730–736. [CrossRef] [PubMed]

12. Tozluoglu, M.; Tournier, A.L.; Jenkins, R.P.; Hooper, S.; Bates, P.A.; Sahai, E. Matrix geometry determines optimal cancer cell migration strategy and modulates response to interventions. *Nat. Cell Biol.* **2013**, *15*, 751–762. [CrossRef] [PubMed]

13. Engler, A.J.; Sen, S.; Sweeney, H.L.; Discher, D.E. Matrix elasticity directs stem cell lineage specification. *Cell* **2006**, *126*, 677–689. [CrossRef] [PubMed]

14. Gilbert, P.M.; Havenstrite, K.L.; Magnusson, K.E.; Sacco, A.; Leonardi, N.A.; Kraft, P.; Nguyen, N.K.; Thrun, S.; Lutolf, M.P.; Blau, H.M. Substrate elasticity regulates skeletal muscle stem cell self-renewal in culture. *Science* **2010**, *329*, 1078–1081. [CrossRef] [PubMed]

15. Bajek, A.; Gurtowska, N.; Olkowska, J.; Kazmierski, L.; Maj, M.; Drewa, T. Adipose-derived stem cells as a tool in cell-based therapies. *Arch. Immunol. Ther. Exp. (Warsz.)* **2016**, *64*, 443–454. [CrossRef] [PubMed]

16. Conde-Green, A.; Marano, A.A.; Lee, E.S.; Reisler, T.; Price, L.A.; Milner, S.M.; Granick, M.S. Fat grafting and adipose-derived regenerative cells in burn wound healing and scarring: A systematic review of the literature. *Plast. Reconstr. Surg.* **2016**, *137*, 302–312. [CrossRef] [PubMed]

17. Mead, B.; Logan, A.; Berry, M.; Leadbeater, W.; Scheven, B.A. Dental pulp stem cells: A novel cell therapy for retinal and central nervous system repair. *Stem Cells* **2016**, *35*, 61–67. [CrossRef] [PubMed]

18. Collart-Dutilleul, P.Y.; Chaubron, F.; De Vos, J.; Cuisinier, F.J. Allogenic banking of dental pulp stem cells for innovative therapeutics. *World J. Stem Cells* **2015**, *7*, 1010–1021. [PubMed]

19. Tajiri, N.; Acosta, S.; Portillo-Gonzales, G.S.; Aguirre, D.; Reyes, S.; Lozano, D.; Pabon, M.; Dela Pena, I.; Ji, X.; Yasuhara, T.; et al. Therapeutic outcomes of transplantation of amniotic fluid-derived stem cells in experimental ischemic stroke. *Front. Cell. Neurosci.* **2014**, *8*, 227. [CrossRef] [PubMed]

20. Waddington, R.J.; Youde, S.J.; Lee, C.P.; Sloan, A.J. Isolation of distinct progenitor stem cell populations from dental pulp. *Cells Tissues Organs* **2009**, *189*, 268–274. [CrossRef] [PubMed]

21. Otto, A.; Schmidt, C.; Luke, G.; Allen, S.; Valasek, P.; Muntoni, F.; Lawrence-Watt, D.; Patel, K. Canonical Wnt signalling induces satellite-cell proliferation during adult skeletal muscle regeneration. *J. Cell Sci.* **2008**, *121*, 2939–2950. [CrossRef] [PubMed]

22. Cornelison, D.D.; Wold, B.J. Single-cell analysis of regulatory gene expression in quiescent and activated mouse skeletal muscle satellite cells. *Dev. Biol.* **1997**, *191*, 270–283. [CrossRef] [PubMed]

23. Zammit, P.S.; Golding, J.P.; Nagata, Y.; Hudon, V.; Partridge, T.A.; Beauchamp, J.R. Muscle satellite cells adopt divergent fates: A mechanism for self-renewal? *J. Cell Biol.* **2004**, *166*, 347–357. [CrossRef] [PubMed]

24. Wu, C.; Asokan, S.B.; Berginski, M.E.; Haynes, E.M.; Sharpless, N.E.; Griffith, J.D.; Gomez, S.M.; Bear, J.E. Arp2/3 is critical for lamellipodia and response to extracellular matrix cues but is dispensable for chemotaxis. *Cell* **2012**, *148*, 973–987. [CrossRef] [PubMed]

25. Krawetz, R.J.; Taiani, J.; Greene, A.; Kelly, G.M.; Rancourt, D.E. Inhibition of rho kinase regulates specification of early differentiation events in P19 embryonal carcinoma stem cells. *PLoS ONE* **2011**, *6*, e26484. [CrossRef] [PubMed]

26. Hetrick, B.; Han, M.S.; Helgeson, L.A.; Nolen, B.J. Small molecules CK-666 and CK-869 inhibit actin-related protein 2/3 complex by blocking an activating conformational change. *Chem. Biol.* **2013**, *20*, 701–712. [CrossRef] [PubMed]

27. Otto, A.; Macharia, R.; Matsakas, A.; Valasek, P.; Mankoo, B.S.; Patel, K. A hypoplastic model of skeletal muscle development displaying reduced foetal myoblast cell numbers, increased oxidative myofibres and improved specific tension capacity. *Dev. Biol.* **2010**, *343*, 51–62. [CrossRef] [PubMed]

28. Cruz-Jentoft, A.J.; Baeyens, J.P.; Bauer, J.M.; Boirie, Y.; Cederholm, T.; Landi, F.; Martin, F.C.; Michel, J.P.; Rolland, Y.; Schneider, S.M.; et al. Sarcopenia: European consensus on definition and diagnosis: Report of the european working group on sarcopenia in older people. *Age Ageing* **2010**, *39*, 412–423. [CrossRef] [PubMed]

29. Nagano, M.; Hoshino, D.; Koshikawa, N.; Akizawa, T.; Seiki, M. Turnover of focal adhesions and cancer cell migration. *Int. J. Cell Biol.* **2012**, *2012*, 310616. [CrossRef] [PubMed]

30. Sanz-Moreno, V.; Gadea, G.; Ahn, J.; Paterson, H.; Marra, P.; Pinner, S.; Sahai, E.; Marshall, C.J. Rac activation and inactivation control plasticity of tumor cell movement. *Cell* **2008**, *135*, 510–523. [CrossRef] [PubMed]

31. Li, W.; Zheng, Y.; Zhang, W.; Wang, Z.; Xiao, J.; Yuan, Y. Progression and variation of fatty infiltration of the thigh muscles in duchenne muscular dystrophy, a muscle magnetic resonance imaging study. *Neuromuscul. Disord.* **2015**, *25*, 375–380. [CrossRef] [PubMed]

32. Cordani, N.; Pisa, V.; Pozzi, L.; Sciorati, C.; Clementi, E. Nitric oxide controls fat deposition in dystrophic skeletal muscle by regulating fibro-adipogenic precursor differentiation. *Stem Cells* **2014**, *32*, 874–885. [CrossRef] [PubMed]

33. Amthor, H.; Christ, B.; Weil, M.; Patel, K. The importance of timing differentiation during limb muscle development. *Curr. Biol.* **1998**, *8*, 642–652. [CrossRef]

34. Condic, M.L.; Rao, M. Alternative sources of pluripotent stem cells: Ethical and scientific issues revisited. *Stem Cells Dev.* **2010**, *19*, 1121–1129. [CrossRef] [PubMed]

35. Porzionato, A.; Sfriso, M.M.; Pontini, A.; Macchi, V.; Petrelli, L.; Pavan, P.G.; Natali, A.N.; Bassetto, F.; Vindigni, V.; De Caro, R. Decellularized human skeletal muscle as biologic scaffold for reconstructive surgery. *Int. J. Mol. Sci.* **2015**, *16*, 14808–14831. [CrossRef] [PubMed]

36. Manchineella, S.; Thrivikraman, G.; Khanum, K.K.; Ramamurthy, P.C.; Basu, B.; Govindaraju, T. Pigmented silk nanofibrous composite for skeletal muscle tissue engineering. *Adv. Healthc. Mater.* **2016**, *5*, 1222–1232. [CrossRef] [PubMed]

37. Kim, T.H.; Kwon, C.H.; Lee, C.; An, J.; Phuong, T.T.; Park, S.H.; Lima, M.D.; Baughman, R.H.; Kang, T.M.; Kim, S.J. Bio-inspired hybrid carbon nanotube muscles. *Sci. Rep.* **2016**, *6*, 26687. [CrossRef] [PubMed]

38. Omairi, S.; Matsakas, A.; Degens, H.; Kretz, O.; Hansson, K.A.; Solbra, A.V.; Bruusgaard, J.C.; Joch, B.; Sartori, R.; Giallourou, N.; et al. Enhanced exercise and regenerative capacity in a mouse model that violates size constraints of oxidative muscle fibres. *eLife* **2016**, *5*. [CrossRef] [PubMed]